Netherlands society for Biomaterials and Tissue Engineering

Program 32nd Annual Meeting, 30 November & 1 December 2023 at the Conference center De Werelt

Conference rooms: AIR & WATER

Thursday, 30 November 2023

9.00-9.45	Registration, coffee & poster mounting
9.45-10.00	Welcome (Room: AIR)
10.00-11.00	**Keynote lecture:** Prof. Hélder Santos (Room: AIR) Full Professor in Biomedical Engineering at The University Medical Center Groningen/University of Groningen *Nanoparticles for boosting cancer antitumor immunity and mitochondria-targeting for reactive oxygen species generation*
11.00-11.15	Short coffee break

11.15-12.30 (10+2 min)	**Oral Presentation Session 1** (AIR) *Smart hydrogel systems* Chair: Piotr Zielinski	**Oral Presentation Session 2** (WATER) *Tissue healing* Chair: Yuewen Zhu
01/02	**Kimberly Brock, University of Twente** *Thiol-mediated Coupling Chemistry as a Crosslinking Method to Prepare Dynamic Self-Healing Hydrogels*	**Gizem Cosar Kutluogu, MedSkin Solutions/Radboudumc** *Mimicking Burn Wound Environment in vitro: Eschar Fibroblasts vs Dermal Fibroblasts*
03/04	**Kirill Mikhailov, University of Groningen/UMC Groningen** *Biomedical self-synthesizing hydrogels with tunable mechanical properties*	**Madalena Gomes, Amsterdam UMC** *Decellularization of extracellular matrix produced in vitro by primary human fetal mensenchymal cells*
05/06	**Sanne van de Looij, Utrecht University** *Diels-Alder Click-Chemistry as a Dynamic Crosslinking Method for Neo-Cartilage Tissue Engineering*	**Merel Gansevoort, Radboudumc** *The prenatal application of functionalized collagen scaffolds in a fetal sheep wound model induces a gene expression profile that results in enhanced skin regeneration*
07/08	**Victor Veenbrink, Technical University Eindhoven**	**Mingjing Zhu, Amsterdam University** *A Novel TGF-β3-Derived Peptide Promotes Chondrogenesis in vitro and in vivo*

	Cell Painting with supramolecular assemblies: exploring biomimicry with high-throughput screening	
09/10	**Alexis Wolfel Sanchez, University of Twente** *Controlled and Tunable Biofunctionalization of Poly(acrylamide) Hydrogels with Cell-Adhesive Ligands*	**Lieke van Dommelen, Radboudumc** *Development of a Biodegradable Porous Hybrid Material to be used as a Patch for Diaphragmatic Hernia Closure*
11/12	**Minye Jin, University of Twente** *Stress-relaxing Bioinspired Dynamic Hydrogels for 3D Cell Encapsulation*	**Roman Krymchenko, Radboudumc** *Preparation of specific elastin hydrolysates and their in vitro evaluation during ECM deposition*

12.30-13.30	Lunch

13.30-14.45 (10+2 min)	**Oral Presentation Session 3** (AIR) *Nano- and micromaterial technologies* Chair: Lizzy Cuypers	**Oral Presentation Session 4** (WATER) *3D printing & additive manufacturing* Chair: Hao Wu
13/14	**Melvin Gurian, University of Twente** *Self-feeding living tissues via nutritional nanoparticles enables long-term stem cell functionality under anoxia*	**Gabriele Addario, Maastricht University** *3D bioprinted human renal tubulointerstitial model to study fibrosis: providing alternatives to in vivo models*
15/16	**Aida Varela-Moreira, Utrecht University** *The media composition influences LNPs internalization by Nucleus Pulposus Cells*	**Essa Al-jehani, Technical University Eindhoven** *3D-printed magneto-active microfiber scaffolds for remote stimulation of skeletal muscle cells in vitro*
17/18	**Mirko D'Urso, Technical University Eindhoven** *Contact guidance triggers fibroblast activation*	**Adrián Seijas Gamardo, Maastricht University** *Modelling the innervation in endometriosis: A biofabrication strategy for generating organized complex 3D in vitro models*
19/20	**Castro Johnbosco, University of Twente** *Modulating microscale mechanics of single cell microenvironment via cell tethering in single cell microgels to guide stem cell function*	**Dmitrii Iudin, Utrecht University** *Shrinkable Hydrogels for Resolution Enhancement in 3D (Bio)printing*
21/22	**Juul Verbakel, Technical University Eindhoven** *Poking inside the cell: Using surface topographies to control Golgi morphology*	**Farhad Sanaei, Radboudumc** *Assessing Printability of Bio-inks by Means of Capillary Rheology*
23/24	**Johanna Husch, University of Twente** *Exploring Microgel Technology for High-Throughput Formation of Osteoclasts*	**Piotr Zielinski, University of Groningen** *Drug-Loaded PLGA Nanoparticles Embedded Within Melt Electrowritten Scaffolds as Drug Delivery Systems*

14.45-15.15	Coffee break & check in into rooms

15.15-16.30 (10+2 min)	**Oral Presentation Session 5** (AIR) *Bone & cartilage regeneration* Chair: Johanna Husch	**Oral Presentation Session 6** (WATER) *Blood and vascular engineering* Chair: Sofia Artomonova
25/26	**Daphne Menssen, Technical University Eindhoven** *Cartilage Organoid Production with Human Induced Chondroprogenitor Cells*	**Encheng Ji, Erasmus MC** *In Vitro Co-Culture Of Tissue-Engineered Mineralised Cartilage And Vessel Networks To Model Endochondral Ossification*
27/28	**Flurina Staubli, UMC Utrecht** *Enhancing Chondrogenic Differentiation for Endochondral Bone Regeneration: The Impact of Cell Number, Signaling Factors and Hypertrophy*	**Francisca Gomes, University of Twente** *Erythrocyte Membrane-Inspired Lipid Coatings For Blood Substitutes*
29/30	**Lena Stoecker, Technical University Eindhoven** *Towards Fabrication of Osteoinductive Scaffolds*	**Magdalena Gladysz, University of Groningen** *Endothelial Cells and Astrocytes Growth Variations on Melt-Electrowritten Scaffolds for Blood-Bain Barrier Modeling*
31/32	**Martyna Nikody, Maastricht University** *Novel Bioactive Glasses From the SiO2-CaO-Na2O System for Bone Regeneration Applications*	**Imke Jansen, Erasmus MC** *A tissue-engineered model of the atherosclerotic plaque cap with microcalcifications*
33/34	**Chong Huang, Radboudumc** *Tooth-on-a-chip co-culture model to study the early-stage interaction between dental epithelial and mesenchymal cells*	**Margot Passier, Technical University Eindhoven** *Computational modeling of sprouting angiogenesis mechanoresponse*
35/36	**Liline Fermin, Maastricht University** *Unravelling the role of biomaterial properties in orchestrating osteoclastogenesis events during biomaterials-driven bone regeneration*	**Jirawat Iamsamang, Technical University Eindhoven** *Designing Fibrous Tubular Scaffolds for Enhanced Mechanical Performance in Vascular Engineering*

16.30-16.45	Coffee break
16.45-18.30	**Thesis award & NBTE general assembly** (Room: AIR)
18.30-19.00	**Sponsor introduction** (Room: AIR)
19.00-20.00	Dinner
20.00-21.00	**Evening lecture:** Prof. Erik van Sebille (Room: AIR) Professor of Oceanography and Public Engagement at Utrecht University *Tackling the plastic soup or saving the climate? The role of academics in major environmental challenges*
21.00-22.00	**Pubquiz** (Room: FIRE)
22.00-0.00	Get together with drinks (Room: FIRE)

Friday, 1 December 2023

7.00-9.00	Breakfast
9.00-10.00	**Rapid-fire poster parallel session** (Rooms: AIR & WATER)
10.00-11.15	**Poster session** (Room: FIRE)
11.15-12.45	**Focus symposium** (Room: AIR) Niloofar Tahmasebi Birgani, Maastricht University *Bone mini-tissues* Monize Caiado Decarli, University of Groningen *Bioprinting of bioactive human based hydrogels* Mani Diba, Radboudumc *Engineering the dynamic behavior of hydrogels as extracellular matrix* Tommaso Ristori, Technical University Eindhoven *Synergy of experiments and simulations to unravel new blood vessel formation*
12.45-14.00	Lunch **Meet the Company**
14.00-15.00	**Panel discussion** (Room: AIR) Young PIs discuss personal experiences on their academic journey (moderator: *Aurelie Carlier*) Panelists: Niloofar Tahmasebi Birgani Monize Caiado Decarli Mani Diba Tommaso Ristori
15.00-15.30	Coffee break

15.30-16.45 (10+2 min)	**Oral Presentation Session 7** (AIR) *Miniaturized systems* Chair: Johanna Husch	**Oral Presentation Session 8** (WATER) *Modulating the immune response* Chair: Martyna Nikody
37/38	**Marta Garcia Valverde, Utrecht University** *Engineering a Biomimetic Glomerular Filtration Barrier Chip for Diabetic Nephropathy Modeling*	**Els Alsema, RIVM/Technical University Eindhoven** *Establishing Predictive Relationships Between In Vitro Macrophage Assays and In Vivo Implant Fibrosis*
39/40	**Ceri-Anne Suurmond, Radboudumc** *Bone Metastatic Spheroid Model for Preclinical Assessment of Novel Anticancer Drugs and Biomaterials*	**Hannah Brouwer, Technical University Eindhoven** *The Interplay Between 3D Extracellular Matrix Organization And Macrophages During Tissue Remodelling*

41/42	**Carolina Serrano Larrera, University of Twente** *Fat Pad-on-chip: Advancing Adipose Tissue Modeling through 3D Culture, Mechanical Stimulation, and Disease Applications*	**Maria Lobita, University of Groningen/UMC Groningen** *Incorporation of Copper Metal Framework Nanoparticles into Polymeric Microneedles to target the M1-type Macrophages*
43/44	**Marieke Meteling, University of Twente** *How 3D microtissue formation directs chondrogenic lineage commitment of stem cells*	**Sofia Artamonova, Technical University Eindhoven** *Spatiotemporal Assessment of Pathophysiological Tissue Remodeling in Resorbable Synthetic In Situ Tissue-Engineered Heart Valves in Sheep*
45/46	**Sarah Pragnere, Technical University Eindhoven** *Engineering Tissue Microarchitecture: The Role of Cell Contractility and Matrix Properties*	**Bram Zoetebier, University of Twente** *Injectable Hydrogels for Neutralizing Inflammatory and Pro-Catabolic Cytokines*
47/48	**Jaehyeon Kim, Maastricht University** *OviChip : 3D in vitro Oviduct Model*	**Yanjing Ji, University of Groningen/UMC Groningen** *Visible Light Responsive Reversible Photoacids-Based Core-Shell Nanogels for Antifouling Surface Coating*

16.45-17.00	Short coffee break
17.00-17.30	**Announcements, awards ceremony & closure of the meeting** (Room: AIR)

Sponsors

GESIM Bioinstruments and Microfluidics

Integrating the Worlds of Micro and Macro Technology

REGENHU

Miltenyi Biotec

Rapid-fire Poster Parallel Session

Friday, 1 December 2023

	Session 1 (AIR)	**Session 2** (WATER)
01/02	**Hannah Abee, RIVM/Maastricht UMC** *In vitro assays for the effect of implant material on the host response to infection*	**Marie Loly, Maastricht University** *Unravelling Kidney Development by Reverse Engineering Branching Morphogenesis*
03/04	**Nancy Avila Martinez, Radboudumc** *Construction of fibrillar collagen and hyaluronan scaffolds and preliminary in vitro evaluation*	**Mattia Manenti, Technical University Eindhoven** *Analysis of the endothelialization of small-diameter in situ tissue-engineered vascular grafts; A systematic review*
05/06	**Gizem Babuccu, Amsterdam UMC** *In vitro evaluation of novel antimicrobial peptides: potential synergy with human plasma*	**Amal Mansoor, Technical University Eindhoven** *Paracrine Effects of Macrophage Phenotype on Tendon Tissue Remodelling*
07/08	**Cécile Bosmans, University of Twente** *Emulating physical dynamicity of arterial blood vessels and neighbouring tissue interaction*	**Rob Meuwese, Radboudumc** *The effect of different sterilization methods on the expandable collagen plug in in vitro and ex vivo setups*
09/10	**Maaike Bril, Technical University Eindhoven** *Protecting Your Precious: Dynamic Topographies Drive Nuclear Reorganization Events*	**Yu Na, University of Twente** *Improving Interfacial Adhesion Properties of Hydrogel Matrices to PDMS-based Microfluidic Platforms*
11/12	**Thijs Conner, Technical University Eindhoven** *To Fuse Or Not To Fuse: The Effect Of Polarization State On The Fusion Of Macrophages Towards Foreign Body Giant Cells*	**Jet Peters, Technical University Eindhoven** *Influence of Tissue Growth on Collagen Orientation in Articular Cartilage*
13/14	**Hasnae El Showk, Technical University Eindhoven** *Investigating the Effects of Cyclic Strain on Macrophage Fusion and Multinucleated Giant Cell Formation*	**Madelief Rous, UMC Groningen** *Investigating the Interaction of Breast Implants and the Surrounding Tissue: An Introduction*
15/16	**Micaela Fernandes, University of Groningen** *Microfabrication of high resolution poly(methyl methacrylate) (PMMA) microfluidic devices*	**Irem Soyhan, University of Groningen/UMC Groningen** *Polyhydroxyalkanoates as biodegradable polymeric biomaterials*

17/18	**Amaia Garmendia Urdalleta, Erasmus MC** *Incorporation of osteoclasts into an in vitro model of mineralised cartilage in the context of endochondral ossification*	**Mariana Harue Taniguchi Nagahara, Maastricht University/University of Campinas** *Wound Healing Electrospun Meshes Incorporating a Natural-based Arrabidaea chica Verlot extract*
19/20	**Devlina Ghosh, University of Groningen/UMC Groningen** *A universal nanogel-based coating approach for medical implants*	**Laure van Hofwegen, Amsterdam UMC** *The bactericidal activity of a graphene quantum dot implant coating*
21/22	**Anniek Gielen, RIVM/Amsterdam University** *In Vitro – In Vivo Predictivity of Osseointegration Markers*	**Noemy Vergara Vera, Technical University Eindhoven** *Influence of macromolecular crowding on collagen I fibrillogenesis in 3D printing*
23/24	**Madalena Gomes, Amsterdam UMC** *Proteomic analysis of primary human fetal, adult dermal and eschar mesenchymal cells and their secreted extracellular matrices*	**Valentine Vetter, Technical University of Eindhoven** *Early host responses to in situ engineered heart valves*
25/26	**Esra Güben Kaçmaz, Maastricht University** *Mineralized Collagen Micro-blocks for Bottom-Up Bone Tissue Engineering*	**Margot Warin, Maastricht University** *Bioactive glasses vs Bacteria: Using the pH to Fight Infections in Long Bone Defects*
27/28	**Yannick Hajee, Radboudumc** *Effect of Hydrogel Viscoelasticity on Osteogenic Differentiation of hMSC Spheroids*	**Hao Wu, Maastricht University** *Investigating the peripheral neurovascular interactions based on an in vitro model using melt electrowriting and collagen/fibrin hydrogel*
29/30	**Jarno Hiemstra, University of Twente** *Bioinspired Hydrogels with Modulated Degradability for 3D Cell Encapsulation*	**Ruichen Zhang, University of Groningen/UMC Groningen** *Sustainability in clinical nanogel coating technology for combating central venous catheter infection*
31/32	**Marlena Maria Księżarczyk, Utrecht University** *Distinct morphological differences in the osteochondral tissue of the humeral head between aquatic, semi-aquatic and terrestrial mammals*	**Yuewen Zhu, University of Groningen/UMC Groningen** *An Injectable Hydrogel Loaded with Dual-coated Nanoparticles for Wound Healing Application*
33/34	**Nguyen Zuan Thanh Le, University of Twente** *Advancing Injectable Hydrogel Scaffold With Tyramine-Functionalized Chondroitin Sulfate For Cartilage Repair*	**Pavan Gudeti, The Silesian University of Technology** *Advancements in hydrogel-based inks for tissue engineering and regenerative medicine*
35/36	**Deeksha Rajkumar, Amsterdam UMC** *Novel Bioactive Glass S53P4 cream as a bactericidal coating to prevent Biomaterial-associated infections*	**David Rojas-Velazquez, Utrecht University** *Using Bayesian Optimization to Calculate Conductivity in an Electrolytic Fluid for the Forward Problem in Electrocardiography*

37/38		**Clara Soeiro Maas, UMC Groningen** *Biofabrication of Osteogenic Spheroids from Human Dental Pulp Stem Cells of Deciduous Teeth (SHEDs)*

Thursday
30 November 2023

Keynote lecture

Nanoparticles for boosting cancer antitumor immunity and mitochondria-targeting for reactive oxygen species generation

Prof. dr. Hélder A. Santos

Prof. Santos (D.Sc. Tech., Chem. Eng.) is a Full Professor in Department of Biomedical Engineering at the University of Groningen. He is also Research Director at the University of Helsinki, Faculty of Pharmacy. Prof. Santos is also the co-founder of the startups Capsamedix Oy and Medixmicro Oy, and Coordinator of MSCA-ITN P4 FIT network in tendon repair (~4.1 m€). He holds Visiting Professorships at the Shanghai Jiao Tong University School of Medicine and University of Tartu, and also Honorary Adjunct Fellow at the University of Technology Sydney. Prof. Santos research interests include the development of nanoparticles/nanomedicines and biomaterials for biomedical applications, particularly cancer and heart diseases. His lab makes the unique bridge between medical engineering, pharmaceutical nanotechnology and tissue engineering by combining unique techniques to develop novel therapeutic formulations for translation into the clinic. He is co-author of +500 publications (+21700 citations; h-index = 88) and 5 patents. He has +220 invited talks around the world. He is also in Editorial board member of Advanced Healthcare Materials, Advanced Therapeutics, Chemical Society Reviews, Journal of Controlled Release, VIEW, Journal of Functional Materials, Frontiers in Bioengineering and Biotechnology and Materials, Frontiers in Biomaterials, Precision Nanomedicine, PLOS ONE, etc. He is Associate Editor of Nano Select, Smart Materials in Medicine, and Drug Delivery and Translational Research, among others.
Prof. Santos has received prestigious awards/grants, for example, the "Talent Prize in Science" in 2010 attributed by the Portuguese Government, ERC Starting Grant in 2013 and ERC Proof-of-Concept Grant in 2018, Young Researcher Award in 2013 attributed by Faculty of Pharmacy, the Academy of Finland Award for Social Impact in 2016, and the CRS Young Investigator Award 2021.

Oral Presentation Session 1

Smart hydrogel systems

Thiol-mediated Coupling Chemistry as a Crosslinking Method to Prepare Dynamic Self-Healing Hydrogels

K.Brock[1], R. Carrillo[2], J.I. Paez[1]
[1]University of Twente, Drienerlolaan 5, 7522NB, Enschede, Netherlands
[2]Instituto de Productos Naturales y Agrobiología, Avda. Astrofísico Fco. Sánchez 3, 38206 La Laguna, Spain
Email: k.brock@utwente.nl

Dynamic covalent chemistry (DCC) provides a versatile toolbox of reactions, consisting of diverse bonds that are strong yet dynamic. The implementation of dynamic covalent bonds in materials enables interesting properties such as self-healing behavior and stress relaxation over a wide timescale. Accordingly, DCC has also attracted interest in the biomedical field. One of the applications is the implementation of DCC in extracellular matrix (ECM) mimics, enabling better resemblance to the natural dynamicity of the ECM than static bonds and being stronger than physical bonds.

In this work, a novel type of thiol-based dynamic covalent chemistry is used as a crosslinking strategy to form tunable, dynamic hydrogels for cell encapsulation.

The system consists of two polyethylene glycol (PEG) precursors, one linear bifunctional precursor, synthesized in good yield (60%) and excellent substitution degree (100%), and the other a 4-arm precursor with four functional groups, commercially available. Hydrogels form rapidly in a few seconds to minutes by mixing the two precursors under physiological conditions (aqueous buffer solution, pH 7.0-8.0, room temperature). The mechanical properties and curing kinetics were characterized by shear rheology. Human mesenchymal stem cells (hMSCs) were encapsulated in the hydrogel and the acute toxicity was assessed by a live/dead assay after 2 hours of encapsulation.

The hydrogels prepared using this thiol-mediated coupling chemistry are formed rapidly in a few seconds to minutes under explored conditions. The shear storage modulus (G') is in the range of 200-3000 Pa, and can be tuned by changing the concentration of the precursors from 7.5 to 10 wt%. Furthermore, the material shows moderate stress relaxation (25-60%) at 10% strain, an important parameter featuring the viscoelasticity of the material. Due to the dynamic character of the bonds, two halves of a cut hydrogel can reconcile in 0.5-3.5 h at room temperature, demonstrating the self-healing properties of the system.

Cell viability results show a viability of 74±15% after 2 h of encapsulation, similar to the static control system of PEG polymer crosslinked with thiol-vinyl sulfone bonds with a similar architecture.

In summary, this study showcases the applicability of this novel thiol-mediated dynamic covalent chemistry to make tunable, self-healing, stress-relaxing hydrogels, that show potential for cell encapsulation applications.

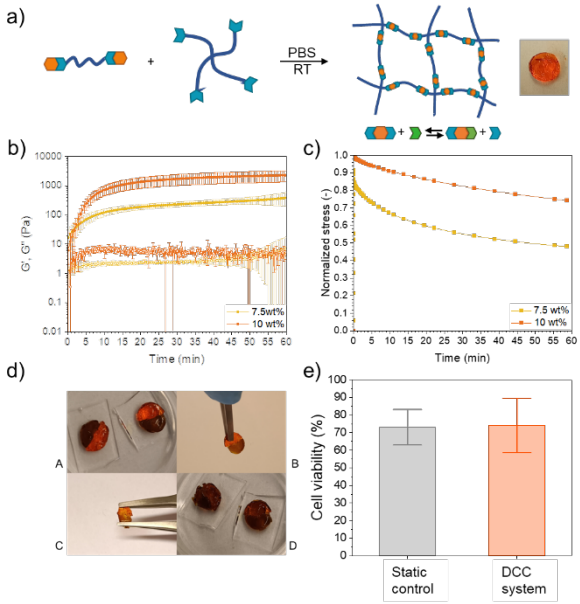

Figure 1: a) Schematic representation of the two precursors that form a crosslinked network, the resulting hydrogel is depicted on the right. b) Curing kinetics and shear modulus of the thiol-mediated DCC hydrogel at 7.5 and 10 wt%. c) Stress relaxation at 10% strain of thiol-mediated DCC hydrogel at 7.5 and 10 wt%. d) Self-healing experiment after 0 min (1), 30 min (2), 3.5 h (3) and overnight. e) Cell viability after 2 h encapsulation in 10 wt% DCC gels, in comparison to a static gel control.

Biomedical self-synthesizing hydrogels with tunable mechanical properties

K. Mikhailov1,2*, I. Marić1, L. Yang2, R. Bron2, P. van Rijn2 and S. Otto1

[1]Stratingh Institute for Chemistry, University of Groningen, Nijenborgh 4, 9747 AG Groningen, the Netherlands
[2]University Medical Center Groningen, Department of Biomedical Engineering and W. J. Kolff Institute, University of Groningen, Antonius Deusinglaan 1, 9713 AV, Groningen, the Netherlands
*k.mikhailov@rug.nl

Key words: dynamic covalent chemistry, self-assembly, supramolecular hydrogels

INTRODUCTION

Peptide-based hydrogels are important materials in cell culture research and are utilized as scaffolds for tissue engineering, wound healing and drug delivery due to their close resemblance to the extracellular matrices [1]. Over the recent years, dynamic structural properties of a biological scaffold were proven to be essential to mimic natural tissues [2,3]. In this work, we utilize orthogonal disulfide and hydrazone dynamic covalent chemistries to create a biocompatible self-synthesizing peptide-based hydrogel scaffold from an ordered self-assembled supramolecular structure.

RESULTS AND DISCUSSION

Oxidation of peptide building block (**1**) modified with a thiol-containing moiety and with a hydrazide moiety results in formation of a dynamic equilibrium of various sized macrocycles. Out of the mixture, only pentamers $\mathbf{1}_5$ stack on each other and form supramolecular fibers with hydrazide groups on their surfaces (Figure 1a). This process is autocatalytic, which increases the fabrication rate and opens up a possibility to precisely control the fiber length [4].

The network of fibers is then cross-linked with a dialdehyde to give a hydrogel through hydrazone bond formation (Figure 1a). Altering the fibers length through autocatalytic fiber formation, the nature of the cross-linker and cross-linking density allowed us to cover a large range of hydrogel stiffnesses with a high degree of controllability ($G' \sim 3*10^2$ – $7*10^3$ Pa).

Utilization of the same hydrazone approach allows these fibers to be decorated with bioactive aldehyde-containing moieties (Figure 1a), which can bring additional functionality to the scaffold and direct the behavior of the cells that are cultured on top of or inside the hydrogel matrix.

To assess biocompatibility of these hydrogels, we investigated cell viability and spreading on unmodified hydrogel ($\mathbf{1}_5$) and hydrogels modified with 10 mol % glyoxylyl-functionalized RGD and LDV peptides. All samples showed high cell viability and spreading after 24 hours of culturing (Figure 1b, c) [5].

We exploited these hydrogels to direct osteogenic differentiation of human mesenchymal stem cells (hMSCs), and are currently investigating the effect of the fiber length controlling gel stiffness on cell behaviour

CONCLUSIONS

Here we show the development of biocompatible and self-synthesizing hydrogels based on two orthogonal dynamic chemistries. Fiber formation is a self-assembly driven and autocatalytic process, which substantially decreases the manufacturing effort, allows fine tuning of the material properties and gives the unique label “self-synthesizing hydrogel” to the material.

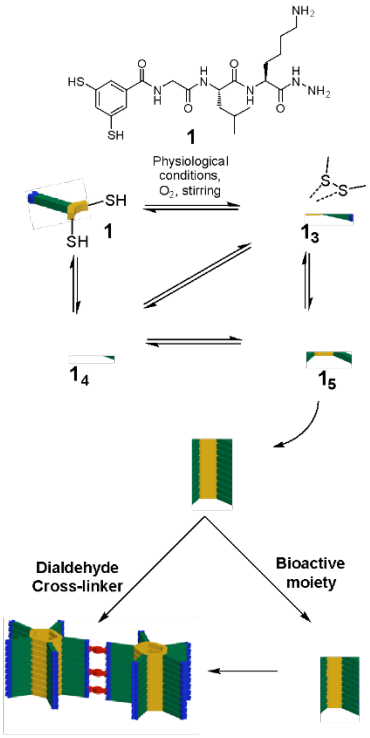

Figure 1. (a) Emergence of the self-replicating supramolecular fibers, decoration of the fibers with bioactive moieties and formation of the hydrogel through hydrazone chemistry. (b) Live/dead staining of hMSCs on hydrogel samples after 24 h of culturing. (c). DAPI and FITC-phalloidin staining, after 24 h of culturing. All scale bars are equal to 150 μm.

REFERENCES

1. X. Ding et al., Adv. Drug Deliver. Rev., 2020, 160, 78–104
2. S. Tang et al., Prog. Mater. Sci., 2021, 120, 100738
3. K. Zhang et al, Chem. Rev., 2021, 121, 11149-11193
4. A. Pal et al., Angew. Chem., 2015, 54, 7852 –7856
5. I. Maric et al., Angew. Chem., 2023, 62, e202216475

Diels-Alder Click-Chemistry as a Dynamic Crosslinking Method for Neo-Cartilage Tissue Engineering

S.M. van de Looij[1], B.G.P. van Ravensteijn[1], T. Vermonden[1] (t.vermonden@uu.nl)
[1]Department of Pharmaceutics, Faculty of Science, Utrecht Institute for Pharmaceutical Sciences (UIPS), Utrecht University, 3584 CG, Utrecht, the Netherlands

Introduction: The stiff yet elastic material of the extracellular matrix (ECM) allows articular cartilage to withstand movement and heavy loads for years. However, partially due to its avascular and alymphatic nature that leads to reduced nutrient access, the tissue hardly recovers after injury or disease. The main goal of this project is to develop a neo-cartilage implant with suitable mechanical properties and biocompatibility, by means of encapsulating mesenchymal stem cells (MSCs) into a bulk hydrogel. Using dynamic-covalent Diels-Alder click-chemistry between furan and maleimide functionalities to crosslink hyaluronic acid, gelatin and PEG into a polymer network (Fig. 1), we aim to design a tuneable platform for cartilage engineering. In this study, we investigate various hydrogel formulations with increasing theoretical maximum crosslinking densities for their chemical and mechanical properties.

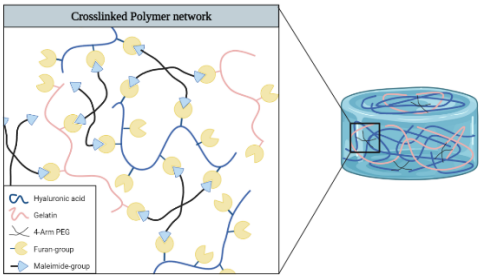

Fig. 1: Graphical overview of hydrogels formed by Diels-Alder Crosslinking.

Materials and Methods: Furan-modified hyaluronic acid (HAFU) and gelatin (GelFU) were synthesised at a degree of substitution of 65% and 85%, respectively. 4-Arm $PEG_{10.000}$-maleimide (4APM) was purchased from JenKem. Several gel formulations named A-D (see Table 1) with increasing crosslinking density were prepared with a standard weight ratio of 4:1 HAFU to GelFU, and 5:1 molar ratio of furan to maleimide moieties.

Table 1: Tested formulations A, B, C and D.

	Total polymer content	HAFU content	GelFU content	4APM content	Crosslinking density
A	3.5%	1.6%	0.4%	1.5%	5.8 mM
B	4.5%	2.1%	0.5%	1.9%	7.5 mM
C	5.5%	2.5%	0.6%	2.3%	9.0 mM
D	6.5%	3.0%	0.8%	2.7%	10.7 mM

The degree of swelling and degradation kinetics of different hydrogel formulations were assessed at 37 °C. Polymers were crosslinked in either PBS or MSC-growth medium, and stored over time in medium. Rheological measurements were conducted to assess the gelation time (defined as the moment the storage modulus (G') overtakes the loss modulus (G'')) and the gel strength (defined as the maximum G').

Results and discussion: We found that the degree of swelling, degradation kinetics (Fig. 2A-B), gelation time (Fig. 2C-D) and gel strength (Fig. 2E-F) can be easily tuned by increasing the theoretical maximum crosslink density. Interestingly, gels crosslinked in PBS initially tend to swell to a lesser extent and have slower degradation kinetics. Similarly, they present a shorter gelation time and higher maximum storage modulus, indicating a higher crosslinking efficiency than gels crosslinked in medium. The thiols present as free cysteine in medium appear to interfere with the Diels-Alder reaction by competing with furan moieties for maleimide binding. However, as the theoretical maximum crosslink density increases in formulations A to D, we note that the effect of this interference on the final gel strength and degradation time is reduced. For formulations C and D, the gelation kinetics are approximately equal in PBS and medium, and the maximum storage modulus only differs a factor ~2 as opposed to a factor ~6 for conditions A and B. Nevertheless, there are still improvements to be made to obtain a sufficient degradation profile of at least two months in medium.

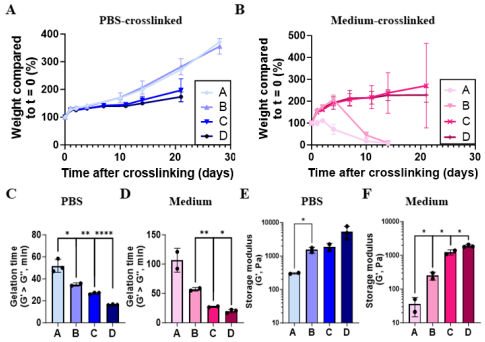

Fig. 2: Chemical and mechanical testing of formulations A, B, C and D. (A) Swelling and degradation study of hydrogels crosslinked in PBS, stored in MSC-growth medium. (B) Swelling and degradation study of hydrogels crosslinked and stored in MSC-growth medium. (C) Gelation time of gels crosslinked at 37 °C in PBS, and (D) MSC-growth medium. (E) Maximum storage modulus of polymers crosslinked at 37 °C in PBS, and (F) MSC-growth medium. Statistical significance is noted with * ($p < 0.05$), ** ($p < 0.01$), *** ($p < 0.001$) or **** ($p < 0.0001$).

Conclusion and future goals: Diels-Alder-crosslinkable hydrogels composed of HAFU, GelFU and PEG have tuneable chemical and mechanical properties, but the crosslinking efficiency is hindered by medium components. Still, gels formed in medium at higher crosslinking densities have mechanical properties that are deemed sufficient for cartilage engineering. Our next steps aim at showing cell viability, proliferation and extracellular matrix deposition after MSC-encapsulation.

Acknowledgements: Funding for the project is provided by LS-CarE consortium (project number NWA.1389.20. 192) of the research programme NWA-ORC which is (partly) financed by the Dutch Research Council (NWO).

Cell Painting with supramolecular assemblies: exploring biomimicry with high-throughput screening

V.A. Veenbrink[1,2], N. Konshin[1,3], J. de Boer[1,3] and P.Y.W Dankers[1,2]
[1] Eindhoven University of Technology, Institute for Complex Molecular Systems
[2] Eindhoven University of Technology, Department of Biomedical Engineering, Laboratory of Chemical Biology
[3] Eindhoven University of Technology, Department of Biomedical Engineering
P.O. Box 513, 5600 MB Eindhoven, The Netherlands

Introduction

One of the main goals of biomaterials research is to develop a synthetic mimic of the extracellular matrix. However, to capture the complexity of nature in a chemically accessible way requires a robust an tunable platform. To this end, our group relies on supramolecular materials based on ureido-pyrimidinone (UPy) chemistry (Figure 1). UPy compounds can form supramolecular assemblies through quadruple hydrogen bonding, π-π interactions and hydrophobic interactions. These assemblies can be made bioactive by introducing peptide-functionalized UPy compounds. The modular nature of supramolecular interactions facilitates the production of large libraries of multifunctional UPy assemblies. This can be achieved through changes to components such as the addition of multiple bioactive UPys, crosslinkers or other functionalized UPy molecules. In this way it is possible to gradually approach the complexity found in the natural ECM. However, to investigate such a large quantity of conditions, a high-throughput screening method is required. To this end the Cell Painting protocol developed by the Broad institute of MIT and Harvard was adapted to work with UPy assemblies in solution. Cell Painting is a high throughput morphological screening method that creates cell level morphological profiles. These profiles are generated by collecting up to 1477 unique measurements across eight cellular compartments stained with six dyes. This wealth of information also makes the technique suitable for a machine learning approach. In this study, U2OS cells were treated with fibronectin or various fibronectin-derived peptide-functionalized UPy assemblies in solution. The cells were then analyzed using the Cell Painting protocol. Cells with similar morphological profiles were identified using a Pearson Correlation matrix. Furthermore, a random forest algorithm was trained to identify morphological profiles relating to cells treated with fibronectin. In doing so, it was demonstrated that complex ECM proteins such as fibronectin can be mimicked through simple peptide-functionalized UPy assemblies. Hereby laying the foundation for future research into other ECM mimicking proteins.

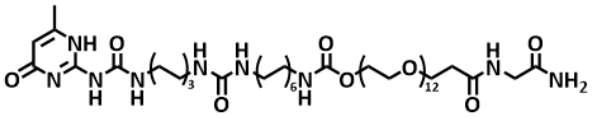

Figure 1: Molecular structure of UPy-Glycinamide

Results and Discussion

It was demonstrated that the morphological profile obtained from treating U2OS cells with fibronectin was significantly similar to that of U2OS cells treated with either the fibronectin fragment III domains 9 and 10 (FNIII(9-10)) and that of U2OS cells treated with UPy-GPHSRN(GS)$_3$GRGDS (Figure 2). However, at higher concentrations of UPy assemblies in solution, the profile appears to be determined primarily by the UPy and not by the specific peptide-functionalized UPys. This effect was eliminated by training a random forest classifier to identify relevant morphological profiles (data not shown here).

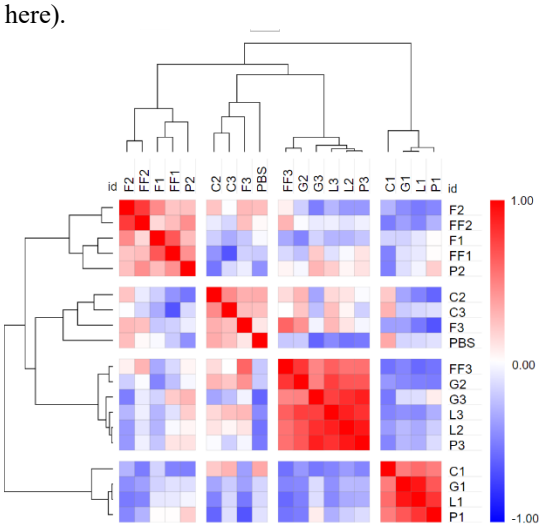

Figure 2: Pearson correlation matrix of the Cell Painting profiles of U2OS cells treated with Fibronectin (F), Fibronectin fragment FNIII(9-10) (FF), UPy-GPHSRN(GS)$_3$GRGDS (P), UPy-GGGRGDS (L) or UPy-cRGDfK (C) at increasing dilutions (1 = 1x, 2 = 10x, 3 = 100x)

Conclusions and Outlook

It was demonstrated through analyzing the Cell Painting profiles of cells treated with fibronectin and fibronectin derived peptide-functionalized UPys, that UPy-GPHSRN(GS)$_3$GRGDS showed the most promise as a fibronectin mimicking supramolecular assembly. In future, more peptides and formulations will be investigated for ECM mimicking properties.

References

1. Diba, M. *et al.* Engineering the Dynamics of Cell Adhesion Cues in Supramolecular Hydrogels for Facile Control over Cell Encapsulation and Behavior. *Advanced Materials* **33**, 2008111 (2021).
2. Bray, M. A. *et al.* Cell Painting, a high-content image-based assay for morphological profiling using multiplexed fluorescent dyes. *Nature Protocols 2016 11:9* **11**, 1757–1774 (2016).

Controlled and Tunable Biofunctionalization of Poly(acrylamide) Hydrogels with Cell-Adhesive Ligands

A. Wolfel[1], M. Jin[1], N. Araújo-Gomes[1], M. Becker[1], J. Leijten[1], L. Moreira Teixeira[2], J. I. Paez[1]*
Developmental Bioengineering[1]/Advanced Organ Bioengineering and Therapeutics[2], TechMed Centre, University of Twente.
Drienerlolaan 5, 7522NB, Enschede, The Netherlands. E-mail: j.i.paez@utwente.nl

Introduction:

Understanding and controlling cell-materials interactions through cell-adhesive ligands is key to modulate cell-behavior in tissue engineered constructs. Synthetic hydrogels such as poly(acrylamide) (PAM) are often used as 2D cell culture platforms to study cell-materials interactions. Because of their characteristic protein repellence, PAM gels need to be chemically treated to be biofunctionalized with cell-adhesive ligands in a controlled and tunable fashion. However, typically applied chemistries for biofunctionalization are not user-friendly, are expensive, and lack chemo-selectivity and reproducibility, impairing ligand functionality and leading to inconclusive results [1]. In this work, we present a novel strategy that facilitates the biofunctionalization of PAM hydrogels with bioligands by means of a chemo-selective reaction: the luciferin-inspired click ligation [2]. We developed a novel comonomer featuring a cyanobenzothiazole (CBT) group, which is compatible with PAM preparation. When copolymerized with acrylamide and a crosslinker via established protocols, PAM-CBT hydrogels are easily obtained. Pendant CBT moieties can later be used to covalently bind *N*-cysteine containing biomolecules in a single step, under physiological conditions, and at tunable concentrations.

Materials and Methods:

Hydrogel synthesis: comonomers were dissolved in a water:DMF mixture (60:40) and degassed before the addition of free radical initiators (APS/TEMED). The curing mixture was spotted onto a hydrophobic glass slide and covered with a freshly prepared acrylated glass coverslip. PAM-CBT gels formed within 10 min, were rinsed with water, and characterized by UV-Vis spectroscopy, confocal microscopy, and nanoindentation. Biofunctionalization: *N*-cysteine containing bioligands were linked to PAM-CBT by reaction in HEPES buffer (20 mM, pH 8) at R.T. during 30 min. Cell culture: hMSCs were seeded on top of the hydrogels at densities of 2.5×10^3 cells.cm^{-2}. Cell adhesion was quantified by collecting the supernatant containing the non-adhered cells after 1 h post-seeding and performing DNA quantification.

Results and Discussion:

PAM hydrogels containing the novel comonomer CBT-AM were prepared using adapted standard protocols for PAM synthesis. The amount of CBT groups in the hydrogels was varied by adjusting the molar concentration of CBT-AM used during the synthesis (0-5 mol%). Thin PAM-CBT hydrogels covalently attached to glass coverslips were obtained in one step and resulted translucid to the naked eye. The increasing amount of CBT-AM in the gels was proven by UV-Vis measurements, which showed an increased absorbance at 320 nm, due to the absorbance of CBT. These results demonstrated the effective incorporation of CBT-AM in PAM hydrogels and the predictive control achieved on the loading of CBT groups. Furthermore, we analysed the effect of CBT-AM concentration in the final properties of PAM-CBT hydrogels. Increasing CBT-AM concentration (0-4 mol%) slightly decreased hydrogel equilibrium swelling ratio (ESR, varied from 95 to 85%), hydrogel thickness decreased from 79.3 to 47.5 µm, and Young's modulus increased from 1.9 to 6.0 kPa. These variations can be attributed to the hydrophobicity of the CBT moiety, which may lead to decreased water uptake at higher CBT-AM concentrations.

We compared the biofunctionalization performance of the new PAM-CBT substrates with that of the golden standard biofunctionalization technique used for PAM hydrogels, known as sulfo-SANPAH (PAM-SS) [1]. Biofunctionalization in PAM-CBT substrates occurred under mild conditions and was completed in less than 30 min at R.T. In contrast, PAM-SS biofunctionalization required of repetitive cycles of intense UV-irradiation (2x, 5 min, 365 nm, 50 mW.cm^{-2}) and overnight reaction to achieve sufficient biofunctionalization. Furthermore, the PAM-CBT approach enabled 55-fold higher immobilization of ligand than SS and with more homogeneous ligand distribution. In PAM-CBT substrates, we demonstrated that the amount of immobilized biomolecule can be finely and reproducibly controlled, by simply modulating the concentration of the bioligand in the incubation solution. This feature is very important considering that biological properties of PAM substrates could be significantly different according to their ligand density. We compared the biological performance of PAM-CBT and PAM-SS hydrogels modified with cell-adhesive ligands (cRGD). PAM-CBT-RGD hydrogels promoted remarkably faster adhesion of hMSCs than PAM-SS-RGD substrates. After 1 h of cell culture, 70 % of seeded hMSCs adhered to PAM-CBT substrate while only 20% were adhered to PAM-SS-RGD. Furthermore, hMSCs seeded in PAM-CBT where more homogeneously distributed, adopted more spread shape and showed higher metabolic activity than in PAM-SS substrates, where cells showed aggregation and clustering.

Conclusions:

CBT-AM incorporation into PAM hydrogels enabled a highly efficient and robust bioconjugation strategy. PAM-CBT outperformed PAM-SS in biofunctionalization efficiency and homogeneity, which led to remarkable differences in the biofunctionality of the substrates. Hence, the presented strategy is anticipated to promote more conclusive studies regarding cell-ligands interaction by enabling a better control of ligand density loading.

References: [1] Wolfel A. *et al*. *Front. Chem.* 10, 2022.
[2] Jin M. *et al*. *ACS Appl. Mater. Interfaces*. 14, 2022.

Stress-relaxing Bioinspired Dynamic Hydrogels for 3D Cell Encapsulation

M.Jin[1], J.I.Paez[1]
[1]University of Twente. Drienerlolaan 5, 7522 NB, Enschede, The Netherlands
m.jin-1@utwente.nl

Introduction. As extracellular matrix mimics, hydrogels have been explored extensively due to their high water content, porosity, and adjustable biochemical and mechanical properties. One of the key features of soft tissues, viscoelasticity, has been increasingly modulated during such artificial matrices design, for example, by introducing dynamic covalent bonds at the crosslink points. Here, we propose a bioinspired thiol-mediated dynamic covalent chemistry to engineer a dynamic hydrogel platform for cell culture. This dynamic network shows tunable viscoelastic properties, stress relaxation, self-recovery and self-healing behavior. Moreover, by combining this novel dynamic chemistry with a static crosslinking chemistry, the properties of the hydrogel matrix could be finely tuned to support 3D cell culture.

Materials and Methods. 4-arm, 20 kDa PEG macromers were used as hydrogel precursors. Hydrogels were prepared under physiological conditions (37°C, 20 mM HEPES buffer, pH 8). Mechanical strength and gelation kinetics of the resulting hydrogels were characterized by shear rotational rheology. Crosslinking process, biofunctionalization with cell-adhesive peptide cyclo(RGDfC), and encapsulation of human mesenchymal stem cells (hMSCs) took place one-pot. The resulting hydrogels were cultured for up to 5 days. Cell viability and cell-materials interactions were evaluated by live/dead assay, cytoskeletal and morphological characterization, respectively.

Results and Discussion. PEG hydrogels, crosslinked via the novel bioinspired dynamic chemistry, were successfully prepared under physiological conditions (Fig. 1a) following established protocols [1, 2]. Hydrogels at 10 wt% polymer concentration in HEPES buffer pH 8.0 showed a fast gelation time (< 45 s) and good mechanical strength (G'~ 4397 Pa), as revealed by time sweep rheology (Fig.1b). In addition, the high dynamicity of this system allowed gel self-recovery and self-healing properties after rupture. Stress relaxation experiments showed that the dynamic hydrogels fully release the stress within ~10 min (Fig.1c), suggesting fast bond reorganization at the macroscopic level. For the end application as artificial cell scaffold, the too fast network dissociation of hydrogels could potentially impede the usage for long term cell culture. To improve matrices stability, besides the dynamic bonds, a well-established thiol mediated covalent chemistry that forms stable, static bonds was introduced for a hybrid hydrogel design. By varying the ratio between static and dynamic crosslinks, a stable hydrogel platform with tunable viscoelasticity was developed. The time sweep rheological data showed a gelation within 2 min for all conditions (Fig. 1d). No significantly differences in stiffness were found among different hydrogel formulations after reaching steady-state. Hybrid hydrogels featuring cell-adhesiveness were fabricated and tested as matrices for culture of hMSCs. A high cell viability (>83%) at day 1 post-encapsulation demonstrated the good cytocompatibility of the hydrogels. On day 3 and day 5, overall cell viability decreased for all hydrogel compositions. But remarkably, the increase of fraction of dynamic crosslinks in the matrix significantly improved cell viability at all timepoints. These results highlight the importance of tunable network viscoelasticity on cell survival in matrices that do not have enzymatically degradable mechanis

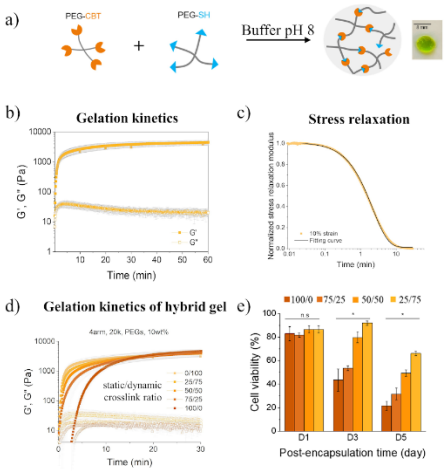

Figure 1. a) Dynamic hydrogel design. b) Gelation rate and c) stress relaxation profile of the dynamic hydrogel. d) Gelation kinetics of static/dynamic hybrid hydrogels, at different bond ratios. e) Cell viability of hMSCs after 1, 3 and 5 days post-encapsulation.

Conclusions. This novel bioinspired dynamic covalent chemistry expands the existing toolbox for engineering matrices for cell encapsulation under physiological conditions. This hydrogel platform exhibits fast and tailorable gelation rate, adjustable mechanical strength and rapid stress relaxation. By combining static and dynamic covalent bonds, an improved hydrogel system suitable for cell culture application is developed. These stress-relaxing cell-encapsulating hydrogels are being further developed as injectable and printable formulations for applications in tissue engineering and regenerative medicine.

Reference. [1] M. Jin, G. Koçer and J. I. Paez, *ACS Applied Materials & Interfaces* **2022**, *14*, 5017-5032. [2] J. I. Paez, A. Farrukh, R. Valbuena-Mendoza, M. K. Włodarczyk-Biegun and A. del Campo, *ACS Applied Materials & Interfaces* **2020**, *12*, 8062-8072.

Oral Presentation Session 2

Tissue healing

Mimicking Burn Wound Environment *in vitro*: Eschar Fibroblasts vs Dermal Fibroblasts

Gizem Cosar Kutluoglu[1,3], Marcel Vlig[2], Anouk Elgersma[2], Bouke Boekema[2], Willeke F. Daamen[3], Claudia Doberenz[1], Dominique Manikowski[1]

[1] MedSkin Solutions Dr. Suwelack, Josef-Suwelack-Straße 2, 48727 Billerbeck, Germany
[2] Preclinical Research, Association of Dutch Burn Centres (ADBC), Beverwijk, The Netherlands
[3] Radboud university medical center, Radboud Research Institutefor Medical Innovation, Dept. of Medical BioSciences, Nijmegen, The Netherlands
Contact: gizem.cosar@medskin-suwelack.com

Introduction

Untreated large skin defects like burn wounds often heal leaving a hypertrophic scar which may be a large burden for patients. One treatment option is the application of dermal substitutes, which act as temporary scaffolds to facilitate cell attachment and vascularization (1). Full skin equivalents (FSEs) are bioengineered skin models of *in vitro* generated dermal-epidermal layers, which might provide a suitable platform for investigating neotissue formation as response to different treatment options (2). So far primary human dermal fibroblasts co-cultured with primary human keratinocytes have been used to generate FSEs. Since it has been shown that fibroblasts isolated from eschar tissue debrided from burn wounds exhibit a different gene expression profile than dermal fibroblasts isolated from healthy donors (3), we analyzed the suitability of eschar fibroblasts for FSE generation in comparison to primary dermal fibroblasts and their potential to generate *in vitro* scar-forming wound tissue model.

Materials & Methods

MatriDerm® (thickness 2 mm; MedSkin Solutions Dr. Suwelack AG, Billerbeck, Germany) was used as a scaffold for FSEs. It was punched into 12 mm diameter cylinders and $2x10^5$ primary human dermal or eschar fibroblasts isolated from 3 donors (admitted to Red Cross Hospital in Beverwijk) were seeded onto the matrices in DMEM + 10 % FCS at 37°C, 5% CO_2 for 4 days. Subsequently, $1x10^5$ primary human keratinocytes isolated from normal skin were seeded on top and the models were cultured for an additional 4 days. On day 8, the FSEs were air-exposed and cultured for 23 days by refreshing the medium twice a week (2). The FSEs were cut in half and one half was used for RNA extractions and subsequent qPCR for the following targets α-smooth muscle actin (SMA), cytokeratin 10 (CK10), COL4α1, COL1α1, COL3α1 whereas the other half was embedded in paraffin, cut into 5 µm thick sections and used for immunohistochemistry staining for the following components α−SMA, CK10, COL IV, dermatan sulfate (DS).

Results

In all FSEs, fibroblasts were present within the matrix structure with a keratinocyte layer on top. In some cases, some keratinocytes were also found in the dermal equivalent. According to CK10 staining, the epidermal layer was observed to be better developed in eschar fibroblast based FSEs. However, the results were variable due to donor differences. DS staining showed that collagen was homogeneously synthesized in both eschar and dermal fibroblast based FSEs. When comparing dermal and eschar fibroblasts, eschar fibroblast based FSEs demonstrated contractile behavior by rolling up in culture, whereas dermal fibroblast based FSEs remained flat. This was in line with higher α-SMA expression in eschar fibroblast based FSEs and positive α-SMA staining, a marker of contractility, only in FSEs generated using eschar fibroblasts.

Discussion

Eschar fibroblast based FSEs may resemble the scar-forming wound tissue more closely than dermal fibroblast based FSEs, because the effect of matrix production, degradation, and contractile protein expression such as α-SMA are more closely related to those found in burn wounds (4). Related to donor differences, a thorough characterization of eschar fibroblasts prior to FSE generation might improve the donor related effects of FSE.

Conclusion

An eschar fibroblast based FSE was made that may be used as a platform to study the effect of different dermal substitutes or treatments on wound healing processes and scarring.

Acknowledgement

The SkinTERM project has received funding from the European Union's Horizon 2020 research and innovation programme under the Marie Skłodowska-Curie grant agreement No 955722.

References

1. Dill et al., Biological dermal templates with native collagen scaffolds provide guiding ridges for invading cells and may promote structured dermal wound healing. Int Wound J. 2020;17(3):618-630.
2. Mulder et al., Full Skin Equivalent Models for Simulation of Burn Wound Healing, Exploring Skin Regeneration and Cytokine Response. *Journal of Functional Biomaterials*. 2023; 14(1):29
3. Van Der Veen et al., Stem Cells in Burn Eschar. Cell Transplantation. 2012;21(5):933-942.
4. Guo et al., Identification of Key Genes in Severe Burns by Using Weighted Gene Coexpression Network Analysis. Comput Math Methods Med. 2022 Jun 28;2022:5220403.

Decellularization of extracellular matrix produced *in vitro* by primary human fetal mensenchymal cells

M. Gomes [1,2,3,4], M. Zhou [5], Z. Jiang [1], M.Vlig [3], M.L. Groot [5], E. Middelkoop [1,2,3,4], H. Niessen [1], P. Krijnen [1], B. Boekema [2,3]

[1] Department of Pathology, Amsterdam UMC (AUMC), location AMC, Amsterdam, The Netherlands
[2] Department of Plastic, Reconstructive and Hand Surgery, AUMC, location VUmc, Amsterdam, The Netherlands
[3] Association of Dutch Burn Centres, Beverwijk, Netherlands
[4] Tissue Function & Regeneration, Amsterdam Movement Sciences Research Institute, Amsterdam, The Netherlands
[5] Laserlab, Vrije Universiteit Amsterdam, Amsterdam, The Netherlands

Introduction: Unlike adult full-thickness wounds, fetal skin wounds in early development heal through tissue regeneration without scarring. To explore the role of the extracellular matrix (ECM) in the regenerative potential of mesenchymal cells (MCs), we constructed an in vitro model of fetal MCs-derived decellularized ECM (dECM).

Methods: Primary human MCs isolated from fetal skin were cultured with vitamin C for 2 weeks to stimulate ECM production. For decellularization four protocols were tested: 1) ammonium hydroxide and Triton X-100, 2) freeze-thawing, 3) disodium phosphate and NP-40, and 4) CHAPS, followed by DNase I treatment (protocols 1, 2 and 4). The decellularization efficiency and ECM integrity were analysed by picogreen assay, western blot and second/third harmonic generation microscopy (S/THGM). To minimize ECM detachment, MCs were cultured on different coatings. Adult dermal MCs were cultured in fetal dECM for 10 days. Cell adherence was verified via bright-field microscopy and cellular activity via resazurin assay.

Results: Protocol 1 led to immediate ECM detachment. dECM obtained from protocols 2, 3 and 4 showed significantly reduced DNA content compared to the non-decellularized control, while protocol 3 was significantly more effective. Type I and III collagen, and fibronectin levels were notably lower in dECM using protocol 4. dECM from protocol 2 showed a net of collagen fibers by SHGM similar to the non-decelllularized control, while fibre morphology was slightly altered in dECM from protocol 3. dECM from both protocols showed low cell content imaged by THGM, in line with DNA measurements. Poly-L-lysin coating showed the least dECM-detachment. Finally, dermal MCs cultured in dECMs showed good cell adhesion and viability.

Conclusion: Our successful fetal dECM model, with poly-L-lysin coating before ECM production and decellularization via protocols 2 or 3, enables studying MCs derived ECM's regenerative potential. Protocol 2 minimizes ECM alteration, while protocol 3 enhances decellularization efficiency, both leading to adult dermal MCs' adherence and proliferation in dECMs.

Acknowledgements: This project has received funding from the European Union's Horizon 2020 research and innovation programme under the Marie Skłodowska-Curie grant agreement No 955722.

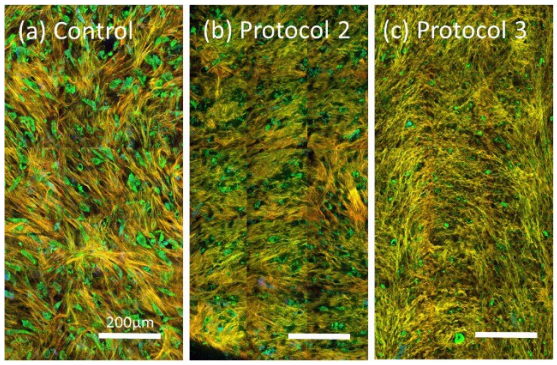

Fig. 1: Second/third harmonic generation microscopy images of fetal-MCs-derived-ECM non-decellularized (a) and decellularized (b, c).

The prenatal application of functionalized collagen scaffolds in a fetal sheep wound model induces a gene expression profile that results in enhanced skin regeneration

Merel Gansevoort[1], Corien Oostendorp[1], Linde F. Bouwman[1], Dorien M. Tiemessen[2], Paul J. Geutjes[2], Wout F.J. Feitz[2], Toin H. van Kuppevelt[1] and Willeke F. Daamen[1]
Departments of Medical Biosciences[1] and Urology[2], Radboud Research Institute for Medical Innovation, Radboud university medical center, PO Box 9101, 6500 HB Nijmegen, The Netherlands

Introduction

Spina bifida is a severe congenital birth defect where the neural tube fails to close during foetal development. Prolonged exposure of the spinal cord to amniotic fluid is detrimental to neurological development and can result in mental and physical disabilities. Inducing fast and efficient closure of the defect without scar formation may greatly improve treatment of spina bifida. Previous experiments using a foetal sheep full thickness wound model demonstrated that prenatal application of porous type I collagen scaffolds functionalized with heparin, fibroblast growth factor 2 (FGF2) and vascular endothelial growth factor (VEGF) induced superior skin regeneration postnatally [1]. Following up on these observations we investigated the early effects of these functionalized collagen scaffolds on the gene expression profile in regenerating skin.

Materials and Methods

Porous type I collagen (COL, bovine origin) scaffolds were prepared through lyophilization. Scaffolds were supplemented with heparin (HEP) and chemically crosslinked using 1-ethyl-3- (3-dimethylaminopropyl) carbodiimide (EDC) and N-hydroxy succinimide (NHS), followed by soaking in a solution of phosphate buffered saline containing FGF2 and VEGF. The resulting COL-HEP/GF scaffolds were washed to remove unbound growth factors. The scaffolds were implanted into Ø 12 mm full thickness wounds on the dorsal side of Dutch Texel breed fetuses at 79 day's gestation (term 140-147 days) [2]. Collagen scaffolds without additives (COL) and untreated wounds (UNTR) were used as controls. Two weeks post implantation the animals were sacrificed and the wound area including scaffold remnants and surrounding tissue was harvested.

Cryosections were prepared and the epidermis and dermis were collected separately using laser dissection microscopy. From each skin layer RNA was isolated, amplified and converted to cDNA. Gene expression levels were measured using the Ovine Gene 1.0 ST Array from Affymetrix. Differentially expressed genes (DEGs) between the conditions were extracted and analyzed for enriched biological processes using DAVID Bioinformatics Recourses. Additionally, DEGs were organized into protein-protein interaction networks using the analysis tool 'String' and clustered by the ClusterONE algorithm in Cytoscape to further define subtle changes in biological processes.

Results and Discussion

When comparing COL to UNTR no enriched biological processes were identified, neither in the epidermis nor dermis, by DAVID. On the other hand, comparing COL-HEP/GF to UNTR revealed various biological processes related to wound healing were enriched. In the epidermis this included the actual term 'wound healing' and in the epidermis 'angiogenesis', 'cell adhesion', and 'positive regulation of cell migration' were found, indicating that the functionalized collagen scaffolds influences the wound healing process.

Intriguingly, when comparing COL-HEP/GF to COL only two terms were found by DAVID (both in the epidermis), which were related to viral response. The COL and COL-HEP/GF-treated wounds already looked markedly different at two weeks post implantation on both the macroscopic and microscopic level. Using Cytoscape, clusters of highly-related DEGs were found in both the epidermis and dermis. Annotation of these clusters with biological processes revealed that the clustered genes were involved with a multitude of wound healing-related processes. This included the regulation of cell mass, cellular signalling and extracellular matrix organization.

Conclusions

Two weeks post wounding the COL-HEP/GF scaffolds induce a subtle gene expression profile, characterized by controlled matrix deposition and cell signalling, which may contribute to the long-term pro-regenerative effects that were seen postnatally.

Acknowledgements

This work was supported by the Radboud Institute for Molecular Life Sciences: PhD round 2020, EU-FP6 project EuroSTEC (grant agreement no. LSHB-CT-2006-037409) and EU-FP7 project EuroSkinGraft (grant agreement no. 279024).

References

1. Oostendorp, C., et al., *Sustained Postnatal Skin Regeneration Upon Prenatal Application of Functionalized Collagen Scaffolds.* Tissue Eng Part A, 2020. **27**(1-2): p. 10-25.
2. Hosper, N.A., et al., *Intra-uterine tissue engineering of full-thickness skin defects in a fetal sheep model.* Biomaterials, 2010. **31**(14): p. 3910-9.

A Novel TGF-β3-Derived Peptide Promotes Chondrogenesis *in vitro* and *in vivo*

Mingjing Zhu[1,2], Siqing Jiang[2], Xingyang Li[2], Wenchao Zhong[2,3,4], Wei Cao[2], Antong Wu[2,5], Gang Wu[1], Qingbin Zhang[2]

1. Department of Oral Cell Biology, Academic Centre for Dentistry Amsterdam (ACTA), University of Amsterdam and Vrije Universiteit Amsterdam, Amsterdam Movement Sciences, Amsterdam, The Netherlands.
2. Department of Temporomandibular Joint, Affiliated Stomatology Hospital of Guangzhou Medical University, Guangdong Engineering Research Center of Oral Restoration and Reconstruction, Guangzhou Key Laboratory of Basic and Applied Research of Oral Regenerative Medicine, Guangzhou, Guangdong 510182, China
3. Department of Human Genetics, Amsterdam UMC Location Vrije Universiteit Amsterdam, Amsterdam, The Netherlands
4. Department of Clinical Chemistry, Amsterdam UMC Location Vrije Universiteit Amsterdam, Amsterdam, The Netherlands
5. Laboratory for Myology, Department of Human Movement Sciences, Vrije Universiteit Amsterdam, Amsterdam Movement Sciences, Amsterdam, The Netherlands

Introduction:

The repair of large cartilage defects remains highly challenging in the fields of orthopedics and oral and maxillofacial surgery, due to lack of chondro-inductive factors present in the damaged chondrogenic microenvironment. One viable approach is to apply chondro-inductive growth factors, such as bone morphogenetic protein-2 (BMP-2) and transforming growth factor-β3 (TGF-β3). However, their use is associated with various limitations, such as low production yield, high cost, and potential immunogenicity. To provide a viable alternative, in this study, we aimed to develop a novel chondro-inductive peptide and functionalized hydrogel, and hypothesized that as a chondro-inductive peptide derived from TGF-β3, this novel chondro-inductive peptide would induce chondrogenic differentiation of mouse bone marrow stem cells (BMSCs) and repair critical-size articular cartilage defect more effectively than TGF-β3.

Materials and Methods:

We analyzed the crystallographic data of the critical binding domain of TGF-β3 with its type II receptor and designed 10 TGF-β3-derived peptides (TPs). We tested the ability to form cartilage of all 10 TPs adsorbed onto collagen sponges transplanted intramuscular in rats. Thereafter, we analyzed the efficacy of TP number 8 (TP8) in inducing *in-vitro* chondrogenesis of mouse BMSCs grown in a micromass. We also explored the molecular mechanisms for the chondro-inductivity of TP8 using western blot and RNA sequencing. Finally, we evaluated the *in-vivo* efficacy of TP8-functionalized gelatin-methacryloyl (Gel-MA) hydrogels to repair critical-size cartilage defects in rabbit medial femoral condyles, using a histological scoring system for evaluation of the repair of full-thickness articular cartilage defects. All data are presented as mean ± SD. All the experiments were performed at least 3 times. Comparisons between groups were made by one-way ANOVA. Post hoc comparisons were made using Bonferroni corrections. The level of significance was set at $p < 0.05$.

Results and Discussion:

We found that TP8, adsorbed onto absorbable collagen sponge, potently induced *de novo* cartilage formation. TP4 stimulated bone formation, while the other TPs were ineffective. TP8 (500 ng/ml) induced a significantly higher area of glycosaminoglycans (GAGs) and proteoglycans (PGs) in the micromass than every other TP, comparable to BMP-2 (500 ng/ml) and TGF-β3 (10 ng/ml). TP8 significantly upregulated the amount of phosphorylated Smad1/5 over total Smad 1/5 in mouse BMSCs by 1.5 -fold. TP8 upregulated 356 mRNAs and downregulated the expression of 104 mRNAs in micromasses of mouse BMSCs in comparison with the untreated BMSCs. Through bioinformatic analysis, we found that TP8 upregulates genes related to cartilage development and regulation, and connective tissue development, such as those involved in TGF-β3 signaling. We found that the expression of low-density lipoprotein receptor (LDLR) -related protein-1 (Lrp1) in the TP8 group was significantly higher than in the control group, and that knockdown of Lrp1 downregulated the expression of chondrogenic-related genes and proteins (Sox9), and inhibited the TP8-induced chondrogenic differentiation of mouse BMSCs. In cartilage defects in rabbits *in vivo*, the ICRS macroscopic scores of the TGF-β3- functionalized Gel-MA hydrogels group and the TP8- functionalized Gel-MA hydrogels group were higher than unfunctionalized ones at 4 weeks (by 1.63-fold and 1.94-fold respectively). TP8 induced the highest score among all groups, which was 1.13-fold higher than TGF-β3, and almost identical to the score reached for normal cartilage.

Conclusions / Summary:

We developed a novel, bioactive, TGF-β3-derived chondro-inductive peptide. TP8 promotes BMSC chondrogenesis *in vitro*. TP8- functionalized GelMA hydrogels induce chondrogenesis and enhance the repair of critical-size cartilage defects in rabbit medial femoral condyles *in vivo*. We thus confirm that TP8, as a chondro-inductive peptide derived from TGF-β3, induces chondrogenic differentiation of BMSCs and stimulates repair critical-size articular cartilage defect, superior to that induced by TGF-β3.

Development of a Biodegradable Porous Hybrid Material to be used as a Patch for Diaphragmatic Hernia Closure

Lieke H.A. van Dommelen[1], Bas van Bochove[2], Luc Vossen[1], Elly M.M. Versteeg[1], Marc J.K Ankoné[2], Dirk W. Grijpma[2], Toin H. van Kuppevelt[1], André A. Poot[2], Willeke F. Daamen[1]

[1]Radboud university medical center, Radboud Research Institute for Medical Innovation, Dept. of Medical BioSciences, Nijmegen, the Netherlands

[2]University of Twente, Dept. of Advanced Organ Bioengineering and Therapeutics, Enschede, the Netherlands

Introduction

Congenital diaphragmatic hernia is a rare but life-threatening condition. It is characterized by one or more defects in the diaphragm, which is the primary skeletal muscle involved in respiration. After birth, large diaphragmatic hernias need patch repair. Currently used patches do not have the required mechanical properties, biodegradability, nor cellular ingrowth characteristics to result in a functional diaphragm for the new-born.[1] We therefore aimed to develop a hybrid patch material from collagen and a slowly degradable polymer. Collagen is biocompatible and biodegradable but largely lacks the required mechanical properties.[2] Biodegradable synthetic polymers may have the necessary mechanical properties, but generally fall short in biointegration.[3] We investigated the production of a porous photo-crosslinked hybrid material, based on collagen and tough poly(trimethylene carbonate) (PTMC).

Materials and Methods

Insoluble type I collagen was functionalised using glycidyl methacrylate (ColMA) and three-armed PTMC using methacrylic anhydride (PTMC-tMA). ColMA was suspended and PTMC-tMA was dissolved in acidified dimethyl sulfoxide. The two components were combined in the weight ratios 3:15 and 3:5 or used separately as controls. Suspensions and solutions were frozen and UV-crosslinked, extracted, and lyophilized. Patch coherency, macroscopic appearance and handleability were investigated. Patch structure was assessed using scanning electron and light microscopy.

Results

Coherent ColMA, PTMC-tMA and ColMA/PTMC-tMA hybrid patches at weight ratios 3:15 and 3:5 were obtained after photo-crosslinking. Patches could be handled without macroscopical morphology changes. ColMA patches were more brittle than PTMC-tMA and hybrids. Hybrids were more rigid than PTMC-tMA or ColMA alone. Scanning electron micrographs revealed a porous structure with large areas where the two components could not be distinguished from each other. Light microscopy (H&E staining) indicated a distribution of collagen throughout the entire hybrid patch.

Conclusions

Porous ColMA/PTMC-tMA hybrid materials were produced for eventual use in congenital diaphragmatic hernia closure.

Future prospects

The produced porous ColMA/PTMC-tMA hybrid materials is further characterized, and the *in vitro* response is being investigated using primary human skeletal muscle myoblasts.

Acknowledgements

This study was funded by the Dutch Research Council (NWO), project number 17562 (DIAPATCH).

References

1. Haroon J, *et al.*, Clin Pediatr. 2013;52(2):115-24.
2. Brouwer KM, *et al.*, J Biomed Mater Res B Appl Biomater. 2014;102(4):756-63.
3. Rongen JJ, *et al.*, J Biomed Mater Res A. 2016;104(11):2823-32.

Preparation of specific elastin hydrolysates and their *in vitro* evaluation during ECM deposition

Roman Krymchenko[1], Nancy Avila-Martinez[1], Bouke Boekema[2], Marcel Vlig[2], Elly M.M. Versteeg[1], Toin H. van Kuppevelt[1], Willeke F. Daamen[1]
[1]Radboud university medical center, Radboud Research Institute for Medical Innovation, Department of Medical BioSciences, Nijmegen, The Netherlands
[2]Association of Dutch Burn Centers, Beverwijk, The Netherlands
Contact: Roman.Krymchenko@radboudumc.nl

Introduction

Elastin is a fibrous extracellular matrix protein involved in tissue elasticity and resilience. After severe skin wounding, elastin synthesis is insufficient during the healing process and usually results in disorganized deposition which does not lead to functional tissue regeneration.[1] Degradation products of elastin direct wound healing by influencing cell growth, migration, proliferation and cellular signalling.[2] Importantly, the presence of elastin and elastin degradation products suppresses the differentiation of fibroblasts into myofibroblasts, modulates elastin expression, fibroblast and keratinocyte migration and angiogenesis.[2] Elastin-based biomaterials may provide a platform for the development of biomimetic wound management therapies that are clinically and economically effective.[3]
In this study, insoluble elastin was purified from pulverized equine *ligamentum nuchae*. Solubilization of elastin fibres was performed in four ways: by oxalic acid (OxA-ELN; stepwise or continuous solubilisation), by potassium hydroxide (KOH-ELN) or by digestion with elastase (Enz-ELN). Biological activity was assessed using fibroblasts using RT-qPCR and Western blotting.

Materials and methods

Purified insoluble elastin was obtained from pulverized equine *ligamentum nuchae*. Acidic hydrolysis was performed in aqueous oxalic acid solution at 95°C with collection of the supernatant after each incubation hour for 12 consecutive hours. For continuous acidic solubilization, without intervening collection of supernatants, 9 hours were needed. Alkaline hydrolysis was done with KOH in 80% EtOH. For enzymatic digestion, elastase from porcine pancreas was used. Solubilized elastin preparations were neutralized, concentrated, and analysed with sodium dodecyl sulfate polyacrylamide gel electrophoresis, Lowry protein assay, 2,4,6-trinitrobenzene sulfonic acid (TNBS) assay and size exclusion chromatography.
Pilot *in vitro* experiments were conducted on primary human dermal fibroblasts (hdFB) and human foetal lung fibroblast cell line (HFL-1), while extracellular matrix (ECM) deposition was stimulated with sodium ascorbate or with a combination of sodium ascorbate and macromolecular crowders. A concentration of 30 µg/ml of each elastin preparations was tested.

Results

SDS-PAGE showed that all preparations formed smears from the beginning of the stacking gel and possessed proteins with different molecular weights. While patterns for OxA-ELN and KOH-ELN were similar, Enz-ELN differed and indicated the presence of lower molecular weight protein.
Size exclusion performed on fast protein liquid chromatography confirmed that the largest molecular weight of soluble elastin was obtained via fractionated oxalic acid hydrolysis, while enzymatic digestion resulted in the peptides with the smallest molecular weights. Analysis of the number of primary amine groups showed highest values for the enzymatic digest, corresponding to the smallest fragments. Fractions showed homogeneity on basis of molecular mass and concentration both theoretically calculated and practically measured.
When HFL-1 cells were stimulated with sodium ascorbate, only KOH-ELN slightly reduced type I collagen deposition on protein level, while all other elastin preparations did not change collagen abundance. However, increased αSMA expression was seen on both gene and protein levels for all tested elastin preparations.
Primary skin fibroblasts stimulated with sodium ascorbate and PVP-40 as a macromolecular crowder showed that collagen deposition was diminished by all preparations except stepwise OxA-ELN, while the biggest impact was seen with KOH-ELN. αSMA expression was not different with qPCR analysis, but protein expression was undetectable for these cells.

Conclusions

Insoluble elastin fibres were solubilized using acidic, alkaline and enzymatic methods. Pilot studies for *in vitro* evaluation of solubilised elastin preparations revealed different behaviour on primary skin fibroblasts and a pulmonary fibroblast cell line. Further experiments are needed for a definite conclusion on myofibroblasts differentiation and their effect during ECM deposition.

Acknowledgements

The SkinTERM project received funding from the European Union's Horizon 2020 research and innovation programme under the Marie Skłodowska-Curie grant agreement No 955722.

References

1. Almine *et al. Birth Defects Res C Embryo Today* **2012**. *96;*3:248-257
2. Daamen *et al. Tissue Eng Part A* **2008**. *14*;3: 349-360.
3. Sarangthem *et al. Adv Wound Care (New Rochelle)* **2021**. *10*:5:257-269.

Oral Presentation Session 3

Nano- and micromaterial technologies

Self-feeding living tissues via nutritional nanoparticles enables long-term stem cell functionality under anoxia

M. Gurian*, N.G.A. Willemen*, I.R. Porsul, S. Jeong, M.C. Kruyt, S.R. Shin, and J. Leijten
Department of Developmental BioEngineering, Faculty of Science and Technology, Technical Medical Centre, University Twente, Drienerlolaan 5, 7522NB Enschede, The Netherlands. Contact: m.gurian@utwente.nl

Introduction:

The creation of tissue engineered constructs offers a promising strategy to replace, restore, and/or regenerate damaged tissue and/or organs. Unfortunately, producing viable tissue engineered constructs is limited to small tissues sizes, which precludes many clinical applications. Increasing tissue size associates with progressively severe oxygen and nutrient diffusion limitations that lead to cellular necrosis and ultimately implant failure. Scaling up engineered tissues towards clinically relevant sizes thus represents a major unresolved challenge in tissue engineering.
Recent approaches to address this issue involve in situ metabolic support continuously providing either oxygen or nutrients throughout the engineered tissues. Although these methods have previously shown promise, they remain limited in their clinical translation due to their dependency on xenogenic enzymes. Xenogenic enzymes are prone to illicit an immunogenic response while rapidly losing efficiency within the host organism due to a myriad of factors (e.g. temperature, pH, etc), limiting their use in clinically sized tissues. Here, we report on the innovative use of glycogen, a naturally occurring nutritional nanoparticle found within mammalian cells that reversibly stores glucose. Surprisingly, we show that human cells (e.g., mesenchymal stem cells; hMSC) can metabolize extracellular glycogen by secreting enzymes, which offers metabolic support for clinically relevant time periods.

Materials and Methods:

Cell culture and metabolic support: hMSC were cultured within nutrient-free DMEM containing 1% Pen/Strep and one specific metabolite type. Viability and metabolic activity were assessed using a live/dead stain and PrestoBlue, respectively. The expression of several pro-angiogenic factors was measured using a customized Illuminex assay. Release of cell-mediated glycogen-degrading enzymes was measured using ELISA.
Glycogen-loaded core shell production: Core-shell precursor droplets composed of glycogen, dextran-tyramine, and horseradish peroxidase in phosphate-buffered saline were emulsified in surfactant-containing oil using a microfluidic droplet generator, and subsequently crosslinked via supplementation with H_2O_2. Glycogen-loaded core shells were consecutively used in 2D cell culture and encapsulated within collagen hydrogels to maintain hMSC viability and metabolic activity.

Results:

Extracellular glycogen nanoparticles were demonstrated to offer the first of its kind self-feeding metabolic support system that is facilitated by cell mediated secretion of glycogen degrading enzymes. This allowed for glucose release in a cell-concentration dependent manner that was sufficient to maintain cell viability and metabolic activity of hMSC for clinically relevant time periods in anoxia. Protein and gene analysis also showed that glycogen enhanced the pro-angiogenic potential of hMSC in anoxia, leading to increased endothelial cell tube formation.
The natural size of glycogen nanoparticles allowed for their encapsulation and retention within core-shell microgels. This offered prolonged glycogen availability within engineered tissues, while providing sufficient metabolic support to maintain hMSC viability and functionality in anoxia.

Conclusion:

In this work, we established extracellular glycogen as the first of its kind self-feeding metabolism support system that maintains cell functionality for clinically relevant time periods. Additionally, the glycogen nanoparticles are retained by small porous hydrogels offering easy incorporation into a wide range of commonly used hydrogels highlighting the versatile potential for various clinical applications.

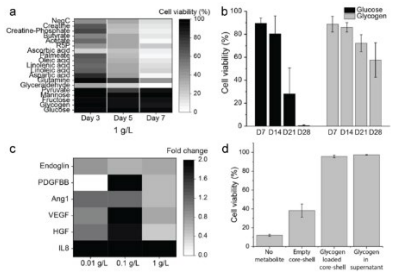

Figure 1: *a) Sugars, glycogen in particular, maintain hMSC viability and metabolic activity in anoxia the best. b) Long-term viability of hMSC when exposed to either 1 g/L glucose or glycogen. c) Pro-angiogenic factor secretion of hMSCs after 7 days in anoxia in chemically defined medium containing only glycogen. d) Effect of glycogen-loaded core-shell microparticles on hMSC viability.*

References:

[1] N. Willemen *et al*., Trends in Biotech., 39 (11), 2021, 10.1016/j.tibtech.2021.01.007
[2] M. Zargarzadeh *et al*., Materials Horizons, 9 (2), (2022), 10.1039/D0MH01982H
[3] N. Willemen *et al.,* Adv. Healthc. Mater., 11 (13), 2022, 10.1002/adhm.202102697

The media composition influences LNPs internalization by Nucleus Pulposus Cells

A. Varela-Moreira[1], C. Voskamp[1], D. Corraini[1], R. M. Schiffelers[2], M.A Tryfonidou[1]

1 Regenerative Orthopaedics, dept. of Clinical Sciences, Faculty of Veterinary Medicine, Utrecht University, The Netherlands
2 CDL Research, University Medical Center Utrecht, The Netherlands

Introduction

Low back pain is the number one cause of years lived in disability since the 90s. The degeneration of the intervertebral disc (IVD) is a common cause of low back pain. Degeneration of the disc starts within its core, the nucleus pulposus (NP). We are developing an injectable cell-free mRNA-based therapeutic approach using Lipid Nanoparticles (LNPs) for mild to moderate disc degeneration. LNPs are the state-of-the art delivery system for nucleic acids. In the degenerate disc, the decrease in tissue osmolarity and pH together with the presence of pro-inflammatory mediators exert catabolic effects. This affects NP cell pathophysiology but may also modulate LNP uptake and RNA translation. In this study we aim to assess the effect of different relevant media compositions for the disc environment (protein content, pH and osmolarity) on the internalization of LNPs in dog NP cells.

Materials and Methods

LNPs were prepared by microfluidic mixing using the NanoAssemblr Benchtop. An ethanol phase of lipids was mixed with an acidic mRNA aqueous phase leading to the formation of the LNPs. LNPs were prepared at a flow rate ratio (aqueous: organic) of 3:1 and a total flow rate of 9 mL/min. LNPs were composed of ionizable lipid, cholesterol, DSPC, PEG_{2000}-DMG at a molar ratio of 50/38.5/10/1.5, respectively. Four different ionizable lipids were used to prepare LNPs, namely DLin-MC3-DMA, C12-200, ALC-0315 and SM-102. To prepare fluorescently labeled LNPs, 0.2 mol% of Cy5.5-PE was added to the lipid mix. Cy5.5-LNPs were prepared at a final total lipid concentration of 2.5 mM. mRNA was encapsulated at a 10:1 wt/wt ratio between ionizable lipid and mRNA. After preparation, LNPs were dialyzed against an excess of TBS (20 mM Tris, 0.9% NaCl pH 7.4) with Slide-A-Lyzer™ G3 Dialysis Cassettes, 20K MWCO, for at least 16h. After dialysis, Cy5.5-LNPs were stored at 4°C and used up to one month. The hydrodynamic diameter of LNPs was measured by Dynamic Light Scattering and the Zeta Potential of LNPs was determined with Zetasizer Nano. Primary dog NP cells (P1) were thawed and expanded in high glucose DMEM supplemented with 10% FCS, 1% P/S, 0.1 mM Ascorbic Acid and 0.5% Fungizone. For internalization studies, cells were seeded in 96 well plates. Next day, culture media was removed, and cells were washed once with FCS-free media. To assess the effect of serum proteins on LNPs internalization, Cy5.5-LNPs were diluted in FCS-free or FCS-rich media from which 100 µL were added to each well and incubated at 37°C with 5% O_2 for 1h, 2h and 4h. To assess the effect of a pro-degenerate environment after 4 hrs of culture, culture media with different osmolarity and pH were prepared to mimic a healthy (450 mOsm/L, pH 7.1) and a pro-degenerate (350 mOsm/L, pH 6.8) IVD milieu. After each time point, cells were transferred to a U-bottom 96 well plate, washed with PBS and fixed with 4% PFA before analysis by Flow Cytometry.

Results and Discussion

LNPs showed an average diameter of 60-80 nm with PdI of 0.05-0.2 for all the formulations prepared (n=5 per formulation). The low PdI < 0.3 indicates the LNPs are monodisperse. The surface charge of the LNPs was neutral with Zeta Potential values between 0 and -5 mV. The effect of serum on LNPs internalization was assessed by adding LNPs to cells with FCS-free or -rich media. After 1h, ~80% of the cells in FCS-rich media internalized LNPs, while only ~5% of the cells in FCS-free media internalized LNPs. In FCS-free media the internalization increased up to 50% after 4h while in FCS-rich media almost 100% of the cells were positive for Cy5.5 at the same timepoint. This indicates that proteins present in the serum adsorb to the LNP surface and mediate a faster and receptor-mediated internalization of the nanoparticles. These results are in line with what is reported for the Onpattro formulation. Upon systemic administration, Apolipoprotein E absorb to the surface of Onpattro that are subsequently internalized via the Low Density Lipoprotein receptor at the surface of hepatocytes. The IVD is an avascular tissue rich in extracellular matrix but also proteins. Apolipoprotein E is upregulated in aged human discs, indicating that the same internalization mechanism can take place in the IVD. The incubation of cells in a pro-degenerate environment (350 mOsm/L, pH 6.8) led to a 2- to 10-fold increase in LNP internalization when compared to a healthy environment (450 mOsm/L, pH 7.1). The low pH (pH 6.8) might induce changes in the LNPs structure that increase their uptake. Higher internalization of extracellular vesicles by cancer cells in acidic environment compared to a buffered one was previously reported.

Conclusion/Summary

In this study we assessed the effect of different media composition on the internalization of LNPs by dog NP cells derived from mild degenerate discs. We observed that serum proteins increase the cell uptake of LNPs. Additionally, a pro-degenerate environment increases the uptake of LNPs when compared to a healthy disc environment. These results will enable us to fine tune the culture conditions to assess protein translation in further experiments while mimicking the degenerate disc environment.

Funding
This work is part of the project NC-CHOICE of the research programme VICI which is (partly) financed by the Dutch Research Council (NWO).

Contact guidance triggers fibroblast activation

M.D'Urso[1,2], I. Jorba[1,2,3], A.v.d.Pol[1,2], C.v.C. Bouten[1,2], N.A. Kurniawan[1,2]

1 Department of Biomedical Engineering, Eindhoven University of Technology, Eindhoven, The Netherlands
2 Institute for Complex Molecular Systems, Eindhoven University of Technology, Eindhoven, The Netherlands
3 Unitat de Biofísica i Bioenginyeria, Facultat de Medicina i Ciències de la Salut, Universitat de Barcelona, 08036 Barcelona, Spain

Fibroblasts play a key role in maintaining the balance of tissues by releasing extracellular matrix components. They have a spindle-shaped appearance and a lower migration ability. When tissues are under stress and inflammation occurs, cytokines and growth factors increase in the wound area. One of the most investigated activation factors is TGF-β1–3, which triggers the activation of fibroblasts and promotes their migration towards the wound site. When activated fibroblasts reach the site, they undergo a transition in phenotype, becoming myofibroblasts with contractile properties due to the incorporation of αSMA into their cytoskeleton.

At the cellular level, cells respond to various environmental cues, such as ligand distribution, by sensing them through adhesion events that alter the cytoskeleton, leading to different cell phenotypes characterized by different morphotypes. However, the transduction of signals from environmental cues to cellular responses is still not fully understood.
Our project aimed to study the behaviour of fibroblast phenotypes by controlling their physical and mechanical environments effectively. We utilized LIMAP technique to achieve spatial control of adhesion contact regions using contact guiance substrates. Additionally, we developed a quantitative, automated morphometric analysis of cell images on these micropatterned substrates and correlated the morphotype with fibroblast phenotypes. We have detected that morphometric parameters such as cell area and FAs eccentricity were higher when cells were activated biochemically and mechanically. The off-nuclei mechanical measurements confirmed that activated fibroblasts showed similar behaviour to the fibroblasts cultured on 2D micropatterns with respect to the one treated with growth factors.

This approach provides deeper insights into the involvement of mechanosensing and focal adhesion morphology in correlating morphotype and phenotype in fibroblast phenotype transition relevant for restoring tissue homeostasis when in a pathological state.

1. Walker, M., Godin, M. & Pelling, A. E. Mechanical stretch sustains myofibroblast phenotype and function in microtissues through latent TGF-β1 activation. Integrative Biology 12, 199–210 (2020).
2. Sagara, H. et al. Activation of TGF-β/Smad2 signaling is associated with airway remodeling in asthma. Journal of Allergy and Clinical Immunology 110, 249–254 (2002).
3. Humeres, C. et al. Smad7 effects on TGF-β and ErbB2 restrain myofibroblast activation and protect from postinfarction heart failure. J Clin Invest 132, (2022)

Modulating microscale mechanics of single cell microenvironment via cell tethering in single cell microgels to guide stem cell function

Castro Johnbosco, Tom Kamperman, Jeroen Leijten

Leijten Laboratory, Department of Developmental Bioengineering, TechMed Centre, University of Twente, The Netherlands

Introduction

Mechanobiological insights are widely studied as they contribute to the guiding of (stem) cell function and fate. Current studies investigate such mechanisms using engineered artificial matrices that are defined by their macro-level mechanical property. Yet, cells inside any matrix can only detect properties at the nano and micro scale. Moreover, heterogeneity in cell populations yields mixed insights into how mechanotransduction affects overall stem cell function and obscures our understanding of subsequent downstream biophysical behavior. Thus, to precisely understand how heterogeneous stem cell populations sense and transduce their microscale mechanics, we developed single cell artificial niches (SCANs), which are composed of an individual cell coated in a few micron thick hydrogel layer that is tethered directly to a cell membrane [1][2]. We tuned the biophysical properties (e.g., hydrogel stiffness) of SCANs to determine how such cues influence stem cell function in 3D environments at single cell resolution.

Materials and Methods

Dextran conjugated with tyramine moieties (Dex-TA, 15% DS) containing mesenchymal stromal cells (MSCs) using a microfluidic chip, allowed for the creation of micrometer-sized microgels containing a single cell. Stem cell-laden microgels of distinct mechanical properties (soft: ~10kPa and stiff: ~40kPa SCANs) using different crosslinker concentrations were stimulated to commit to the chondrogenic lineage. The differentiation process was mapped at distinct time points using nanoindentation, immunohistochemistry, and holotomography to determine protein expression levels and biophysical alterations like cell volume, macromolecular crowding, and histone methylation.

Results and Discussion

The soft and stiff SCANs were analyzed for the increase in the microscale mechanical property as a measure of protein deposition. Cell tethering was confirmed using phenolic oxidative coupling of naturally available tyrosines on the cell membrane and tyramine present in the polymer material used to produce cell tethering SCANs. Immunofluorescence images revealed soft matrices favor stem cells towards chondrogenesis rather than stiff microenvironment. However, mechanotransduction in stem cell differentiation was independent of matrix binding cues and the YAP-TAZ mechanotransduction pathway. Moreover, alterations were observed in cytoplasmic and nuclear volume as a result of macromolecular crowding and histone methylation among soft and stiff SCANs which potentially influence cell fate decisions. Overall, biophysical alterations inside a cell are highly dictated by the immediate pericellular environment, which leads to altered programming of stem cell function.

Conclusion

SCANs represent a novel platform that could provide the opportunity to precisely tune microscale mechanics for each cell of a stem cell population. Moreover, we can better mimic cell-matrix interaction using tethering to direct mechanotransduction all at single-cell resolution.

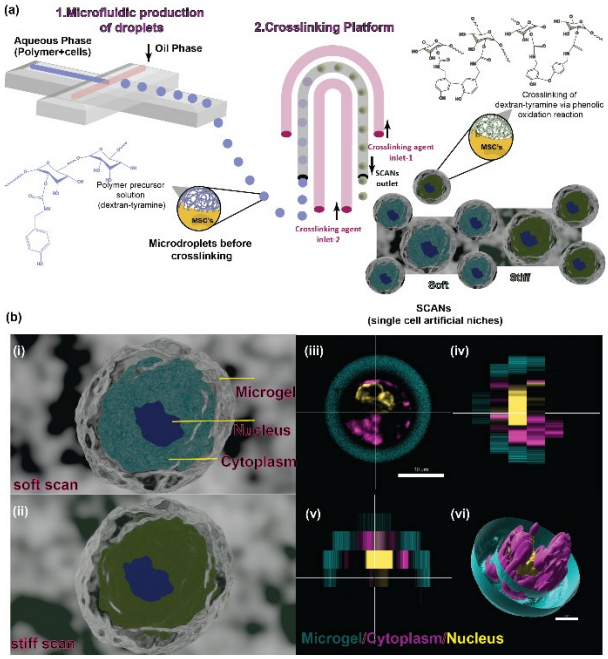

Figure 1: (a) Scalable production of SCANs using a flow-focusing microfluidic device, (b) SCANs influence cell function soft (i), stiff (ii), centered cell in a SCAN (iii), cross-sectional views of centered cells (iv-v), the 3D reconstructed image of the microgel, cytoplasm and nucleus (vi).

References

Kamperman, T., et al., Advanced Materials, 2021. **33**(42): p. 2102660.

Mao, A.S., et al.,. Nature Materials, 2017. **16**(2): p. 236-243.

Acknowledgments

This work was funded by (NWO, Vidi Grant, #17522).

Poking inside the cell: Using surface topographies to control Golgi morphology

J. Verbakel, R. S. Polishchuk, A. Khodjakov, and J. de Boer
Eindhoven University of Technology, Department of Biomedical Engineering and Institute for Complex Molecular Systems, Eindhoven, The Netherlands
2 Telethon Institute of Genetics and Medicine, Pozzuoli, Italy
3 Wadsworth Center, New York State Department of Health, New York, USA

Background. Surface topographical cues provide cells with signals to maintain or change their physiology and play therefore an essential role in controlling cell phenotype. Mechanosensitive signaling pathways influenced by these surface structures control expression of genes involved in differentiation, proliferation and metabolism. Evidence for the significant role of the Golgi apparatus (GA) in the regulation of these higher order cellular processes has been emerging and the precise structural organization of the GA has shown to be relevant to the regulation of these processes. Organization and localization of the Golgi mini-stacks varies among different organisms, cell types and physiological conditions. Since structure and morphology is relevant for functional Golgi capacity, we hypothesize that Golgi morphology and thus function can be directed by making use of biomaterial properties, in particular surface topographies. Current models suggest that the assembly of the characteristic Golgi ribbon is both an actin and microtubule dependent process. In addition to inducing morphological and functional changes on a cellular and organelle (nuclear) level, previously observed active remodeling of the microtubule and actin network indicates the potential of topography-aided control of Golgi dynamics.

Experimental design. Mesenchymal stem cells (MSCs) were cultured on flat control surfaces and seven polystyrene topographies that span the phenotypic space to assess whether cellular confinement induces structural changes in Golgi morphology. In order to examine the contribution of actin and microtubule filaments in these morphological changes, MSCs were exposed to small molecules inducing actin (Cytochalasin D) and microtubule (nocodazole) depolymerization, or stabilization of actin filaments (jasplakinolide) and microtubules (paclitaxel). Transcriptome analysis was performed in order to identify topography-induced changes in gene expression profiles.

Results. Contrary to the distinct continues Golgi ribbon structure consisting of multiple interconnected Golgi stacks and surrounding vesicles and tubule in MSCs cultured on flat surfaces, physical confinement induced by unique surface topographies results in differential reorganization of the Golgi architecture. Spatial reorganization and increased ribbon surface density was consistently evident on all topographies. In addition, variable compaction of the Golgi complex and collapse of the characteristic ribbon structure could be observed. These differences are accompanied by differential organization of the actin cytoskeleton and microtubule network. Transverse arcs and dorsal stress fibers can be observed in MSCs on flat surface, whereas long, thick ventral stress fibers are formed when cells settle between the confining topographies. Contrary to the characteristic linear bundles of antiparallel microtubule organization on flat surfaces, microtubule bundles re-orient and align parallel along the grooves between topographical features in case of topographically enhanced surfaces. In order to classify established signaling pathways in which topography-induced differentially expressed genes were predominantly involved, pathway over-representation analysis was performed. Significantly overrepresented signalling pathways primarily involved protein trafficking and post-translational protein modification, irrespective of the topographical feature design.

Conclusion. Whereas topography-induced changes in Golgi morphology and Golgi-related gene expression profiles can be observed, identifying the functional effects on Golgi activity is challenging due to technical limitations of known functional assays.

J. Verbakel (J.verbakel@tue.nl)
R. S. Polishchuk (polish@tigem.it)
A. Khodjakov (alexey.khodjakov@health.ny.gov)
J. De Boer (j.d.boer@tue.nl)

Exploring Microgel Technology for High-Throughput Formation of Osteoclasts

J.F.A. Husch[1,2], N.M. Araújo-Gomes[1], N.G.A. Willemen[1], J.C.H. Leijten[1], J.J.J.P. van den Beucken[2]
[1]Leijten Laboratory, Developmental BioEngineering, University of Twente, Drienerlolaan 5, 7522NB Enschede, [2]Regenerative Biomaterials, Dentistry, Radboudumc, Philips van Leydenlaan 25, 6525EX Nijmegen, The Netherlands

Introduction: Osteoclasts are multinuclear cells of hematopoietic origin responsible for bone resorption (1). Due to their crucial role in bone homeostasis and pathologies, osteoclasts are investigated in multiple research areas relating to bone health and disease (2). However, in vitro research on osteoclasts remans challenging due to the intrinsic heterogeneity of the cultures (3). Consequently, there is a need for establishing pure osteoclast cultures. Here, we investigate whether encapsulation of osteoclast precursors in microfluidically generated hollow microgels composed of a tyramine-conjugated dextran shell (4) could facilitate cell aggregate formation and subsequent cell fusion thus forming a single osteoclast with predetermined number of nuclei per microgel. Due to the sacrificial nature of the microgel, generated osteoclasts can be released to obtain pure osteoclast cultures.

Methodology: Primary human mononuclear cells were isolated from buffy coats and differentiated toward macrophages. Macrophages were detached and encapsulated in microgels as described previously (4). Encapsulated macrophages were differentiated toward osteoclasts for up to 29 days. During the culture period, morphology, and viability were observed using light, and fluorescence microscopy. To assess osteoclast formation with confocal microscopy, microencapsulated cells were stained for β_3 integrin as an osteoclast marker.

Results and Discussion: We successfully encapsulated primary human macrophages in 90 µm diameter microgels. Cells survived the encapsulation procedure, as was demonstrated by viability of more than 80%. Although limited aggregation of macrophages occurred, immunofluorescent staining revealed formation of a number of high quality osteoclasts within the microgels.

Conclusions: We successfully managed to differentiated encapsulated primary human macrophages toward osteoclasts. In further studies, we will investigate protocol optimization to augment cellular aggregation rates and increase production throughput to realize scalable production of high quality osteoclasts.

Acknowledgements: This study received financial support from the Twente University RadBoudumc Opportunities (TURBO) program.

References:

1. Sims NA & Gooi JH. Bone remodeling: Multiple cellular interactions required for coupling of bone formation and resorption. Semin Cell Dev Biol. 2008;19(5):444-51.
2. Henriksen K, et al. Osteoclast activity and subtypes as a function of physiology and pathology--implications for future treatments of osteoporosis. Endocr Rev. 2011;32(1):31-63.
3. Madel MB, et al. A Novel Reliable and Efficient Procedure for Purification of Mature Osteoclasts Allowing Functional Assays in Mouse Cells. Front Immunol. 2018;9:2567.
4. van Loo B, et al. Enzymatic outside-in cross-linking enables single-step microcapsule production for high-throughput three-dimensional cell microaggregate formation. Mater Today Bio. 2020;6:100047.

Oral Presentation Session 4

3D printing & additive manufacturing

3D bioprinted human renal tubulointerstitial model to study fibrosis: providing alternatives to *in vivo* models

G. Addario, S. Djudjaj, Peter Boor, L. Moroni, C. Mota*

G. Addario, L. Moroni, C. Mota
Maastricht University, MERLN Institute for Technology-Inspired Regenerative Medicine, Complex Tissue regeneration Department, 6229 ER Maastricht, The Netherlands. g.addario@maastrichtuniversity.nl;
S. Djudjaj, Peter Boor Institute of Pathology, RWTH University of Aachen, Aachen, Germany.

Introduction

Chronic kidney disease induces a gradual loss of kidney functions with fibrosis being the pathological endpoint, characterized by a remodeling of the extra-cellular matrix (ECM). Currently, murine *in vivo* models are used to study interstitial fibrosis, affecting locally the renal tubulointerstitium, through histological characterization of biopsy tissue. However, animal models are unable to completely recapitulate human diseases, hence physiologically relevant humanized 3D *in vitro* models are needed.

Materials and Methods

A protocol for the decellularization of fresh kidney pig tissue (dECM) was optimised. Primary human proximal tubular epithelial cells were bioprinted in a core-shell filament architecture, wrapped around by human primary renal fibroblasts encapsulated in dECM, mimicking the interstitium *in vitro* (Fig. 1). To study the induction and progression of fibrosis *in vitro,* cells were treated with TGF-β1 and the dECM further crosslinked with vitamin B2 (dECM+B2+TGF-β1), and compared to dECM control as healthy condition. Fibrotic genes were investigated using qPCR, together with histology and immunostaining to evaluate protein secretion, alongside with the study of the mechanical properties using a nanoindenter. Finally, perfusion was included in the model, by manufacturing an in house perfusion chamber.

Results and Discussion

Results showed an increase in Young's Modulus for the dECM+B2+TGF-β1 condition over time, alongside with an increased secretion of collagen proteins by primary cells as proven by histology and immunostaining. Multiple fibrotic genes as *ACTA-2, VIM, FIN, Col1a1, Col3a1* and *Col4a1* (Fig.2) showed a statistical significant increase for the diseased-simulated condition in comparison with control, which further increased when exposed to dynamic flow. The proposed *in vitro* model was compared to human fibrotic tissues, proving the validity of our approach, in terms of morphology and collagen deposition (Fig. 3).

Conclusion

We showed a physiologically relevant *in vitro* model to study human kidney fibrosis and its multiple factors. This offers an advanced solution that can allow researchers to investigate the effect of compounds such as TGF-β1 with more relevance. Furthermore, bioprinting can enhance the level of complexity, mimicking more closely the architecture of the native tissue. We believe our approach might be used in the future to test drugs and possible therapies for arresting, or even reversing fibrosis.

Acknowledgments

This project has received funding from the European Union's Horizon 2020 research and innovation programme under the Marie Skłodowska-Curie grant agreement No 860715.

Figures

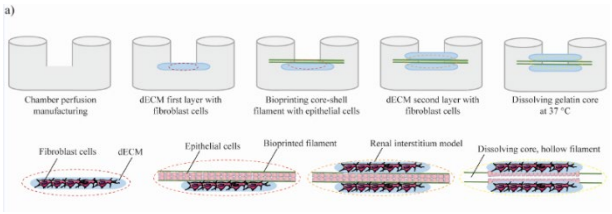

Fig.1: **Bioprinting design of the model.** Schematic of the bioprinting strategy. A core-shell filament was bioprinted between two layers of dECM-based gels. By dissolving the gelatin core, a hollow filament was produced and the perfusion chamber allowed to perfuse the entire structure, mimicking the renal interstitium *in vitro*. Image was adapted from Servier Medical Art, by Servier, licensed under a Creative Commons Attribution 3.0 unported license.

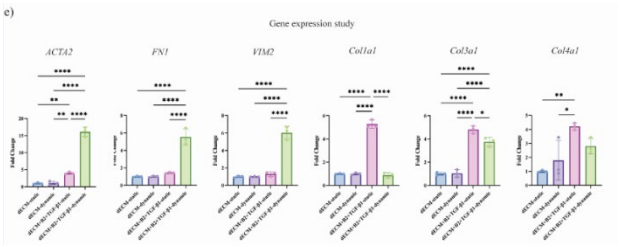

Fig.2: **Gene expression on the bioprinted model.** Gene expression study comparing dECM and dECM+B2+TGF-β1, static and dynamic states on day 14. A p value smaller than 0.05 was considered statistically significant (*p < 0.05, **p < 0.01, ***p < 0.005, ****p < 0.0001 and ns for p > 0.05). Results are shown as mean ± standard deviation.

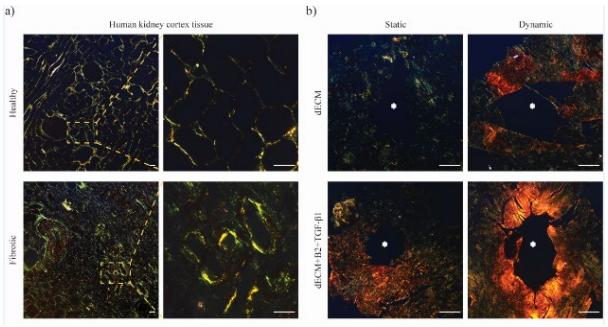

Fig.3: **Histological comparison of the model with primary tissue.** a) Human kidney cortex tissue was kindly provided by Uniklinik in Aachen, Germany. The healthy and fibrotic tissue was then stained for picrosirius red, highlighting the different morphology and collagen content. Scale bar: 50 µm; b) Cross-section of the bioprinted tubulointerstitium, with the white asterisks showing the hollow area. Collagen I is marked in yellow-orange, while collagen III in green. Scale bar: 400 µm

.

3D-printed magneto-active microfiber scaffolds for remote stimulation of skeletal muscle cells *in vitro*

G. Cedillo-Servin[1], O. Dahri[2], J. Meneses[3], J. van Duijn[1], F. Sage[2], J. Silva[3], A. Pereira[3], F.D. Magalhães[3], J. Malda[1,4], N. Geijsen[2], A.M. Pinto[3], M. Castilho[1,5]

[1] Department of Orthopedics, University Medical Center Utrecht, Utrecht, The Netherlands
[2] Department of Anatomy and Embryology, Leiden University Medical Center, Leiden, The Netherlands
[3] Department of Chemical Engineering, Faculty of Engineering, University of Porto, Porto, Portugal
[4] Department of Clinical Sciences, Faculty of Veterinary Medicine, Utrecht University, Utrecht, The Netherlands
[5] Department of Biomedical Engineering, Institute for Complex Molecular Systems, Eindhoven University of Technology, The Netherlands

Introduction: Current therapies against muscular dystrophies do not generally address losses in myotube alignment that support muscle contraction. Moreover, mechanical stimulation of injured skeletal muscle alone has been shown to facilitate functional regeneration *in vivo* [1]. Here, we hypothesized that magneto-active scaffolds with well-organized fiber architectures can guide myotube growth and remotely stimulate muscle contraction. To achieve this, melt electrowriting (MEW) —a unique technique for fabricating highly ordered microfiber scaffolds [2]— was performed from blends of polycaprolactone (PCL) and iron oxide nanoparticle (ION)-modified partially reduced graphene oxide nanoplatelets (rGNP), generating magneto-active scaffolds that support muscle cell growth.

Materials and Methods: ION-decorated rGNP (rGNP@) was obtained by *in situ* deposition in alkaline dispersion. rGNP@ was then melt-blended with medical grade PCL, yielding magneto-active composites (rGNP@ content of 2–20 wt.%). Their processing was systematically assessed based on key MEW parameters in a custom device [2]. Well-organized fiber scaffolds with hexagonal micro-structures were fabricated, and their assembly into cartesian or polar grid macrostructures was explored. The effect of rGNP@ content and MEW parameters on scaffold morphology, magnetic properties, and mechanical performance was studied. Finally, MEW PCL/rGNP@ scaffolds were embedded in cast Matrigel/type-I collagen hydrogels seeded with immortalized mouse myoblasts (C2C12 cell line). Cell viability, differentiation efficacy, and fusion were studied after 1 and 8 days in culture.

Results and Discussion: ION deposition on rGNP yielded well-dispersed rGNP@ particles with sizes above 0.5 µm and low aspect ratio (Fig. 1a). Homogeneous PCL/rGNP@ composites with very high magnetic filler content (up to 20 wt.%) were obtained by melt-blending in a solvent-free manner (Fig. 1b). MEW enabled the design of magnetic hexagonal scaffolds with tunable fiber diameter, modularity, and zonal distribution of magneto-active and nonactive material (Fig. 1c). Hexagonal scaffolds (thickness of 400 µm, pore size of 600 µm, fiber diameter of 18–22 µm) displayed elastic deformability under tension, mitigating limitations due to high filler content. External magnetic fields below 300 mT triggered out-of-plane reversible deformation and effective contraction up to 17% in scaffolds with filler content above 10 wt.% (Fig. 1d). Moreover, C2C12 cell culture on Matrigel/collagen/ MEW scaffolds showed that the presence of magnetic particles did not significantly affect viability after 8 days, compared to scaffolds lacking magnetic filler. Under static conditions, myoblasts underwent similar differentiation rates regardless of the presence of magnetic particles (Fig. 1e).

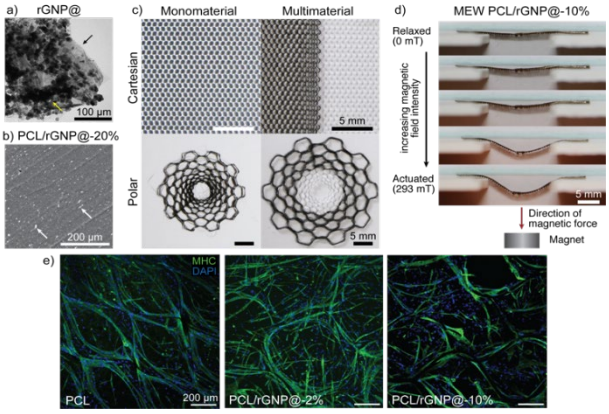

Figure 1. a) *TEM of rGNP@; rGNP (black arrow); ION (yellow arrow).* ***b)*** *SEM of PCL/rGNP@-20% filament cross-section; rGNP@ (arrows).* ***c)*** *Modular MEW scaffolds based on PCL (white) and PCL/rGNP@ (black).* ***d)*** *Deformation of PCL/rGNP@-10% scaffold under external magnetic fields.* ***e)*** *Confocal imaging of C2C12-seeded Matrigel/collagen/MEW scaffolds after 8 days of static culture. MHC (myosin heavy chain); DAPI (nuclei).*

Conclusions: We showed that highly ordered microfiber scaffolds based on PCL/rGNP@ blends can be reproducibly fabricated by MEW, allowing for controlled deposition of zonally distributed magneto-active materials with customized geometries. This enabled the design of actuating scaffolds that support skeletal cell growth and differentiation *in vitro*, as well as remotely triggered mechanical stimulation. These findings provide new perspectives for the development of consistent and scalable soft-robotic skeletal muscle microtissues *in vitro*.

References:

[1] Cezar C., *et al*. 2016. Proc. Natl. Acad. Sci.
[2] Castilho M., *et al*. 2018. Adv. Funct. Mater.

Acknowledgments: This work was funded by the NWO (024.003.013; OCENW. XS5.161), the EU's H2020 program (874827), Novo Nordisk Foundation (NNF21CC0073729), FSHD global, Singelswim Utrecht, the Portuguese FCT (LA/P/0045/2020; UIDB/00511 /2020; UIDP/00511/2020; CEECIND/03908/2017; UIDB/ 04293/2020), UT Austin/PT (UTAP-EXPL/NPN/0044/2021), and FEDER-NORTE (NORTE-01-0145-FEDER-000054).

Modelling the innervation in endometriosis: A biofabrication strategy for generating organized complex 3D *in vitro* models

A.Seijas-Gamardo[1], A. Schulten[1], Victor de la Rosa[2], Richard Hoogenboom[3], A. Romano[4], L.Moroni[1] and P. Wieringa[1]

[1]MERLN Institute, Maastricht University, The Netherlands
[2]Avroxa BV, Ghent, Belgium
[3]Supramolecular Chemistry department, Ghent University, Belgium
[4]GROW, School for Oncology and Reproduction, Maastricht University, The Netherlands

Endometriosis is a chronic condition characterized by the ectopic growth of endometrial-like tissue outside the endometrial lining. Its symptoms are very diverse, including common manifestations like inflammation and pain, and in severe cases, resulting in infertility. This condition is estimated to affect roughly 10% of women of reproductive age, although this number may fluctuate due to some individuals being asymptomatic and, consequently, undiagnosed.

Significantly, the precise etiology of endometriosis remains elusive. The disease's inherent heterogeneity, combined with a historical lack of research, has limited our understanding of the disease, having just theories regarding its origin and constraining the efficacy of available treatments. While exact cause of endometriosis is not understood, there is evidence to suggest that the extracellular matrix (ECM) at the lesion site may play a role in the development and progression of the disease. Changes in the ECM composition may influence the adhesion of endometrial cells, facilitating their implantation and growth. These changes can also contribute to their inflammatory environment and fibrosis, seen in endometriotic lesions. Moreover, they can influence nerve growth and sensitivity in the lesions area, potentially explaining the pain suffered by patients.

Additionally, hormones play a significant role in the development and progression of endometriosis. In endometriosis there is often an imbalance between estrogen and progesterone. The high levels of estrogen compared to progesterone stimulate the growth of endometriotic lesions since these are responsive to the hormonal changes.

The multifactorial and heterogeneous nature of this condition require more complex *in vitro* models that can recapitulate these key factors.

Here we present the development of a 3D *in vitro* model for the study of endometriosis using a novel sacrificial templating strategy to organize and give structure to soft hydrogel coculture systems. Using this technology, we generate a hydrogel platform that better emulates the spatial organization of different cell types and related ECM composition that are relevant for the disease. The sacrificial template is fabricated from a novel thermoresponsive polymer (OXA) that is stable at cell culture conditions, but it quickly dissolves at standard refrigerator temperatures. With this we were able to generate high resolution microchannels between two mini-wells within a hydrogel. After screening different hydrogel compositions, we found that polyacrylamide (PAM) was the best choice for generating this model based on its optimal optical properties and stability. By placing IPSC-derived nociceptive neurons in one mini-well and patient-derived endometrial organoids in another, we were able to promote axonal outgrowth and innervation of a model endometrial lesion. By adding an increasing concentration of collagen into the endometrial mini-well, we can emulate an increasingly fibrotic microenvironment around the lesion. We validate this mimetic fibrotic environment through comparison with histological samples from patients suffering from endometriosis. When culturing the organoids in this higher collagen concentration hydrogel we observed an effect in the morphology of the organoids, demonstrating an effect derived from the ECM composition. To mimic the hormonal disbalance and secretion of hormones in the lesion estrogen can also be added into the culture system. The effects of this hormonal treatment and ECM composition were assessed quantifying the proliferation, viability and gene expression of the endometrial organoids and the outgrowth of the nociceptor neurons.

The development of this *in vitro* model provides an essential tool for the endometriosis research field to put a spotlight on this long overlooked disease and to test new treatments that can alleviate the burden of the patients suffering from it.

Shrinkable Hydrogels for Resolution Enhancement in 3D (Bio)printing

D. Iudin, M. J. van Steenbergen, M. Neumann, B. G. P. van Ravensteijn, T. Vermonden
Div. Pharmaceutics, Utrecht Institute of Pharmaceutical Sciences, Utrecht University, 3584 CG, Utrecht, The Netherlands

Introduction:

A major challenge in 3D bioprinting of functional parts of organs using soft hydrogel materials is reaching sufficient resolution to mimic the complex organization in many tissues. Although higher resolutions can be obtained by adjusting the printing hardware parameters, such a machine-based approach generally results in high shear strains on the printing inks which could be harmful to incorporated cells.

For this reason, we are developing hydrogel materials that can shrink on demand after the printing step. This post-processing leads to smaller dimensions of the (bio)printed structures, allowing us to create in vitro models of complex tissues containing structural features of realistic dimensions.

The shrinking approach relies on electrostatic interactions between hydrogels consisting of crosslinked anionic polymers and cationic polymers, which effectively act as shrinking agents. These interactions lead to (partial) charge neutralization and an increase in hydrophobicity, promoting water expulsion, that, in turn, results in hydrogel shrinkage (Figure 1).[1]

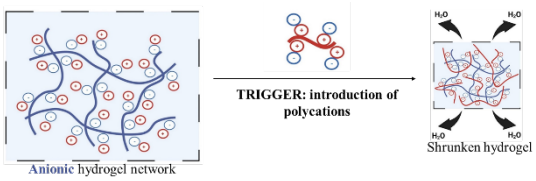

Figure 1. Mechanism of the shrinking process.

Although conceptually sound, the previously developed shrinkage procedure faces two limitations:

1) Prolonged exposure to high concentrations of cytotoxic polycations limits cytocompatibility.

2) The process is limited to charged hydrogels.

Initially, to maximize cytocompatibility we decided to minimize exposure to cytotoxic polycations. Partially, this was achieved by determining the minimal amount of polycation required to induce effective shrinking and following the shrinkage kinetics in detail.

The next strategy to address both limitations simultaneously is the development of a new shrinking approach relying on inherently cytocompatible supramolecular driving forces.

Materials and methods:

1. To determine the minimum amount of polycation for effective electrostatic-based shrinking, poly(2-(dimethylamino)ethyl methacrylate) (pDMAEMA) fluorescently labeled with Cy3 was synthesized and used to quantify the polycation uptake into hyaluronic acid (HA) based hydrogel matrices by analyzing the fluorescent signal reduction of the supernatant. Next, the cytocompatibility of the shrinking process was investigated on HA hydrogels containing conditionally immortalized proximal tubular epithelial cells (ciPTECs) by applying the minimal required polycation concentration.

2. To develop a new shrinking strategy, hyaluronic acid and dextran (DEX) were selected and modified with specific complementary self-assembling groups. Then, hydrogels based on the mixture of the obtained smart polymers were prepared and investigated in terms of their shrinking efficiency.

Hydrogels for both studies were casted in PDMS molds. Size measurements before and after shrinking were performed using Vernier calipers. All experiments were conducted in PBS buffer, pH = 7.4 at room temperature.

Results and discussion:

1. Detailed investigation into the electrostatically-mediated shrinkage of HA hydrogels revealed that the shrinking efficiency and its rate depends on the initial concentration of pDMAEMA-Cy3. Moreover, the analysis of the absorbed amounts of pDMAEMA-Cy3 showed that high shrinking efficiency (8 times in hydrogel volume, Figure 2) for the minimal required polycation concentration was achieved close to the theoretical point of charge neutralization. The analysis of the cytocompatibility of hydrogels containing ciPTECs under the exposure to identified polycation concentration showed significantly improved cell viability.

2. The newly developed shrinking approach based on the interaction of modified HA and DEX demonstrated a high shrinking efficiency up to 7 times in hydrogel volume. The shrinking process is reversible and mechanical testing showed an increase in stiffness upon shrinking. The cytocompatibility of the new approach is currently being investigated.

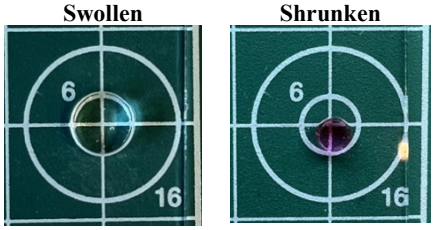

Figure 2. HA-based hydrogel before (left) and after (right) polycation-driven shrinkage.

Conclusions:

l. Cytocompatibility of the electrostatic-based approach was significantly improved by applying a minimal amount of polycation that is just sufficient to achieve effective shrinking.

2. A new, potentially more cell-friendly shrinking approach was developed demonstrating a shrinking efficiency up to 7 times in hydrogel volume.

Reference:

1. Gong, J., Schuurmans, C.C.L., et al., Complexation-induced resolution enhancement of 3D-printed hydrogel constructs, *Nat. Commun.* 11, 1267 (**2020**).

Acknowledgements: Funding for this project is provided by the Dutch Research Council: NWO-VICI 18673.

Assessing Printability of Bio-inks by Means of Capillary Rheology

F. Sanaei[1], P. Bertsch[1], S.C.G. Leeuwenburgh[1], M. Diba[1]

Department of Dentistry-Regenerative Biomaterials, Radboud Institute for Medical Innovation, Radboud University Medical Center, Nijmegen, The Netherlands

Conventional in vitro tissue models lack native tissue-like architecture. 3D bioprinting offers enhanced control over tissue model architecture, thereby opening the ways for fabrication of near-physiological tissue models. Printable biomaterials, known as bio-inks, play a crucial role in 3D bioprinting. Recent progress in materials science has led to the development of various bio-inks for extrusion-based bioprinting –most common type of 3D bioprinting. Despite this progress and technological advancement in 3D bioprinting technology, achieving reliable and reproducible printing with existing bio-inks remains a widespread challenge, necessitating extensive experimental optimizations.

Viscoelastic properties of bio-inks play a critical role in their printability and shape fidelity of printed filaments. Rotational and oscillatory rheological measurements are currently gold standards for assessing the flow and viscoelastic behavior of bio-inks. However, these approaches do not accurately mimic the physical process of bio-ink extrusion, making it challenging to predict printability using data obtained based on these methodologies.

To address this limitation, we have developed a methodology based on capillarity rheology (CR) for assessing printability of bio-inks. This method replicates the physical conditions bio-inks undergo during 3D bioprinting. In this system, the bio-ink flows with various flowrates through a defined-size capillary -narrow cylindrical conduit. A pressure sensor integrated at the beginning of the capillary measures the pressure of extrusion. Subsequently, pressure values combined with the temperature values of the material are collected which can give insights about the viscoelastic and shear-thinning behavior of materials. As a proof of principle, we have employed Pluronic F-127, cellulose nanocrystals, and gelatin methacrylate (GelMa) as commonly used inks to assess their extrusion in this system.

Our preliminary results show a discrepancy between rotational rheology and the CR methods, which indicate differing properties for the same material. Interestingly, rotational rheology shows a high shear-thinning behavior for GelMa under commonly utilized print settings which contradicts the results obtained from CR method. This result necessitates a re-evaluation of current evaluation techniques for printability of bio-inks, emphasizing the significance of employing methodologies that mimic the printing process more closely. To this end, our ongoing experiments employ this CR-based for in-depth evaluation of bio-ink printability. Overall, this approach offers new insight into the rheological properties of the bio-inks during the printing process and provides a new tool for more effective optimization of 3D printing process for the design of tissue models.

Drug-Loaded PLGA Nanoparticles Embedded Within Melt Electrowritten Scaffolds as Drug Delivery Systems

Piotr Zielinski[1], Shree Bagchi[1], Marcus Koch[2], Marleen Kamperman[1], Malgorzata Wlodarczyk-Biegun[1,3]
[1]Polymer Science - Zernike Institute for Advanced Materials, University of Groningen,
Nijenborgh 4, 9747 AG Groningen, The Netherlands
[2]Leibniz Institute for New Materials, Campus D2 2, 66123 Saarbrücken, Germany
[3]Biofabrication and Bio-Instructive Materials- Biotechnology Center, Silesian University of Technology,
B. Krzywoustego 8, 44-100 Gliwice, Poland
Contact: p.s.zielinski@rug.nl

Introduction:

3D scaffolds are commonly used in tissue engineering as they provide a suitable microenvironment for cells to proliferate and differentiate. One of the production methods is Melt Electrowriting (MEW) which allows the fabrication of scaffolds with precise microarchitecture [1]. Drug delivery systems can be incorporated into these scaffolds to enhance cell differentiation or impart antibacterial properties.
In this project, we will evaluate a novel approach that involves embedding drug nanocarriers within the polycaprolactone (PCL) matrix of MEW scaffolds. This approach holds the potential to obtain drug delivery system with high-release precision.

Materials and Methods:

Gentamicin-loaded PLGA nanoparticles (NPs) were fabricated using a double emulsion technique with solvent evaporation. The average size and polydispersity index were characterized by dynamic light scattering. Drug release studies from drug-loaded NPs and encapsulation efficiency were performed. NPs with encapsulated fluorescent dye were fabricated in order to visualize the NPs in the PCL matrix. Fluorescent-labeled NPs were mixed with PCL powder at different concentrations (0.01%, 0.05%, and 0.1%), dispersed in 0.5% (w/v) PVA, and then freeze-dried. After freeze-drying the composite material was melted in the oven at 70°C. Confocal microscopy was used to verify the homogenous distribution of NPs after mixing them with PCL. Next, the composite material was cut into smaller pieces and used for printing with the MEW printer. The printability of PCL with different concentrations of NPs was checked.

Results:

The NPs were in nanometer size (≈220 nm) with a low polydispersity index (≈0.06) and showed high encapsulation efficiency (70%). The NPs also showed a biphasic drug release mechanism with an initial burst release within the first few hours and subsequent sustained release. The confocal microscopy images of fluorescent-labeled NPs showed homogenous dispersion on NPs within the PCL matrix after mixing for all the NPs concentrations (Fig. 1A). The increasing of NPs concentration resulted in a higher fluorescent signal. After obtaining the homogenous distribution of fluorescent-labeled NPs within the PCL matrix, scaffolds with different concentrations of rhodamine-loaded NPs were successfully fabricated using MEW. The dispersion of NPs remained homogenous after printing the composite material with the MEW printer (Fig. 1B). The fiber diameter in printed scaffolds was around 70 µm.

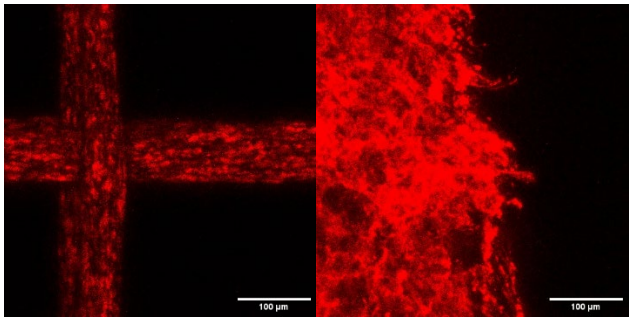

Fig.1. Distribution of fluorescent NPs (A) within the PCL matrix and (B) in PCL fibers after MEW printing.

Summary and Conclusions:

Gentamicin-loaded NPs were successfully fabricated with homogenous size distribution and a high level of drug entrapment. Encapsulation of fluorescent dye allowed visualization of NPs dispersion within the PCL matrix. The mixing process allowed for the homogenous distribution of NPs in PCL, maintained after material printing using the MEW method.

In the future, the printability of drug-loaded NPs in the PCL matrix will be studied and optimized as high-precision drug delivery systems. Mechanical analysis will be performed to analyze the influence of NPs on the scaffold's mechanical properties. In addition, drug release studies from MEW scaffolds with drug-loaded NPs will be performed.

References:

[1] P. Zielinski et al., *3D printing of bio-instructive materials: Toward directing the cell*, Bioactive Materials, 2023

Oral Presentation Session 5
Bone & cartilage regeneration

Cartilage Organoid Production with Human Induced Chondroprogenitor Cells

D.M.A. Menssen[1], G. Mazzini[2], Y.F.M. Ramos[2], I. Meulenbelt[2], F. Abinzano[1], and K. Ito[1]
[1]Orthopaedic Biomechanics, Dept. of Biomedical Engineering, Eindhoven University of Technology, The Netherlands [2]Molecular Epidemiology, Dept. of Biomedical Data Sciences, Leiden University Medical Center, The Netherlands

Introduction: Regeneration of damaged articular cartilage using human primary articular chondrocytes (hPACs) is a promising clinical procedure. However, their 2D expansion is slow and causes dedifferentiation which in turn can lead to inferior fibrocartilaginous repair tissue. Recently, the use of spinner flasks (SFs) has shown to be an efficient method to create self-assembled cartilage organoids using notochordal cell-derived matrix (NCM), where hPACs can proliferate without dedifferentiating[1]. These organoids could be used in cartilage repair strategies or personalized models. However, the number of organoids is limited by the number of chondrocytes obtained during a biopsy. To solve this problem, human induced chondroprogenitor cells (hiCPCs) could be used. Therefore, the goal of this study was to create cartilage organoids using hiCPCs and compare them to those made with hPACs.

Methods: After hiCPC colonies were produced at Leiden UMC[2], they were dissociated into single cells and cultured in the SFs according to an established protocol[1] using either 10 ml expansion medium[2] or maturation medium[3] with NCM. SF cultures with colonies in maturation medium without NCM and a hPAC control[1] were also included. Furthermore, a standard static pellet culture without NCM was included. After 14 days, organoids and pellets were harvested, the Feret diameter was measured, and biochemical assays (glycosamino-glycans (GAGs) and DNA), histology (picrosirius red and alcian blue) and immunohistochemistry (Ki67 and SOX9) were conducted (n=2 or 3 for organoids and pellets). Quantitative data were statistically analyzed with either a one-way ANOVA with Tukey's multiple comparisons or a Kruskal-Wallis with Dunn's multiple comparisons tests for size and GAG content per DNA, respectively.

Results: SF culture with single hiCPCs resulted in only five large organoids regardless of medium type. Brightfield microscopy showed that the hiCPC organoids in maturation medium were less dense compared to those in expansion medium. The hPAC organoids were 4x smaller than hiCPC organoids (Figure 1A), and there were considerably more hPAC organoids present (±300 organoids per SF). hiCPC colonies were still intact after SF culture and did not merge with each other. The alcian blue showed the typical lining of cells at the outside of the hPAC organoids (Figure 2A), whereas this lining of cells was absent on the hiCPC organoids (Figures 2C and B). Furthermore, the alcian blue staining barely showed GAGs in the hiCPC colonies (Figure 2D). However, biochemistry showed no significant differences in GAG content per DNA for all groups (Figure 1B). For the static culture, the hiCPCs in maturation medium did not form a pellet while the hiCPCs in expansion medium and the hPACs did. Biochemistry showed no significant differences of GAG content per DNA for the static groups (results not shown).

Discussion: The results showed that it is possible to produce cartilage organoids from hiCPCs with NCM. However, these organoids are different compared to hPAC organoids in terms of size, number, and cellular organization. Interestingly, the hiCPCs seem to perform more like hPACs in expansion than in maturation medium during both SF and static culture. As maturation medium is used for the chondrogenesis of hiCPCs colonies[3], it is hypothesized that the dissociation of the hiCPC colonies into single cells, followed by pelleting or organoid formation alters the cells. However, further study is needed to understand this effect. For the cartilage organoids to be effective in either cartilage repair strategies or personalized models, future studies should improve the SF protocol in order to decrease the size and increase the number of cartilage organoids with hiCPCs.

Acknowledgements: This work was supported by the LS-NeoCarE research program, funded by the Netherlands Organization for Scientific Research.

References: [1]Crispim J.F. et al., *Acta Biomater*. 2021 [2]Adkar S.S. et al., *Stem Cells,* 2019 [3]Ruiz A.R. et al., *Cell and Tissue Res.* 2021

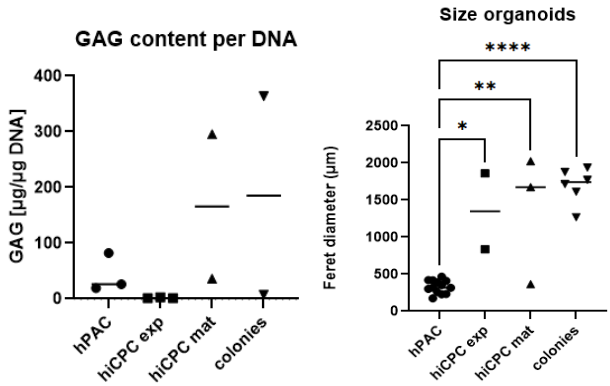

Figure 1: Size and biochemical analysis of the organoids afterva 14-day SF culture. (A) The Feret diameter of the hPAC organoids was significantly smaller than the hiCPC organoids in expansion medium (exp), hiCPC organoids in maturation medium (mat), and hiCPC colonies. (B) No differences between GAG content per DNA in the organoids were found. **p<0.01, ***p<0.001, and ****p<0.0001.

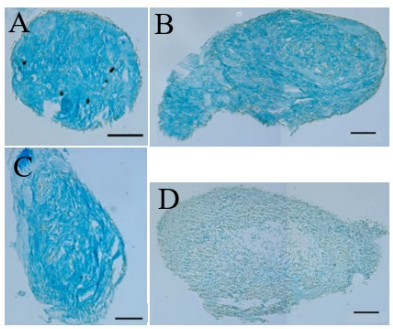

Figure 2: Alcian blue staining showing the GAG content in the organoids produced in the SFs. (A) hPAC organoid. (B) hiCPC organoid in expansion medium. (C) hiCPC organoid in maturation medium. (D) colony. Scale bar is 100 µm.

Enhancing Chondrogenic Differentiation for Endochondral Bone Regeneration: The Impact of Cell Number, Signaling Factors and Hypertrophy

F. Staubli[1,2], S. Degiovanni Morales[1,2], A. J. W. P. Rosenberg[1], D. Gawlitta[1,2]
[1]Dept. of Oral and Maxillofacial Surgery & Special Dental Care, [2]Regenerative Medicine Center Utrecht, University Medical Center Utrecht, Utrecht, The Netherlands

In the process of endochondral bone regeneration (EBR), a cartilaginous structure is implanted to generate bone through endochondral ossification[1]. This method primarily relies on the chondrogenic differentiation of mesenchymal stromal cells (MSCs) to form cartilage tissues within 3-dimensional cell culture systems. However, there is no consensus on ideal culture conditions, including carrier material, number of cells per tissue, applied growth factors, and hypertrophy induction. Understanding how these factors affect cartilage composition and structure is crucial to optimize implant production for EBR and ultimately translate this approach to the clinic.

Human MSCs from 3 donors (passage 4) were differentiated chondrogenically *in vitro* either in biomaterial-free pellet culture ($2.5*10^5$ cells) or embedded in rat tail collagen I biomaterial as carrier (4mg/ml; 10^6 cells/tissue). Up to 21 days of culture, tissues were cultured in chondrogenic medium supplemented with either TGF-β only, or TGF-β and BMP2. On day 21, half of the tissues were switched to hypertrophic medium, while the other half was kept in the corresponding chondrogenic medium until day 28. Tissues were analyzed using Safranin O, Collagen type II, and von Kossa staining; and content of glycosaminoglycans (GAGs) and DNA were quantified on days 21 and 28. Additionally, samples for bulk RNA sequencing were collected on day 28.

Chondrogenesis was confirmed (Safranin O and Collagen II staining) in samples of all donors, but overall, GAG deposition and response to culture conditions varied among donors. Further, mineralization was confirmed for samples of all donors that were cultured in hypertrophic medium (von Kossa staining). In biomaterial-free tissues, donor 3 MSCs showed limited GAG deposition when cultured without BMP2 (Figure 1). When BMP2 was introduced to chondrogenic medium, GAG deposition comparable to donors 2 and 3 MSCs was observed. Further, for donor 3 tissues, a breakdown of GAGs after hypertrophic induction, independent of the type of growth factor supplementation, was observed. In contrast, for donors 2 and 3 no differences in GAG content between the TGFβ and TGFβ/BMP2 groups on day 21 or 28 in chondrogenic medium was distinguished. However, for donor 2 a reduction of GAGs after hypertrophic induction if exposed to TGFβ/BMP2, which was not present if only exposed to TGFβ, was shown. No significant differences in GAG deposition depending on growth factor exposure was seen in donor 1 tissues. Our analysis of collagen-embedded samples revealed trends mirroring those in biomaterial-free tissues. While the total GAG content was consistently higher in collagen-tissues, GAG/DNA was generally lower, indicating that the smaller, biomaterial-free pellets induced more GAG production per cell.

In conclusion, our study underscores the intricate interplay between culture conditions, donor-specific factors and cartilage composition in the context of MSC chondrogenesis. Our results indicate that BMP2 supplementation might support chondrogenesis of MSCs with low chondrogenic potential, such as MSCs derived from elderly patients. Furthermore, BMP2 might enhance hypertrophic progression in certain donors. Currently, staining of collagen type X to evaluate hypertrophy is ongoing. Additionally, bulk RNA sequencing data have been generated and will be analyzed to reveal gene expression differences among donors and groups.

Next, differentially regulated genes, especially related to chondrogenesis and hypertrophy, will be confirmed at the protein level. In this way, small changes in cartilage composition, which might affect bone formation upon implantation, can be detected and identified.

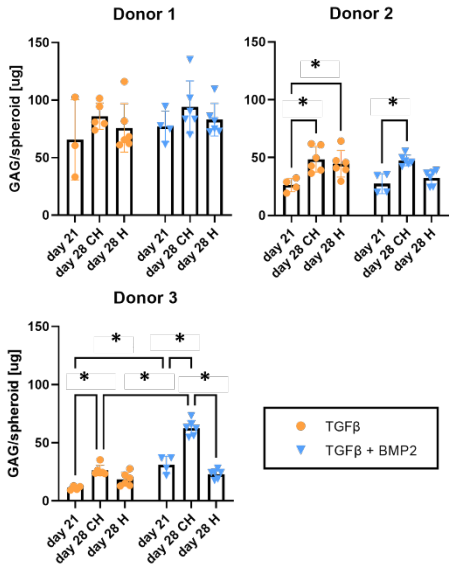

Figure 1: Glycosaminoglycans (GAGs) in biomaterial-free tissues at day 21 and 28 (n = 6) of culture for 3 donors. CH = chondrogenic. H = hypertrophic. $p < 0.05$ = *.

In the future, *in vitro* or *in vivo* models can be employed to evaluate bone formation capacity and its dependence on conditions for MSC differentiation and the resulting cartilaginous tissue composition.

Reference: [1]Longoni A *et al*. Adv Sci 9:e2103284, 2022.

Acknowledgment: This abstract is part of the project XLbone (with project number 19260) of the research programme OTP which is financed by the Dutch Research Council (NWO).

Towards Fabrication of Osteoinductive Scaffolds

L. Stoecker[1], C. Villette[2], L. Geris[2], M. Castilho[1]
[1] Eindhoven University of Technology, De Zaale, Eindhoven, The Netherlands;
[2] KU Leuven, Oude Markt 13, 3000 Leuven, Belgium

Contact: l.stoecker@tue.nl

Introduction: In bone tissue engineering, there is a growing interest in the development of scaffolds that can enhance osteoinduction by stimulating mechano-transduction processes in cells. To achieve this goal, researchers need to gain precise control of the scaffold's local deformation under physiological loading conditions. As of today, creating these type of scaffolds bears two challenges. Firstly, the scaffold's design, which is case-specific and accounts for various potentially conflicting parameters such as stiffness and porosity. Secondly, the scaffold's production within a process that is capable of manufacturing highly engineered and individualized scaffolds with pore sizes down to 200 µm [1] both fast and on demand. In recent work our team has developed an heuristic strain-based optimization algorithm which automatically generates scaffolds that meet both local strain and porosity targets under a specified load, addressing the first challenge. [2] In this study, it is now investigated whether the generated scaffolds can be produced with additive manufacturing (AM) to meet a porosity of 80 % and homogeneously distributed physiological strains of 0.5 % under prescribed compression loading of 0.5 N.

Materials and Methods

The outer shape of the scaffolds is defined as a cylinder with a diameter of 20 mm and a height of 10 mm. The inner volume is divided into 1,100 cubic elements and the aforementioned optimization algorithm is used to individually and iteratively optimize each element to meet the objective of a homogeneous strain distribution (Fig. 1b). As a control, the non-optimized cylinder is used (Fig. 1a). To investigate the suitability of the algorithm and printing technology for more complex shapes, a second shape is introduced, which contains a centered hole (Fig. 1c,d).

A stereolithography (SLA) system Form 3B+ (Formlabs, United States of America) with a laser spot size of 85 µm is used to manufacture the scaffolds from biocompatible resin Bioflex A50 MB (Resyner Technologies S.L, Spain). Parts are post-processed within a two-step washing procedure in isopropyl alcohol and post-cured with ultraviolet light. The geometry of post-processed parts is assessed with the MicroCT80 (Scano Medical AG, Switzerland) and the porosity is determined by a threshold-controlled reconstruction. Compression testing is conducted with the universal mechanical tester MTS Criterion (MTS Systems Corporation, United States of America) and a 500 N load cell at a speed of 0.085 mm/s. During testing, load and displacement are acquired and failure behavior is monitored. Apparent stiffness is calculated from engineered stress-strain curves. Data is compared to simulated results obtained by a finite element analysis.

Results and Discussion: The highest porosity of 46 ± 5 % is present in the complex optimized scaffold (Fig.1d) but is significantly different from the computed porosity of 80 %. The lowest porosity of 27 ± 2 % is measured for the simple control (Fig. 1a). The scans shows a considerable accumulation of material in the scaffold. Control scaffolds tend to fail brittle while optimized scaffolds show a ductile failure behavior. While failure occurs at similar displacements, simple controls withstand the highest load of 52.5 N. Complex optimized scaffolds show maximal loads of 13.9 N. The apparent stiffness is in the range between 6 – 12 N/mm and thus significantly higher than simulated. Deviation is smaller for optimized scaffolds, being 1.8 – 2.2 times higher than computed. Findings align with the amount of material accumulation in the scaffolds: lower porosities result in higher stiffnesses. The accumulation of material might result from a lower actual printing resolution, an insufficient washing step, or missing consideration of design guidelines for AM in the scaffold design process.

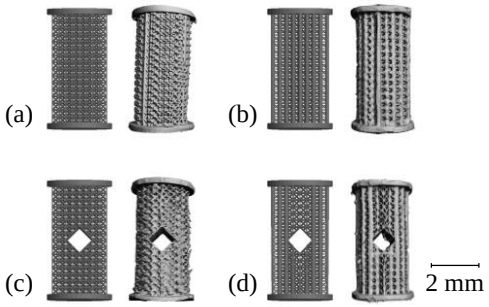

Figure 1: Comparison between CAD (left) and CT-scan (right) for the simple control (a), the simple optimized (b), the complex control (c), and the complex optimized (d) scaffold.

Conclusions and Summary: The porosity of 80 % is not reached with the employed SLA. Low porosities of the printed scaffolds lead to a higher stiffnesses and inhomogeneous material accumulation prevents the generation of a homogeneous strain. In further research, a high resolution machine with a spot size of 27 µm will be employed to investigate, if the material accumulation can be significantly reduced. Furthermore, scaffold scans will be conducted under compression to assess the strain distribution and potentially fulfill the requirements for osteoinductive scaffolds in the future.

References:

[1] Doktor et al., Conf. of Engineering Mechanics, 2011
[2] Phillips et al., International Biomechanics, 2, 2015

Complete listing of e-mail addresses:

C. Villette: claire.villette@kuleuven.be
L. Geris: liesbet.geris@kuleuven.be
M. Castilho: m.dias.castilho@tue.nl

Novel Bioactive Glasses From the SiO2-CaO-Na2O System for Bone Regeneration Applications

Martyna Nikody [a,b], Lilian Kessels [c], Matthias Schumacher [a], Tim Wolfs [c], Lizette Morejón [d], José A. Delgado [d], Timo Rademakers [a,b], Pamela Habibovic [a], Lorenzo Moroni [b], Elizabeth R. Balmayor [a,e]

[a] Department of Instructive Biomaterials Engineering, MERLN Institute for Technology-Inspired Regenerative Medicine, Maastricht University, Maastricht, the Netherlands
[b] Department of Complex Tissue Regeneration, MERLN Institute for Technology-Inspired Regenerative Medicine, Maastricht University, Maastricht, the Netherlands
[c] Department of Paediatrics, Maastricht University, Maastricht, the Netherlands
[d] Department of Ceramics and Composite Materials, BIOMAT Center for Biomaterials, University of Havana, Havana, Cuba
[e] Experimental Orthopaedics and Trauma Surgery, Department of Orthopaedic, Trauma, and Reconstructive Surgery, RWTH Aachen University Hospital, Aachen, Germany.

Introduction

Angiogenesis is essential for successful bone regeneration and repair. It is particularly indispensable in the repair of critical-sized bone defects as a lack of vascular network can lead to insufficient nutrient and oxygen supply with subsequent graft failure. Bioactive glasses are a group of ceramic biomaterials finding numerous applications due to their excellent biocompatibility and bioactivity. Depending on their composition, bioactive glasses can have various properties resulting from altered amount and proportions of the main components. In this study, we investigated both angiogenic and osteogenic properties of novel bioactive glasses from the SiO_2-CaO-Na_2O system.

Materials & Methods

Three bioactive glasses from the SiO_2-CaO-Na_2O system were previously synthesized from calcite minerals and silica sands extracted from natural deposits in Cuba. Silica sand used for the synthesis of each glass was obtained from a different depth of the deposit, resulting in a different color of the sand (grey, white, and yellow). To characterize the atomic and molecular structure of the materials, Fourier transform infrared spectroscopy (FTIR) and X-ray diffraction spectroscopy (XRD) were performed. The viability of human mesenchymal stromal cells (hMSCs) was investigated through a direct culture with bioactive glass particles at different concentrations. Furthermore, DNA quantification, alkaline phosphatase (ALP) activity, and expression of relevant osteogenic and angiogenic gene markers were investigated. Finally, angiogenic properties were further confirmed in a chick chorioallantoic membrane (CAM) model.

Results

FTIR spectra revealed the composition of the bioactive glasses, while XRD patterns confirmed their amorphous character and suggested the presence of nanocrystalline domains. Overall, cell proliferation increased over the period of 14 days, while the ALP activity varied between samples and concentrations. Further analysis showed that all tested formulations induced changes at the gene expression level. Finally, all bioactive glasses tested in a CAM model influenced the number, distribution, and branching of the blood vessels. The glass synthesized with white silica sand influenced parameters associated with angiogenesis in the most consistent way.

Conclusions

Overall, our results demonstrated that the novel bioactive glasses from the SiO_2-CaO-Na_2O system have both osteogenic and angiogenic properties. Furthermore, a correlation between different material compositions with the angiogenic properties of these materials was observed. Future work will focus on additive manufacture and characterisation of three-dimensional, porous polymer-bioactive glass composites.

Acknowledgements

This work was supported by the Netherlands Organization for Scientific Research, Applied and Engineering Sciences (NWO-AES, Grant # 16711).

Tooth-on-a-chip co-culture model to study the early-stage interaction between dental epithelial and mesenchymal cells

Chong Huang [1], Farhad Sanaei [1], Wei Ji [2], Fang Yang [1], X. Frank Walboomers [1]

1.Department of Dentistry-Regenerative Biomaterials, Radboud University Medical Center, Research Institute for Medical Innovation, Nijmegen, the Netherlands. chong.huang@radboudumc.nl
2.School & Hospital of Stomatology, Wuhan University, Wuhan, China

Introduction:

The tooth is a complex organ with intricately organized hard and soft tissues e.g. enamel, dentin, and pulp. While various materials have been applied clinically to replace the missing tooth structures, synthetic materials fall short in recreating the complex physical patterns and biological functions of natural teeth. Thus, tooth regenerative therapy seeks to engineer living teeth by orchestrating the behavior of tooth cells in the way natural teeth develop. Although it is widely recognized that teeth are generated from the dental epithelial (DE) and mesenchymal cells (DM), the complex cascade of DE-DM interactions has not been elucidated. In this study, we aim to establish a tooth-on-a-chip, providing a reliable in vitro platform for studying the spatial-temporal cues involved in DE-DM interaction. This innovative approach holds promise for shedding light on the complex processes underpinning tooth development and regeneration.

Materials and Methods:

Chip design and fabrication: A 3-parallel-channel design was used in this study. Three distinct pillars were designed to connect these paralleled channels. The negative chip molds were crafted by a 3D printer. Liquid PDMS was prepared by mixing Sylgard 184 and its curing agent at a 10:1 ratio. After degassing, the liquid PDMS was poured onto the molds and cured at 90 °C for 30 min. Polymerized PDMS was then peeled off from the molds. Inlets and outlets were punched and then the chip was closed by a coverslip using an air plasma.
Cell culture: Primary porcine DE cells and human DM cells were extracted by enzymatic digestion. They were cultured in LHC-8 and αMEM medium, respectively, and cryopreserved until use.

Tooth-on-a-chip development: The DM cells were resuspended fibrin gel with a final concentration of 1000 cells/μL. The mixture was gently injected into the central channel by a micropipette. After fibrin polymerization, a DE cell suspension of 1000 cells/μL was injected into the apical channel. Next, the chip was tilted vertically for 2h, allowing DE to settle onto the interconnecting pores. To inhibit fibrin degradation, 20μg/mL aminocaproic acid (ACA) was added to the medium. Media were replenished daily to maintain the static co-culture.
Cell viability: Samples were imaged at day 1, day 7, and day 14 with epifluorescence microscopy. A live-dead cytotoxicity Kit was used on day 1, day7, and day 14 following the manufacturer's guidelines. Briefly, after rinsing with PBS, samples were incubated for 1h with 100X ethidium homodimer-1 and 400X calcein acetoxymethyl ester.
Immunofluorescent staining and imaging: Samples were fixed and permeabilized with paraformaldehyde and Triton-X100 respectively. After blocking in bovine serum albumin, samples were incubated first with primary antibodies (anti-cytokeratin 14 and vimentin) and then secondary antibodies. All samples were examined, and 3D reconstructed under confocal laser scanning microscopy (CLSM).

Results:

Chip validation: Initial testing of pillar designs revealed some issues. Trapezoidal pillars led to chip bonding failure due to poor fidelity. Hexagonal pillars hindered medium supply due to the trapping of air bubbles. Only a pillar design that included a dent led to successful device assembly, facilitated medium transport, and provided spatial control of hydrogel. Consequently, this design was selected for later experiments.
Stability of long-term 3D culturing: The mixture of DM cells and fibrin gel effectively filled the central channel. Live-dead staining results showed that cell-embedded fibrin successfully kept integrity in the central channel for up to 2 weeks. DM cells were evenly distributed in gel, exhibiting a fibroblast-like morphology on day 7. Over the course of 2 weeks, DM cells kept proliferating and accumulated in the spaces between each two pillars where the interface was expected to form.
DE-DM interface development on chip: After coculturing 3D DM cells in the central channel with the DE cells for 12h, the sample was stained with cell-specific markers. The reconstructed image showed that DM cells grew to the surface of fibrin into the interconnecting spaces between pillars. The loaded DE cells were successfully attached to fibrin gel and established physical interaction with DM cells in the superficial layer.

Conclusions:

3D printing is an effective tool for designing tooth-on-chip systems, offering rapid chip production and adaptability.
The culturing system on the chip was cytocompatible and provided a stable 3D in vitro model for tooth-on-a-chip experiments.
The early-stage tooth-on-a-chip displayed biomimicry by recreating physically structured interaction between DE and DM cells.

Unravelling the role of biomaterial properties in orchestrating osteoclastogenesis events during biomaterials-driven bone regeneration

L. Fermin[1], D. de Melo Pereira[1,2], H. Yuan[4], N. Davison[1,2], E. Rosado Balmayor[3], P. Habibovic[1], Z. Tahmasebi Birgani[1]
[1] Department of Instructive Biomaterials Engineering, MERLN Institute for Technology-Inspired Regenerative Medicine, Maastricht University, Universiteitssingel 40, 6229 ER Maastricht, The Netherlands
[2] Instructure Labs, Herderslaan 13, 2526 KL The Hague, The Netherlands
[3] Experimental Orthopaedics and Trauma Surgery, Department of Orthopaedic, Trauma, and Reconstructive Surgery, RWTH Aachen University Hospital, 52074 Aachen, Germany
[4] Kuros Biosciences A.G., Wagistrasse 25, 8952 Schlieren, Switzerland

Introduction: Biomaterial-driven osteoinduction is the ability of a biomaterial to trigger bone formation in a non-bone environment, often assessed by ectopic bone formation *in vivo*. Some, yet not all, calcium phosphates (CaPs) exhibit osteoinductive potential. It was shown earlier that CaPs with similar chemical composition, but different surface topography and microstructure led to different osteoinductive properties.[1] Specifically, CaPs with smaller grains and pores simultaneously favored ectopic bone formation[2], and osteoclast attachment and resorption.[3] The effect of biomaterial properties on osteoclasts, and the effect of osteoclast on osteoinduction has yet to be investigated thoroughly**.** Here, we aim to decouple the microstructure and topography of two CaPs with different osteoinductive potential from their chemical composition, and to investigate the role of the topography on osteoclastogenic events in the presence of these biomaterials.

Material and Methods: Grained topographies of osteoinductive (TCP S) and non-osteoinductive (TCP B) tricalcium phosphates (TCP) were replicated onto nickel shims via galvanoforming, which were in turn used to replicate the topographies onto thermal polyurethane (TPU) films using a nanoimprinting technique. TPU replicates were analyzed with confocal laser scanning profilometry, scanning electron microscopy (SEM), mechanical testing, contact angle measurement and Fourier transform infrared spectroscopy (FTIR). Buffy coat-derived peripheral blood mononuclear cells (PBMCs) were seeded onto TPUs with and without the topographies, as well as onto control bone slices. Cells were seeded at a density of $3x10^6$ cells/cm^2 in osteoclast differentiation medium. Cell morphology and osteoclastic markers were analyzed at multiple time points.

Results and Discussion: Nanoimprinting fatefully replicated the intricate three-dimensional topographies of TCP onto TPU substrates. PBMCs differentiated into osteoclasts on TPU replicates; yet the SEM analysis showed differences in cell morphology between substrates with different topographies. More and larger cells were observed on the TCP S topography compared to the TCP B topography (Figure 1). This was also observed in previous research, where a higher number of osteoclasts was found on TCP S.[3] Expression of osteoclastic markers at mRNA level showed differences at early time points; however, these differences seemed to disappear after 21 days (Figure 2). Both Cathepsin K (CTSK) and TRAP are genes specific for osteoclast activation and resorption. This can indicate that TCP S topography leads to earlier osteoclast differentiation and activation. A larger panel of genes will be analyzed to further understand the change in cell behavior on the topographies, with specific markers related to actin dynamics.

Conclusion: In this research, we have shown a fabrication method for faithful replication of TCP topographies onto polymer films. Using this approach, we could effectively decouple the chemical composition from the topographical properties of TCPs, and showed that osteoclasts respond differently to these two topographies in terms of attachment, morphology and (early) mRNA expression of osteoclastic markers. Further analysis is ongoing to understand how topographies drive these osteoclastic responses.

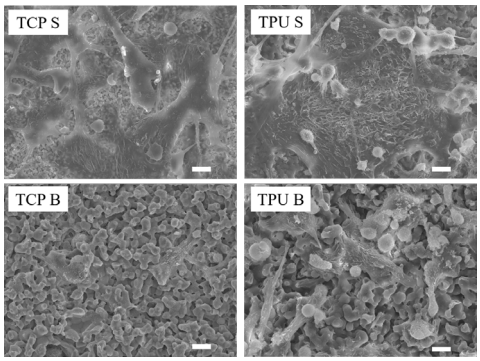

Figure 1. Osteoclast attachment and morphology on TCP discs (left) and TPU replicates (right) visualized by SEM.

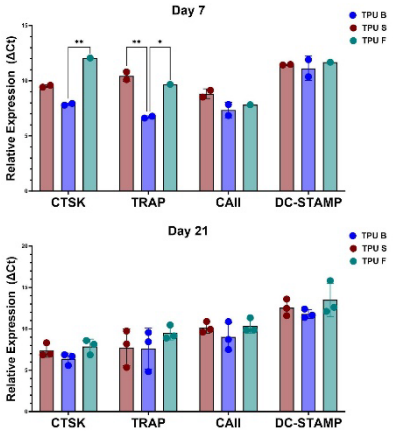

*Figure 2. Relative mRNA expression of relevant osteoclast markers in the cells cultured for 7 and 21 days on TPU replicates and flat TPU films (TPU F). * represents $p \leq 0.01$ and ** represents $p \leq 0.05$.*

References

1. J. Zhang et al., 2014, Acta Biomaterialia 10(7), 3254-3263
2. N.L. Davison et al., 2015, European Cells and Materials 29, 314–329.
3. N.L. Davison et al., 2014, Biomaterials 35, 7441-7451.

Acknowledgements: This research has been made possible by the Materials-Driven Regeneration Gravitation Program of the Dutch Research Council (NWO).

Oral Presentation Session 6

Blood and vascular engineering

In Vitro Co-Culture Of Tissue-Engineered Mineralised Cartilage And Vessel Networks To Model Endochondral Ossification

E. Ji[1], L. Leijsten[1], J. Witte-Bouma[1], A. Rouchon[2], N. Di Maggio[2], A. Banfi[2], G.J.V.M. van Osch[3,4], E. Farrell[1], A. Lolli[1]
1: Department of Oral and Maxillofacial Surgery, Erasmus University Medical Center, Rotterdam, The Netherlands
2: Department of Biomedicine, Basel University Hospital, Basel, Switzerland
3: Department of Orthopaedics & Sports Medicine and Department of Otorhinolaryngology, Erasmus MC University Medical Center, Rotterdam
4: Department of Biomechanical Engineering, University of Technology, Delft, The Netherlands

Introduction: Endochondral ossification (EO) is the process of bone development via a cartilage template. It involves multiple stages, including chondrogenesis, mineralisation and angiogenesis. Importantly, how cartilage mineralisation affects angiogenesis during EO is not fully understood. Here we aimed to develop a new *in vitro* co-culture model to recapitulate and study the interaction between mineralised cartilage generated from human mesenchymal stromal cells (hMSCs) and microvascular networks.

Methods: Chondrogenic hMSC pellets were generated by culture with transforming growth factor (TGF)-β3 (10ng/ml). For mineralised pellets, β-glycerophosphate (BGP) (10mM) was added from day 7 and TGF-β3 was withdrawn on day 14. To evaluate the effect of the pellet secretome on angiogenesis, conditioned medium (CM) was produced by culturing the pellets for 24h in basal medium. Transwell migration, EdU-proliferation and 3D-tube formation assays were employed to evaluate the effect of the CM on human umbilical vein endothelial cells (HUVECs). To perform direct co-cultures, d14 chondrogenic or mineralised pellets were embedded in fibrin hydrogels containing vessel-forming cells (HUVECs, adipose stromal cells). The pellets were characterised by immunohistochemistry (IHC). Furthermore, the hydrogels were subjected to whole-mount staining for laminin and the vessel length density (VLD) was quantified by confocal imaging.

Results: The CM from d14 chondrogenic or mineralised pellets significantly stimulated HUVEC migration and proliferation, as well as *in vitro* vascular network formation. When CM from pellets subjected to prolonged mineralisation (d28) was used, these effects were strongly reduced. When d14 chondrogenic and mineralised pellets were directly co-cultured with vessel-forming cells in fibrin hydrogels, the cartilage matrix (collagen type II /X stainings) and the mineral deposition (von Kossa staining) were well preserved. Confocal imaging analyses demonstrated the formation of physiologically differentiated microvascular networks (Fig. A), showing apicobasal polarisation as well as well-formed lumina of a regular size compatible with blood flow. Importantly, microvascular structures were formed in the proximity of chondrogenic or mineralised pellets and contact between vessels and pellets was achieved (Fig. B).

Discussion & Conclusions: The angiogenic properties of tissue engineered cartilage are significantly reduced upon prolonged mineralisation. Based on this evidence, we developed a 3D co-culture model of vessel network formation in the presence of chondrogenic or early mineralised pellets. This model can help us to better understand the role of angiogenesis in endochondral bone formation, or find applications in disease modelling studies.

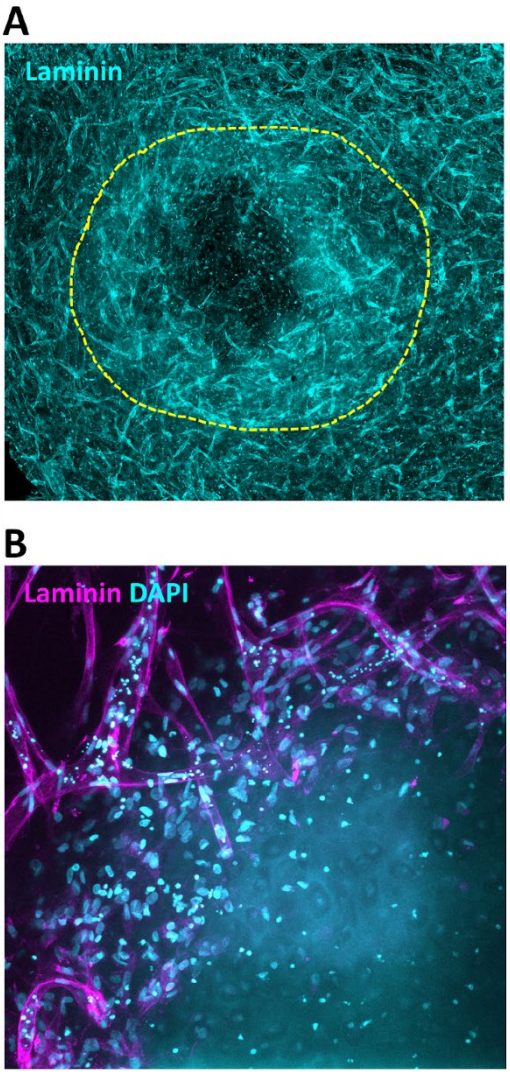

Fig. Confocal imaging of the 3D co-culture model of vessel network formation with chondrogenic/ mineralised pellets. (A). Microvessels in the co-culture model were stained with Laminin (Cyan) and visualised by confocal imaging. The yellow dotted line indicates the position of a chondrogenic pellet. Imaged with Leica Stellaris 5 LIA .(B) DAPI (Cyan) and Laminin (Fuchsine) staining was performed to assess the contact between pellets and microvessels. Imageds with Leica SP5 Intravital.

Acknowledgements: The European Union Horizon 2020 Research and Innovation Program under grant agreement 801159 supported this study.

Erythrocyte Membrane-Inspired Lipid Coatings For Blood Substitutes

Francisca L. Gomes[1,2], Rick Edelbroek[2], Indra Mooij[1,2], Jasper van Weerd[3], Pascal Jonkheijm[2*], and Jeroen Leijten[1*]

[1]Leijten Lab, Dept. of Developmental BioEngineering, Faculty of Science and Technology, Technical Medical Centre, University of Twente; [2]Dept. of Molecules and Materials, Laboratory of Biointerface Chemistry, Faculty of Science and Technology, MESA+ Institute for Nanotechnology, University of Twente; [3]LipoCoat BV. Enschede, The Netherlands. *authors contributed equally*

Introduction: Blood is a scarce life-saving resource with a labile supply-and-demand equilibrium. Supplies for transfusions are often limited due to the incompatibility of blood types, a low percentage of universal blood donors, and a short shelf-life. Moreover, the urgent need for blood in situations of war, natural disasters, or pandemics further increases its demand. To reinforce its supply, blood substitutes have strongly emerged. Hemoglobin-based oxygen carriers and perfluorocarbons have been the most successful blood substitutes to date. Nevertheless, production and use of hemoglobin has limited scalability due to its dependence on blood, and use of perfluorocarbons still warrants adaptations for improved biological response. Overall, engineering the ideal blood substitute requires universality, safety, scalability, and a long shelf-life.

In this work, we developed a bio-inspired lipid coating as a synthetic erythrocyte membrane. We first established a bottom-up lipid coating method, compatible with a wide range of particle suspensions, and studied the effect of different erythrocyte membrane-mimicking lipid formulations in particle hemocompatibility. Having determined the safest formulation, we applied this new synthetic membrane to oxygen-generating microparticles (OG-MPs) to assess their potential as self-oxygenating blood cells.

Methods: A solvent gradient-based lipid coating method was first developed and validated in-house, based on the solvent assisted lipid bilayer method.[1] Briefly, a concentrated lipid-particle mixture was first prepared in isopropanol, into which an aqueous buffer was then injected to induce lipid re-assembly. The gradient was finally heated to form a conformal coating. Four synthetic lipid formulations of increasing complexity (D, C, S, and I) were then designed, inspired by the outer leaflet of the native erythrocyte membrane, starting with phosphatidylcholine (formulation D) and cumulatively adding cholesterol (C), sphingomyelin (S), and phosphatidylinositol (I), at molar ratios described elsewhere.[2] For confocal imaging, 0.1 mol% Texas Red™-DHPE were added. Hemolysis, plasma coagulation time, and whole blood biomarker assays were conducted. Next, OG-MPs were produced by incorporating CaO_2 crystals onto polycaprolactone microparticles, after which these constructs were lipid-coated and characterized in terms of structure and hemocompatibility *in vitro*.

Results and Discussion The effects of solvent type, buffer addition rate, lipid concentration and gradient ratio on coating formation were first validated on microparticles. The four erythrocyte-inspired lipid coatings were then applied to silica microparticles (SiO_2 MPs, Figure 1a), nanoparticles (SiO_2 NPs), and polycaprolactone microparticles (PCL MPs). Overall, the most complex coatings (S and I) displayed the highest lipid coating efficiency and colloidal stability for all substrates. All coatings remarkably reduced the hemolysis of SiO_2 NPs (Figure 1b), while complex coatings evidenced the most delayed coagulation. Complex coatings also demonstrated the lowest complement, platelet, and immune-activating profiles on PCL MPs (Figure 1c). Lastly, OG-MPs were characterized, evidencing a controlled release of oxygen over 3 days. Fluorescence microscopy confirmed lipid coating formation.

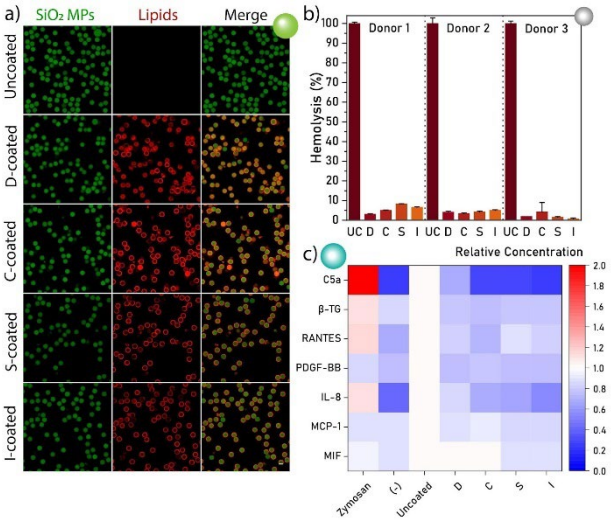

Figure 1. a) Confocal microscopy images of lipid coatings on SiO_2 MPs. Scale bar equals 5 µm. b) Hemolysis assay. c) Whole blood biomarker analysis after incubation with zymosan, no materials (-), uncoated PCL MPs, or coated PCL MPs.

Conclusions: We describe a novel, bio-inspired lipid coating as a synthetic erythrocyte membrane and its application in a blood substitute. Ongoing and following work will focus on particle characterization and *in vitro/in vivo* hemocompatibility testing.

Acknowledgements: F.L.G. acknowledges the TechMed Donor Service of the University of Twente and its donors. Authors acknowledge financial support from Health~Holland (Project LSHM19074).

References

1 Ferhan, A. R. *et al. Nat Protocols* **14**, 2091-2118 (2019).
2 Lorent, J. H. *et al. Nat Chem Biol* **16**, 644-652 (2020).

Endothelial Cells and Astrocytes Growth Variations on Melt-Electrowritten Scaffolds for Blood-Brain Barrier Modeling

M.Z. Gładysz[1,2], Marcus Koch[3], Marleen Kamperman[1], Anika Nagelkerke[2], Malgorzata Wlodarczyk-Biegun[1,4]
[1] Polymer Science, University of Groningen, Nijenborgh 4, 9747 AG Groningen, The Netherlands
[2]Pharmaceutical Analysis, Groningen Research Institute of Pharmacy, University of Groningen, Antonius Deusinglaan 1, 9713 AV Groningen, The Netherlands
[3]Leibniz Institute for New Materials, Campus D2 2, 66123 Saarbrücken, Germany
[4]Biotechnology Centre, Silesian University of Technology, Krzywoustego 8, 44-100 Gliwice, Poland
Contact: m.z.gladysz@rug.nl

Introduction: Melt electrowriting (MEW) is a high-resolution 3D printing method resulting in the fabrication of fibrous scaffolds with highly controlled architecture, holding promise for tissue engineering applications. However, the success of cell growth on these scaffolds is cell type-specific, necessitating a detailed study to optimize conditions.

Goal: This study examines the growth patterns of endothelial cells and astrocytes - key components of the blood-brain barrier (BBB)[1], on MEW scaffolds for the development of an in vitro BBB model.

Materials and Methods: Scaffolds, fabricated from medical-grade poly(ε-caprolactone) using MEW (Spraybase), were surface modified, treatments included poly-L-lysine (PLL), poly-D-lysine (PDL), fetal bovine serum (FBS), L-DOPA coatings, NaOH etching, and oxygen plasma activation, to facilitate cell adhesion. Two distinct cell types, murine brain endothelial cells (bEnd.3) and primary mouse astrocytes, were separately and co-cultured on these scaffolds. Cytoplasmic fluorescent labeling was employed for co-culture purposes. bEnd.3 cells were cultured on both scaffolds and flat control surfaces for seven days, followed by proteomic analysis. Live cell imaging monitored the behaviour of bEnd.3 and astrocytes on scaffolds over 19 days. The expression of astrocyte A1 and A2 phenotype markers, such as C3 and S100a10 was investigated via fluorescence microscopy. Scanning electron microscopy assessed cellular morphology.

Results and Discussion: Optimal cell attachment occurred on samples subjected to oxygen plasma treatment, followed by PLL or L-DOPA coating. Astrocytes exhibited accelerated growth and greater surface coverage compared to bEnd.3. They demonstrated a neuroprotective phenotype (A2) on all tested scaffold architectures (square, triangular, rhombus, and random). However, when bEnd.3 cells were co-cultured on these scaffolds they formed agglomerates, indicating challenges related to cell attachment (**Fig. 1.**). Moreover, proteomics analysis revealed significant alterations in bEnd.3 cells, particularly in pathways associated with the IL-17A signaling, inflammatory response, and blood clotting cascade, which are undesirable (**Fig.2.**).

Outlook: Diverse cell types exhibit unique responses and morphologies on MEW scaffolds, shedding light on tissue development. Astrocytes grew faster and bridged the gaps quicker than bEnd.3 when cultured on MEW scaffolds. Integrating proteomics into MEW research holds promise for uncovering understudied cellular disparities and can reveal currently overlooked cell-specific differences. Subsequent mass spectrometry studies will delve deeper into these variations, advancing our understanding.

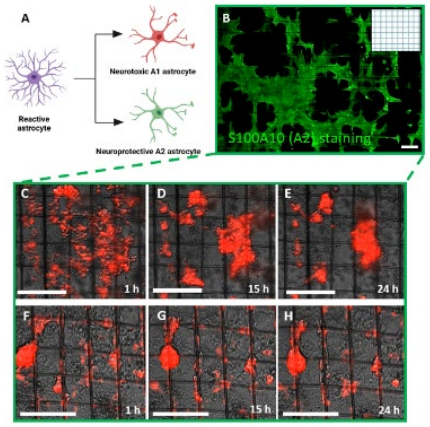

Fig. 1. A) schematic representation of astrocyte polarization. B) astrocytes labeled with S100a10 grown on a square mesh scaffold on day 4. Scale bar: 100 µm. Bottom: Live imaging of co-culture of bEnd.3 labeled with mKate2 seeded on top of a confluent astrocyte layer on square MEW scaffolds. C), D), E) Day 0 for bEnd.3 and day 33 for astrocytes. F), G), H) Day 4 for bEnd.3 and day 37 for astrocytes. Scale bars: 200 µm

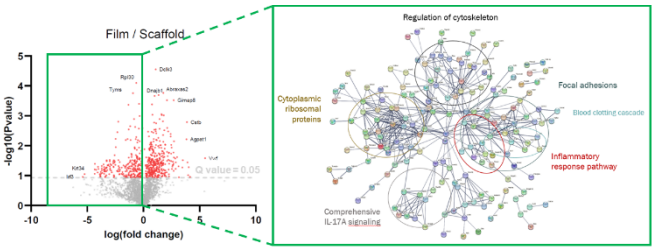

Fig. 2. Left: volcano plot of protein expression of bEnd.3 cells grown for 7 days on PCL scaffolds and PCL films, plotting statistical significance (-log10 Pvalue) vs. magnitude of fold change (log2FC), n=3.
Right: downregulated protein expression – high confidence (0.7) in String DB, cross-referenced with Gene Set Enrichment Analysis

References:

1. Gładysz, M. Z., Stevanoska, M., Włodarczyk-Biegun, M. K. & Nagelkerke, A. Breaking through the barrier: Modelling and exploiting the physical microenvironment to enhance drug transport and efficacy. *Adv. Drug Deliv. Rev.* **184**, 114183 (2022).

A tissue-engineered model of the atherosclerotic plaque cap with microcalcifications

I. Jansen[a], H. Crielaard[a], T. Wissing[a], C. Bouten[b,c], F. Gijsen[a,d], A. Akyildiz[a,d], E. Farrell[c], K. van der Heiden[a]
a Department of Biomedical Engineering, Erasmus MC, University Medical Center Rotterdam, the Netherlands
b Department of Biomedical Engineering, Eindhoven University of Technology, Eindhoven, The Netherlands.
c Institute for Complex Molecular Systems (ICMS), Eindhoven University of Technology, Eindhoven, The Netherlands.
d Department Biomechanical Engineering, Delft University of Technology, Delft, The Netherlands
e Department of Oral and Maxillofacial Surgery, Erasmus MC, University Medical Center Rotterdam, the Netherlands

Introduction

Rupture of the cap of an atherosclerotic plaque can lead to thrombotic cardiovascular events, such as myocardial infarction and stroke. The atherosclerotic cap is often characterised by a heterogenous composition, and can contain inflammatory cells and microcalcifications (diameter < 50 µm) embedded in a collagenous matrix. Current computational models suggest that the presence of microcalcifications in the atherosclerotic cap can increase the risk of cap rupture, but experimental verification of the mechanical effect of microcalcifications is lacking. Previously, we created a tissue-engineered (TE) fibrous atherosclerotic cap model with controllable collagen content, suitable for mechanical testing[1]. In the current study, we extended the TE model to include and mimic microcalcifications and assess the impact of microcalcifications on collagen organization and cap mechanics.

Materials and methods

First, human carotid plaque caps were histologically analysed to determine the distribution, size, and density of microcalcifications in human cap tissue obtained from carotid endarterectomy (CEA) samples. Hydroxyapatite (HA) particles were used as mimic of microcalcifications in the TE-cap, since HA is the main component of microcalcifications in human plaques (Fig 1A). Human myofibroblasts were cultured in 1 x 1.5 cm-sized fibrin-based constrained gels, according to previously established protocols[1]. Clusters of hydroxyapatite particles were injected at the start of the culture. During a 21-culture period, the myofibroblasts deposited a collagenous matrix around the particles, (Fig 1B). At day 21, all samples were exposed to multiphoton microscopy with second harmonic generation (SHG) to determine the local collagen fiber orientation, using a fiber orientation analysis tool (FibLab)[2]. Hydroxyapatite particles were visualized using a hydroxyapatite (HA)-targeting probe (IVISense Osteo 680). After vital imaging, the samples were subjected to uniaxial tensile tests until rupture[3].

Results and discussion

In CEA samples microcalcification particles were present in clusters. Particles were observed to be 2 - 15 µm (84%), while only 3% was larger than 30 µm. HA particles with similar size and distribution were used to mimic microcalcifications in the tissue-engineered constructs and verified against the human situation (Fig. 1A). SHG revealed higher local collagen fiber dispersion in regions of hydroxyapatite clusters compared to control samples (Fig. 1B). Engineered caps with HA particles demonstrated lower stiffness and ultimate tensile stress than control samples (Fig. 1C), suggesting increased rupture risk in atherosclerotic plaques with microcalcifications. Furthermore, sample stiffness negatively correlated with dispersion of collagen fibers (Fig. 1C), highlighting the effect of fiber orientation, due to microcalcifications, on tissue mechanics.

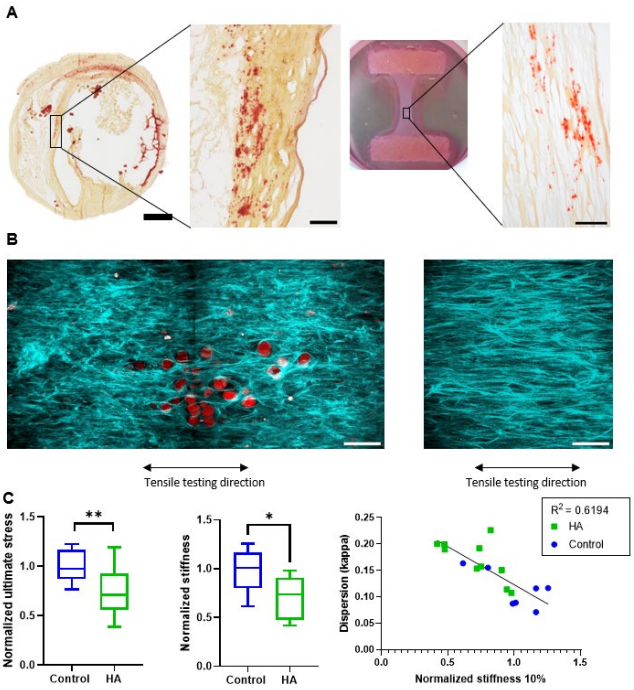

*Figure SEQ Figure * ARABIC 1. (A) Comparison of microcalcification distribution in the human atherosclerotic cap compared to HA particles in the TE-cap. (B) Collagen organisation around microcalcifications and in control area at day 21. (C) Global mechanical characterisation of tissues: normalised ultimate stress, stiffness and correlation between the collagen fiber dispersion and stiffness. Scale: (A) 1 mm, 100 µm, 100 µm. (B) 100 µm, 100 µm*

Conclusions

We have created a TE fibrous cap model with a mimic of microcalcifications to study the effect on cap mechanics and collagen organization. This model supports previous computational finding regarding a detrimental role for microcalcifications in cap rupture risk, due to a lowered ultimate tensile stress and stiffness. Ongoing research focusses on the effect of microcalcification size, shape and density on cap rupture mechanics. The model can be further deployed to elucidate tissue mechanics in pathologies with calcifying soft tissues.

References

[1] Wissing, T. B. *et al.* Tissue-engineered collagenous fibrous cap models to systematically elucidate atherosclerotic plaque rupture. *Sci. Rep.* **12**, 1–13 (2022).
[2] Van Haaften, E. E. *et al.* Decoupling the Effect of Shear Stress and Stretch on Tissue Growth and Remodeling in a Vascular Graft. *Tissue Eng. - Part C Methods* **24**, 418–429 (2018)
[3] Crielaard, H. *et al.* A Method to Study the Correlation Between Local Collagen Structure and Mechanical Properties of Atherosclerotic Plaque Fibrous Tissue. *J. Vis. Exp.* **2022**, 1–24 (2022).

Funding: This work was funded by a NWO-Vidi grant (18360)

Computational modeling of sprouting angiogenesis mechanoresponse

M. Passier[1], R. Jacobs, K. Bentley[2], S. Loerakker[1], T. Ristori[1]
1. Department of Biomedical Engineering and Institute for Complex Molecular Systems, Eindhoven University of Technology, The Netherlands; 2. Francis Crick Institute, United Kingdom

Introduction: Understanding and controlling angiogenesis, i.e. the process of blood vessel formation from pre-existing ones, are crucial requirements to enable the development of large tissue-engineered constructs. Recent experiments have shown that the extracellular matrix stiffness affects the process of endothelial tip/stalk cell selection, a key step of angiogenesis [1]; however, the underlying molecular mechanisms are largely unclear. Crosstalk between the mechanosensitive YAP/TAZ proteins and the Notch pathway [2], fundamental for tip cell selection, could potentially explain this mechanoresponse. Specifically, we hypothesize that this signaling crosstalk affects the temporal dynamics of tip/stalk cell selection, a key feature in angiogenesis influencing the final vascular topology [3].

Materials and Methods: To test this hypothesis and gain valuable insight in the angiogenesis mechanoresponse, previous computational models of Notch [4] and YAP/TAZ [5] were coupled by assuming an inhibitory effect of YAP/TAZ on the Notch ligand Dll4 (Fig. 1), as motivated by literature [6]. To fully characterize Dll4 regulation, the Notch model was further enhanced by including DLL4 upregulation resulting from Notch activation [7], as well as Dll4-Notch cis-inhibition [8] (Fig. 1). The YAP/TAZ-mediated DLL4 inhibition was fitted against previous *in vitro* data [9]. A parameter exploration was performed concerning the Notch-mediated DLL4 upregulation and cis-inhibition. Then, to investigate the temporal dynamics of cell fate selection, Endothelial Cells (EC) in our simulations were exposed to VEGF for 24 hours, after which the EC phenotype was assigned based on the filopodia content.

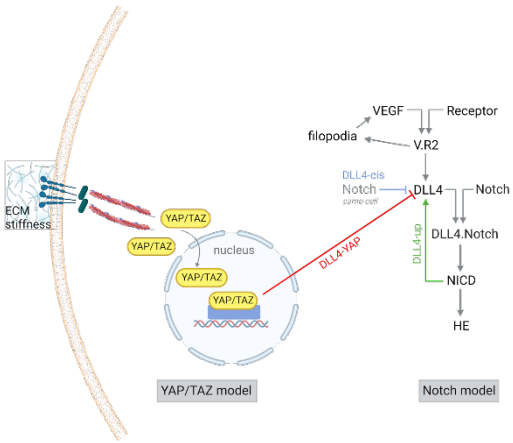

Figure 1: Schematic of the computational model and the added interactions related to DLL4. Created with BioRender.com

Results: As described by previous experimental findings, DLL4 production was predicted to decrease as stiffness increased, resulting from a mechanoregulated higher nuclear YAP/TAZ fraction. In the tip/stalk cell patterning speed, we found a biphasic response to this interaction. For 5 kPa, ECs patterned for all hypotheses. Generally, small increases compared to that stiffness slightly increased patterning speed, till a threshold above which much slower patterning speeds were observed (Fig. 2). DLL4 upregulation increased this stiffness threshold, since the cells kept patterning relatively fast for a broader range of stiffnesses. In contrast, cis-inhibition lowered this threshold: patterning speed decreased already for lower stiffnesses, thereby possibly counteracting Notch-mediated Dll4 upregulation when combined.

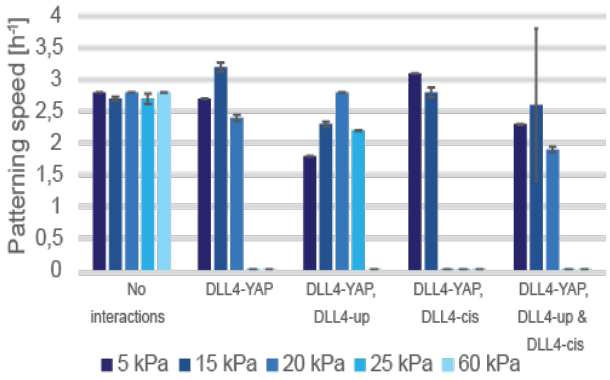

Figure 2: Patterning speed (how fast the cells become either a tip cell [>25 filopodia] or a stalk cell [<25 filopodia]) for varying stiffnesses and for a range of DLL4 interactions.

Discussion and Conclusion: Our study suggests that the Notch-YAP/TAZ crosstalk indeed affects the temporal dynamics of tip/stalk selection via DLL4 inhibition. From 5kPa, increasing stiffness increases the nuclear YAP/TAZ content and increases patterning speed, whereas above a threshold, patterning speed is reduced and finally, we observe hypersprouting (all cells have many filopodia, there is no real pattern). Notch-mediated upregulation can affect this response: the patterning speed decreases only for higher stiffnesses. This effect could be counteracted by cis-inhibition. Although in the future the proposed model could be extended by including additional YAP/TAZ-Notch interactions, here we provided a first model of the Notch-YAP/TAZ crosstalk in sprouting angiogenesis, which can already generate insights and form a basis for stiffness tuning of tissue-engineered scaffolds for future applications.

References

[1] Guo, Y. et al, Bioact. Mater. 7:364-376, 2021.
[2] Neto, F. et al, Elife, 7:e31037, 2018
[3] Bentley, K. Et al, Phil. Trans. R. Soc. B., 2017
[4] Venkatraman L et al. PLoS One, 11:e0166489, 2016
[5] Sun, M. et al, Biophys J., 110:2540-2550, 2016
[6] Yasuda, D. et al, JCI, 129:4332-4349, 2019
[7] Benedito, R. et al, Cell, , 2009
[8] Sprinzak, D. et al, Nature letters, 456:86-91, 2010
[9] Matsuo, E. et al, Exp Cell Res., 408:112835, 2021

Designing Fibrous Tubular Scaffolds for Enhanced Mechanical Performance in Vascular Engineering

J. Iamsamang[1], S. Pragnere[1], I. Donker[2], D. van den Broek[3], N.A. Kurniawan[1,4], M. Castilho[1,4]
[1] Department of Biomedical Engineering, Eindhoven University of Technology, The Netherlands
[2] Department of Orthopaedics, University Medical Center Utrecht, The Netherlands
[3] Department of Chemical Engineering and Chemistry, Eindhoven University of Technology, The Netherlands
[4] Institute for Complex Molecular Systems, Eindhoven University of Technology, The Netherlands

Introduction: Designing and fabricating vascular replacements for treating the dysfunction of small blood vessels poses significant challenges, primarily due to the relatively small vessel diameter (≤6 mm), the need to withstand hemodynamic pressure, and the requirement for long-term patency. A promising approach to address this challenge is *in situ* tissue engineering vascular replacements, that utilizes the surrounding microenvironment as a natural bioreactor to guide the tissue formation and remodeling, ultimately leaving no foreign material in long-term. To achieve this, an optimal scaffold (micro)structure is required, allowing for cell infiltration while maintaining adequate strength to keep the lumen open under hemodynamic conditions. In this study, we investigated the potential to melt electrowriting (MEW) – a relatively new printing method capable of producing controlled microstructures – to produce highly porous fibrous tubular scaffolds with hexagonal shaped micropores. We hypothesized that such tubular scaffolds with hexagonal micropores would allow for cell infiltration and providing distensibility at low strains to accommodate pulsatile blood flow, while offering increased stiffness at high strains to prevent rupture and ensure elastic stability. Also, we explored whether printing paths influenced scaffold distensibility and stiffness.

Materials and Methods: The scaffolds with hexagonal micropores were designed with two orientations (0° and 90°) with the same pore area (0.32 mm^2). Each design was then printed in both axial and circumferential (circ.) directions, resulting in four variants: 0°-axial, 0°-circ., 90°-axial, and 90°-circ. (Fig.1 A). All designs were fabricated using a custom-built MEW set up. Specifically, the melted poly(ε-caprolactone) was extruded at a temperature of 88°C with air pressure of 2 bars through a 27G needle. The material was then deposited on a cylindrical collector at voltages ranging from 5.5-7.5kV. The dimension of the printed scaffolds was evaluated using optical microscopy and their circumferential tensile performance was tested using a uniaxial ring test with two pins (Ø0.8mm).

Results and Discussion: The fibrous tubular scaffolds (Ø2 mm, thickness 0.2 mm) with a fiber diameter of ~10 µm and pore sizes of 300-400 µm were successfully fabricated with <25% deviation from the intended path (Fig.1 B,C). Notably, the circumferentially-printed scaffolds displayed a significant 3-5 fold increase in circumferential modulus ($E_{circ.}$) compared to axial scaffolds (Fig. 1 D,E). Furthermore, the axial scaffolds (0°-axial and 90°-axial) experienced rupture at strains ranging from 0.5-1, whereas most circumferential scaffolds (0°-circ. and 90°-circ.) exhibited plastic deformation within this strain region and only failed at strains exceeding 2. These results showed that not only the orientation of hexagonal micropores but also the printing direction of MEW noticeably impact the circumferential stiffness. Thus, aligning the fiber in the loading direction can improve the scaffold's stiffness. However, this stiffness is only comparable to that of the intima and media layers of human coronary arteries (HCA) [1,2], not of the overall vessel (Fig. 1 E). This is because the wall thickness of printed scaffolds is thinner than that of HCA (0.55-1 mm). Therefore, there is still room for improvement before achieving optimal vascular replacements.

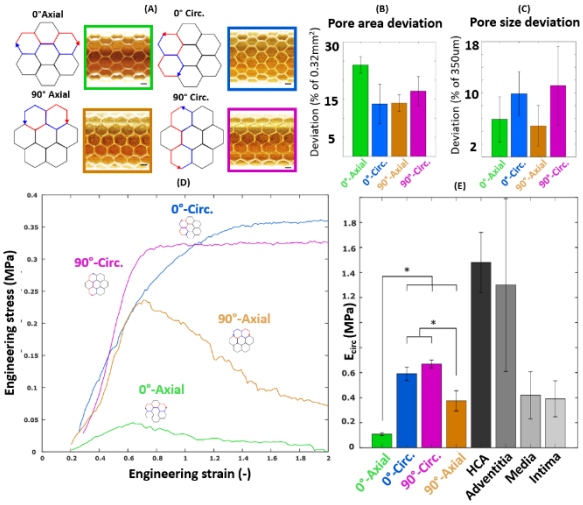

*Figure 1: (A) Four different variants, featuring red and blue arrows to depict printing directions (scale bar: 300µm), (B) Pore area deviation, (C) Side length deviation, (D) The stress-strain curves, and (E) their $E_{ring.}$ compared with HCA (*p<0.01).*

Conclusions: A novel fabrication technique has been employed to create highly porous, tubular scaffolds consisting of organized fibers with native-like stiffness. Notably, the proper alignment of the fibers in the direction of loading has yielded improvements of the final scaffold's stiffness. While E_{circ} of all scaffolds falls short of the healthy HCA observed in young patients, the scaffolds printed in circumferential direction have exhibited comparable stiffness to the media and intima layer within HCA. Therefore, by strategically considering the printing and fiber alignment, it is possible to optimize the scaffold mechanical performance to achieve the optimal vascular replacement. Based on these findings, the 0°-circ. and 90°-circ. designs have been selected for *in vitro* cell studies under dynamic stretch and shear stress which are currently in progress.

References:

[1] Karimi A. et al, Mater Biol Appl, 33(5):2550-4, 2013.
[2] Holzapfel G.A. et al, Am J Physiol Heart Circ Physiol 289:H2048-2058, 2005.

Evening lecture

Tackling the plastic soup or saving the climate? The role of academics in major environmental challenges

Prof. dr. Erik van Sebille

Erik van Sebille is Professor in Oceanography and Public Engagement, at Utrecht University. He investigates climate change and plastic pollution in the ocean, among others in a recently-started Vici project on the transport of large plastic items by ocean circulation in the North Sea. He also holds a 20% appointment at the Freudenthal Institute, where he investigates the role and effectiveness of scientists in science communication. He is also a member of De Jonge Akademie of the KNAW.

Friday
1 December 2023

Focus symposium

Bone mini-tissues

Niloofar Tahmasebi Birgani

MERLN-Institute for Technology-Inspired Regenerative Medicine, Maastricht University

Dr. Niloofar Tahmasebi Birgani, an Assistant Professor at Maastricht University with a profound passion for biomaterials in regenerative medicine, earned her Master's degree in Biomedical Engineering with a specialization in Biomaterials at AmirKabir University of Technology in her homeland, Iran, back in 2009. She then pursued her PhD in the Tissue Regeneration department at the University of Twente in the Netherlands. Niloofar's doctoral research was a dedicated exploration of calcium phosphate-based biomaterials enriched with inorganic additives to promote essential bone regeneration processes, such as osteogenic differentiation and vascularization. Following the successful completion of her PhD, Niloofar embarked on a new adventure as a Biomedical Engineer and R&D Team Leader at Materiomics, a pioneering startup. There, her work revolved around the discovery of surface microtopographies that could influence cell behavior, ultimately dictating specific cell fates.

Driven by her ambitions for academic excellence, Niloofar made the decision to delve deeper into her research within an academic setting. In 2018, she began her post-doctoral journey at the MERLN Institute for Technology-Inspired Regenerative Medicine at Maastricht University, where her research focused on developing cutting-edge platforms for the biological screening of biomaterials in 3D, the advancement of microbiomaterials, and the bottom-up engineering of musculoskeletal tissues, with a particular emphasis on bone.

In 2020, she was awarded the NWO Incentive Grant for Women in STEM, and in 2022, she received the Maastricht Young Academy Interdisciplinary Grant. Currently, Niloofar is an Assistant Professor at the MERLN Institute, where her research pursuits encompass advanced technologies for crafting micro-scale biomaterials, utilizing biomaterials for regenerative therapies, advancing the field of bottom-up tissue engineering, and constructing *in vitro* miniaturized models, all with a strong emphasis on musculoskeletal tissues.

Bioprinting of bioactive human based hydrogels

Monize Caiado Decarli

The University Medical Center Groningen

Pursuing her interest for Biotechnology and Tissue Engineering, Monize completed her bachelor's and master's degrees in Biotechnology at Federal University of São Carlos (São Paulo, Brazil). During this time, Monize also acquired experience in the clinical environment. First, she did a clinical research training at the Cell-based Therapies at Medical School (University of São Paulo, Brazil). Subsequently, working in a multidisciplinary team at Butantan Institute (São Paulo, Brazil) aiming at developing a recombinant vaccine against rabies.

Due to her passion for human stem cells, in 2017 Monize embarked on a Double Doctoral PhD Degree Program between Maastricht University (The Netherlands) and University of Campinas (Brazil). Her research focuses on the use of stem cell spheroids for the biofabrication of cartilage tissues through 3D Bioprinting. More recently, she developed her post-doctoral project at the MERLN Institute for Technology-Inspired Regenerative Medicine (The Netherlands). As a key-member of the InterLynk European Consortium, she expanded her focus on innovative strategies for bioprinting bioactive hydrogels, such as embedding bioprinting and a multimaterial approach combining melt-electrowritting and bioprinting.

From January 2024 onwards, Monize will be starting as Principal Investigator at the Department of Biomedical Engineering, University Medical Center Groningen (UMCG). As the Group Leader in Bioprinting, she will be focusing on bioprinting bioactive hydrogels based on proteins, polysaccharides and extra vesicles, to be applied for the tissue regeneration of several tissues of the human body. Her carrier vision in science is to become a full professor in the biomedical translational field, converting science into practice to benefit human health.

Engineering the Dynamic Behavior of Hydrogels as Extracellular Matrix

Mani Diba

Regenerative Biomaterials–Dentistry, Research Institute for Medical Innovation, Radboud University Medical Center

Mani Diba is an Assistant Professor and a Hypatia Fellow at Radboud University Medical Center. He received a B.Sc. degree in Materials Engineering from Isfahan University of Technology and an M.Sc. degree in Advanced Materials and Processes from University of Erlangen–Nuremberg. He carried out his Ph.D. in the field of self-healing biomaterials at Radboud University Medical Center. After his Ph.D., he performed postdoctoral research at Eindhoven University of Technology, Rice University, and Harvard University. His research interests include bottom-up biomaterial design and biofabrication strategies.

Synergy of experiments and simulations to unravel new blood vessel formation

Tommaso Ristori

Biomedical Engineering Department, Eindhoven University of Technology (TU/e)

Tommaso Ristori is Assistant Professor at the Eindhoven University of Technology (TU/e), in the Biomedical Engineering Department. After receiving a joint MSc degree in Mathematics and Mathematical Engineering from the University of Florence (Italy) and Universidad Complutense de Madrid (Spain), Tommaso completed a PhD in Biomedical Engineering at the TU/e, with a thesis focused on the computational analysis of cell-mediated collagen remodelling. His experience at the TU/e continued then as a postdoctoral researcher, in strong collaboration with the Abo Akademi of Turku (Finland), developing computational models of cell-cell signalling mechanosensitivity underlying blood vessel remodelling. Tommaso then worked for two years at the Boston University (Boston, USA), funded by the NWO Rubicon and the Marie Sklodowska-Curie Fellowships, to perform research focused on blood vessel development via 2D and 3D cell culture techniques. In March 2021, he was appointed Assistant Professor at the TU/e, in the Biomedical Engineering Department.

Currently, Tommaso's research focuses on investigating blood vessel formation and designing regenerative medicine approaches to induce physiological vascularization of diseased and engineered tissues. Particular attention is devoted to the mechanobiology and cell signalling underlying sprouting angiogenesis, the process leading to the formation of new blood vessels from pre-existing ones. Controlling this process is not only the target of several medical therapies, but also key to enable the development of relatively large tissue-engineered constructs. To unravel the mechanisms of angiogenesis, Tommaso develops multiscale computational models synergistically integrated with targeted experiments, essential to inform and validate the simulations. Moreover, strategies to better leverage on this integration between simulations and experiments are also developed.

Oral Presentation Session 7

Miniaturized systems

Engineering a Biomimetic Glomerular Filtration Barrier Chip for Diabetic Nephropathy Modeling

M.G. Valverde[1], L. Wubbolts[1], J. Faria[1], T.K. van der Made[1], R. Masereeuw[1], S.M. Mihăilă[1]
[1] Division of Pharmacology, Utrecht Institute for Pharmaceutical Sciences, Utrecht University, Universiteitsweg 99, 3584 CG Utrecht, The Netherlands

Introduction: Diabetic nephropathy (DN) is a chronic microvascular complication of diabetes mellitus and is the leading cause of end-stage kidney diseases. One of the features of DN is proteinuria, protein leakage from the capillaries into urine caused by severe damage to the glomerular filtration barrier (GFB). Endothelial cells, glomerular basement membrane (GBM) and podocytes are the components of the GFB, and therefore, targets for the study of DN. While traditional *in vitro* DN models have offered valuable insights on GFB biology, they are oversimplistic, the cell-microenvironment interactions are limited and often do not allow transport studies [1]. Besides tuning the extracellular matrix and stiffness of the substrate [2], recent evidence suggests that podocytes are responsive to topographical cues, such as microscale curvatures [3]. In this study, we developed and characterized a 3D microphysiological model of the GFB by culturing conditionally immortalized podocytes (ciPODs) on hollow fiber membranes (HFM, 500 µm outer diameter) mounted in a perfusable chamber. The HFM provides topographical guidance to the ciPODs whilst allowing for perfusion studies in which apical and basal compartments are accessible. Guided by the surface curvature, the podocytes tightly surround the engineered barrier, similar to the podocyte-capillary interaction *in vivo*.

Methods: HFM were sterilized with EtOH, and biofunctionalized with subsequent coatings of L-DOPA and a collagen IV-laminin 511 blend for ensuring cell attachment. ciPODs were then seeded on the surface of the fiber and grown until forming a confluent layer (7 days, 33ºC) and further maturated (14 days, 37ºC) to develop the differentiated cell markers. Next, fibers were fixed and imaged with scanning electron microscope (SEM) to assess morphology, or immuno-stained for mature podocyte marker expression (nephrin, podocin, WT1, and ECM components) and imaged with confocal microscopy (**Fig. 1**).

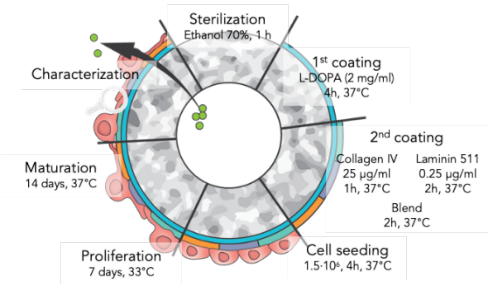

Figure 1: Biofunctionalization and cell seeding protocol.

Assembly of the HFM-GFB system in a chamber and perfusion of FITC-inulin (14kDa) and FITC-dextran (40kDa, 77kDa, 250kDa) allowed for determining the selectivity of the established barrier. Acute DN-like injury was modeled by exposing the HFM-GBF fibers to a high-glucose cocktail for 72h and marker expression and leakage were compared with control conditions.

Results: Upon coating optimization, the podocytes were able to form a cell layer around the fiber. While collagen alone was able to ensure cell attachment (75% coverage of the surface), the presence of laminin, another GBM component, rendered a >85% in cell coverage and a 1.3-fold increase in the number of cells attached (**Fig. 2A**). With the collagen-laminin blend coat, the cells show enhanced cellular protrusions (**Fig. 2B**), increased GBM deposition (collagen-IV, laminin-5) (**Fig. 2C**) and upregulated expression of known mature markers (nephrin, podocin) (**Fig. 2D**).

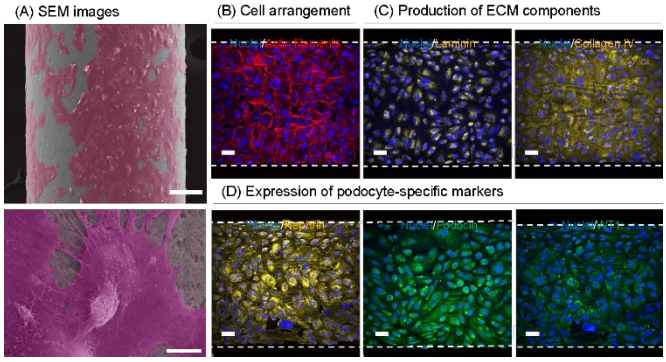

Figure 2: (A) Arrangement of cells (pink) in the fiber (grey) with SEM microscopy. (B) Actin arrangement of the cells in the fiber. Presence of GBM components (C) and expression of podocyte specific markers (D).

Furthermore, our model showed size selectivity comparable to the *in vivo* GFB, as proven by proteinuria assays based on a library of FITC-inulin and various molecular weigth FITC-labeled dextrans. Cell viability markers and sieving capacity were disrupted in DN conditions, induced by high-glucose exposure.

Conclusion: In conclusion, our novel curved substrate-based approach, combined with perfusion capabilities, offers an advanced *in vitro* model for mimicking the GFB of the kidney. The replication of physiological topographical cues and dynamic flow conditions provides a more accurate representation of the native microenvironment, enabling investigations into the barrier's structure, function, and response to injury. This model holds significant promise for advancing our understanding of kidney diseases and facilitating the development of targeted therapeutic interventions.

References

[1] Valverde, M, Nat. Rev. Nephrol. 2022
[2] Yaoita, E, Kidney Int. 93, 519–524. 2018
[3] Korolj, A, Lab Chip 18, 3112–3128. 2018

Bone Metastatic Spheroid Model for Preclinical Assessment of Novel Anticancer Drugs and Biomaterials

C.E. Suurmond[1*], R. Wang[1], M. Iafisco[2], N. Margiotta[3], M. Diba [1], J.J.P. van den Beucken[1], S.C.G. Leeuwenburgh[1]

[1]Department of Dentistry – Regenerative Biomaterials, Research Institute for Medical Innovation, Radboudumc, Nijmegen, The Netherlands. [2]Institute of Science, Technology and Sustainability for Ceramics (ISSMC, ex ISTEC), National Research Council (CNR), Faenza, Italy. [3]Dipartimento di Chimica, Università degli Studi di Bari Aldo Moro, Bari, Italy

INTRODUCTION

Prostate and breast cancer are primary cancer types that metastasize frequently and predominantly to bone. Direct treatment of bone metastases comprises chemotherapy combined with surgical resection, the latter creating a bone defect that requires filling with a suitable graft material[1]. Ideally, such bone graft material would have dual functionality by exhibiting both bone regenerative and anticancer efficacy toward remaining cancer cells. Recently, hydroxyapatite nanoparticles (nHA) loaded with the chemotherapeutic drug cisplatin have been proposed to achieve this dual functionality[2]. However, biomaterials with anticancer efficacy are currently evaluated using relatively simple 2D cell culture models that overestimate their efficacy due to limited resemblance of the 3D physiological bone tumor conditions[3]. Therefore, we previously developed an easy-to-use but clinically relevant 3D humanized bone metastatic spheroid model showing abundant cancer cell manifestation. Here, we aim to use this bone metastatic spheroid model to preclinically assess the therapeutic efficacy of cisplatin and cellular uptake of nHA in 3D.

MATERIALS AND METHODS

Primary human bone marrow stromal cells (hBMSC; stained with CellTrace CFSE green) were combined with prostate cancer (PC3) or breast cancer cells (MDA-MB-231; both stained with CellTrace Far Red), such that the cancer cells constituted 10% of the total cell population. The cells were then seeded in ultra-low attachment plates with 30 µg/mL of collagen type 1A to generate bone metastatic spheroids. Cisplatin was added at 10, 50, and 100 µM for a 24h exposure period. Subsequently, spheroids were imaged using confocal microscopy. nHA were prepared by mixing 83.5 mM $Ca(CH_3COO)_2$ with 50 mM Na_3PO_4, followed by aging for 24h at 60 °C under continuous stirring. nHA were then collected by centrifugation, thoroughly washed and diluted to 1 mg/mL. nHA were stained with IRDye 680RD overnight and subsequently supplemented to the media of bone metastatic spheroids at 25-100 µg/mL.

RESULTS AND DISCUSSION

Spheroids showed a dose-dependent response to cisplatin administration (Figure 1). Both types of cancer cells were more susceptible to cisplatin than hBMSCs, as evidenced by relative increase of green staining at higher cisplatin concentrations.

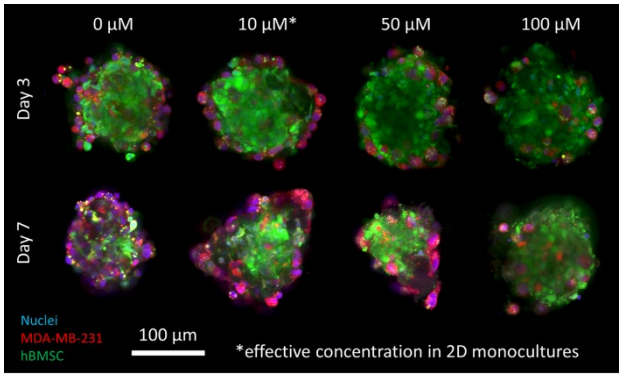

Figure 1: *Bone metastasis spheroids (hBMSCs (green), MDA-MB-231 (red), nuclei (blue)) treated with various concentrations of cisplatin imaged with confocal laser scanning microscopy after 3 and 7 days of culture.*

In addition, uptake of nHA by cells within the bone metastatic spheroids was observed after a 24h incubation period, suggesting that this spheroid model can be used for 3D preclinical evaluation of nanobiomaterials with anticancer activity (Figure 2).

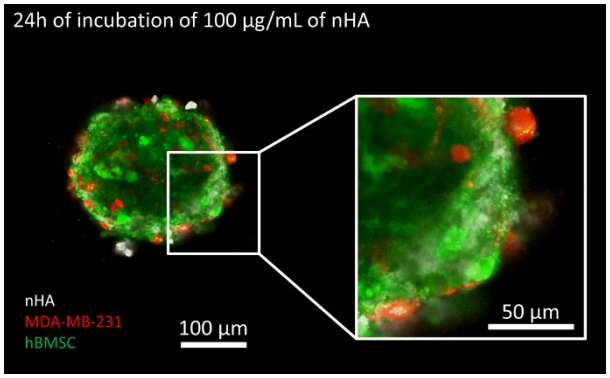

Figure 2: *Bone metastatic spheroid (hBMSCs (green), MDA-MB-231 (red), nHA (white)) showing uptake of nHA at 24h after nHA supplementation.*

CONCLUSIONS

The data presented here justify further validation of bone metastatic spheroids for screening of chemotherapeutic drugs and nanobiomaterials toward bone cancer treatment.

REFERENCES

1. Cooper DM, et al. Cortical Bone Porosity: What Is It, Why Is It Important, and How Can We Detect It? Curr Osteoporos Rep. 2016;14(5):187-98.
2. Nadar RA, et al. Preclinical evaluation of platinum-loaded hydroxyapatite nanoparticles in an embryonic zebrafish xenograft model. Nanoscale. 2020;12(25):13582-94.
3. Li F, et al. A bifunctional MXene-modified scaffold for photothermal therapy and maxillofacial tissue regeneration. Regenerative Biomaterials. 2021;8(6).

Fat Pad-on-chip: Advancing Adipose Tissue Modeling through 3D Culture, Mechanical Stimulation, and Disease Applications

A. C. Serrano Larrea, T. X. T. Le, B. Zoeteber, M. Karperien
Department of Developmental BioEngineering, Faculty of Science and Technology, University of Twente, The Netherlands

Organ-on-chip (OoC) technology has revolutionized the *in-vitro* modeling of human tissues, enabling more physiologically relevant studies and reducing reliance on animal models. This work introduces a novel Fat Pad-on-Chip (FPoC) platform that seamlessly integrates mechanical actuation and a soft hydrogel matrix to faithfully replicate the extracellular matrix (ECM) dynamics within adipose tissue. Tailored for disease modeling and drug testing, the FPoC enables detailed studies for its role in degenerative joint diseases.

This study focuses on the development of adipose tissue constructs utilizing hybrid hydrogels, specifically modified Hyaluronic Acid (HA), Dextran (Dex), and Gelatin (Gel) with tyramine (-TA) groups, in combination with either mesenchymal stem cells (MSCs) or adipose-derived stem cells (ADSCs). HA-TA, Dex-TA, and Gel-TA were synthesized with a degree of substitution of 13.3% per disaccharide, 10.2% per saccharide, and 18.9% per carboxyl group, respectively. A mixture of 1:1 HA-TA: Dex-TA was used to generate 1.25%, 2.5% and 5% w/v hydrogels, Gel-TA concentration of 0.05% w/v was constant in all the hydrogels. The mechanical properties of each concentration were assessed using rheology, yielding a storage moduli of 0.23 kPa, 0.85 kPa and 5.5 kPa, respectively. The 2.5% hydrogel (0.85 kPa) closely mimics the adipose tissue's native modulus (0.73 kPa). Subsequently, MSCs and ADSCs were encapsulated in each hydrogel formulation and assessed for cell viability, proliferation, and adipogenic differentiation potential. All the hydrogel formulations displayed high cell viability, with concentration-dependent cell migration and stretching.

The FPoC design incorporates microscale mechanical actuators to replicate the dynamic environment of the fat pad faithfully. Validation experiments are underway to evaluate adipocyte differentiation, lipid metabolism, and inflammatory responses within the microfluidic chip under static and actuated conditions. The integration of mechanical actuation significantly elevates the physiological fidelity of our FPoC, offering unprecedented utility for emulating adipose tissue behavior during joint movement compared to conventional static *in-vitro* models. Consequently, this technology holds immense promise for advancing our understanding of the fat pad in degenerative joint disorders.

In conclusion, our FPoC represents a significant advancement in *in-vitro* adipose tissue modeling. Its capacity to faithfully recapitulate the Fat Pad cellular microarchitecture and physiological function of adipose tissue positions our platform as a pivotal tool for disease modeling and drug testing applications.

Keywords: Organ on chip, fat pad, hydrogel, soft tissue, adipocytes.

How 3D microtissue formation directs chondrogenic lineage commitment of stem cells

M. Meteling[1], B. van Loo[1], C. Suurmond[1], M. Kern[1], K. Govindaraj[1], I. Meulenbelt[2], L. Geris[3,4], F.P. Luyten[3,4], Y.F.M. Ramos[2], L.S. Moreira-Teixeira[5], and J. Leijten[1]

[1] Leijten Lab, Department of Developmental BioEngineering, TechMed Centre, University of Twente, Enschede, The Netherlands. [2] Department of Biomedical Data Sciences, Section Molecular Epidemiology, Leiden University Medical Center, Leiden, The Netherlands. [3] Prometheus, Division of Skeletal Tissue Engineering, KU Leuven, Leuven, Belgium [4] Skeletal Biology and Engineering Research Center, Department of Development and Regeneration, KU Leuven, Leuven, Belgium. [5] Department of Advanced Organ Bioengineering and Therapeutics, TechMed Centre, University of Twente, Enschede, The Netherlands. Contacts: m.a.w.meteling@utwente.nl, jeroen.leijten@utwente.nl

Introduction: Three-dimensional (3D) cell culture sytems are known to mimic the native cell environement better, and elicit a more physiologically-relevant cell behavior. However, how 3D cell culture systems lead to this more native-like cell behavior, in terms of changes in intracellular processes, remains unclear. An often neglected parameter in cell culture systems is molecular crowding [1]. Specifically, intracellular molecular crowding which affects virtual all cellular processes including protein folding, enzyme kinetics, and gene transcription [2]. Surprisingly, the effect of 3D cell culture on intracellular crowding has remained largely unexplored. A well-known example of 3D cell culture augmenting cell function is microtissue culture of stem cells, which facilitates chondrogenic differentiation. Hence, we investigated how microtissue culture causes intracellular changes in stem cells facilitating chondrogenesis. Here, we demonstrate that cellular aggregation and subsequent 3D microtissue formation resulted in an increase of cellular crowding that altered cell metabolism and associated expression of transcription factors, which guided chondrogenic lineage commitment.

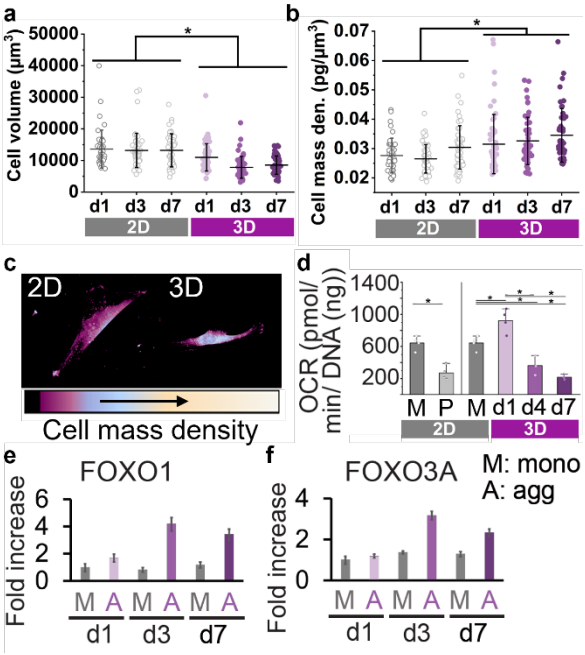

Figure 1: a) Cell volume decrease over time in aggregates (3D). b-c) Crowding increase in 3D compared to monolayer (2D). d) Decrease in ATP production in 3D over time. e-f) Increase in FOXO1/3A expression in 3D compared to 2D . d: day, P: PEG, mono: monolayer, agg: aggregates, * $p < 0.05$

Methods: Human periosteum derived stem cells (hPDCs) were seeded either in monolayer or agarose microwell inserts, containing microwells of 200 µm [3], at a seeding density of about 100 cells per microwell. The resulting aggregates were cultured in proliferation medium or chondrogenic differentiation medium. Inhibition studies were performed in both media. Aggregate size, cell size, and cell volume were investigated using brightfield and confocal imaging. Intracellular crowding was determined with flow cytometric and holotomographic microscopy analysis. Cellular metabolism was assessed with Seahorse assays. FOXO1/3A levels were determined with RT-qPCR, Western blot, and immunostaining. Mitochondria were assessed with MitoTracker staining and TEM imaging. Changes in RNA expression were assessed by RNA sequencing. Artificial crowding was performed with PEG300 or salt.

Results and Discussion: A transition from monolayer to aggregate culture was found to decrease cell volume and increase intracellular crowding (Figure 1a-c) and intra-organellar crowding (e.g. mitochondrial crowding). This associated with a reduced glycolysis rate and mitochondrial ATP production in aggregates (Figure 1d). The observed decrease in ATP-linked mitochondrial respiration could be emulated in monolayer by artificially crowding the cells (Figure 1d). Investigating the molecular mechanism, we revealed that the pro-chondrogenic transcription factors FOXO1 and FOXO3A were upregulated upon transition to 3D microtissue culture (Figure 1e, f). Moreover, inhibition of FOXO1 rescued the decrease in cell volume and inhibited chondrogenic differentiation. Also, inhibition of glycolysis resulted in increased cell volume and decreased FOXO expression.

Conclusion: In summary, we revealed that 3D microtissue culture alters both intracellular crowding levels and energy metabolism, and identified FOXO1 and FOXO3A as lead candidates for regulating the identified intracellular changes enhancing chondrogenesis in 3D microtissues. We thus revealed a new mechanism via which 3D cell culture regulates cellular function.

References

1. Ellis RJ. Trends Biochem Sci. 26 (2001)
2. Mourao MA, et al. Biophys J. 12 (2014)
3. Leijten J, et al. Scientific reports. 6 (2017)

Acknowledgements: Financial support was received from the European Research Council (StG, #759425) and the Dutch Research Council (Vidi Grant, #17522).

Engineering Tissue Microarchitecture: The Role of Cell Contractility and Matrix Properties

S. Pragnere, N.A. Kurniawan
Department of Biomedical Engineering, Eindhoven University of Technology, Eindhoven, 5600 MB The Netherlands
Institute for Complex Molecular Systems, Eindhoven University of Technology, Eindhoven, 5600 MB The Netherlands
s.c.m.pragnere@tue.nl

Introduction

Different tissue engineering methods are used to produce *in vitro* tissues that faithfully mimic *in vivo* tissues. Most studies adopt a "top-down approach" to produce 3D in vitro tissues: they embed the cells in a pre-defined geometry[1]. These approaches entail or even require a homogeneous distribution of the cells in the matrix. This is disadvantageous because it precludes control of the microarchitecture, which is important to replicate the function of native tissues, and therefore limits the biological relevance of the produced tissues[2]. For example, collagen fibers in the articular cartilage are parallel to the surface in the superficial zone, but transition to a perpendicular orientation in the deeper zone[3]. This organization is optimized to sustain the mechanical load that the tissue faces. Thus, it would be of particular interest to reproduce such a gradient of fiber organizations. Cells can generate traction forces on their surrounding fibers, which affects the alignment of the fibers in the matrix. Our aim is to use this specificity of the cells to control the micro-architecture of in vitro tissues. We hypothesize that it can be achieved by controlling: 1) the contractile phenotype of the cells and 2) the mechanical properties of their environment.

Materials and Methods

To control the contractile phenotype of the cells, we selected the BJ1 cell line (hTERT immortalized foreskin fibroblasts) as they lost their ability to express α-SMA fibers. To confirm their phenotype, cells were seeded in 96 multi-well plates and cultured for 7 days with 10 ng/mL TGF-β. Their α-SMA expression was evaluated by microscopy. To control the mechanical properties of their environment, we chose to work with collagen-alginate hydrogels. Cells were suspended in solutions of collagen, alginate and calcium sulfate ($CaSO_4$) at different concentrations and molded in 8 mm Teflon molds. Once the gels were crosslinked (90 minutes), culture medium was added to cover the gels. Contraction was measured for 14 days on macroscopic images of the gels. To evaluate the simultaneous impact of both environment and cell phenotype, cells were embedded in collagen-alginate hydrogels 1.5 mg/mL collagen, 5 or 10 mg/mL alginate and 5 mM $CaSO_4$ and contraction was measured for 14 days. After 14 days, 20 µM cytochalasin D was added overnight to disrupt the actin cytoskeleton.

Results

Our 2D experiments confirmed that BJ1 cells, unlike primary dermal fibroblasts, did not express α-SMA upon stimulation with TGF-β. However, they expressed strong actin stress fibers.
We identified two formulations of the collagen-alginate hydrogels that enabled cell spreading while limiting the macroscopic contraction of the gel without the addition of TGF-β: 1.5 mg/mL collagen, 5 or 10 mg/mL alginate and 5 mM $CaSO_4$. These two conditions were further selected to evaluate the impact of TGF-β on cell contraction. Even though BJ1 cells cannot express α-SMA fibers, they induced more contraction when stimulated with TGF-β, in both the 5 mg/mL and 10 mg/mL alginate gels (figure 1). Addition of cytochalasin D overnight after 14 days showed no release of the compaction of the gels, indicating that cells induced a plastic (permanent) deformation of the gels.

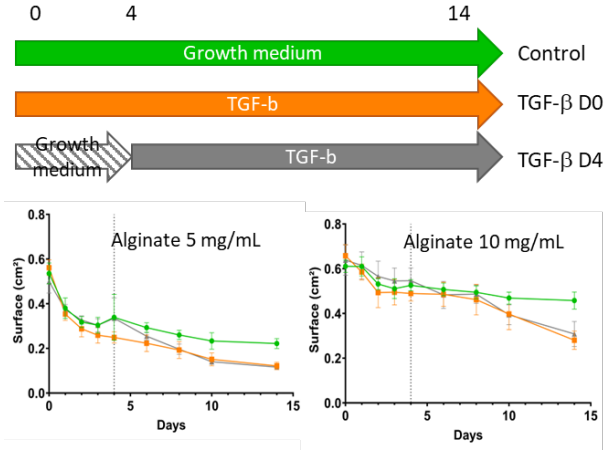

Figure 1:Effect of TGF-β on macroscopic contraction. TGF-β was added either from D0 or from D4 and cells were embedded in collagen-alginate gels with either 5 or 10 mg/mL alginate.

Conclusion

By controlling both the contractile phenotype of the cells and the mechanical properties of their environment, we were able to control the contraction rate of collagen-alginate hydrogels. Even though BJ1 cells do not differentiate in myofibroblasts upon stimulation with TGF-β, they still respond to it by increasing their contractility. We believe that this is the first step toward the control of the microstructure. Further experiments will focus on biofabrication methods that enable the precise positioning of the cells in the hydrogels to induce preferential fiber alignment through cell contraction.

References

1. Subramanian Sundaram & Christopher S Chen. Next-generation engineered microsystems for cell biology: a systems-level roadmap. *Trends in Cell Biology* (2022) doi:10.1016/j.tcb.2022.01.003.
2. Schot, M., Araújo-Gomes, N., van Loo, B., Kamperman, T. & Leijten, J. Scalable fabrication, compartmentalization and applications of living microtissues. *Bioactive Materials* **19**, 392–405 (2023).
3. Klika, V., Gaffney, E. A., Chen, Y.-C. & Brown, C. P. An overview of multiphase cartilage mechanical modelling and its role in understanding function and pathology. *Journal of the Mechanical Behavior of Biomedical Materials* **62**, 139–157 (2016).

OviChip : 3D in vitro Oviduct Model

J. Kim, E. Escarda Castro, M. Corrales Terron, R. Hoogenboom, L. Moroni, P. Wieringa
Department of Complex Tissue Regeneration, MERLN Institute for Technology-Inspired Regenerative Medicine, Maastricht University, Universiteitssingel 40, 6229 ER Maastricht, The Netherlands

Introduction: The increasing amount of research into the oviduct microenvironment signifies its importance not just as a passage for gametes and embryo, but as a location for early embryo's epigenetic reprogramming [1]. The oviduct luminal epithelium is composed of mostly secretory and ciliated cells, which is supported by underlying stroma. Secretory cells release various substances into the lumen to provide nutritional support for the gametes and embryo, while ciliated cells create fluid currents that facilitate their movement and transport [2-4]. Interestingly, the proportion of these two cell types changes along the tube, resulting in different functions within the oviduct as shown in Figure 1. Furthermore, fluctuations in female hormone levels induce alterations in the epithelium composition, with menstrual changes in estrogen and progesterone regulating the proliferation of secretory cells and the differentiation of secretory cells into ciliated cells [3-6]. The stroma, located beneath the epithelium, is composed of extracellular matrix components and various cell types including fibroblast, immune cells and nerves. Recent study on the crosstalk between oviduct epithelium and stroma has shown its importance in regulating protein expression within the epithelium and forming its microfold architecture. [7-9].

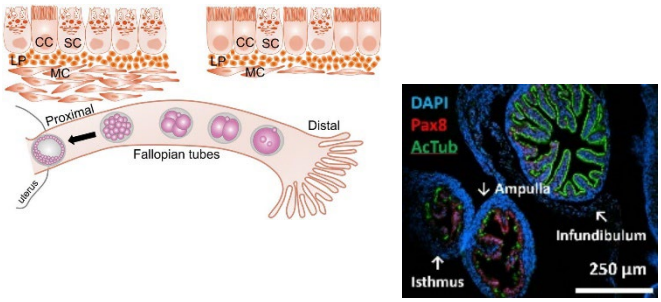

a. b

Figure1. a) Oviduct epithelium along the tube. b) histology of mouse oviduct. Pax8, a marker for secretory cell & AcTub, a marker for cilia. Image adapted from Reproduction 159, 3; 10.1530/REP-19-0189 [5].

Despite their importance, oviduct models to date have tended to focus on its epithelial aspect rather than incorporating essential stromal elements. This restricts accurate simulation of biological characteristics brought by its novel architecture such as alterations in cellular composition or disease progression along the tube [1, 10].
Therefore, we propose the development of a standardized and reproducible 3D in vitro oviduct model with multi-key compartments. This abstract outlines characterization of mouse oviduct epithelial organoid as cell source for the oviduct model, fabrication of the channel device, and finally, the oviduct model with biological complexity by introducing stroma and female steroid hormones within the system.

Materials and methods: Epithelial cells isolated from mouse oviduct were seeded in Geltrex dome to form organoids. When organoids were formed after 7 days in Geltrex, 1 µM dibenzazepine (DBZ) was added in organoid culture medium for 7 days. In parallel, a channel platform reflecting the isthmus structure of oviduct was fabricated by following steps. After bonding a coverslip on the bottom of polydimethylsiloxane (PDMS) device, the surface of the device was modified with 5% 3-aminopropyltriethoxysilane (APTES) and 1% glutaraldehyde. Then, ø 1 mm polyoxazoline filament was fixed within the middle-chamber of the device and 4.5 mg/ml bovine collagen type I with or without fibroblast was added embedding the filament. When the hydrogel was crosslinked, the device was cooled below lower critical solution temperature (LCST) triggering filament dissolution and formation of a channel. Afterwards, cells isolated from mouse oviduct epithelial organoids were seeded by gentle pipetting in the channel. When the lumen was completely covered with cells, hormones of interest (β-Estradiol and Progesterone) were added in the culture medium for 14 days.

Results & Discussions: Our result showed successful mouse oviduct epithelial organoid culture as evidenced by morphology and gene expression analysis responding to stimuli (DBZ). In parallel, the channel device with 4.5 mg/ml bovine collagen I showed similar stiffness to that of mouse oviduct found in the literature. Furthermore, our result successful cultivation of oviduct epithelial cells from the organoid and fibroblast within the device. Additionally, by exposing the device with female steroid hormones, we observed a responsive behaviour in epithelial cells within the channel.

Conclusion & Perspective: Our study highlights the potential of a channel device with epithelium-stroma interaction that can be used for hormone responsive 3D in vitro human oviduct model. Our next objective is the transition from mouse model to human model. In parallel, structural complexity will be added in the device such as fluidic system and auxiliary channel to better mimic the original tissue. Ultimately we expect to address inflammatory and fibrotic response observed during induced tubal infection within our device.

References:

[1] M. Ferraz et al., 2018, Nature communications, 9(1), 4934.
[2] S. Yuan et al., 2021, PNAS, 118 (22)
[3] M. Ford et al., 2021, Cell Reports Cell, 36, 109677.
[4] H. Yamanouchi et al., 2010, Biology of Reproduction, 82, 528-533
[5] B. Bartton et al., 2020, Reproduction, 159 R125–R137.
[6] Y. Chang et al., 2019, Journal of cancer, 10(13).
[7] R. Yokomizo et al., 2021, Stem Cell Research & Therapy, 12 :130
[8] A. J. Crawfold et al., 2023, bioRxiv preprint
[9] T. Umezu et al., 2004, Zoological Science, 21(3) 319-326.
[10] R. Heremans et al., 2021, Front. Cell Dev. Biol. 9:661472.

Oral Presentation Session 8

Modulating the immune response

Establishing Predictive Relationships Between *In Vitro* Macrophage Assays and *In Vivo* Implant Fibrosis

E.C. Alsema[1,2], J. de Boer[2,3], N.R.M. Beijer[1]
[1]Centre for Health Protection, National Institute for Public Health and the Environment (RIVM), Bilthoven, The Netherlands.
[2]Department of Biomedical Engineering, Eindhoven University of Technology, Eindhoven, The Netherlands.
[3] Institute for Complex Molecular Systems, Eindhoven University of Technology, Eindhoven, The Netherlands

Introduction

Medical implants, such as pacemakers, hip replacements or surgical meshes, are commonly used to treat a wide range of medical issues. The vast majority of patients benefit from these implants. However, some patients can develop health complaints, such as excessive fibrosis and chronic pain, despite rigorous preclinical testing. Many of these adverse effects are a result of the immune response to the implanted material, the foreign body response, which results in fibrotic encapsulation of the implant. Currently, it is difficult to screen for this adverse effect in early stage development of novel biomaterials as no validated, human biology-based models exist to predict this outcome. Our aim is to improve the predictivity of *in vitro* assays for fibrotic encapsulation. As this process is largely driven by the response of macrophages to the material surface, we focus on THP-1 derived macrophages as an *in vitro* model.

Approach

The performance of common *in vitro* read-outs, including cell attachment, cell death, metabolic activity and profile, and cytokine secretion (13-plex panel) is evaluated for a set of previously *in vivo* tested materials, selected as pairs of low vs high fibrosis materials. To increase the discriminatory power of the model, 18 different culture conditions are also screened for the potential to increase differences observed between materials, using one model material pair (polypropylene membranes with varying pore size). These conditions were based on signals present in the *in vivo* implant environment (e.g. TLR2/4 agonists, tissue injury factors or hypoxia) and expected to alter *in vitro* macrophage responses.

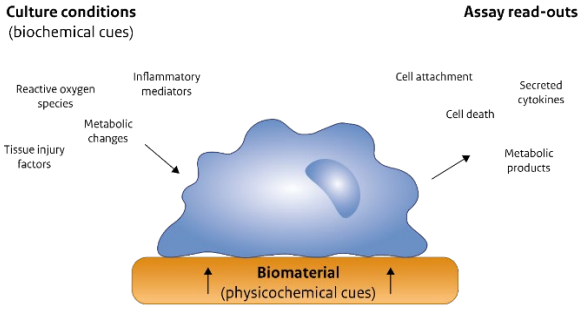

Results

For the first set of tested materials, no large differences in cell attachment, cell death or metabolic activity and profile were observed. Minor differences in cytokine secretion (TNF-a, IL-1b, IL1-RA) could be observed, but cytokine levels were generally low. In the screening of inflammatory conditions, several conditions that increased the level of cytokine secretion were identified, as well as conditions inducing secretion of additional cytokines not secreted by unstimulated macrophages (IL-6, CCL-17, CXCL-10). However, several of the cytokine secretion-inducing conditions (e.g. M1 stimuli) also reduced the differences observed between low vs high fibrosis materials, lowering the discriminatory power of the model.

Outlook

In further experiments, more material pairs will be evaluated to systematically correlate *in vitro* macrophage responses to *in vivo* fibrosis. The applicability of the identified culture conditions to other materials will also be tested.

The Interplay Between 3D Extracellular Matrix Organization And Macrophages During Tissue Remodelling

H.F.M. Brouwer[1,2*], T.B. Wissing[3*], N.H.M. van Hooren[2], C.V.C. Bouten[1,2], K. van der Heiden[3], J. Foolen[1,2], A.I.P.M. Smits[1,2]
[1] Department of Biomedical Engineering, Eindhoven University of Technology, Eindhoven, The Netherlands
[2] Institute for Complex Molecular Systems (ICMS), Eindhoven University of Technology, Eindhoven, The Netherlands
[3] Department of Biomedical Engineering, Cardiology, Thorax Center Erasmus MC, Rotterdam, The Netherlands

Introduction: During tissue repair, homeostasis is restored after functional remodelling of newly formed extracellular matrix (ECM) and the resolution of inflammation. Properly resolving this response is a complex and tightly regulated process.[1] Key players are the immune system, and macrophages in particular, ECM producing cells and ECM organization. Macrophage polarization into a spectrum of phenotypes is hypothesized to play an important regulatory role in ECM degradation and remodelling, and macrophage polarization has been shown to be influenced by steering their morphology.[2] However, it is not known to what extent ECM organization (aligned versus chaotic) affects macrophage polarization state and matrix remodelling capacity. Therefore, this study presents the design and validation of a 3D *in vitro* model, with either an anisotropic or isotropic structured ECM, that enables us to better understand and eventually steer macrophage remodelling behaviour in differently organized physiological matrices.

Methods: *In vitro,* 3D anisotropic and isotropic matrices were produced by human vena saphena cells (HVSCs)[3] by using respectively 2 or 4 constraints (Figure 1). Then the tissues were decellularized and re-seeded with macrophages. Collagen and collagen hybridizing peptide (CHP, indicative of collagen damage) staining, cellular (DNA), glycosaminoglycan (GAG) and hydroxyproline (HYP) assays, and qPCR were performed to characterize macrophage phenotype and tissue remodelling. A pilot experiment was performed for which THP-1 derived macrophages were seeded on the decellularized isotropic and anisotropic constructs and cultured for 6 days.

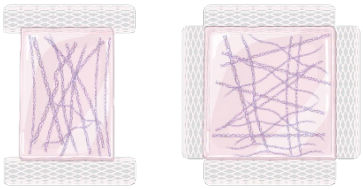

Figure 1. Graphic of in vitro 3D tissue engineered anisotropic (left) and isotropic (right) ECM models

Results and Discussion: After 21 days of culture, collagen fiber staining and quantification of its orientation indicates a clear anisotropic organization in the 2-constraint tissues (Figure 2A, in red) and an isotropic organization in the 4-constraint tissues (in blue). Quantitative tissue assays show negligible differences in DNA, GAG and HYP content per tissue weight between the anisotropic and isotropic samples (data not shown). Decellularization of the samples resulted in a 10-fold reduction of DNA content, while the detected GAG, and HYP content were not affected by the process (Figure 3). Initial results of THP-1 derived macrophages seeded on the decellularized tissues indicate that they introduce collagen damage (Figure 4).

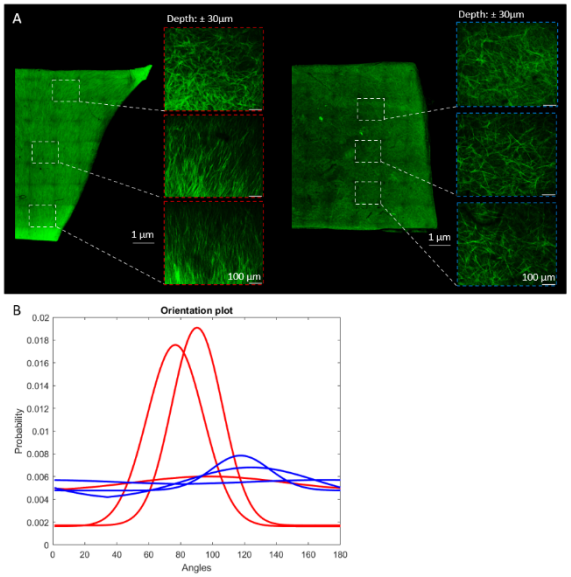

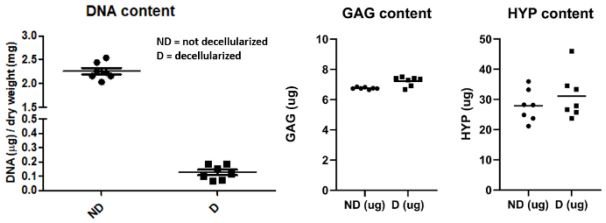

Figure 3. Quantification of the cellular content (DNA, µg) per tissue dry weight (mg), glycosaminoglycan content (GAG, µg), and hydroxyproline (HYP, µg) content.

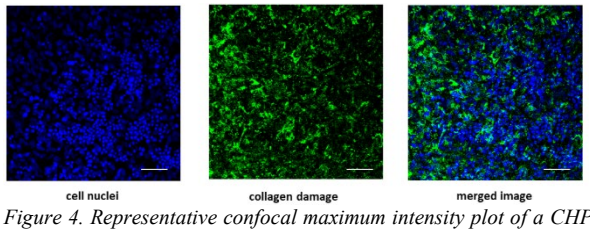

Figure 4. Representative confocal maximum intensity plot of a CHP-stained macrophage seeded tissue (day 6) showing collagen damage.

Outlook: We present decellularized isotropic and anisotropic ECM models that can be used to study the interplay between ECM organization and macrophages. Current work focuses on further assessing macrophage polarization, and macrophage-driven ECM remodelling. This will eventually help us identify the key mechanisms that should be steered to improve tissue healing.

References:

[1] Wissing et al. **(2017)** *NPJ Regenerative medicine.*
[2] McWhorter et al. **(2013)** *PNAS.*
[3] Wissing et al. **(2022)** *Scientific Reports.*

Contact details presenting author: h.f.m.brouwer@tue.nl
This research was financially supported by the Gravitation Program "Materials Driven Regeneration", funded by the Netherlands Organization for Scientific Research (024.003.013).

Incorporation of Copper Metal Framework Nanoparticles into Polymeric Microneedles to target the M1-type Macrophages

M.M. Lobita[1,2,*], Han Gao[1], Ruoyu Cheng[1,3], Gabriela Snachez[1,2], P. van der Meer[1], M.-A. Shahbazi[1,2], H.A. Santos[1,2,3]

[1] Department of Biomedical Engineering, University Medical Center Groningen, University Groningen, 9713 AV Groningen, The Netherlands
[2] W.J. Kolff Institute of Biomedical Engineering and Materials Science, University Medical Center Groningen, University Groningen, 9713 AV Groningen, The Netherlands
[3] Drug Research Program, Division of Pharmaceutical Chemistry and Technology, Faculty of Pharmacy, University of Helsinki, FI-00014, Helsinki, Finland
*Email: m.lobita@umcg.nl

Introduction

Myocardial infarction is one of the most common causes of early death in adults worldwide. Two inflammatory phases are present after MI. The M1 macrophages appear in a higher number, in the infarcted area, leading to a dysregulated inflammation, which interferes with cardiac repair[1].
Metal framework nanoparticles are crystalline porous materials with metal nodes linked by organic ligands. Copper is one of the most represented metal ions in the cellular system, showing high biocompatibility[2].
Furthermore, microneedles (MNs), a three-dimensional microstructure, are an outstanding transdermal delivery system capable of immunomodulation in a non-invasive and painless manner[3,4].
Our hypothesis relies on developing and fabricating dissolving MNs with suitable mechanical properties by micromolding method with the aim of piercing into skin barrier and delivering the desired cargos, Cu-MOF-NPs.

Materials and Methods

The selected method for MNs production was micromolding[5]. Firstly, the polymeric solutions were prepared and, afterwards, the same solution was poured into the top of the molds, followed by centrifugation and vacuum techniques. All the patches were removed from the molds after drying, visualized under bright field microscopy, and characterized using texture analyzer. Cu-MOF-NPs were characterized after production using transmission electron microscopy.

Results and Discussion

Different concentrations of the selected polymer were tested to form MNs with the proper characteristics. MNs arrays presented an average height of 690±19 µm. These MNs patches showed suitable mechanical properties being able to reach completely the fourth layer of Parafilm M® membrane with a depth of approximately 500 µm. All three types of MNs showed similar mechanical behavior (**Figure 1**A).

Conclusion

This preliminary data shows the successful formation of MNs with suitable properties, capable of reaching the desired layer to efficiently deliver the cargos.
We look forward to, after collecting all data, effectively delivering the Cu-MOF-NPs, while stimulating macrophage polarization in order to regulate inflammation.

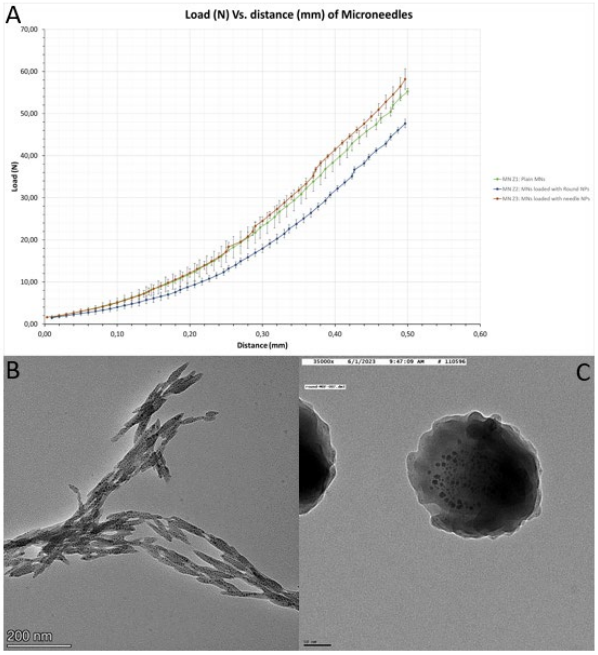

Figure 1: (A) Fracture Evaluation study of the three types of MNs: plain MNs, MNs loaded with round shape Cu-MOF-NPs, and MNs loaded with needle shape Cu-MOF-NPs. (B) and (C) transmission electron microscopy images form the needle shape Cu-MOF-NPs and round shape Cu-MOF-NPs, respectively.

Acknowledgments: This work was supported by the University Medical Center Groningen Research Funds.

References

1. Zhang, Q. *et al.* Signaling pathways and targeted therapy for myocardial infarction. *Signal Transduct. Target. Ther.* **7**, 78 (2022).
2. Kirandeep *et al.* Fabrication of novel copper MOF nanoparticles for nanozymatic detection of mercury ions. *J. Mater. Res. Technol.* **22**, 278–291 (2023).
3. Ali, M., Namjoshi, S., Benson, H. A. ., Mohammed, Y. & Kumeria, T. Dissolvable polymer microneedles for drug delivery and diagnostics. *J. Control. Release* **347**, 561–589 (2022).
4. Prausnitz, M. R. Engineering microneedle patches for vaccination and drug delivery to skin. *Annu. Rev. Chem. Biomol. Eng.* **8**, 177–200 (2017).
5. Sabbagh, F. & Kim, B. S. Recent advances in polymeric transdermal drug delivery systems. *J. Control. Release* **341**, 132–146 (2022).

Spatiotemporal Assessment of Pathophysiological Tissue Remodeling in Resorbable Synthetic In Situ Tissue-Engineered Heart Valves in Sheep

Sofia Artamonova[1,2], E. Middendorp[1,2], S. Dekker[1], B.J. de Kort[1,2], A. Lichauco[1], E.M. Brauchle[3], J. Kluin[4], E. Aikawa[5], K. Schenke-Layland[3], F.P.T. Baaijens[1,2], C.V.C. Bouten[1,2], S. Loerakker[1,2], A.I.P.M. Smits[1,2]

[1] Department of Biomedical Engineering, Eindhoven University of Technology, Eindhoven, The Netherlands
[2] Institute for Complex Molecular Systems (ICMS), Eindhoven University of Technology, Eindhoven, The Netherlands
[3] Department for Women's Health, University Women's Hospital, Tübingen, Germany
[4] Academic Medical Center, Amsterdam, The Netherlands
[5] Department of Medicine, Brigham and Women's Hospital, Harvard Medical School, Boston, MA, United States

Introduction: The use of acellular resorbable synthetic scaffolds to replace diseased heart valves represents a translationally attractive strategy, for which proof-of-concept has been shown in recent preclinical and clinical trials [1,2]. This strategy, also known as *in situ* tissue engineering (TE), involves the immune-driven process where a resorbable synthetic scaffold is gradually replaced by endogenous living tissue, directly *in situ* [3]. Notwithstanding the promising results obtained so far, the processes of inflammation-driven *in situ* tissue regeneration remain poorly understood and recent studies have reported on strong spatial heterogeneities in tissue formation and scaffold resorption, which makes outcome unpredictable [4]. Given that heart valves are continuously subjected to heterogeneous mechanical loads (cyclic stresses and strains), we hypothesized that the spatial heterogeneity in inflammation and tissue formation is, at least partly, driven by the variations in local stresses or strains. To test this hypothesis, the overall aim of this study was to map the spatiotemporal expression of neomatrix and cell phenotypes in our *in situ* tissue-engineered heart valve implants during long-term follow-up in a sheep model, and to correlate the expression patterns to the local stresses and strains as determined via computational modeling.

Methods: We performed a detailed retrospective analysis on the explanted *in situ* TE valves from one of our previous preclinical studies [1]. Upon implantation in the pulmonary position in sheep, 3/4 of the valves were functional over 12 months follow-up, with 1 valve showing grade 3 regurgitation. Paraffin-embedded longitudinal sections of explanted *in situ* TE heart valves, with 6 and 12 months follow-up (n=4 sheep timepoint), were analysed using Raman microspectroscopy and comprehensive immunohisto-chemistry (IHC). IHC analysis was performed using a dedicated sheep specific antibody panel (>40 antibodies) for valvular interstitial cell-, extracellular matrix-, elastogenesis- and inflammation-associated markers, which we recently developed and validated [5].
In order to correlate local marker expression in each individual explant to the local mechanical loads, finite element models were used to calculate local maximal-principal stresses and strains within the individual explants, using the measured mechanical properties and geometry of each individual explant as input.

Results and Discussion: Overall, the Raman spectra revealed progressive development of the newly formed matrix in the fibrosa and spongiosa layers of *in situ* TE valves towards their native counterparts. The ventricularis-like tissue in TE valves did not fully resemble the composition of native ventricularis due to the limited development of an elastic network. Degradation of the synthetic scaffold associated with inflammatory cell infiltrates was most pronounced in the remodeling area localized in the middle portion. Of note, Raman spectrometry was able to clearly identify the 12-month malfunctioned explant that was previously diagnosed as regurgitant. IHC analysis corroborated Raman spectra data and demonstrated an extensive expression of fibrotic-like markers in this specific valve, thus differentiating it from the other functional 12-month valves.
The local stresses and strains in the different regions of the valves showed increasing variation with prolonged implantation time. Over time, the local strains tended to increase, while stresses decreased. Strikingly, when correlating the local mechanics with the IHC marker expression, several cell markers were found to correlate positively with local strain, but not with the local stress. These included markers related to tissue formation (e.g. TGF-β1, TGF-β3, vimentin) as well as inflammation (e.g. IL-10, CD163, TNF-α).

Outlook: The observed differential marker expression between functional and regurgitant valves can provide us with a diagnostic set of histopathological biomarkers, which could discriminate between functional regeneration and pathologic fibrotic repair. Moreover, our findings suggest that strain is a dominant mechanical cue that drives the cell-driven transformation of the scaffold into a living valve and the differences in local stress in the neo-valve are mainly determined by differences in the underlying tissue formation and scaffold resorption. These findings enhance our mechanistic understanding of the inflammation-driven *in situ* regenerative processes and will contribute to our ability to design rationally engineered second-generation heart valve grafts with predictable long-term outcome, by creating valve designs with favorable mechanical loading patterns (e.g. by modifying valve geometry and/or microarchitecture).

References:

[1] Kluin et al. *Biomaterials.* 2017;125.
[2] Morales et al. *Front. Cardiovasc. Med.* 2021;7.
[3] De Kort et al. *Adv. Drug Deliv. Rev.* 2021;178.
[4] De Kort et al. *Acta Biomater.* 2021;135.
[5] Dekker et al. *Front. Cardiovasc. Med.* 2018;5.

Contact details presenting author: s.artamonova@tue.nl

Visible Light Responsive Reversible Photoacids-Based Core-Shell Nanogels for Antifouling Surface Coating

Y. Ji [1], G. Pacella [2], G. Portale [2], P. van Rijn [1]
[1] W.J.Kolff Institute for Biomedical Engineering and Materials Science, University of Groningen/ University Medical Center Groningen (UMCG), Ant. Deusinglaan 1, Groningen, The Netherlands
[2] Zernike Institute for Advanced Materials, University of Groningen, Nijemborg 4, 9747 AG Groningen, The Netherlands
y.ji@umcg.nl

Introduction

Surface fouling is a persistent problem across various industries, leading to reduced efficiency and increased maintenance costs. Prosthetic implants, biosensors, catheters, vascular stents, dental implants, and other medical equipment are prone to surface biofouling due to the adhesion of microbial or thrombotic agents. Infection from these biomedical devices and implants can lead to the death of the patient [1]. Traditional antifouling coatings often rely on toxic or environmentally harmful components, necessitating the development of environmentally friendly and sustainable alternatives. In the pursuit of innovative materials for combating surface fouling, we introduce a novel approach utilizing visible-light-responsive reversible photoacids (PAHs) based core-shell nanogels (nGels) as highly effective antifouling surface coatings.

Our core-shell nGels (named as pNIPMAM-*co*-PAHs nGels) are designed by PAHs and N-Isopropylmethacrylamide (NIPMAM) as copolymer shell binding to small volume NIPMAM core, providing a multifaceted approach to antifouling. The merocyanine-type PAHs can reversibly alter in an aqueous solution [2]. The shell material undergoes a reversible protonation and deprotonation process upon exposure to visible light, resulting in surface acidity changes that disrupt the adhesion and growth of fouling organisms and contaminants. Meanwhile, the highly hydrated state of these kinds of coatings is presumably a contributor to the antifouling effects due to the size increase of nanogels after visible light irradiation [3]. The phototunable nature of our nanogels allows for control over antifouling activity, promoting their versatility across various application domains.

Methods

This research outlines the synthesis, characterization, and performance evaluation of pNIPMAM-*co*-PAHs nGels as antifouling surface coatings. We aim to investigate their efficacy in deterring the adhesion of biofilms on different substrates. Furthermore, we are about to assess their stability, longevity, and environmental impact, highlighting their potential as sustainable alternatives to conventional antifouling methods.

Results

The PAHs are relatedly difficult to polymerize due to steric hindrance itself. In our work, we first formed a small volume of pNIPMAM core, and then PAHs were introduced by the copolymerization of NIPMAM comonomer on the surface of the pNIPMAM core. From TEM images, the pNIPMAM-*co*-PAHs nGels are spherical with fuzzy edges, monodispersed. The size varies from 400 nm to 200 nm as the PAHs uptake of nanogels increases.

Figure 1 (A) provides a visual representation of the photoreaction of the pNIPMAM-*co*-PAHs nanogels. To adhere these nanogels to glass substrates, we employed a straightforward, cost-effective, and time-efficient spraying deposition technique grounded in electrostatic interactions. This method utilized polyethyleneimine (PEI) as an anchoring polymer. Examining the surface coating with Atomic Force Microscopy (AFM) revealed dense coverage, depicting a tightly packed arrangement of the pNIPMAM-*co*-PAHs nanogels, as shown in Figure 1 (B).

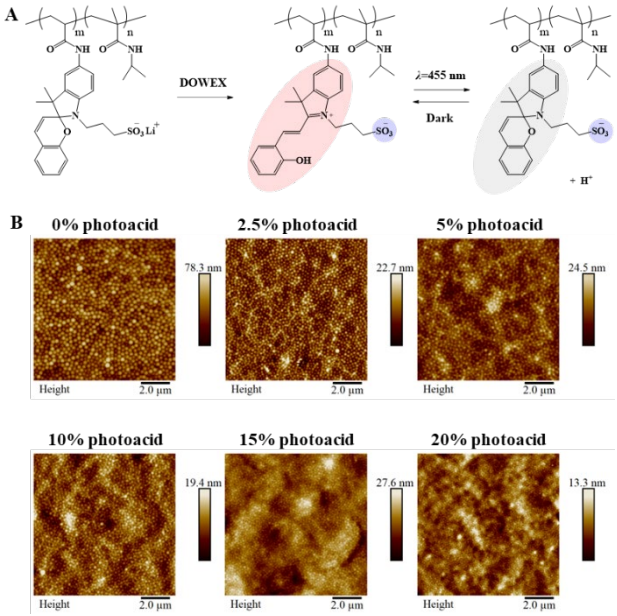

Figure 1 (A) Photoreaction of merocyanine PAHs nanogels. (B) AFM images of homogenous merocyanine PAHs nanogels.

Conclusion

The visible-light-responsive reversible PAHs-based core-shell nanogels presented in this study offer a promising avenue for developing next-generation antifouling surface coatings. In our upcoming research endeavors, our focus will be on further investigating the coating's multifaceted capabilities. Firstly, we aim to delve into its efficacy in resisting fouling. Secondly, we will rigorously evaluate its biosafety properties to ensure that it meets the highest standards for compatibility with biological systems.

References

[1] A. B. Asha et al. *Chem. Soc. Rev.* **2021**, *50*, 11668.
[2] V. K. Johns et al. *Chem. – A Eur. J.* **2014**, *20*, 689.
[3] D. Keskin et al. *Biomacromolecules* **2019**, *20*, 243.

Posters

Number	Name
1	**Hannah Abee, RIVM/Maastricht UMC** *In vitro assays for the effect of implant material on the host response to infection*
2	**Nancy Avila Martinez, Radboudumc** *Construction of fibrillar collagen and hyaluronan scaffolds and preliminary in vitro evaluation*
3	**Gizem Babuccu, Amsterdam UMC** *In vitro evaluation of novel antimicrobial peptides: potential synergy with human plasma*
4	**Cécile Bosmans, University of Twente** *Emulating physical dynamicity of arterial blood vessels and neighbouring tissue interaction*
5	**Maaike Bril, Technical University Eindhoven** *Protecting Your Precious: Dynamic Topographies Drive Nuclear Reorganization Events*
6	**Thijs Conner, Technical University Eindhoven** *To Fuse Or Not To Fuse: The Effect Of Polarization State On The Fusion Of Macrophages Towards Foreign Body Giant Cells*
8	**Hasnae El Showk, Technical University Eindhoven** *Investigating the Effects of Cyclic Strain on Macrophage Fusion and Multinucleated Giant Cell Formation*
9	**Enrique Escarda-Castro, Maastricht University** *Exploring the Dynamic Interplay of Neuroinflammatory Signals in the Intestine: Insights into Pro- and Anti-Inflammatory Cytokines and Neuropeptides*
10	**Tianqi Feng, University of Groningen/UMC Groningen** *Topography-mediated muscle engineering using Alginate-based scaffold*
11	**Micaela Fernandes, University of Groningen** *Microfabrication of high resolution poly(methyl methacrylate) (PMMA) microfluidic devices*
12	**Han Gao, University of Groningen/UMC Groningen/University of Helsinki** *Polysaccharide-based RNAi nanomedicine for promoting cardiac repair post-myocardial infarction*
13	**Amaia Garmendia Urdalleta, Erasmus MC** *Incorporation of osteoclasts into an in vitro model of mineralised cartilage in the context of endochondral ossification*
14	**Devlina Ghosh, University of Groningen/UMC Groningen** *A universal nanogel-based coating approach for medical implants*

15	**Anniek Gielen, RIVM/Amsterdam University** *In Vitro – In Vivo Predictivity of Osseointegration Markers*
16	**Madalena Gomes, Amsterdam UMC** *Proteomic analysis of primary human fetal, adult dermal and eschar mesenchymal cells and their secreted extracellular matrices*
17	**Esra Güben Kaçmaz, Maastricht University** *Mineralized Collagen Micro-blocks for Bottom-Up Bone Tissue Engineering*
18	**Yannick Hajee, Radboudumc** *Effect of Hydrogel Viscoelasticity on Osteogenic Differentiation of hMSC Spheroids*
19	**Jarno Hiemstra, University of Twente** *Bioinspired Hydrogels with Modulated Degradability for 3D Cell Encapsulation*
20	**Pardis Keikjosravani, UMC Utrecht** *Antibacterial Peptide-loaded Chitosan Nanoparticles to Treat Staphylococcus aureus Biofilm*
21	**Marlena Maria Księżarczyk, Utrecht University** *Distinct morphological differences in the osteochondral tissue of the humeral head between aquatic, semi-aquatic and terrestrial mammals*
22	**Nguyen Zuan Thanh Le, University of Twente** *Advancing Injectable Hydrogel Scaffold With Tyramine-Functionalized Chondroitin Sulfate For Cartilage Repair*
23	**Marie Loly, Maastricht University** *Unravelling Kidney Development by Reverse Engineering Branching Morphogenesis*
24	**Mattia Manenti, Technical University Eindhoven** *Analysis of the endothelialization of small-diameter in situ tissue-engineered vascular grafts; A systematic review*
25	**Amal Mansoor, Technical University Eindhoven** *Paracrine Effects of Macrophage Phenotype on Tendon Tissue Remodelling*
26	**Rob Meuwese, Radboudumc** *The effect of different sterilization methods on the expandable collagen plug in in vitro and ex vivo setups*
27	**Yu Na, University of Twente** *Improving Interfacial Adhesion Properties of Hydrogel Matrices to PDMS-based Microfluidic Platforms*
28	**Jet Peters, Technical University Eindhoven** *Influence of Tissue Growth on Collagen Orientation in Articular Cartilage*
29	**Madelief Rous, UMC Groningen** *Investigating the Interaction of Breast Implants and the Surrounding Tissue: An Introduction*

30	**Irem Soyhan, University of Groningen/UMC Groningen** *Polyhydroxyalkanoates as biodegradable polymeric biomaterials*
31	**Lennard Spauwen, UMC Utrecht** *Mechanical Anisotropic Properties in Biofabricated Cartilage Implants*
32	**Janne Spierings, Technical University Eindhoven** *Can macrophage polarization be an early indicator of outcome after ACL reconstruction?*
33	**Kaja Stradovnik, Technical University Eindhoven** *Exploring the Role of Morphogens in Adolescent Idiopathic Scoliosis*
34	**Mariana Harue Taniguchi Nagahara, Maastricht University/University of Campinas** *Wound Healing Electrospun Meshes Incorporating a Natural-based Arrabidaea chica Verlot extract*
35	**Laure van Hofwegen, Amsterdam UMC** *The bactericidal activity of a graphene quantum dot implant coating*
36	**Noemy Vergara Vera, Technical University Eindhoven** *Influence of macromolecular crowding on collagen I fibrillogenesis in 3D printing*
37	**Valentine Vetter, Technical University of Eindhoven** *Early host responses to in situ engineered heart valves*
38	**Margot Warin, Maastricht University** *Bioactive glasses vs Bacteria: Using the pH to Fight Infections in Long Bone Defects*
39	**Niels Willemen, University of Twente** *Steering Stem Cell Behaviour within 3D Living Composite Tissues using Stimuli-responsive Cell-adhesive Micromaterials*
40	**Hao Wu, Maastricht University** *Investigating the peripheral neurovascular interactions based on an in vitro model using melt electrowriting and collagen/fibrin hydrogel*
41	**Ruichen Zhang, University of Groningen/UMC Groningen** *Sustainability in clinical nanogel coating technology for combating central venous catheter infection*
42	**Yuewen Zhu, University of Groningen/UMC Groningen** *An Injectable Hydrogel Loaded with Dual-coated Nanoparticles for Wound Healing Application*
43	**Pavan Gudeti, The Silesian University of Technology** *Advancements in hydrogel-based inks for tissue engineering and regenerative medicine*
44	**Deeksha Rajkumar, Amsterdam UMC** *Novel Bioactive Glass S53P4 cream as a bactericidal coating to prevent Biomaterial-associated infections*

45	**David Rojas-Velazquez, Utrecht University** *Using Bayesian Optimization to Calculate Conductivity in an Electrolytic Fluid for the Forward Problem in Electrocardiography*
46	**Clara Soeiro Maas, UMC Groningen** *Biofabrication of Osteogenic Spheroids from Human Dental Pulp Stem Cells of Deciduous Teeth (SHEDs)*

In vitro assays for the effect of implant material on the host response to infection

Hannah. S. Abee[1,2], Chris J. J. Arts[2,3], , Nick R.M. Beijer[1]
[1]Centre for Health Protection, National Institute for Public Health and the Environment (RIVM), Bilthoven, The Netherlands.
[2]Department of Orthopedic Surgery, Maastricht University Medical Center Plus, Maastricht, the Netherlands.
[3]Department of Biomedical Engineering, Eindhoven University of Technology, Eindhoven, the Netherlands

Introduction

Bacterial infection is one of the most severe complications of orthopedic implants which often leads to implant failure [1]. In addition to the hard substrate of the implant, which provides an excellent substrate for bacterial adhesion and biofilm formation, the presence of the implanted foreign body leads to a dysregulation of the local immune system. This altered peri-implant immune system results in a decreased bacterial clearance capacity of the host and an increased risk for infection [2]. Currently, pre-clinical tests for novel implants mainly assess for biocompatibility in sterile environments. Additionally, the potential anti-infective properties of the implant are often tested for their direct anti-bacterial effect (e.g., bacterial killing, prevention of adherence). Currently no *in vitro* test models are established that include the effect of the implant on the hosts' own response to an infection. Here we explore several *in vitro* assays that might be used to evaluate the effects of the implant's mechanical characteristics on several immune cell functions (activation, phagocytosis, intracellular killing) in order to unravel underlying mechanisms and to more accurately predict the risk for implant related infection.

Approach and aim

The behavior of immune cells cultured on implant materials will be evaluated by looking at different aspects of the anti-bacterial response, including immune cell activation, phagocytosis, and intra-cellular killing. Our model consists of three main components: (1) the material, (2) the host, and (3) the bacteria. For the material, we use a titanium alloy (Ti6Al4V) with different surface structures (i.e., smooth and 3 levels of increasing roughness). This is a material that is already commonly used for hip implants in the clinic. The host is represented by human macrophages (THP1 cell line). Macrophages are key players in the host response to biomaterials, as well as the response to infection [3]. Additionally, macrophages are mechanosensitive and respond to surface structure, and change their behavior accordingly [4]. For the bacteria we use Staphylococcus aureus, the species that is the most common cause of implant related infection [5], in different conditions (i.e., heat-killed and live, as well as non-opsonized and opsonized with human serum). The aim is to develop *in vitro* assays that balance predictivity and complexity to more accurately predict the risk for implant associated bacterial infection *in vivo.*

Outlook

Currently, pre-clinical tests for innovative anti-infective implants are mainly focused on their direct anti-bacterial capacity by testing the effect of the material on bacteria. Additionally, separate tests are performed to determine the implants biocompatibility with the host without the presence of bacteria. Besides testing the implant for direct anti-bacterial activity and biocompatibility, future pre-clinical safety assessment might benefit from incorporating tests that assess the effect of the implant on the hosts' immune response to infection.

References

[1] Kaufman, Matthew G., Jesse D. Meaike, and Shayan A. Izaddoost. "Orthopedic prosthetic infections: diagnosis and orthopedic salvage." *Seminars in Plastic Surgery*. Vol. 30. No. 02. Thieme Medical Publishers, 2016.
[2] Riool, Martijn, and Sebastian AJ Zaat. "Biomaterial-Associated Infection: Pathogenesis and Prevention." *Urinary Stents: Current State and Future Perspectives*. Cham: Springer International Publishing, 2022. 245-257.
[3] Martin, K. E., & Garcia, A. J. (2021). Macrophage phenotypes in tissue repair and the foreign body response: Implications for biomaterial-based regenerative medicine strategies. *Acta biomaterialia*, *133*, 4-16.
[4] Chen, S., Jones, J. A., Xu, Y., Low, H. Y., Anderson, J. M., & Leong, K. W. (2010). Characterization of topographical effects on macrophage behavior in a foreign body response model. *Biomaterials*, *31*(13), 3479-3491.
[5] Bernard, Louis, et al. "Value of preoperative investigations in diagnosing prosthetic joint infection: retrospective cohort study and literature review." *Scandinavian journal of infectious diseases* 36.6-7 (2004): 410-416.

Construction of fibrillar collagen and hyaluronan scaffolds and preliminary *in vitro* evaluation

Nancy Avila-Martinez[1], Roman Krymchenko[1], Bouke Boekema[2], Marcel Vlig[2], Elly M.M. Versteeg[1], Toin H. van Kuppevelt[1], Willeke F. Daamen[1]

[1]Radboud university medical center, Radboud Research Institute for Medical Innovation, Department of Medical BioSciences, Nijmegen, The Netherlands

[2]Association of Dutch Burn Centers, Beverwijk, The Netherlands

Contact: Nancy.AvilaMartinez@radboudumc.nl

Introduction

Scars are formed after deep skin wound injuries like burns. The fetal skin microenvironment, however, allows for scarless skin regeneration without scarring and contraction[1]. An abundant component in the embryonic extracellular matrix is hyaluronan (HA).[2] It has been shown that hyaluronan helps to moisturize the skin and stimulate cell migration in excisional wounds.[3] To study whether biomaterials with hyaluronan improve wound healing, type I collagen scaffolds with and without hyaluronan were prepared and characterized. Fibrotic response was tested using fibroblasts focusing on α-smooth muscle actin (SMA) expression.

Materials & Methods:

Two different types of scaffolds were prepared from a suspension of type I collagen in 0.25 M acetic acid without (COL) or with 0.05% (w/v) of HA (COL-HA). Suspensions were frozen and lyophilized. Scaffolds were chemically crosslinked with 1-ethyl-3-(dimethyl aminopropyl) carbodiimide (EDC) and N-hydroxysuccinimide (NHS) and lyophilized again. Scaffold characterization included morphology by scanning electron microscopy (SEM), HA content by stains-all analysis, HA distribution by staining with biotinylated hyaluronic acid binding protein on cryosections, and extent of crosslinking by amine group quantification and differential scanning calorimetry assay.

For cell culture, Ø 12 mm gamma-sterilized scaffolds were evaluated with primary human dermal fibroblasts (hdFB) and a human fetal lung fibroblast cell line (HFL-1). Gene and protein expression of α-SMA was measured with RT-qPCR assay and Western blot, using GAPDH as a reference gene.

Results

Pore morphology did not alter after adding hyaluronan to the collagen scaffolds. Pores were roundish with a diameter mostly between 75-125 µm. Hyaluronan was successfully incorporated and evenly distributed through the scaffolds as indicated by immunostaining. The amount of incorporated hyaluronan was 92 ± 13 µg/mg. COL scaffolds and COL-HA scaffolds had a degree of crosslinking of 58 ± 6 and 67 ± 4 %, respectively, according to the reduction in amine groups. Chemical crosslinking increased the thermal stability by ~18 °C for both types of scaffolds.

Preliminary results showed that after 5-7 days of culturing, α-SMA decreased both at gene and protein level in HFL-1 cells. For primary human dermal fibroblasts, a similar trend was observed at gene expression level, but the protein was not detected after Western blotting.

Conclusion

Porous fibrillar collagen scaffolds incorporated with hyaluronan could be prepared. Preliminary *in vitro* results showed a reduced α-SMA gene expression for two types of fibroblasts. Further *in vitro* analysis with additional markers will be performed to evaluate the regenerative capacity of fibroblasts in these scaffolds.

Acknowledgement

The SkinTERM project has received funding from the European Union's Horizon 2020 research and innovation programme under the Marie Skłodowska-Curie grant agreement No 955722.

References

1. Lorenz *et al.*. Plast Reconstr Surg. 1995;96(6):1251-9.
2. Karppinen *et al*. F1000Res. 2019;8.
3. Tolg *et al.* PLoS One. 2014;9(2).

In vitro evaluation of novel antimicrobial peptides: potential synergy with human plasma

Gizem Babuccu[1], Jan Wouter Drijfhout[2], Robert A. Cordfunke[2], Martijn Riool[1*], Sebastian A.J. Zaat[1]

*[1]Dept. of Medical Microbiology and Infection Prevention, Amsterdam institute for Infection and Immunity, Amsterdam UMC, University of Amsterdam, [2]Dept. of Immunology, Leiden University Medical Center, Leiden, The Netherlands, *Current address: Laboratory for Experimental Trauma Surgery, Dept. of Trauma Surgery, University Hospital Regensburg, Regensburg, Germany.*

g.babuccu@amsterdamumc.nl

Introduction: The skin functions as a physical barrier against Gram positive and negative pathogens. Gram-negative bacteria are resistant to the action of many antibiotics due to their impermeable outer membrane. An important player of the immune system is the complement system, a protein network in the blood plasma and tissue fluids that directly kills Gram-negative bacteria through pore-formation by the Membrane Attack Complex (MAC). Once our skin is disrupted by wounding, microbial pathogens can gain access to tissues. Invasion of these microbial pathogens causes wound infection by degrading or damaging tissues through the production of a variety of enzymes and toxins. In order to treat wound infections, antibiotics are applied topically on open wounds; however, microorganisms are becoming resistant to conventional antibiotics at an alarming rate, and therefore alternatives are needed. One class of such novel agents for infected wound treatment are antimicrobial peptides (AMPs), which comprise a major component of the non-specific innate defense system in most multicellular organisms, forming the first line of defense against invading microbes.

Goal: In the present study, we aimed to determine whether the antibacterial activity of selected AMPs against *Acinetobacter baumannii* RUH875 was affected by blood components such as plasma, particularly by interaction with the complement system.

Method: A set of so-called "Leiden-Amsterdam Pearls" (LAP)-peptides were tested against *A. baumannii* RUH875 in RPMI-1640 medium [99.9% ($LC_{99.9}$)] in the absence or presence of human plasma. Then, a subset that had increased activity in the presence of the plasma were tested in a dose-dependent manner in the presence of different concentrations of pooled human plasma ranging from 1.56% to 50%, and in 50% heat-inactivated human plasma, which does not have a functional complement system anymore due to the heating.

Results: When we screened the LAP peptides in RPMI-1640 with and without 50% pooled human plasma, we observed that for some of the peptides, the plasma addition did not negatively affect the AMP's activity against *A. baumannii*, but on the contrary, the activity was enhanced in 50% plasma. The $LC_{99.9}$ of these peptides in RPMI-1640 ranged from 60 to 120 µM to *A. baumannii*. The $LC_{99.9}$of LAP-012, one of the best-performing peptides in plasma, in the presence of human plasma was between 3.75 – 7.50 µM (see figure). LAP-012 showed 8-fold enhanced activity even in the presence of as little as 1.56% plasma, and the best activity was seen in between 6.25% – 50% plasma concentration with an $LC_{99.9}$ of 3.75 µM.

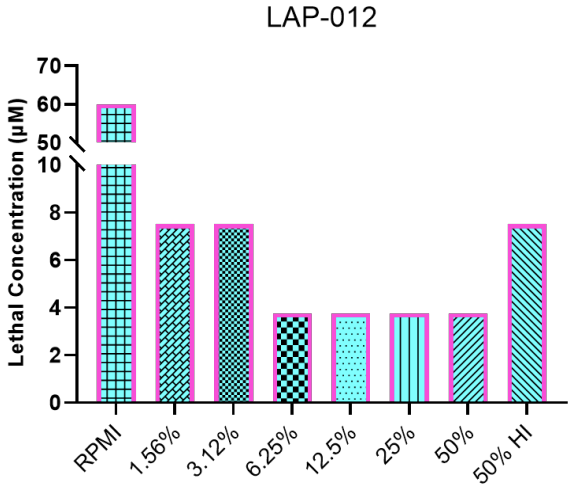

Figure: Bactericidal activity of LAP-012 in RPMI, in RPMI with 1.56 - 50% human plasma, and 50% heat-inactivated (HI) plasma against *A. baumannii* RUH875. Results are expressed as the lethal concentration ($LC_{99.9}$), which is the lowest AMP concentration that killed ≥99.9% of the bacteria within ≦24 hours compared to the inoculum.

When we inactivated the complement proteins in plasma by heat, the efficacy of LAP-012 with this plasma decreased to 7.5 µM.

Conclusion: We identified a set of peptides of which the activity against *A. baumannii* is potentiated by human plasma. As this potentiation was abolished when the plasma was heat-treated, inactivating the complement system, we hypothesize that synergistic interactions with complement likely are involved. In that case, a membrane attack complex formed by the complement system in the outer membrane might allow the AMPs to more easily reach their most likely target, the inner membrane. As a future direction, the effects of purified complement proteins, and inner and outer membrane damage will be investigated.

This project received funding from the Dutch Scientific Council (NWO) LIFT program (729.001.024) and has been supported by the STIMULUS project, European Union's Horizon 2020 research and innovation program under the Marie Skłodowska-Curie grant agreement No. 955664.

Emulating physical dynamicity of arterial blood vessels and neighboring tissue interaction

C. Bosmans[1], M. Becker[1], L. Moreira Teixeira[2], J. Leijten[1]
[1]Department of Developmental Bioengineering, University of Twente, Enschede, The Netherlands
[2]Advanced Organ bioengineering and Therapeutics, University of Twente, Enschede, The Netherlands

Vasodilation and vasoconstriction are inherent to the circulatory system as part of biological response to various stimuli [1]. While the engineering of multiscale, branched, and interconnected blood vessels has been a well-investigated challenge, mimicking the dynamic (e.g., dilating – deflating) behavior of native arterial vessels has remained understudied. In addition, reproducing the diffusion in pulsatile flow as well as the mechanical actuation transmitted by blood vessels to neighboring cells and tissues remains an unexplored area of research in the tissue engineering and organ-on-chip (OoC) fields.

Here, we utilized a highly elastic hydrogel composed of tyramine-conjugated alginate (A-TA) to enable controlled and reversible dilation during steady as well as pulsatile flow. The influence of pulse frequency on diffusion and dilation was investigated. This novel approach offers improved supply nutrition, which can prevent the formation of necrotic cores in larger organotypic cultures. Moreover, it represents an actuation approach that mimics native mechanical stresses caused by pulsatile blood flow, thus, enhancing differentiation and functionalization as a response to mechanical and biochemical cues [2-3]. The flow-related shear stresses are monitored by flow modelling to investigate the influence of the dilation onto the maximum shear within the channels. Furthermore, local stiffening (locally limiting the dilation) can be a potential tool to model disease phenomena, such as in stenosis or aneurysm.

The next step of this study is to integrate such dynamic biomaterial into an OoC platform for added complexity and dynamicity by diffusing nutrients and cyclically actuate the model, to ultimately emulate the effects of the arterial blood flow.

1 Fung, Y.-c. (1993) Biomechanics: mechanical properties of living tissues. Springer

2 Park, D., et al. (2020) Integrating Organs-on-Chips: Multiplexing, Scaling, Vascularization, and Innervation. Trends in Biotechnology 38, 99-112

3 Rouwkema, J., et al. (2008) Vascularization in tissue engineering. Trends in Biotechnology 26, 434-441

Protecting Your Precious: Dynamic Topographies Drive Nuclear Reorganization Events

M.J. Bril[1,2], J.N. Boesveld[1,2], L. Rato[3], C.M. Sahlgren[1,2,3] & N.A. Kurniawan[1,2]

[1] Department of Biomedical Engineering, Eindhoven University of Technology, PO Box 513 5600 MB Eindhoven, The Netherlands

[2] Institute for Complex Molecular Systems, Eindhoven University of Technology, PO Box 513 5600 MB Eindhoven, The Netherlands

[3] Faculty of Science and Engineering, Åbo Akademi University, FI-20520 Turku, Finland

Introduction *In vivo*, cells are surrounded by a dynamic extracellular matrix (ECM) that provides numerous physical and mechanical cues. For example, micro- to macroscale topographies can be found as small capillaries or brain tissue. Environmental factors, such as topography and stiffness, are known to affect nuclear morphology, epigenetic modifications and chromatin architecture. However, most *in vitro* studies lack the dynamic properties of the ECM and are thus a poor recapitulation of the native environment. Stimuli-responsive materials offer an attractive platform to investigate mechanobiological behavior of cells in a more dynamic setting. In this project, we examined the impact of dynamic topographies on nuclear morphology and epigenetic modifications in fibroblasts.

Materials & Methods We used a photoresponsive hydrogel, which can change its surface topography on demand when exposed to blue light, to subject fibroblasts to changing topographies. Human dermal fibroblasts (hDF) or vimentin depleted hDF were seeded on top and subjected to multiple rounds of topographical changes. Next, the morphology and distribution of fibroblast nuclei were investigated and examined for their histone acetylation and methylation levels using fluorescence microscopy.

Results & Discussion Fibroblasts compact and relocate their nuclei towards the static regions of the hydrogel, and increasing the frequency of topographical changes enhances this relocation effect. Vimentin intermediate filaments are found to be crucial for these nuclear relocation events. Moreover, genome-wide epigenetic levels were assessed, and dynamic topographies were found to affect global histone acetylation and methylation levels, possibly resulting in more condensed chromatin to protect the nuclear material against unwanted deformations. Preliminary results show that the observed changes in chromatin architecture result in a more quiescent-like fibroblast.

Conclusion To protect nuclear matter against unwanted deformations, fibroblasts compact and relocate their nuclei away from dynamic regions using vimentin intermediate filaments. Besides, dynamic topographies are associated with genome-wide changes in epigenetic modifications, thereby influencing cell fate. This knowledge can be useful for designing tissue engineering strategies.

To Fuse Or Not To Fuse: The Effect Of Polarization State On The Fusion Of Macrophages Towards Foreign Body Giant Cells

T.S. Conner*, B.J. de Kort, C.V.C. Bouten, A.I.P.M. Smits.
Department of Biomedical Engineering and the Institute for Complex Molecular Systems, Eindhoven University of Technology, Groene Loper 3 5612 AE Eindhoven, Netherlands
*email: t.s.conner@tue.nl

Introduction: Macrophages are important regulators of scaffold degradation and neo-tissue formation in *in situ* tissue engineering (TE) [1]. In addition to their remarkable plasticity, macrophages are also able to fuse together and form foreign body giant cells (FBGCs) that can degrade biomaterials with more efficiency than their unfused counterparts [2]. Macrophage fusion is known to be induced by IL-4 [3]. However, little is known about whether the macrophage polarization state (e.g. M0, M1, M2) play a role in FBGC formation and function. In this research, we investigated the effects of polarization on FBGC formation. This study was divided into two parts. In the first part, a robust culture protocol for the FBGC formation from primary human macrophages was established. In the second part, the optimized culture protocol was used to study the influence of macrophage polarization state on fusion potential. We hypothesized that due to the higher IL-4Rα expression on M1 macrophages, higher fusion rates would be obtained with M1 macrophages when stimulated with IL-4.

Methods: Human peripheral blood mononuclear cells (hPBMCs) were isolated from buffy coats from healthy donors. Subsequently CD14+ monocytes were isolated and depending on the experiment polarized into M0 (M-CSF), M1 (M-CSF, IFN-y, LPS), or M2 (IL-4, IL-13) macrophages. Polarization efficiency was confirmed using flow cytometry measurements for CD80 and CD206 expression, and RT-qPCR measurements for IL-6, CCR7, TNF-a, CD206, CD163, and IL-10expression. Furthermore, NOX2, LIPA, NFkB, CD44, CD47, SIRPa, and P2RX7 mRNA expression was measured with RT-qPCR, representing genes that are related to ROS and enzyme production, as well as cell fusion. After macrophage polarization, IL-4 was used to induce fusion into FBGCs. The same panel of genes was measured in combination with an MDA assay to measure the oxidative stress. Immunofluorescent images were made at different time points in the fusion process to quantify fusion. To establish the culture protocol, we compared different seeding densities and the use of RPMI-1640, MEM-α, human platelet lysate (hPL), and human serum (hS) on their ability to support FBGC formation.

Results: RPMI-1640 in combination with hS resulted in noticeably lower FBGC formation for each phenotype when compared to MEM-α conditions. The influence of serum additives was less impactful, with hPL seeming to have a slightly increased performance in supporting FBGC formation when compared to hS. Lastly, seeding density drastically impacted fusion, with too high densities leading to fusion even without stimulation and too low densities completely lacking any fusion. Having established a robust culture protocol, we then investigated the influence of macrophage polarization state on fusion potential. M1 macrophages had an increased expression of IL4Rα as expected. However, in contrast to our hypothesis, M1 polarization led to a significant reduction in FBGC formation upon stimulation with IL-4, when compared to M0 and M2 polarization. However, it must be noted that a large donor-to-donor variability was seen in terms of number and size of FBGCs. Interestingly, M1 macrophages before stimulation with IL-4 showed the highest relative expression of all cell fusion genes, highest expression of ROS and enzyme production genes, and seemed to have an increased oxidative stress, which is seemingly in contrast with the reduced number of FBGCs. Lastly, gene expression measurements on FBGCs did not show a clear pro- or anti-inflammatory phenotype, or upregulations in genes related cell fusion or ROS and enzyme production.

Discussion: In this study we explored the effects of culture conditions and phenotype on the formation of IL-4 induced FBGCs from primary human macrophages. Surprisingly, our results demonstrate a strong effect of basal medium choice on FBGC formation. Especially nucleosides and ascorbic acid are thought to be the most noteworthy differences between the basal media, as these have previously been shown to affect macrophage fusion towards osteoclasts. Surprisingly, M1 priming led to a reduction in FBGC formation, despite increase IL-4Rα expression. We suspect that this lack of fusion may be due to differences in metabolism or the inhibitory effects of LPS on fusion.

Conclusion: These findings contribute to our understanding of macrophage fusion and enable the development of robust, and potentially personalized *in vitro* models based on primary human macrophages to systematically unravel the processes of macrophage/FBGC-driven *in situ* TE.

This research was financially supported by the gravitation program “Materials Driven Regeneration”, funded by the Netherlands Organization for Scientific Research (024.003.013)

[1] De Kort & Koch et al. *Adv Drug Deliv Rev* 2021.

[2] Anderson, Rodriguez & Chang. *Semin Immunol* 2008.

[3] Helming & Gordon. *Trends Cell Biol* 2009.

Investigating the Effects of Cyclic Strain on Macrophage Fusion and Multinucleated Giant Cell Formation

Hasnae El Showk[1,2], B.J. de Kort[1,2], T.S. Conner[1,2], L. Angeloni[1,2], C.V.C. Bouten[1,2], A.I.P.M. Smits[1,2]

[1] Department of Biomedical Engineering, Eindhoven University of Technology, Eindhoven, The Netherlands
[2] Institute for Complex Molecular Systems (ICMS), Eindhoven University of Technology, Eindhoven, The Netherlands

Introduction:

Macrophages play a crucial role in orchestrating inflammation and tissue repair [1]. They are highly versatile cells whose behavior and phenotype is mainly dictated by their microenvironment. While much is known about the effect of biochemical cues on macrophage behavior, the effect of mechanical cues has been largely neglected. Macrophage fusion and subsequently multinuclear giant cells (MNGCs) formation, is a behavior that is characteristic of the Foreign Body Response, in response to persistent presence of a foreign material, such as a medical implant, in the body. MNGCs play key roles in fibrous encapsulation and production of degradative molecules, such as reactive oxygen species (ROS) and enzymes. Consequently, when derailed, MNGCs can cause implant failure. Strong spatial heterogeneity in the presence of MNGCs observed in previous preclinical studies with *in situ* TE heart valves [2], suggests that mechanical cues and specifically cyclic strain might influence MNGC formation. Macrophage fusion is a very complex and understudied process which involves biochemical stimuli and cytoskeletal rearrangements [3, 4], both of which are known to be influenced by cyclic strain. Therefore, the goal of this study was to investigate the influence of cyclic strain on MNGC formation.

Methods:

Primary human macrophages were isolated from peripheral blood-derived buffy coats from anonymized healthy donors (Sanquin, Nijmegen). Pre-polarized macrophages were exposed to low (<10%) and high (>10%) uniaxial strains while simultaneously being stimulated with interleukin-4 (IL-4) to induce fusion. After 1 and 3 days of dynamic culture, macrophage morphology, podosome formation and fusion were assessed using cytoskeletal stainings (actin, tubulin, vimentin), as well as integrin stainings. Furthermore, we analyzed cell phenotype (qPCR) and ROS production (MDA assay) as a measure for degradative capacity.

Results and Discussion:

Cyclic strain did not show any significant effect on the formation of MNGC in the presence of IL-4 stimulation (Fig. 1). Neither the fusion index nor the size of MNGCs showed any significant differences in the different strain conditions. However, both unfused macrophages and MNGCs showed mechanosensitive behavior by aligning in the direction of the applied strain, especially in high strain conditions (Fig. 1). Moreover, immuno-fluorescence imaging showed higher expression of podosome-rich regions in MNGCs compared to their unfused counterparts and gene expression of macrophages/MNGCs indicated a possible effect of strain on the expression of genes involved in degradation and fusion.

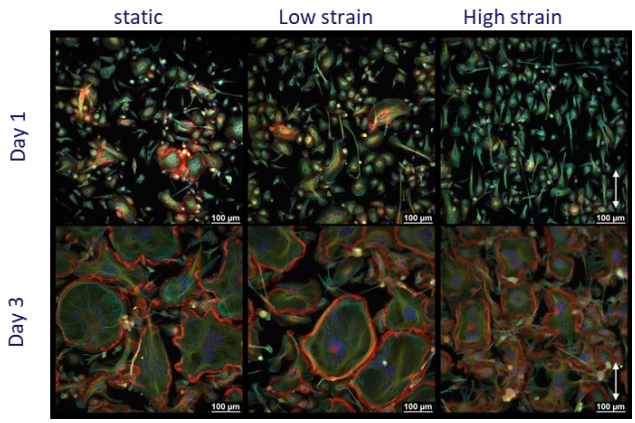

Fig. 1. Cytoskeletal rearrangements of primary human macrophages exposed to static or cyclic strain conditions for 1 or 3 days, with tubulin (green), actin (red) and cell nuclei (blue). All samples were stimulated with IL-4 to induce fusion. Arrows indicate the direction of strain.

Despite the fact that no effect of cyclic strain was observed on MNGC formation, the results indicate that MNGCs are able to sense mechanical strain and that cytoskeletal rearrangement plays an important role in fusion and MNGC formation. However, further investigation is needed to confirm these observations. A possible explanation for the lack of effect of cyclic strain on MNGC formation is the potent role that IL-4 seems to play in the fusion of macrophages, overruling the effects of cyclic strain. Therefore, the next step should be to decouple the effect of cyclic strain and IL-4 on macrophage fusion. This would enable a better understanding of the effects of cyclic strain on fusion and MNGC formation including the pathways involved in this complex process.

Acknowledgements:

This research was financially supported by the Gravitation Program "Materials Driven Regeneration", funded by the Netherlands Organization for Scientific Research (024.003.013) and by the European Union, ERC Starting Grant 101042538 'MACxercise'.

References:

[1] Wissing et al. *NPJ Regen. Med.* 2017;2:18.
[2] De Kort et al. *Acta Biomater.* 2021;135:243.
[3] Helming & Gordon. *Trends Cell Biol.* 2009;19:514.
[4] Faust et al. *Mol. Biol. Cell.* 2019;30:2254.

Contact details presenting author: h.el.showk@tue.nl

Exploring the Dynamic Interplay of Neuroinflammatory Signals in the Intestine: Insights into Pro- and Anti-Inflammatory Cytokines and Neuropeptides

E. Escarda-Castro, L. Moroni, P. Wieringa

MERLN Institute (Maastricht University), Universiteitssingel 40, 6229 ER Maastricht / Room C3.577, The Netherlands

Introduction

The intestine is a major organ of the body with incredible homeostatic capacity, being able to self-regulate multiple aspects such as cell differentiation and barrier integrity. However, it operates within a dynamic interplay influenced by external regulation coming from the peripheral nervous system (PNS) and the immune system. Currently, the precise contributions of these regulatory elements, as well as their interplay, remain unclear and are only partially understood. In this study, we aimed to unravel the complex neuroinflammatory interplay between pro- and anti-inflammatory cytokines and neuropeptides within the intestinal microenvironment, deciphering the role of the PNS in inflammation and immune regulation in the gut.

Materials and Methods

We selected differentiated Caco-2 monolayers, a well-established model of the intestinal epithelium. For the cytokine stimulation of the monolayers and mimicking the role of the immune system, we selected a panel of pro- and anti-inflammatory cytokines. Specifically, we chose TNF-α, IL-1β, and IFN-γ as pro-inflammatory signals known for their roles in promoting intestinal inflammation. In contrast, we included IL-10, recognized as an anti-inflammatory cytokine crucial for maintaining immune balance and suppressing excessive inflammation [1]. As neural signals on the intestine and aiming to uncover their potential involvement in intestinal neuroinflammatory signaling, we selected different neuropeptides secreted by the PNS: Substance P, VIP, CGRPα, CGRPβ, and NPY. By studying the effects of neuropeptides in different inflammatory states induced by cytokines, we seek to reveal their specific contributions to inflammation, immune responses, and gut homeostasis.

We evaluated the intestinal epithelium model in terms of metabolic activity and performed cell viability assessments to understand the impact of neuropeptides on epithelial cell function. Additionally, we measured the release of IL-6 and IL-8 from intestinal epithelial cells. Epithelium-secreted IL-6 has both pro-inflammatory and anti-inflammatory effects, while IL-8 acts as a potent chemoattractant for immune cells. These readouts provide valuable insights into the effects of neuropeptides on cellular viability, inflammatory mediators, and the intricate interplay between neuroinflammatory signaling, epithelial function, and immune regulation in the intestine.

Results and Discussion

As a starting point, we studied the effects of the cytokines in the intestinal epithelium, and we selected working concentrations and combinations for the following experiments. Then, we defined 4 possible scenarios for the neuropeptide studies: basal, in which there were no cytokines present; pro-inflammatory, with the presence of TNF-α, IL-1β, and IFN-γ; anti-inflammatory, with just the presence of IL-10; and resolving, in which both pro- and anti-inflammatory cytokines were present.

By exposing the intestinal epithelium monolayers to different cytokines in different inflammation contexts, we aimed to find the contributions of each neuropeptide to each specific state. Our findings revealed distinct responses of the epithelium to CGRPα and CGRPβ, highlighting their unique characteristics despite their similar nature as peptides. Even though they have been treated as equivalent in the literature, CGRPα responses seem to stimulate inflammation, and CGRPβ seems to mitigate it [3]. Additionally, while VIP is generally considered an anti-inflammatory factor in the intestine, our research demonstrated its contribution to the inflammatory environment under pro-inflammatory scenarios [4]. On the other hand, Substance P appeared to have a minor role in intestinal inflammation. Interestingly, NPY exhibited pleiotropic effects, with its impact on inflammation being dependent on the specific conditions under investigation, demonstrating its complexity in modulating inflammatory responses.

Conclusion

Our study revealed intriguing and unexpected roles of neuropeptides in various inflammatory environments within the intestinal epithelium. Notably, we reported distinct behaviors of the neuropeptides, demonstrating their responsiveness to the inflammation state of the epithelium. These new findings demonstrate the complex functions of neuropeptides in intestinal inflammation, while highlighting their context-dependent roles in the epithelium.

References

[1] Andrews, C., McLean, M. H., & Durum, S. K. (2018). Cytokine Tuning of Intestinal Epithelial Function. *Frontiers in immunology*, *9*, 1270. https://doi.org/10.3389/fimmu.2018.01270

[2] Wei, P., Keller, C., & Li, L. (2020). Neuropeptides in gut-brain axis and their influence on host immunity and stress. *Computational and structural biotechnology journal*, *18*, 843–851. https://doi.org/10.1016/j.csbj.2020.02.018

[3] Russell, F. A., King, R., Smillie, S. J., Kodji, X., & Brain, S. D. (2014). Calcitonin gene-related peptide: physiology and pathophysiology. *Physiological reviews*, *94*(4), 1099–1142. https://doi.org/10.1152/physrev.00034.2013

[4] Iwasaki, M., Akiba, Y., & Kaunitz, J. D. (2019). Recent advances in vasoactive intestinal peptide physiology and pathophysiology: focus on the gastrointestinal system. F1000Research, 8, F1000 Faculty Rev-1629. https://doi.org/10.12688/f1000research.18039.1

Topography-mediated muscle engineering using Alginate-based scaffold

Tianqi Feng, Roderick H.J. de Hilster, L.E. Tromp, T.A.B. van der Boon, Patrick van Rijn
W.J. Kolff Institute for Biomedical Engineering and Materials Science, University of Groningen/ University of Groningen, University Medical Center Groningen, Deusinglaan 1, 9713 AV Groningen, The Netherlands
t.feng@umcg.nl

Introduction: Facial palsy, the paralysis of facial muscles, is a major social burden for affected patients which profoundly alters an individual self-image and ability to communicate and express emotion.[1-3] One of the efficient treatment approaches of facial palsy is muscle engineering which means using biological scaffolds combined with bioactive tissues or cells in order to repair or construct tissue or organ[4]. Skeletal muscle tissue engineering is a promising alternative to traditional volumetric muscle loss surgical treatments that use autogenic tissue grafts, and rather use isolated stem cells with myogenic potential to generate new skeletal muscle tissues to treat volumetric muscle loss[5]. Biological scaffolds used for medical implants, tissue engineering scaffolds, not only provide structural support for the promotion of cellular ingrowth but also impart potent modulatory signaling cues that may be beneficial for tissue regeneration[6]. Among the different kinds of materials, Alginate act as an efficient and popular natural material could form egg-box model in micro-size and gelate in the presence of calcium ions[7].

So the main idea is essentially to combine bio-interfaces to explore the full potential of existing clinical biomaterials currently serving as implants and tissue scaffolds. Using modified-scaffolds would offer control over cellular arrangement, differentiation and functions and yield a construct that closely resembles natural striated muscle. Combining applicable physical surface parameters with Alginate-based hydrogels will drive differentiation and align all three essential constituents of muscle i.e. myofibers, vasculature and neurons[8-9] and bring these into contact with each other.

Key words:
Muscle tissue engineering, Biological scaffolds, Alginate

Method: Imprint technology is used to prepare hydrogel wrinkle topography to form topography surface of hydrogel This approach will function as a screening platform together with altering the stiffness via cross-linking to determine the influence on cells of combined parameters and thereby offering a superior choice of biomaterial properties. We aim to explore the full potential of existing clinical Alginate sources to greatly enhance the clinical translation.

Results and Discussion: Topography Mediating biomaterial surface character could endow new functions for Alginate-based materials to direct cellular behavior to a great extent as excellent biocompatible biomaterials and implant. Transferring topography from PDMS to Alginate-based material through Imprint technology worked well. It is expected that the wrinkled Alginate-based hydrogels will provide the optimum bio-interface for offering striking detailed insights for cell behavior towards enabling it to be transferred to clinical applications such as the development of implantable tissue-engineered constructs.

Conclusion: The approach will explore full potential of Alginate-based material, which could increase new function and diminish implant associated medical complications as a secondary problem and thereby reducing implant impairment as well as lowering patient morbidity and mortality.

References:

1. Langhals NB, Urbanchek MG, Ray A, Brenner MJ. Update i n facial nerve paralysis: tissue engineering and new technologies. Curr Opin Otolaryngol Head Neck Surg. 2014 Aug;22(4):291-9.
2. George E, Richie MB, Glastonbury CM. Facial Nerve Palsy: Clinical Practice and Cognitive Errors. Am J Med. 2020 Sep;133(9):1039-1044.
3. O TM. Medical Management of Acute Facial Paralysis. Otolaryngol Clin North Am. 2018 Dec;51(6):1051-1075.
4. Nakayama KH, Shayan M, Huang NF. Engineering Biomimetic Materials for Skeletal Muscle Repair and Regeneration. Adv Healthc Mater. 2019 Mar;8(5):e1801168.
5. Pantelic MN, Larkin LM. Stem Cells for Skeletal Muscle Tissue Engineering. Tissue Eng Part B Rev. 2018 Oct;24(5):373-391.
6. Lenci E, Menchi G, Saldívar-Gonzalez FI, Medina-Franco JL, Trabocchi A. Bicyclic acetals: biological relevance, scaffold analysis, and applications in diversity-oriented synthesis. Org Biomol Chem. 2019 Jan 31;17(5):1037-1052.
7. dos Santos Araújo P, Belini G B, Mambrini G P, et al. Thermal degradation of calcium and sodium alginate: A greener synthesis towards calcium oxide micro/nanoparticles[J]. International journal of biological macromolecules, 2019, 140: 749-760.
8. Andrew, Dunn, Muhamed, et al. Biomaterial and stem cell-based strategies for skeletal muscle regeneration.[J]. Journal of Orthopaedic Research Official Publication of the Orthopaedic Research Society, 2019.
9. Xie Y, Schneider KJ, Ali SA, Hogikyan ND, Feldman EL, Brenner MJ. Current landscape in motoneuron regeneration and reconstruction for motor cranial nerve injuries.

Microfabrication of high resolution poly(methyl methacrylate) (PMMA) microfluidic devices

M. Fernandes[1,*], W.Meshabi[2], M.M.G. Kamperman[1], O. Fournier[2], H.A. Santos[3,4], M.K. Wlodarczk-Biegun[1,5]

[1]Zernike Institute for Advanced Materials, University of Groningen, Nijenborgh 4, 9747 AG Groningen, The Netherlands
2 Elvesys Microfluidic Innovation Center, 75011 Paris, France
3 Department of Biomedical Engineering, University Medical Center Groningen, University Groningen, 9713 AV Groningen, The Netherlands
4 Drug Research Program, Division of Pharmaceutical Chemistry and Technology, Faculty of Pharmacy, University of Helsinki, FI-00014, Helsinki, Finland
5 Biotechnology Centre, The Silesian University of Technology, Bolesława Krzywoustego 8, 44-100 Gliwice, Poland
*Email: m.gaspar.goncalves.fernandes@rug.nl

Introduction Microfluidics is the science and technology that manipulates fluids at the micrometer or nanometer scale[1]. In recent years, microfluidics-based technology, such as microfluidic devices, offered a tremendous technological breakthrough for various applications, namely biomedical research, diagnostics, drug encapsulation and delivery, cell analysis, and organ-on-a-chip[2]. These consist of a precise network of micro-sized channels, molded or engraved where the fluids are directed, separated, mixed, or manipulated. Advantages of microfluidic devices include analysis, use, and handling of less volume of samples, fast reaction time, enhanced analytical sensitivity, portability, easier automation, and parallelization.

Materials and Methods Material selection is a crucial part of the design process since it can affect the flow, biocompatibility, and absorptivity of microfluidic chips[3]. To date, the materials commonly used for microfluidic chip fabrication are inorganic (e.g., silicon, glass, and ceramic); and polymeric such as (e.g., poly(dimethylsiloxane) (PDMS), poly(methyl methacrylate) (PMMA) and SU-8 photoresist)[4]. PMMA is a synthetic polymer, characterized by high thermal resistance (stable between -70°C to 100°C) and mechanical strength (high Young's modulus and a low elongation at breakage), produced by methyl methacrylate monomer polymerization[5]. These outstanding characteristics, added to optical transparency, hydrophilicity, cost-effectiveness, and easy handling make it one of the most used polymers in microfluidics. Any microfabricated device is the result of a multifaceted process that involves the coordination and collaboration of diverse disciplines. The developed protocol has two main steps: (1) the first stage involves making the master mold by photolithography, a commonly used microfabrication technique for creating features on a dry photo-sensitive chemical, called photoresist[6] (Figure A, 1-5); and (2) the last stage uses the fabricated mold to create the device by hot embossing, a promising technique to fabricate cost-effective structures with high aspect ratios[7] (Figure A, 6-8).

Results and Discussion Different materials (glass and steel), and conditions (lamination temperature, exposure and baking time, baking temperature) were tested to produce reusable molds by photolithography. Hot embossing was performed after optimizing the mold fabrication. Variables, for instance, embossing time, pressure, and temperature were controlled to have the complete transfer of the microfeatures from the mold to the PMMA substrate. This method allowed the fast prototyping of microfluidic devices with resolution of 30µm and 1:1 aspect ratio.

Conclusion This preliminary data shows the successful production of high-resolution PMMA devices. The Inexpensive and innovative protocol developed allows the fast fabrication (less than five hours) of a highly reproducible, versatile, and biocompatible microfluidic device. Future considerations include testing the produced chip for different applications under multiple conditions.

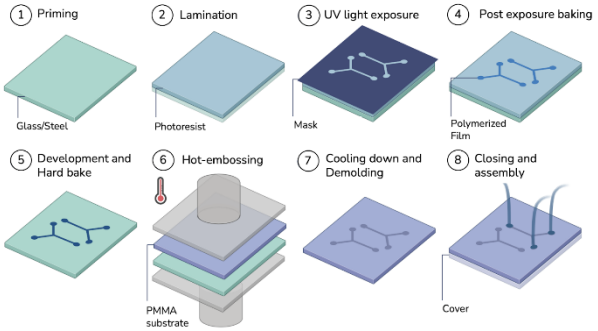

Figure A: Microfabrication protocol, from mold fabrication (1-5) to device assembly (6-8).

Acknowledgments This work was supported by the Biopros and Micro4nano projects, funded by the European Union's Horizon research and innovation program under Horizon-CL4-2021-Digital-Emerging-01-27, grant agreement no. 101070120 and the European Union under H2020-MSCA-Rise-2020, grant agreement No. 101007804.

References

1. Stroock AD. Optical Biosensors, Microfluidics. In: Ligler FS, Taitt CRBTOB (Second E, eds. 2nd ed. Elsevier; 2008:659-681. doi:https://doi.org/10.1016/B978-044453125-4.50019-X
2. Varala S, Satish T, Kumari A, Singh AK. Handbook of Biomolecules, Microfluidic devices. In: Verma C, Verma DKBTH of B, eds. Elsevier; 2023:241-256. doi:https://doi.org/10.1016/B978-0-323-91684-4.00031-1
3. Nielsen JB, Hanson RL, Almughamsi HM, Pang C, Fish TR, Woolley AT. Microfluidics: innovations in materials and their fabrication and functionalization. *Anal Chem*. 2020;92(1):150-168. doi:10.1021/acs.analchem.9b04986
4. Ren K, Zhou J, Wu H. Materials for microfluidic chip fabrication. *Acc Chem Res*. 2013;46(11):2396-2406. doi:10.1021/ar300314s
5. Olabisi O, Adewale K. Handbook of Thermoplastics: Second Edition. *Handbook of Thermoplastics: Second Edition*. 2016;(January 2016):1-956. doi:10.13140/RG.2.1.2068.4881
6. Cardoso S, Silverio V. *Introduction to Microfabrication Techniques for Microfluidics Devices*. Elsevier Inc.; 2020. doi:10.1016/B978-0-12-819838-4.00026-2
7. Becker H, Heim U. Hot embossing as a method for the fabrication of polymer high aspect ratio structures. *Sens Actuators A Phys*. 2000;83(1):130-135. doi:10.1016/S0924-4247(00)00296-X

Polysaccharide-based RNAi nanomedicine for promoting cardiac repair post-myocardial infarction

H. Gao[a,b,*], S.Q. Wang[b], Q. Long[c], Z.H. Liu[b], X.F. Ye[c], H.A. Santos[a,b]

[a] Department of Biomedical Engineering, University Medical Center Groningen, University of Groningen, Ant. Deusinglaan 1, 9713 AV Groningen, The Netherlands.
[b] Drug Research Program, Division of Pharmaceutical Chemistry and Technology, Faculty of Pharmacy, University of Helsinki, FI-00014 Helsinki, Finland.
[c] Department of Cardiovascular Surgery, Ruijin Hospital, Shanghai Jiao Tong University School of Medicine, Shanghai 200020, China.
*Email: h.gao@umcg.nl

Introduction:
Targeting delivery of small interfering RNA (siRNA) by non-viral nanoparticles (NPs) is revolutionizing the biomedical area. However, conventional nanocarriers are limited to undergo clinical translation due to the lack of intracellular delivery and targeting capability in cardiac ischemia lesions. Here, we designed a simple siRNA delivery system with conformational changes properties in a pH-dependent manner. As a proof of concept, the produced RNAi NPs showed inherent targeting affinity towards Dectin-1$^+$ monocytes/macrophages in lesional site. In particular, the RNAi based gene therapy effectively mitigate the formation of fibrotic tissue post ischemic injury.

Methods and Results:
β-glucan based nanoparticles were designed and modified for siRNA delivery. Human hemolysis assay was conducted to assess the pH-responsive properties of NPs, suggested its hemolytic activity at pH 5.5. For in vivo biodistribution and fluorescence assay, near infrared fluorescent dye Cyanine7 (Cy7) was used to conjugate with NPs, a significantly higher fluorescent signal from heart was observed from Cy7-NPs group in mice with ischemic injury. Moreover, the accumulation of β-glucan based NPs was correlated with the overexpressed Dectin-1 expression in infarct area, as calculated by Manders' Colocalization Coefficients (MCC). A MCC of 0.9 confirmed the targeting capability of β-glucan based NPs in heart lesional site. As a proof-of-concept, siRNA interfering transforming growth factor (TGF)-β therapeutics was encapsulated for intravenous injection. As proved by Masson's trichrome staining, the developed siTGF-β NPs effectively reduced the formation of fibrotic tissue. By calculating the ratio of collagen volume fraction (CVF), siTGF-β NPs group reduced 19% of CVF (38.7 ± 7.6% versus 20.5 ± 3.7%), suggesting the therapeutic potential of the developed nanosystem.

Conclusions
In summary, a RNAi-based nanoformulation has been developed for myocardial therapy. As a series of proof-of-concept experiments, the designed siRNA NPs showed superior targeting efficacy and therapeutic effects in infarct area. This β-glucan based nanoplatform holds the potential for treating heart diseases and promoting cardiac regeneration.

Acknowledgments
H. Gao acknowledges financial support from the Chinese Scholarship Council. S.Q. Wang acknowledges the financial support from Academy of Finland (Grant No. 331106). Z.H. Liu acknowledges the financial support from Finnish Red Cross Research Foundation and Academy of Finland (Grant No. 340129). H.A. Santos acknowledges the Sigrid Jus´elius Foundation, the Academy of Finland (Grant No. 331151), and UMCG Research Funds for financial support.

References
1. Z. Liu, S. Wang, C. Tapeinos, G. Torrieri, V. K¨ank¨anen, N. El-Sayed, A. Python, J. T. Hirvonen, H.A. Santos. Adv. Drug Deliv. Rev. 174 (2021) 576–612.
2. Q. Fan, R. Tao, H. Zhang, H. Xie, L. Lu, T. Wang, M. Su, J. Hu, Q. Zhang, Q. Chen, Y. Iwakura, W. Shen, R. Zhang, X. Yan. Circulation 139 (2019) 663–678.
3. B. Bhandary, Q. Meng, J. James, H. Osinska, J. Gulick, I. Valiente-Alandi, M.A. Sargent, M.S. Bhuiyan, B.C. Blaxall, J.D. Molkentin, J. Robbins. J. Am. Heart Assoc. 7 (2018), e010013.
4. S. Hinderer, K. Schenke-Layland. Adv. Drug Deliv. Rev. 146 (2019) 77–82.
5. H.S. Goodridge, C.N. Reyes, C.A. Becker, T.R. Katsumoto, J. Ma, A.J. Wolf, N. Bose, A.S.H. Chan, A.S. Magee, M.E. Danielson, A. Weiss, J.P. Vasilakos, D.M. Underhill. Nature 472 (2011) 471–475.

Incorporation of osteoclasts into an *in vitro* model of mineralised cartilage in the context of endochondral ossification

A. Garmendia Urdalleta (1), J. Witte-Bouma (1), A. Lolli (1), E. Farrell (1)

1. Department of Oral and Maxillofacial Surgery, Erasmus MC University Medical Centre Rotterdam, Doctor Molewaterplein 40, 3015 GD Rotterdam, The Netherlands

Introduction. Bone formation via the process of endochondral ossification (EO) is an extremely complex process involving multiple cell types and interactions as well as the formation and remodelling of multiple extracellular matrices. To date modelling endochondral ossification *in vitro* is mainly limited to the initial steps of the process, namely induction of chondrogenesis and mineralisation of the newly formed matrix. Osteoclasts mediate one of the subsequent stages of EO, which consists of the remodelling of the transient mineralised cartilage developed in the initial steps of the process. The absence of these multinucleated cells was shown to cause disturbances on the EO process [1], [2], highlighting their indispensable role during EO. In this work we introduced a new level of complexity in the *in vitro* modelling of EO through co-culture of transient cartilage undergoing mineralisation and monocyte-derived osteoclasts. With this model we aimed to mimic the remodelling stage that happens during EO *in vivo* in an *in vitro* setting.

Materials and methods. Chondrogenic and mineralised pellets were generated from paediatric human marrow stromal cells (hMSCs) and cultured for 21 days. Cultures were supplemented with transforming growth factor beta-3 (TGF-β3) and dexamethasone up to 18 days (TGF(2w)) or 21 days (TGF(3w)) and β-glycerophosphate (BGP) (TGF(2W)/BGP) for up to 18 days, allowing the induction of mineralisation. Indirect and direct co-culture systems were performed by co-culturing pellets with CD14+ human monocytes in a consensus medium (αMEM 5% FCSi, ascorbic acid, RANKL and M-CSF) within a transwell, or seeding monocytes directly on the pellet surface, respectively. Osteoclastogenesis was evaluated by tartrate-resistant acid phosphatase (TRAP) staining and gene expression analysis (*DC-STAMP, OC-STAMP*, *CTSK, TRAP* and *ATP6V0D2*). Chondrogenesis was assessed by thionine, and collagen type II/X staining, as well as gene expression analysis (*COL2A1* and *COL10A1*). Mineralisation was determined by von Kossa staining.

Results. We achieved osteoclastogenesis in the presence of both TGF(2w) or TGF(2w)/BGP pellets in an indirect co-culture setting, as demonstrated by a similar amount of positively TRAP stained multinucleated cells and expression of osteoclastogenic markers between both TGF(2w) and TGF(2w)/BGP groups. Interestingly, we found that osteoclast formation was significantly reduced in the TGF(3w) group, highlighting the need to remove these factors at least 3 days prior to the start of the co-culture. Upon co-culture, TGF(2w), TGF(3w) and TGF(2w)/BGP pellets presented no clear differences in terms of presence of glycosaminoglycans and collagen type II and X content and expression between co- and mono-cultured pellets. Finally, we successfully set-up a direct co-culture system of monocytes and TGF(2w) as well as TGF(2w)/BGP pellets. Our results showed that monocytes can not only attach to both types of pellets but also differentiate *in situ* into multinucleated TRAP positive and osteoclast marker expressing cells.

Conclusions. This study demonstrates that osteoclasts can be generated in the presence of TGF(2w) and TGF(2w)/BGP pellets, and interactions between them can be studied. Further development of this model will provide us with a tool to further increase our understanding of the EO process in a controlled *in vitro* environment, especially regarding the resorption and remodelling phases. This could be useful for the investigation of bone diseases related to the action of osteoclasts such as osteopetrosis, osteoporosis or breast cancer metastasis.

References:

[1] Dougall, W. et al., Genes & Dev 13, 2412–2424 (1999)
[2] Li, J. et al., Proc. Natl. Acad. Sci. USA. 97, 1566–1571 (2000)

A universal nanogel-based coating approach for medical implants

D. Ghosh[1], D. Keskin[1], A.M. Forson[1], R. Bron[1], C.W.K. Rosman[1], C. Siebenmorgen[1], G. Zu[1], A. Lasorsa[2], P. C.A. van der Wel[2], T. van Kooten[1], M.J.H. Witjes[3], J. Sjollema[1], H. van der Mei[1], P. van Rijn[1]

[1]*University of Groningen, University Medical Center Groningen, Department of Biomedical Engineering, Groningen, The Netherlands*
[2]*Zernike Institute for Advanced Materials, University of Groningen, The Netherlands*
[3]*University of Groningen, University Medical Center Groningen, Department of Oral and Maxillofacial Surgery, Groningen, The Netherlands*

Introduction

The use of implants have increased the quality of life, for patients. However, secondary complications in the host body can lead to implant failure. Coatings have been regarded as an excellent possibility to induce desired responses or to prevent complications, as the bulk implant material does not need to be altered. However to apply a coating, a diverse range of chemical approaches have to be implemented owing to the distinct physiochemical and structural properties of the different classes of implant materials. The aim of the study is to develop a universal nanogel (nGel) coating approach that can be applied to most implant materials, ranging from bioglass, polymers, metals and rubbers and furthermore, investigate the stability of the coating in vitro and in vivo conditions.

Materials and methods

N-Isopropylacrylamide–*co*-*N*-(3-Aminopropyl)methacr ylamide dihydrochloride p(NIPAM-*co*-APMA) core shell nGel particles were synthesized by free-radical precipitation polymerization reaction.[1] The particles were characterized by zeta potential, while the coating was visualized by atomic force microscopy (AFM). The positively charged particles were spray coated and bound on the plasma oxidized, negatively charged implant surface by electrostatic interactions. The stability of the coating was determined in vitro by exposing nGel coated Teflon surfaces to physiological conditions in a shaker incubator for 21 days and in vivo by implanting methacryloxyethyl thiocarbonyl Rhodamine B (MRB) labeled nGel coated (polyvinylidene fluoride) PVDF hernia mesh in mouse model for 13 days.

Results and Discussion

The positive zeta potential, 15.83 ± 0.11 mV at 24°C was attributed to the presence of V50 along with the protonated primary amine groups,[2] introduced by APMA. On plasma oxidation, the surface of the material acquired negative charge. The positively charged nGel particles were deposited on the surface by spray coating technique and the particles were bound to the activated surface via electrostatic interactions[3] **(Figure 1)**. The homogenous uniform coating was characterized by AFM. In vitro data analyzed by AFM showed that the nGel coatings on teflon were stable after 21 days (data not shown), while the in vivo data demonstrated that the coatings on PVDF mesh were stable enough up to 13 days, after which the fluorescent signal was decreasing **(Figure 2b)**. The short term in vivo test is considered as an initial proof for the stability of the nGel coating.

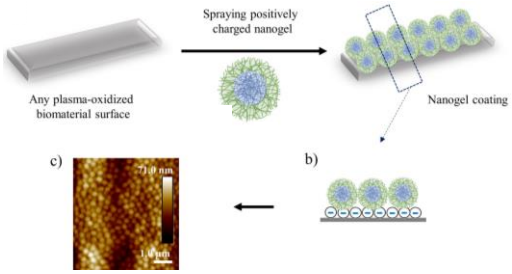

Figure 1: Schematic illustration of the universal nGel-based coating approach on implant surface.

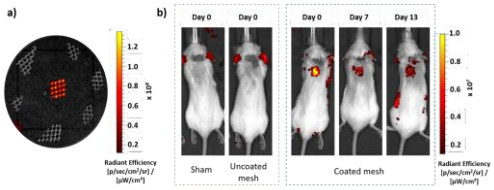

Figure 2: **a)** Representative fluorescence images of nGel coated mesh (labeled with MRB dye, in the middle) and uncoated meshes (grey) taken by IVIS before the implantation in the mice. **b)** Representative fluorescence images of mouse taken without and with the uncoated PVDF mesh and nGel-coated PVDF meshes at different time points.

Summary

The coating approach successfully formed a homogenous uniform coating on most implant surfaces, belonging to different classes of materials. The coating showed high stability in both in vitro and in vivo conditions.

References:

[1] W. H. Blackburn, L. A. Lyon, *Colloid Polym. Sci.* **2008**, *286*, 563.

[2] L. Sigolaeva, D. Pergushov, M. Oelmann, S. Schwarz, M. Brugnoni, I. Kurochkin, F. Plamper, A. Fery, W. Richtering, *Polymers (Basel).* **2018**, *10*, 791.

[3] D. Keskin, O. Mergel, H. C. van der Mei, H. J. Busscher, P. van Rijn, *Biomacromolecules* **2019**, *20*, 243.

In Vitro – In Vivo Predictivity of Osseointegration Markers

Anniek .M.C. Gielen[1,2], A.G. Oomen[1,2], N.M. Leijten[1], N.R.M. Beijer[1]
[1]Centre for Health Protection, National Institute for Public Health and the Environment (RIVM), Bilthoven, The Netherlands.
[2]Institute for Biodiversity and Ecosystem Dynamics (IBED), University of Amsterdam, Amsterdam, The Netherlands.

Introduction

Osseointegration of implants is described as the direct connection between bone and implant [1], and is one of the most determinative factor for successful implantation. This process can be influenced by several factors, including material properties (roughness, porosity, etc.) and the host response to the implant. The growing research into bone regenerative and orthopedic biomaterials warrants increased research investment into early stage development assays, that are predictive of *in vivo* success or failure of the implant. Currently, several different *in vitro* markers are used to assess osseointegration. However, do these *in vitro* evaluations effectively predict *in vivo* osseointegration? Research by Hulsarts-Billström et al. found deficiencies in the *in vivo* predictivity of some markers and indicated that there is a need for proven *in vitro* assays allowing assessment of the *in vivo* osseointegration potential of biomaterials [2]. The research found a mean covariance of *in vitro* scores to *in vivo* score of 58%. The *in vitro* markers used were alkaline phosphatase (ALP) assay, biocompatibility with MTS assay, gene expression of early (RUNX2) and late (osteopontin) markers and mineralization assay. In literature a of lot different markers and combinations of markers with different cell lines are used to predict osseointegration. Commonly used markers will be assessed in this study, building further on the Hulsarts-Billström et al. research.

Aim and Approach

The aim of this research is to assess the predictivity of often used *in vitro* biomarkers for osseointegration. The *in vitro* markers that will be tested include, metabolic activity, cell morphology, alkaline phosphatase, matrix mineralization, osteocalcin, osteoprotegerin, osteopontin, collagen I, prostaglandin E2 and gene expression. The predictivity of the selected markers will be assessed on previously *in vivo* tested materials, ranging from poor to excellent osseointegration. Two osteosarcoma cell lines (MG-63; Saos-2) will be used , where the suitability of the specific cell line per *in vitro* marker will be assessed. Not all assay methods are applicable to all biomaterial types, due to difference in size, form and intrinsic properties (e.g. autofluorescence, porosity). Therefore, the applicability of the assays to different types of biomaterials will be reviewed.

Outlook

In vitro assays can play an increasingly important role in screening the functionality and safety of biomaterials prior to *in vivo* testing. However, proven *in vitro* assays for *in vivo* predictivity are demanded to help innovators early on in the development process of innovative biomaterials. This study will pave the way to the understanding of the difference between *in vitro* osseointegration markers in terms of *in vivo* osseointegration predictivity.

References

[1] Nobles, K. P., et al. (2021). "Surface modifications to enhance osseointegration–Resulting material properties and biological responses." Journal of Biomedical Materials Research Part B: Applied Biomaterials 109(11): 1909-1923.

[2] Hulsart-Billström, G., Dawson, J. I., Hofmann, S., Müller, R., Stoddart, M. J., Alini, M., Redl, H., El Haj, A., Brown, R., Salih, V., Hilborn, J., Larsson, S., & Oreffo, R. O. C. (2016). "A surprisingly poor correlation between in vitro and in vivo testing of biomaterials for bone regeneration: results of a multicentre analysis." European Cells and Materials 31: 312-322.

Proteomic analysis of primary human fetal, adult dermal and eschar mesenchymal cells and their secreted extracellular matrices

M. Gomes [1,2,3,4], P. Karthaka [5], H. Schiller [5], J. Gote-Schniering [5,6,7], R. Scheltema [8], P. Albanese [8], E. Middelkoop [1,2,3,4], H. Niessen [1], P. Krijnen [1], B. Boekema [2,3]

[1] Department of Pathology, Amsterdam UMC (AUMC), location AMC, Amsterdam, The Netherlands
[2] Department of Plastic, Reconstructive and Hand Surgery, AUMC, location VUmc, Amsterdam, The Netherlands
[3] Association of Dutch Burn Centres, Beverwijk, Netherlands
[4] Tissue Function & Regeneration, Amsterdam Movement Sciences Research Institute, Amsterdam, The Netherlands
[5] Institute of Lung Health and Immunity, Comprehensive Pneumology Center, Helmholtz Zentrum München, Munich, Germany
[6] Department of Rheumatology & Immunology and Department of Pneumology, Inselspital, Bern University Hospital, University of Bern, Switzerland
[7] Lung precision medicine program, Department of Biomedical Research, University of Bern, Switzerland
[8] Hecklab, Utrecht University, Utrecht, Netherlands

Introduction: During wound healing, mesenchymal cells (MC) rebuild tissue through extracellular matrix (ECM) secretion. While early fetal skin regenerates, adult skin forms scars in full-thickness wounds. We aim to identify the underlying differences by comparing MC populations and their ECMs: fetal vs adult (regeneration vs repair), and dermal vs eschar (healthy vs wounded).

Methods: Samples of MC (isolated from fetal/adult skin, or eschar tissue from burn patients) and their ECMs, after a 2-week culture with vitamin C, were processed by protein aggregation capture and mass spectrometry. Quality control, principal component, differential expression, proteome/matrisome profiling, gene ontology, and pathway analysis were conducted.

Results: Fetal and adult samples revealed remarkable differences in their proteomic profiles, including ECM compositions. Fetal samples displayed downregulation of contractile phenotype, proteins related to the LIM domain, focal adhesion, and platelet aggregation compared to adult. These features were also downregulated in adult dermal vs eschar samples. Fetal samples presented upregulated proteoglycans and vitamin C cofactors. Proteins differentially expressed in fetal vs adult showed enrichment in the innate immune system pathway, particularly neutrophil degranulation. Differences between fetal vs adult noticeably fade at gestational week 22, when skin regeneration ability ceases.

Conclusion: Our results highlight distinct phenotypic and compositional features, at MC and ECM levels, respectively, between fetus and adult, showing their differential contribution to the wound microenvironment. These differences are remarkable up to the ontogenic transition from scarless healing to scarring and some involved proteins were also differentially expressed in healthy vs wounded adult conditions, emphasizing their potential impact on the wound healing outcome.

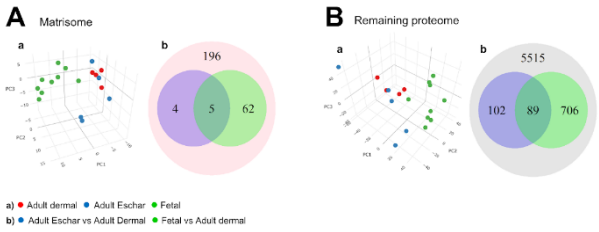

Figure 1 : (A) Matrisome. B) Remaining proteome (total proteome excluding the matrisome). (A-B) a) 3D PCA plot showing each sample of the three mesenhcymal cell types. b) Venn diagram identifying the number of differentially expressed proteins : adult eschar or fetal vs adult dermal within the total matrisome/remaining proteome, including the number of commonly differential expressed proteins.

Acknowledgements: This project has received funding from the European Union's Horizon 2020 research and innovation programme under the Marie Skłodowska-Curie grant agreement No 955722.

Mineralized Collagen Micro-blocks for Bottom-Up Bone Tissue Engineering

E. Güben Kaçmaz, P. Habibović, R. Truckenmüller, Z. Tahmasebi Birgani
Department of Instructive Biomaterials Engineering, MERLN Institute for Technology-Inspired Regenerative Medicine, Maastricht University, Universiteitssingel 40, 6229 ER Maastricht, Netherlands
e.gubenkacmaz@maastrichtuniversity.nl

INTRODUCTION

The self-healing ability of bone is insufficient to heal critical-sized defects and therefore, often in these cases tissue transplantation is needed. As an alternative, engineered bone matrix-mimetic biomaterials, alone or combined with cells, are used[1]. Engineering these alternatives can be approached bottom-up, by co-aggregating cell and microscale matrix-mimetic building blocks to create microtissues with hierarchical, cell-guided organization[2]. Here, we used this approach to create bone-like microtissues using (mineralized) collagen-based microparticles as building blocks.

EXPERIMENTAL METHODS

Collagen microparticles were fabricated by pumping an 8 mg/ml bovine hide collagen methacrylate (CMA) solution containing 1% wt Lithium phenyl-2,4,6-trimethylbenzoylphosphinate, and mineral oil containing 10% v/v TWEEN® 80-Span® 80, as water and oil phases, respectively, into a microfluidic flow-focusing water-in-oil droplet generator. Collected microparticles were incubated at 37 °C, crosslinked using UV light at 405 nm, oil-purified by ethanol, and intra- or extrafibrillar mineralized by 7-day incubation at 37 °C in either poly (L-aspartic acid) solution containing 100 µg/ml calcium and phosphate salts, or 5X-concentrated simulated body fluid. The CMA-based microparticles were characterized with Fourier transform infrared spectroscopy (FTIR), scanning electron microscopy (SEM) and transmission electron microscopy (TEM), and co-aggregated with human mesenchymal stem cells (hMSCs) in non-adherent microwells to analyze their role on hMSCs osteogenic differentiation in the microtissues.

RESULTS AND DISCUSSION

CMA-based microparticles were water-insoluble after crosslinking, showing typical collagen bonds and fibrous microstructures[3-4] (Figure 1a-c). Mineralization of the CMA fibers was observed (Figure 2). While extrafibrillar mineralization showed the globular microstructure of biomimetic CaP on the fibers non-homogenously distributed, intrafibrillar mineralization expectedly preserved the fibrous microstructure and minerals cover the whole fibers[5]. The CMA-based microparticles participated in hMSCs-guided assembly and supported microtissues formation is still ongoing (not shown).

CONCLUSION

We fabricated CMA-based microparticles, and used them to create spheroids with hMSCs. We will next investigate the role of microparticles in inducing osteogenesis in the spheroids, aiming to form bone-like microtissues.

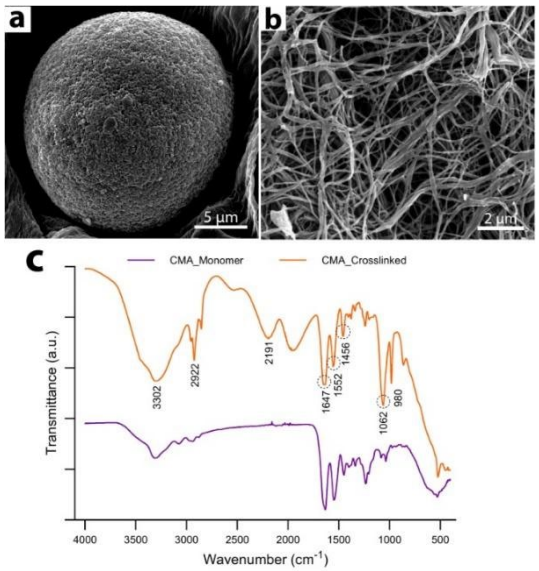

Figure 1. (a) CMA microparticles with (b) a fibrous microstructure, and (c) FTIR spectra of fibrillated and crosslinked CMA. Dashed circles indicate amide bonds in CMA.

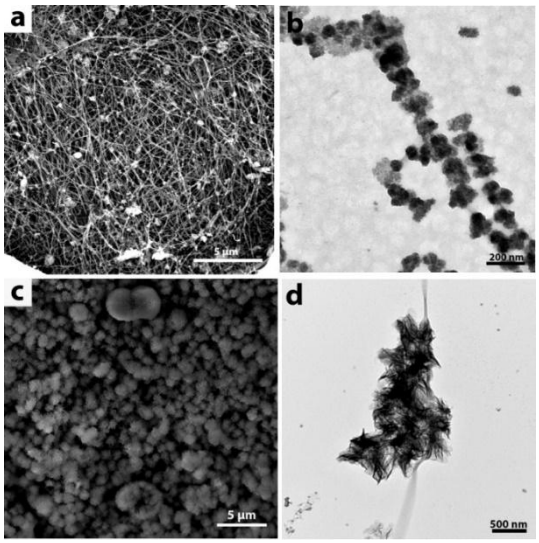

Figure 2. Micro- (left) and nanostructures (right) of CMA fibers in microparticles with (a-b) intra- and (c-d) extrafibrillar mineralization.

REFERENCES

1. Oryan et al. J. Orthop. Surg. Res. 2014.
2. Leferink et al. Adv. Mater. 2014.
3. Ryglova et al. Macromol. Mater. Eng. 2017.
4. Drzewiecki et al. Langmuir. 2014.
5. Pereira et al. Front. Bioeng. Biotechnol. 2020.

ACKNOWLEDGEMENTS

This study was supported by the Study Abroad Program of the Turkish Ministry of National Education, the Dutch Province of Limburg, and the NWO Gravitation Program "Materials-Driven Regeneration" and Incentive Grant for Women in STEM.

Effect of Hydrogel Viscoelasticity on Osteogenic Differentiation of hMSC Spheroids

Y.Hajee[1], D.T. Wu[2,3,4], D.J. Mooney[2,3], M. Diba[1,2,3]

1. Department of Dentistry-Regenerative Biomaterials, Research Institute for Medical Innovation, Radboud University Medical Center, Philips van Leydenlaan 25, 6525 EX Nijmegen, the Netherlands.
2. John A. Paulson School of Engineering and Applied Sciences, Harvard University, Cambridge, Massachusetts, USA
3. Wyss Institute for Biologically Inspired Engineering, Harvard University, Boston, Massachusetts, USA
4. Department of Oral Medicine, Infection, and Immunity, Harvard School of Dental Medicine, Boston, Massachusetts, USA

Introduction

Spheroids are attractive systems for studying the 3D tissue environment due to their high cell density and cell-cell interactions. Hydrogels are commonly employed as 3D mimics of extracellular matrix and therefore used to encapsulate cells and spheroids in organ-on-a-chip models. Although the viscoelasticity of hydrogels can have a significant effect on cell behavior, this aspect has not been investigated for application in organ-on-chip systems. Previous investigations have shown that fast stress relaxation in hydrogels can enhance cell migration and fusion of human mesenchymal stem cell (hMSC) spheroids and increase bone formation based on single hMSCs or pre-differentiated hMSC spheroids. In this study, we investigated the effect of hydrogel viscoelasticity on the osteogenic differentiation of non-differentiated hMSC spheroids.

Materials and methods

Spheroids were prepared using pooled primary human bone marrow MSCs cells (Lonza) by means of low cell adhesion plates. Spheroids were allowed to formed in microwells overnight. Thereafter, hMSC spheroids were encapsulated in RGD-modified alginate hydrogels with equal stiffness but slow or fast stress relaxation profiles (Fig. 1) and cultured for up to 21 days in growth or osteogenic medium. Osteogenic differentiation was assessed by quantifying cellular alkaline phosphatase (ALP) activity and calcium deposition. Additionally, cytological staining and microscopic imaging were caried out with stains for calcium, calcium phosphate minerals, and connective tissue.

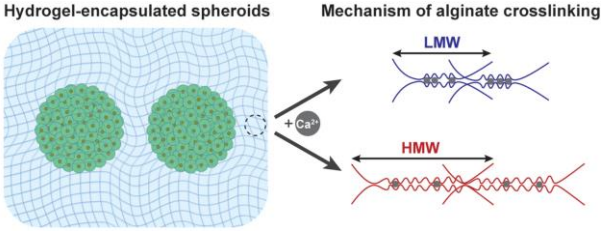

Fig. 1. [1] Alginate stress relaxation is tuned by varying alginate molecular weight and Ca2+ content. Low molecular weight (LMW) gels are fast relaxing, while high molecular weight (HMW) gels are slow relaxing.

Results & Discussion

Whether the gels were cultured in growth (G) or osteogenic (O) medium had a larger effect than gel stress relaxation on ALP activity. Cell migration from the spheroids into the surrounding matrix was observed in the fast relaxing (F) gels, which was not evident in the slow relaxing (S) hydrogels (Fig. 2). In the FO group, spheroids' 'cores' appeared to exhibit an enhanced level of mineralization, as compared to the migrating cells. Nevertheless, further quantitative assessments are needed to confirm this observation.

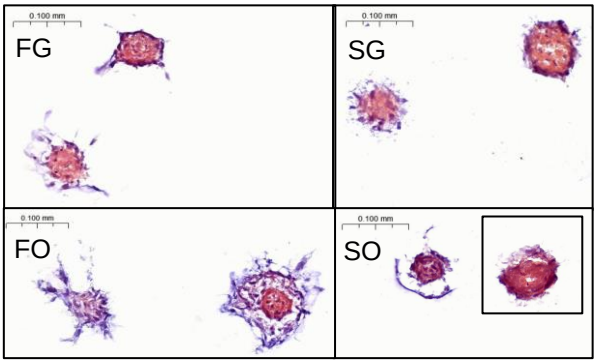

Fig. 2. Representative Alizarin Red (calcium) stains of gel slices with encapsulated spheroids after 21 days. Blue is cytoskeleton counterstain. All samples show calcium deposition.

Conclusion / Summary

Overall, this study sheds light on the role of matrix of stress relaxation on hMSC behavior in 3D tissue models. Early analysis of Alizarin Red stains suggest that cells that migrate away from the 'core' of the spheroids may differentiate into bone less than cells in the core. Ongoing experiments investigate these differences more in detail to reveal the potential interplay between hydrogel viscoelasticity and osteogenic media supplements for *in vitro* bone micro-tissue formation, as critical biophysical and biochemical factors, respectively.

[1] Wu, David T. et al., Bioeng. transl. med.: e10464

Bioinspired Hydrogels with Modulated Degradability for 3D Cell Encapsulation

J. Hiemstra, M. Jin, J.I. Paez
Developmental Bioengineering, TechMed Centre, University of Twente. Drienerlolaan 5, 7522NB, Enschede, The Netherlands.

j.hiemstra-1@student.utwente.nl

Introduction. Hydrogels, hydrated 3D crosslinked polymer networks, have emerged as promising candidates for mimicking the extracellular matrix (ECM). Previous literature showed the importance of matrix remodelling in hydrogels for cell fate [1], however, more detailed information regarding the influence of hydrogel degradability rate on cell fate in 3D cell encapsulation is still subject of investigation. To address this gap, in this work, a polyethylene glycol (PEG) based hydrogel platform that allows matrix remodelling was designed by incorporating matrix-metalloproteinase (MMP)-cleavable peptides with variable degradation rates as crosslinker. We used luciferin-bioinspired click ligation as crosslinking strategy for hydrogel formation. This approach had previously shown efficient gelation kinetics, excellent cytocompatibility and tunable mechanical properties for 3D cell encapsulation [2]. In this work, fundamental hydrogel properties, including gelation time, mechanical properties, pore sizes were characterized. Additionally, cell viability, cell morphology and cell-materials interactions were explored to elucidate their correlation with degradation rate of the matrix. The findings of this study could potentially expand the toolbox of biomaterials for 3D cell encapsulation in the tissue engineering field.

Materials and Methods. 4-arm PEG-CBT (20 kDa) was prepared at 4 wt% in 20 mM HEPES (pH 8.0) as polymer precursor to crosslink with 3 different MMP-cleavable peptides (denoted as VPM, GPQA and GPQW). A macroscopic gelation test was performed to measure gelation times, while mechanical properties were assessed using rheology. For cell studies, 1 mM cyclo(RGDfK(C)) was added to promote cell adhesion and human mesenchymal stem cells (hMSCs) were encapsulated at a density of 500.000 cells/mL. 3D cell distribution and cell viability were evaluated at 1, 3 and 7 days post-encapsulation by live/dead assay. Furthermore, cell-materials interactions were investigated by cytoskeleton and morphological characterization at 0, 3 and 7 days post-encapsulation.

Results and Discussion. MMP-cleavable PEG hydrogels were successfully prepared under physiological conditions (Fig. 1a). All hydrogels showed a fast gelation time of about 25 seconds (Fig. 1b). Rheological analysis indicated a similar G' plateau value (~2300 Pa) for all peptides (Fig 1c). A homogeneous cell distribution across the hydrogel was observed in all cases after 1 day post-encapsulation (VPM-based gel shown as example, Fig. 1d). A high cell viability (>95%) was observed up to 7 days post-culture, which demonstrated the good cytocompatibility of these matrices (Fig. 1e). Cell spreading in all dimensions was observed for all hydrogels, alongside with increased cell volume, which showed no significant difference across the different groups (Fig. 1f). Interestingly, cell sphericity was significantly higher at day 3 in hydrogels prepared with the GPQA peptide (Fig. 1g). According to previous literature, this peptide has the slowest degradation rate, which supports this observation [3].

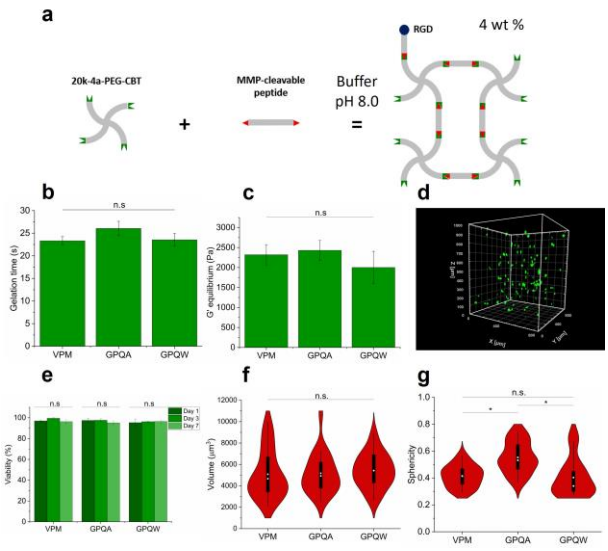

Figure 1: a) MMP-cleavable hydrogel design. b) gelation time and c) G' plateau values during in-situ curing by rheology. d) 3D cell distribution for VPM peptide at 1 day culture. e) Cell viability of encapsulated hMSCs at 7 days of *culture. f) Cell volume and g) sphericity of encapsulated hMSCs at 3 days* of *culture.*

Conclusions. We present a bio-inspired hydrogel platform with tunable degradation rate for 3D cell encapsulation. This platform shows an efficient gelation rate and is suitable for cell culture application. Encapsulated cells responded to the degradability rate of the matrices, evidenced by increased spreading and cell volume and variable cell sphericity. These hydrogels could provide the possibility for development of model scaffolds to study cell-materials interactions.

References.

1. Chaudhuri, O. et al. Nature Mater **2016** 15, 326–334
2. M. Jin, G. Koçer, and J.I. Paez. ACS Applied Materials & Interfaces **2022** 14, 5017-5032
3. Patterson J, Hubbell JA. Biomaterials **2010** 30, 7836-45.

Antibacterial Peptide-loaded Chitosan Nanoparticles to Treat *Staphylococcus aureus* Biofilm

Pardis (P.) Keikhosravani[1,*], Azin Khodaei[1], Tim bollen[1], Floris J. Bikker[2], Kamran Nazmi[2], Bart Van der Wal[1], Charls Vogely[1], Harrie Weinans[1], Saber Amin Yavari[1]

[1] Department of Orthopedics, University Medical Center Utrecht, Utrecht, The Netherlands
[2] Department of Oral Biochemistry, Academic Center for Dentistry Amsterdam (ACTA), the Netherlands
*Email address: p.keikhosravani-2@umcutrecht.nl

Introduction

Bone implant-related infections (IRI) occur when bacteria initially colonize on the implant surface and form a biofilm. These bacteria are encased in an extracellular matrix and are resistant to immune cell clearance [1]. Antibacterial peptides (AMP) are promising agents for disrupting the extracellular matrix of biofilms, destabilizing bacterial membranes and avoiding antibiotic resistance problem [2]. Utilizing cationic nanoparticles such as chitosan nanoparticles (CSNPs), enables targeted penetration into the negatively charged biofilm, facilitating efficient drug delivery, and enabling localized drug release [3]. In this study, peptide-loaded CSNPs were optimized for biofilm penetration and antibacterial properties. The cytotoxicity and antibiofilm activity of varying concentrations of peptide-loaded CSNPs was evaluated. At the optimum concentration, these nanoparticles achieved 99.99% killing efficacy against Staphylococcus aureus (*S. aureus*) biofilms while exhibiting no cytotoxic effects on human mesenchymal stem cells (hMSCs).

Materials and Methods

Ionic gelation was used to prepare peptide-loaded CSNPs based on Piras et al.'s method, with minor modifications [2]. The chitosan solution was made by dissolving chitosan (1 mg/ml) in 1% (v/v) acetic acid. Then peptide and sodium tripolyphosphate (STPP) under magnetic stirring was added, followed by centrifugation at 14,000 RPM for purification. Trehalose was added as a cryoprotectant to prevent agglomeration during lyophilization. Dynamic light scattering (DLS) and zetasizer were used to measure sizes and charges of particles, respectively. The BCA assay kit was used to quantify the drug loading efficacy and measure the amount of peptide released from CSNPs. To assess the diffusion and antibiofilm activity of varying concentrations of peptide loaded-CSNPs, the samples were tested against bioluminescent methicillin-resistant *S. aureus* (Strain: USA300) biofilm through a colony forming unit (CFU) assay. The cytotoxicity of varying concentrations of peptide loaded-CSNPs against hMSCs was also tested. Confocal microscopy was used to visualize live-dead (green-red) stained cells.

Results and Discussion

The peptide-loaded CSNPs were successfully formed with the ionic gelation method. The size, mean zeta potential and drug loading efficacy of peptide-loaded CSNP was calculated 172.63 nm and 39.57 mV and 92%, respectively. In general, small and cationic nanoparticles can carry drugs to the target site. The antibacterial activity of different concentrations of peptide-loaded CSNPs was reported by CFU counting (Figure 1). Peptide-loaded CSNPs at high concentrations (24 mg/ml) eradicated all bacteria. Where 21 mg/ml of peptide-loaded CSNPs showed 4-log (99.9%) eradicating bacteria compared to the control group. Cytotoxicity of the peptide-loaded CSNPs was investigated using live-dead staining (Figure 2). High concentrations of peptide-loaded CSNPs (27 and 24 mg/ml) showed cytotoxicity while lower concentrations did not. Therefore, 21 mg/ml of peptide loaded nanoparticles was chosen as the therapeutic concentration with 99.9% killing efficacy.

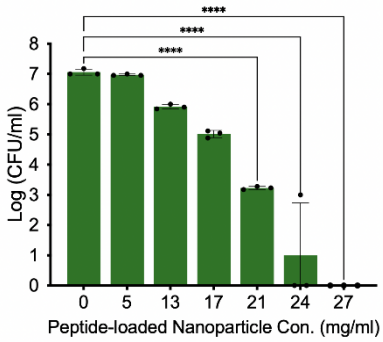

Figure 1: CFU analysis different concentrations of peptide-loaded CSNPs

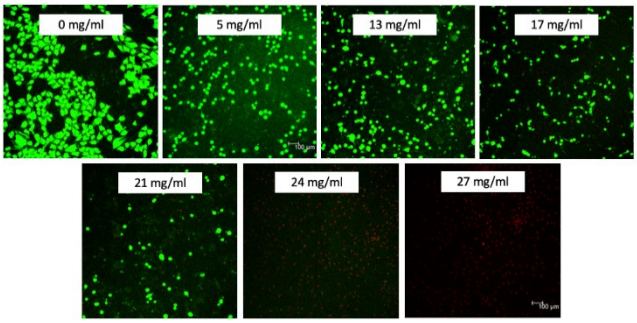

Figure 2: cytotoxicity effect of different concentrations of peptide-loaded CSNPs

Conclusion

To conclude, CSNPs served as a promising system to deliver AMP to treat bone IRI. The optimum concentration of peptide-loaded CSNPs, 21 mg/ml, is not cytotoxic while killing 99.99% of the bacteria inside the biofilm. In clinical settings, the use of nanoparticles for biofilm treatment can offers precise drug delivery and enhanced penetration through biofilm barriers, significantly improving therapeutic outcomes while minimizing systemic side effects.

References

[1] S. Amin Yavari, et al., Advanced Materials, 2020.
[2] A. M. Piras, et al., Pharmaceutical research, 2015.
[3] X. Lv, et al., Small, 2023

Distinct morphological differences in the osteochondral tissue of the humeral head between aquatic, semi-aquatic and terrestrial mammals

M.M. Księżarczyk [3], M.H.P. van Rijen [2,3], L.L. IJsseldijk [4], M. Kik [4], R. Levato [1,2,3], P.R. van Weeren [1,2], J. Malda [1,2,3]*

[1]Department of Clinical Sciences, Faculty of Veterinary Medicine, Utrecht University, the Netherlands
[2]Regenerative Medicine Utrecht, Utrecht University, Utrecht, the Netherlands
[3]Department of Orthopedics, University Medical Centre Utrecht, Utrecht, the Netherlands
[4]Division of Pathology, Department of Biomolecular Health Sciences, Faculty of Veterinary Medicine, Utrecht University, Utrecht, the Netherlands
Corresponding author: Prof. Jos Malda
mail: j.malda@umcutrecht.nl

Purpose
Mammals living on land or in water experience hugely differing loading conditions, which can be supposed to affect their skeletal system. Some differences in structure of both cartilage and bone of the osteochondral unit have been demonstrated between mammals living on land and water. However, data are limited and semi-aquatic mammals, which bridge the divide between an aquatic and terrestrial lifestyle, have not been researched. Therefore, the aim of this study was to establish morphological features of the osteochondral unit, and particularly the calcified cartilage layer, in mammals living in different loading conditions.

Material and methods
Osteochondral tissue samples, each with a diameter 8.5 mm, were collected post-mortem from the central area of the humeral head in aquatic (n=5), semi-aquatic (n=4), and terrestrial (n=5) mammals. The collected material was fixed and then prepared for histological analysis. The following staining methods were applied: Hematoxylin and eosin, safranin-O, picrosirius red, and RGB-trichrome stains. Additionally, Micro-CT analysis was conducted to investigate morphological differences in the osteochondral unit among mammals living in widely different loading environments.

Results
In terrestrial and semi-aquatic mammals, the collagen network of the articular cartilage shows a division into superficial, intermediate, and deep layers. However, in aquatic mammals, the collagen content appeared less organized, and no such distinction could be identified. The calcified layer was observed solely in semi-aquatic and terrestrial animals, with a relatively thinner layer in semi-aquatic mammals. Moreover, in semi-aquatic mammals, the calcified layer displayed irregular formation compared to terrestrial mammals. Only in aquatic mammals were observed highly porous subchondral bone plates, with randomly located cartilage tissue patches.

Conclusion
We have demonstrated considerable differences in the osteochondral units of aquatic, semi-aquatic and terrestrial mammals, which emphasizes the impact of loading. These results are essential for the in-depth understanding morphology of articular cartilage in mammals and hence for the development of future therapeutic approaches.

Advancing Injectable Hydrogel Scaffold With Tyramine-Functionalized Chondroitin Sulfate For Cartilage Repair

N.X.T. Le, B. Zoetebier, M. Karperien
Developmental BioEngineering Department, University of Twente, Enschede, Netherlands

Email: n.x.t.le@utwente.nl

Introduction: Osteoarthritis is a degenerative joint disease that affects millions of people worldwide, and vast efforts have been made to intensively study this disorder to develop effective treatments. One of the promising regenerative therapies is intra-articular injection with *in situ*-forming hydrogels as fillers of focal cartilage defects which can emulate the cartilage environment and promote cell proliferation, differentiation, and extracellular matrix (ECM) formation. Previously, a hybrid hydrogel including tyramine (TA) functionalized hyaluronic acid (HA) and dextran (Dex) was proven to have promising potential in cartilage repair. *In situ* gelation is achieved by co-injection of these polymers with horseradish peroxidase as enzyme and hydrogen peroxide as oxidant. Chondroitin sulfate (CS) is a major component of cartilage which determines the hydration and elasticity of the cartilage as well as promotes the synthesis of collagen II and HA. We anticipated that the addition of TA-functionalized chondroitin sulfate (CS-TA) to this hybrid hydrogel would improve the chondrogenic activity of chondrocytes as well as the deposition of cartilage-like matrix. Therefore, we investigated the hybrid hydrogel including CS-TA, HA-TA, and Dex-TA with various polymer ratios in terms of mechanical properties and their potential to promote cartilage matrix formation.

Materials and Methods: The hydrogel solutions containing Dex-TA, HA-TA, and CS-TA were prepared at 6 different ratios, with a final concentration of 5% wt. The hydrogel solution is enzymatically crosslinked via TA-TA covalent bonds in the presence of horseradish peroxidase (HRP) and hydrogen peroxide (H_2O_2) as an oxidizing agent. Hydrogels were made in a cylindrical shape using a PTFE mold. Mechanical properties of the hydrogel were assessed by rheology. Human nasal chondrocytes were encapsulated at a density of 10 million cells/ml and cultured in the cylindrical hydrogels for 21 days in a standard chondrogenic culture medium including TGF-β3. Then, the hydrogels were collected to perform PCR for RNA expression, histology for proteoglycan content, and immunohistochemistry (IHC) staining for collagen type II deposition.

Results and Discussion: The hydrogels were made by dissolving polymers and HRP in PBS and adding H_2O_2 to initiate the crosslinking. In this study, the final concentration of HRP and H_2O_2 were 3 U/mL and 0.015%, respectively. With these conditions, the hydrogels successfully formed after 45 seconds upon the addition of H_2O_2, given that the hydrogel solutions were pre-cooled on ice. All hydrogel conditions showed excellent cell viability with more than 90% of cells viable at 24h after encapsulation. After 21 days of culture, the cell viability slightly decreased but still, 80% of cells remained viable. Hydrogels with CS-TA had higher cell viabilities as compared to gels with only Dex-TA and HA-TA. Moreover, cell stretching and cell division were only observed in hydrogels with CS-TA. The addition of CS-TA in the hybrid hydrogels increased cell proliferation. The storage moduli of cell-free hydrogels were around 2500 to 3500 Pa depending on the ratios of Dex-TA, HA-TA, and CS-TA. Cell-laden hydrogels had a slightly lower storage modulus of around 1500 Pa at day 1. However, after 21 days in culture, the storage modulus of cell-encapsulated hydrogels was increased which indicated the deposition of ECM. Hydrogels with CS-TA were observed to have lower storage modulus than Dex-TA and HA-TA hydrogels at day 1, however, their stiffness increased most and to highest values after 21 days of culture. In terms of mRNA expression, the relative fold expression of ACAN, COLI, and COLII was most up-regulated in hydrogels containing CS-TA. The IHC staining of COLII and histology staining also showed higher deposition of collagen type II as well as proteoglycans in hydrogels with CS-TA. These results corresponded to the enhanced stiffness of hydrogels after culturing.

Conclusions: According to our results, the addition of CS-TA significantly increased ECM production and consequently the mechanical properties of the chondrocyte-laden hydrogels after 21 days of culture compared to hydrogels consisting of Dex-TA and HA-TA alone. An improvement in chondrocyte proliferation and cartilage matrix deposition is also observed in Dex-TA/HA-TA/CS-TA hydrogels. Therefore, this hybrid hydrogel is a promising approach for cartilage tissue engineering.

Unravelling Kidney Development by Reverse Engineering Branching Morphogenesis

M. Loly, M. Kern, N. Khoshdel Rad, G. Sahin, L. Lins, R. Grant, P. Habibovic, S. Giselbrecht
Department of Instructive Biomaterials Engineering, MERLN Institute for Technology-Inspired Regenerative Medicine, Maastricht University, Universiteitssingel 40, 6229 ER Maastricht, The Netherlands

INTRODUCTION

The human kidney is a remarkably intricate organ and holds great importance because of its complex functions, architecture, and developmental processes. In the early stages of the development, there are three primary cells compartments: Ureteric Bud (UB), nephron progenitor cells and stromal progenitor cells, all undergoing different developmental processes in close and reciprocal interaction. However, studying this developmental process, known as branching morphogenesis, remains difficult due to the lack of appropriate in vitro models.

The UB is a highly regulated structure capable of branching in various complex patterns, including terminal bifid or trifid, and lateral branching. These branching patterns provide a general overview of the mature Collecting Duct (CD) system in the metanephric kidney in vivo. In light of this idea, this project aims to unravel the tightly regulated communication between these three main cellular compartments of the metanephric kidney. Our focus is on the development of complex but artificial CD systems by design, because the collecting duct is considered the key player in determining the number of nephrons and the spatial organization of the entire organ. To guide spatiotemporally the budding and branching of our stem cell-derived ureteric bud organoids, we utilize an innovative compartmentalized microfluidic chip to manipulate and control the branching patterns. The chip platform is used to create local sources of soluble factors and to control biophysical properties of the Extra Cellular Matrix (ECM) in a region-specific manner. Unlike the lung and other branching organs, the underlying mechanisms of kidney branching morphogenesis are not fully elucidated yet. By providing time-lapse data derived from defined 3D in vitro models, we hope to contribute to this challenging endeavor.

Our research seeks to advance the field of regenerative medicine by offering a high-throughput culture and analysis platform for systematic kidney branching morphogenesis study. The ability to comprehend the mechanisms of this developmental process holds vast potential for personalized medicine and opens doors to the development of novel therapies for renal disorders.

MATERIALS AND METHODS

For our experiments, we based on the Taguchi protocol (2017). Mouse embryonic stem cells are cultured at 37°C and 5% CO_2 in feeder-free condition on 0.1% gelatin and used for UB differentiation. At day 0, cells were dissociated with accutase, counted, and seeded in a 96 U-bottom well plate with low attachment properties. The concentrations and components of the medium were changed daily until day 6.5 after obtaining Wolffian Duct progenitor cells organoids. On this day, organoids were dissociated and reseeded in the chamber of an H-designed thermoformed microarray (non-porous Polycarbonate (PC) 50µm thick) to form UB organoids. From day 7.5, we added 10% matrigel to embed the organoid. Two biochemical compounds, BMP4 and GDNF, were applied with flow on each side of the H to respectively inhibit and activate the branching of the structure.

RESULTS AND DISCUSSION

As mentioned above, branching is an important organ patterning mechanism involving multiple embryonic lineages, resulting in a tree-like epithelial structure. To create a faithful UB organoid model, we investigated how external factors, such as growth factors or ECM variations, affect branching patterns. By applying a flow with various soluble molecules, each different on each side of the design, the organoid responds differently to these influences. In this case, an activator flow facilitates the budding and branching of the structure while the other side inhibits its progression. By controlling the direction, division and growth of the branches during the differentiation process, we are able to recreate a higher-order structure of the CD and, subsequently, a complete kidney, including the three cellular compartments.

CONCLUSION

The application of flows with different compositions in an H-design pattern on UB organoids allows for the control of structural growth and one-sided branching. This gives rise to organoids resembling an early branching kidney, with space left for ureter growth. The growth and maturation of such a structure, including its architecture, remain a challenge in the field of regenerative medicine. However, this UB-on-chip model paves the way for a promising and functional CD design-controlled organoid model.

REFERENCES

1. Yuri, S., Nishikawa, M., Yanagawa, N. *et al.* (2017). *Stem cell reports*, *8*(2), 401–416.
2. Taguchi, A., & Nishinakamura, R. (2017). *Cell stem cell*, *21*(6), 730–746.e6.
3. Zeng, Z., Huang, B., Parvez, R.K. *et al. Nat Commun* **12**, 3641 (2021).
4. Tanigawa, S., Tanaka, E., Miike, K. *et al. Nat Commun* **13**, 611 (2022).

Analysis of the endothelialization of small-diameter *in situ* tissue-engineered vascular grafts; A systematic review

M. Manenti [a,b*], D.M. Ibrahim [a,b*], S. Koch [a,b], N.V. Hooren [a], B.D. Kort [a,b], C.V.C. Bouten [a,b], A.I.P.M. Smits [a,b]

[a] Department of Biomedical Engineering, Eindhoven University of Technology, Eindhoven, The Netherlands
[b] Institute for Complex Molecular Systems, Eindhoven University of Technology, Eindhoven, The Netherlands
*Contributed Equally

Introduction

Vascular diseases are leading causes of death and impaired quality of life. Current clinically available treatments comprise either autologous blood vessels or synthetic non-resorbable grafts. Nevertheless, both of them are associated with complications, such as low availability and morbidity for autologous grafts and thrombus and stenosis for the synthetic counterpart. In situ tissue engineered vascular grafts (TEVGs) may represent a promising alternative, able to exploit the body self-capability to grow and remodel new tissue. Moreover, having a bioresorbable, cell-free and off-the-shelf available scaffold can reduce the lengthy and costly in vitro culture procedures. In order to achieve a new functional tissue, a proper integration into the host is a crucial step to attain. As such, after the implantation, the lumen of the graft must be covered by a fully confluent and functional endothelial monolayer.

Due to the dynamic in vivo environment, endothelial coverage is a complex multifactorial process. In this regard, the aim of this systematic review is to assess the influence of the animal model, the graft characteristics and the study design on the formation of a ECs monolayer in small diameter vascular grafts.

Methods

This review is a follow-up on a previously published work focused on the experimental design and the quality of small diameter TEVGs in in vivo models between 1950 and 2020. For the bibliography search, we used the same search strategy to retrieve studies between 2020 and 2023 (**Fig. 1**).

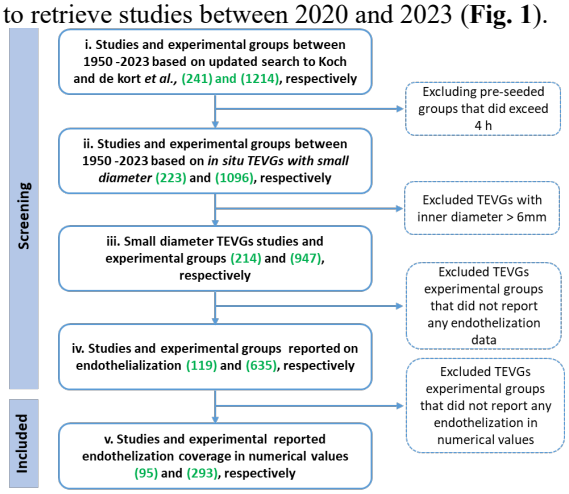

Fig.1 Flow chart for the number of studies and corresponding experimental groups.

Results and discussion

Endothelial coverage: choosing the right animal model

We first show the link between endothelial coverage and animal model (**Fig. 2a,b**). Excluding big animal models for which only 3 experimental groups have been included in the analysis, other animals showed a good endothelial coverage between 84% and 67%. However, since small animals are mostly used in these in vivo studies, it is still difficult to translate those results to the clinic: in fact, while they undergo to transanastomotic endothelialization, in humans other routes are preferred (transmural or fall out).

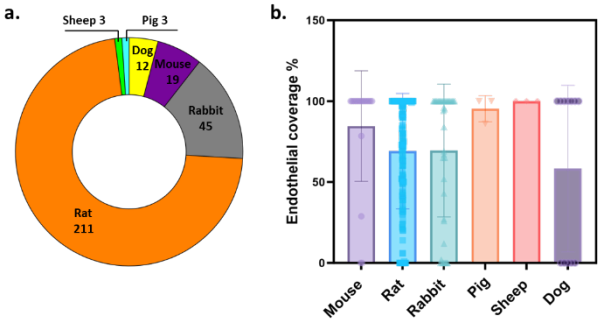

Fig.2 Number of animals per experimental group (a). Relation between animal species and endothelial coverage (b).

Endothelial coverage: just a matter of time?

From our analysis it ended up that the endothelium coverage process is highly dependent on the follow up time (**Fig. 3a**). Hence, we investigate a possible link with the graft characteristics and we found out that, for long follow up time, the geometry of the graft has no direct influence on the endothelium coverage (**Fig. 3b-d**).

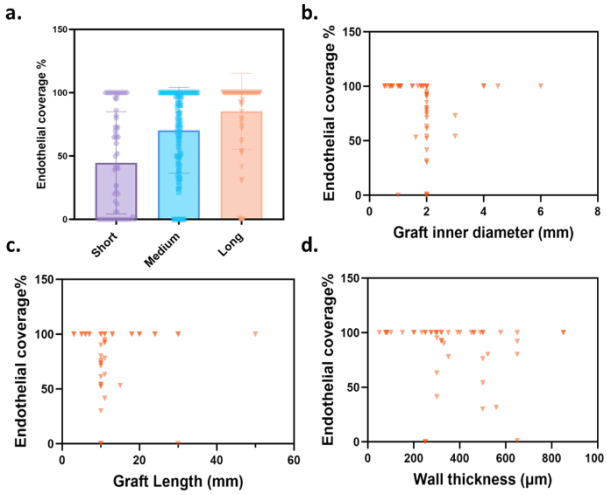

Fig.3 Follow up time (based on animal lifetime) vs endothelium coverage (a). Relation between endothelium formation and graft inner diameter (b), length (c) and wall thickness (d) for long follow up time.

Conclusions

In this study, we found that, in small animal models, one of the most important factor that influence endothelium formation is the follow up time. Nevertheless, for a better translation into the clinic, more investigations on larger animals are needed.

Acknowledgments

This study is part of the Hybrid Heart project funded by European Union's Horizon 2020 1091 research and innovation program under grant agreement No 767195 and part of the Gravitation Program "Materials Driven Regeneration", funded by the Netherlands Organization for Scientific Research (024.003.013).

Paracrine Effects of Macrophage Phenotype on Tendon Tissue Remodelling

A. Mansoor[1,2]*, H. Brouwer[1,2]*, L. Verberne[1,2], C. Bouten[1,2], A. Smits[1,2], J. Foolen[1,2]

[1] *Department of Biomedical Engineering, Eindhoven University of Technology, The Netherlands*

[2] *ICMS, Eindhoven University of Technology, The Netherlands. *HB & AM contributed equally.*

Introduction

Tendinopathy is characterized by tissue degeneration and the transformation of the aligned anisotropic extracellular matrix (ECM) towards a disorganized isotropic ECM. Simultaneously, spindle-shaped tenocytes change into stellate tenocytes [3]. Restoration of the healthy tissue organization is an important challenge to restore its function. Macrophages are thought to be one of the key regulators during remodelling, and their polarization into a spectrum of phenotypes is hypothesized to play a vital role in both tissue remodelling and fibrosis [2]. Their function is influenced by environmental cues such as cytokines and topographies [1]. The interplay between macrophages and tenocytes, and how this influences tendon remodelling remains largely unknown. To get a better understanding of the processes involved, we aim to elucidate the effect of paracrine signalling of distinct macrophage phenotypes on tendon-like tissue remodelling.

Methods

3D constrained microtissue platforms were used *in vitro* to create aligned tendon-like tissues consisting of fibroblasts in a collagen type I gel (Figure 1). The microtissues were cultured in conditioned media (CM) produced from macrophages in three different biochemically induced polarization states, (IFN-γ+LPS stimulated M1, IL-4+IL-13 stimulated M2a, and IL-10 stimulated M2c) and in control RPMI medium. Microtissue waistcoat contraction, gene expression and cellular orientation were analysed to get more insight into the remodelling behaviour.

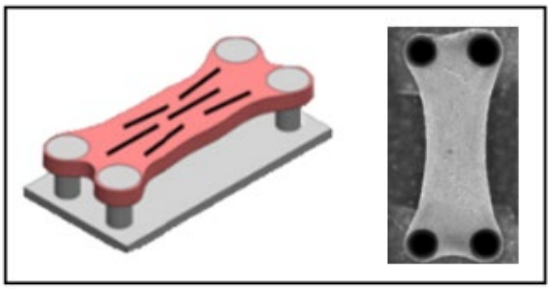

Figure 1. 3D microtissue model using constraints [3]

Results

Control medium resulted in a higher waistcoat contraction in comparison to the CM groups, while the contraction between the CM groups were comparable (Figure 2). The alignment and elongation of the cells appeared to be the strongest in the control groups as compared to the CM groups (Figure 3). Difference in gene expression between CM groups were comparable (Results not shown).

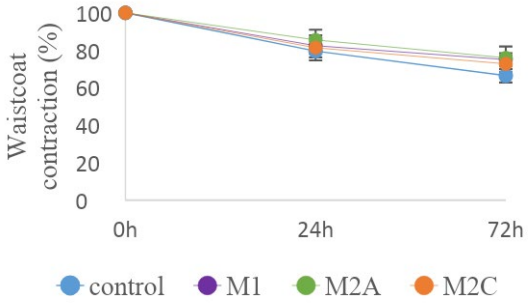

Figure 2. Percentage waistcoat contraction plotted against three time points (0, 24 and 72 hours)

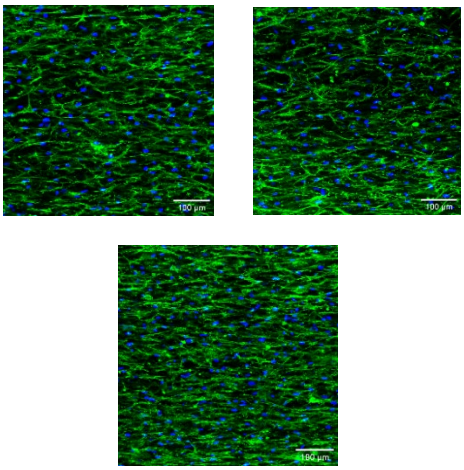

Figure 3. Phalloidin Actin and DAPI stained cells

Discussion

Macrophage-secreted factors were found to have a minimal influence on tissue remodelling in terms of contraction, orientation, and remodelling marker genes. Quantitative analysis of cell orientation and morphology will be done. The minimal differences seen can be attributed to the CM that only had macrophage secreted factors, without stimulating factors. It is likely that the concentration of the macrophage secreted factors was too low to have had a pronounced varied effect. Nevertheless, some factors did have an effect since a difference in waistcoat contraction and morphology was seen between the control and CM groups. A multiplex-ELISA is being done on the conditioned medium to measure the concentrations of the secreted factors. Based on the ELISA results, stimulation of the tissue with specific inflammatory and anti-inflammatory factors at higher concentrations will be done. Further unravelling of the interplay between macrophages and tenocytes is crucial for steering functional tendon healing.

References

[1] Luu et al, ACS Appl Mater Interfaces, 7:28665-28672, 2015. [2] Wissing et al, NPJ Regen Med, 2, 2017. [3] Foolen et al, Matrix Biology, 65:14-29, 2018.

The effect of different sterilization methods on the expandable collagen plug in *in vitro* and *ex vivo* setups

Rob Meuwese[1*], Elly Versteeg[1], Anne Reitsma[1], Mona Al-Areeqi[2], Hugo Nachtegaal[2],
Toin van Kuppevelt[1], Joris van Drongelen[3], Willeke Daamen[1]
[1] Radboud university medical center, Radboud Research Institute for Medical Innovation, Dept of Medical BioSciences, Nijmegen, the Netherlands
[2] HCM Medical, Kerkenbos 10-113, 6546 BJ Nijmegen, the Netherlands
[3] Radboud university medical center, Dept of Obstetrics & Gynecology, Nijmegen, the Netherlands
*Corresponding author: Rob.Meuwese@radboudumc.nl

Introduction.
For the prevention of preterm birth after minimally invasive endoscopic surgery on the fetus an expandable collagen plug is constructed [1]. This plug is made of type I collagen only and expands as it comes into contact with an aqueous solution. Thereby it is able to fit through the fetoscope, fix itself in the endoscopic entry point in the fetal membranes and rapidly seal the defect to prevent leakage and enable cellular influx.
Medical devices like this can be sterilized using different methods, which may have a major effect on the function and tissue response. It is known that gamma irradiation results in protein degradation and induction of crosslinks [2]. Supercritical CO_2 treatment ($scCO_2$) is an upcoming sterilization method for sensitive biomaterials [3]. In this study, both sterilization methods are compared to study the effect on the expandable collagen plug.

Methods.
Lyophilized type I collagen plugs were chemically crosslinked and crimped to fit through a fetoscopic cannula (Ø 3 mm). The crimped plugs were sterilized using gamma irradiation or $scCO_2$ treatment. After sterilization, expansion was studied in PBS, degradation products with SDS-PAGE and time to degrade by collagenase in 0.1 M TRIS-HCL with 0.05 M $CaCl_2$. Degradation was examined macroscopically and with a hydroxyproline assay. To study cellular influx, sterilized plugs were placed in *ex vivo* fresh human fetal membranes and cultured for up to 3 weeks.

Results.
Both sterilization methods resulted in a functional plug that expanded when placed in PBS. SDS-PAGE indicated that only gamma irradiation resulted in protein degradation products. In collagenase the gamma irradiated plugs degraded faster compared to the $scCO_2$ and non-sterile group, leading to higher hydroxyproline values in the supernatant.
Gamma irradiated and $scCO_2$ treated collagen plugs could be cultured for 3 weeks and indicated leakage prevention over this period based on macroscopic evaluation. Histological examination for cellular influx is ongoing.

Discussion and Future Outlook.
Both gamma irradiation and $scCO_2$ treatment are suitable methods for sterilization of the expandable collagen plug. Although differences are seen in degradation products and degradation time, at this level, both sterilization methods result in a functional collagen plug that could seal the endoscopic entry point in an *ex vivo* setup using human fetal membranes. Histology and further analysis will be performed to study the effects of the sterilization methods more closely to appoint the optimal sterilization method for the expandable collagen plug.

Acknowledgments.
This study is funded by ZonMw & Health Holland, project number 40-44600-98-624.

References.
1. Meuwese, R.T.C., et al. Bioactive Materials, 2023. **20**: p. 463-471.
2. Faraj, K., et al. Tissue Engineering and Regenerative Medicine, 2011. **8**: p. 460-470.
3. Op 't Veld, R.C., et al. Tissue Eng Part C Methods, 2020. **26**(2): p. 132-141.

Improving Interfacial Adhesion Properties of Hydrogel Matrices to PDMS-based Microfluidic Platforms

Y. Na[1], U. Devamoglu[2], S. Le Gac[2], J. I. Paez[1]
[1] Developmental BioEngineering, and [2] Applied Microfluidics for BioEngineering Research, TechMed Centre and MESA+ Institute for Nanotechnology, University of Twente, Drienerlolaan 5, 7522 NB, Enschede, The Netherlands

Introduction

Hydrogel matrices are often incorporated in microfluidic platforms as extracellular matrix (ECM) mimics to offer a controlled environment, and they can be used as in vitro models for tissue engineering and drug testing. These microfluidic devices are typically poly(dimethylsiloxane) (PDMS)-based, which can often lead to a mismatch in hydrophilicity and mechanical properties at the interface with the hydrogel material. Such mismatch can either impede the conformality of the hydrogel matrices or cause posterior delamination of the hydrogel during cell culture. Traditionally, methods such as plasma treatment, silanization, and polydopamine coating have been used to mitigate this effect, but they all have different limitations, leading to the instability of the adhesion or an undesirable environment for cell culture.

In this project, we adapt an interpenetration strategy [1], which was reported recently using a combination of hydrophobic and hydrophilic initiators, for incorporating tunable hydrogel matrices suitable for cell culture, on 2D PDMS substrates and in 3D microfluidic platforms, and compare this strategy with traditional approaches including plasma treatment, silanization, and polydopamine coating. As for hydrogel matrix, we used photopolymerized poly(ethylene) glycol (PEG) thiol-norbornene (SH-Nor) hydrogels, which involve a radical-mediated step-growth addition polymerization [2].

Methods

In-situ photorheology was used to study the mechanical properties and gelation kinetics of the hydrogel. Scanning Electron Microscope (SEM) and Energy Dispersive X-ray element mapping were used to study the success of the reaction at the interface and the interpenetration effect. Quantitative adhesion strength was measured by tensile and lap shear tests, while a qualitative study via aqueous immersion was performed to assess the stability of the PEG/PDMS interface. Cell culture studies were performed to assess the biocompatibility of the hydrogel and the hydrogel morphology change during culture in the microfluidic platform.

Results & Discussion

Photorheological results confirm that the PEG thiol-norbornene hydrogels have tunable mechanical properties and gelation times that depend on the specific gel composition and are convenient for cell encapsulation. By varying the hydrogel composition from 20 to 4 wt%, we get average storage modulus of 47 ~ 5.5 kPa, and the crosslinking time is within 3 min. Additionally, the interpenetration group showed higher lap shear strength compared to other control groups (Fig. 1). Furthermore, when cells were encapsulated in the hydrogel and cultured in the PDMS device, the interpenetration approach showed high cell viability (> 80 %) after 1 day of culture in the microfluidic platform (Fig. 1). The hydrogel/PDMS interface appears to be robust both in the presence and absence of cells.

Conclusions

A mechanically tunable PEG SH-Nor hydrogel matrix for cell encapsulation, enabled by thiol-ene photopolymerization, was successfully prepared and the improved interfacial adhesion between this hydrogel and PDMS substrates via the interpenetration approach was demonstrated. The improved adhesion strength between the hydrogel and PDMS via the interpenetration approach was confirmed by the lap shear test and SEM imaging. Furthermore, in terms of biological performance, the PEG SH-Nor hydrogel proved to be highly biocompatible for encapsulation of normal human dermal fibroblast (NHDF) cells in a microfluidic platform, with cell viability over 80 % after 1 day of culture.

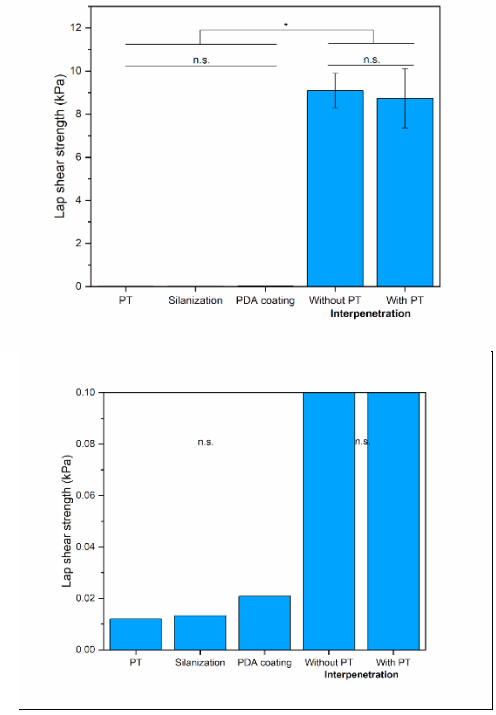

Figure 1. Lap shear strength of different groups, for the interpenetration group, samples without and with oxygen plasma pre-treatment were tested (PT stands for plasma treatment). Statistical significance analysis was performed by one-way ANOVA followed by the Tukey test (*p < 0.05 used for statistical significance; n.s. = not significant).

References

1. Yu, Y., Yuk, H., Parada, G. A., Wu, Y., Liu, X., Nabzdyk, C. S., Youcef-Toumi, K., Zang, J., & Zhao, X. (2018). Multifunctional "hydrogel skins" on diverse polymers with arbitrary shapes. *Advanced Materials*, 31(7), 1807101.
2. Lin, C.-C., Ki, C. S., & Shih, H. (2014). Thiol-norbornene photoclick hydrogels for tissue engineering applications. *Journal of Applied Polymer Science*, 132(8).

Influence of Tissue Growth on Collagen Orientation in Articular Cartilage

J.R. Peters, M. Hoogenboom, F.Abinzano, J. Foolen, K. Ito
Orthopaedic Biomechanics, Department of Biomedical Engineering, Eindhoven University of Technology, The Netherlands

Introduction

Articular cartilage exhibits a distinct structural arrangement of collagen fibers, extending upright from the underlying bone, through the deep cartilage zone, arching over and lying flat in the superficial zone. This arcade-like organization was originally described by Benninghoff [1] and plays a crucial role in the functional properties of cartilage. Consequently, it is important for the mechanical function of tissue engineered cartilage to replicate this distinct collagen architecture [2]. Previous research has found that the apophyseal neoformation of cartilage during postnatal development coincides with change from isotropic to this unique anisotropic fiber organization [3]. This would suggest that localized and directional stimulation of growth is important and could drive the fiber alignment perpendicular to the surface. Therefore, this study aims to investigate the influence of the direction and manner of growth of engineered cartilage to achieve collagen fiber alignment.

Materials & Methods

Chondrocytes were isolated from bovine metacarpal articular cartilage (n=5) and cultured in spinner flasks for 12 days, supplemented with porcine derived notochordal cell matrix (NCM) to induce self-assembled cartilage organoids [4]. Organoids were cultured for 49 days on culture transwell inserts whose membranes were coated with collagen type I. After 7 days, culture medium was supplemented with 10 ng/mL human transforming growth factor β1 (TGF-β1) either in the upper compartment for the top-down (TD) stimulation of cartilage growth, or in the lower compartment for bottom-up (BU) stimulation. On days 7 and 49, constructs were evaluated for dry weight, sulfated glycosaminoglycan (GAG), and hydroxyproline (HYP) content. Moreover, the distribution of collagen and GAG was examined, respectively, with picrosirius red and alcian blue staining. Collagen fiber organization was visualized with polarized light microscopy (PLM). The orientation of alignment was quantified using a fiber-tracking image analysis tool and the proportion of fiber alignment in the angular range of 70° to 105°, with respect to the surface, versus other orientations of alignment was determined [5].

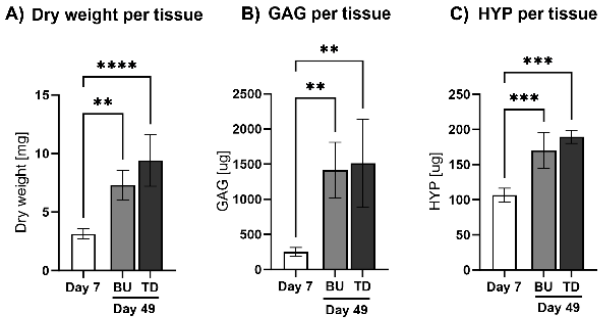

Figure 1: A) Dry weight, B) GAG and C) HYP content per tissue. **p<0.005 and ***p<0.0005

Results & Discussion

Substantial tissue growth occurred for both TD and BU groups (no difference between groups), with over 2x increase in dry weight and collagen and 6x increase in GAG content at day 49 (Fig. 1). Staining of picrosirius red (Fig. 2A and 2C) and alcian blue showed differences in the manner of growth. Regions of new tissue were observed between and underneath the organoids for the BU group, whereas for the TD group only new tissue formed between the organoids (Fig. 2C). The neo-tissue areas underneath the organoids for the BU group displayed collagen type II fiber alignment that
was perpendicular to the surface along the direction of growth (confirmed using antibody staining against type I and II collagen), similar to the deep zones of native articular cartilage. In the newly formed tissue, the BU group show increased proportion of perpendicularly aligned fibers compared to the TD group (59±9% vs. 30±12%, respectively, Fig. 3). It is unknown whether the fibers are deposited in an aligned manner or are subsequently stretched into orientation. However, as the fibers showing alignment were predominantly found in the new tissue underneath the organoids and not in the pre-existing fibers originating from the organoids, fiber alignment perpendicular to the surface is most likely derived from the former. Optimization of native cartilage-like fiber alignment using directional stimulation of growth could lead to improvements in functional tissue engineering grafts in the future.

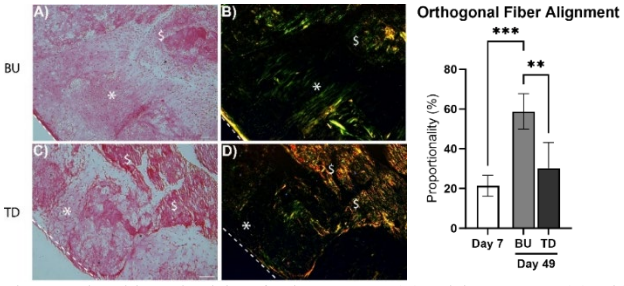

Figure 2: picrosirius red stainings for the BU-group (A) and the TD-group (C), with corresponding PLM images (B and D). Samples are oriented in 45°. Dotted line represents the bottom of the samples,
* neo-tissue formation, $ organoid structures. Scale bar = 100µm.

Figure 3:
Proportion of perpendicular fiber alignment versus other orientations. **p<0.005 and ***p<0.0005

References

[1] Benninghoff A., *Z Zelforsch Mikrosk Anat.,* 1925. [2] Nagel T, Kelly DJ *Tissue Eng Part A.* 2013. [3] Hunziker EB et al., *Osteoartritis and Cartilage*, 2007. [4] Crispim JF et al., *Acta Biomater.* 2021. [5] Dittmar R et al., *Global Spine J.*, 2016.

Acknowledgements

This research was financially supported by the Gravitation Program “Materials Driven Regeneration”, funded by the Netherlands Organization for Scientific Research (024.003.013).

The Interaction of Breast Implants and the Surrounding Tissue: An Introduction to

M.O. Rous, P. van Rijn, T.G. van Kooten, H.A. Santos
University Medical Center Groningen, Department of Biomedical Engineering, A. Deusinglaan 1, 9713 AV Groningen, Netherlands

Breast implant illness (BII)) is a condition associated with implantation that lacks a precise and widely accepted definition, leading to extensive discussions and debates. Women often present with non-specific local and systemic symptoms, which reduce upon explantation of the breast implants, suggesting a causal relationship with the implant and the associated symptoms. However, the lack of replicable studies investigating the direct connection between symptoms, physiological changes, and the underlying causes has left the etiology of these symptoms largely unexplained and enigmatic. It is hypothesized that shell degradation leads to a loss of structural integrity, resulting in the migration (i.e. bleeding) of silicone from the implant into the surrounding tissue (e.g. fat. Muscle) and lymph nodes and the claimed inert nature of the breast implants would be thereby rejected.

To substantiate this hypothesis, research efforts will be focused on understanding the effects of the implant on the surrounding tissue and identifying differences in cell behavior of M0 macrophages, adipocytes, and fibroblasts in exposure to the implants' external and internal silicone. Moreover, the reaction of these cells to specific implant material released by the implant in extraction assays, which will have been previously identified and quantified, will be examined. Furthermore, we will investigate possible ingrowth of cells and microorganisms into the silicon by means of explants as well as use these explants to characterize the alteration of mechanical properties after implantation.

Yearly, 1.7 million breast implants are placed, both for reconstructive and aesthetic purposes. Identifying correlation between the symptoms and the physiology can not only result in answers for a large patient group suffering from symptoms with unknown causes, but also can show the need of in depth revision of the consequences of silicone breast implantation by regulatory parties.

Polyhydroxyalkanoates as biodegradable polymeric biomaterials

Irem Soyhan, Lei Li, Nout van Loenen, Patrick van Rijn
W.J.Kolff Institute for Biomedical Engineering and Materials Science, University of Groningen/University Medical Center Groningen, Ant. Deusinglaan 1, Groningen, The Netherlands
i.soyhan@umcg.nl

Keywords: Polyhydroxyalkonate (PHA), Biodegradation, Hydrolysis, Biodegradable Polymers

Introduction: As the biomedical world seeks better sustainable and non-toxic substates for petroleum-driven polymers, polyesters such as polyhydroxyalkonate (PHA) present an appealing solution. PHA have garnered significant attention due to their biodegradability, low inflammatory response, biocompatibility, non-toxic degradation products, renewable resources, and lower carbon foot printing because of their microbial fermentation production[1,2].

Their aforementioned astonishing properties have emerged PHAs as an invaluable material in a wide range of application areas in biomedicine. Their utility in tissue engineering as biodegradable scaffolds providing cells to grow on and regenerate the damaged tissues. Their slow degradation rate shows promising properties for applications in wound healing or for orthopedic implants. For the latter, slow degradation and the absorbance by the body prevents drastic interventions, such as second surgery, or pH change that may lead to acidosis[3].

For clinical translation it is crucial to further elaborate on the degradation process of PHA.

However, studying the degradation behavior of PHA is not limited to buffer solutions with enzyme alone; it should also extend to biological assessments to mimic the in-vivo environment to ultimately enhance its clinical translation.

Method: The degradation process of PHA was investigated using a buffer systems at different pH and various compositions including cells (fibroblasts and immune cells/macrophages) at either 50℃ for accelerated hydrolytic degradation and at 37℃ for biological degradation approaches over the course of 10 weeks with two types of polymers namely PHA and PHBV (3-hydroxybutyrate-co-3-hydroxyvalerate).

We aim to explore the complete degradation profile of PHA in terms of both pure hydrolysis and biological assessment.

Results and Discussion: The hydrolytic degradation process of both compounds were determined gravimetrically, analyzed with Scanning Electron Microscopy (SEM) and Differential Scanning Calorimetry (DSC). Purely hydrolytic degradation under accelerated conditions did not lead to any significant weight loss while in vivo it is known to degrade over the course of a few years, indicating that biological degradation provides the key mechanism.

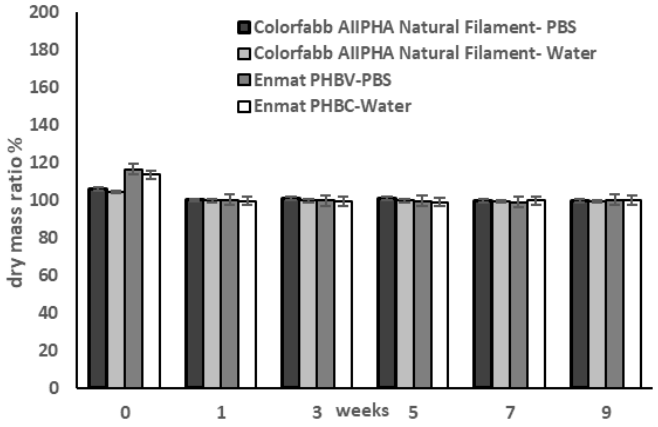

Figure 1. Dry mass ratio (%) of PHBV pellets and PHA filaments.

Conclusion: This approach shows the importance of further understanding the influencing factors of the degradation process of PHA, ultimately, broadening the applicability of these polymers in biomedicine.

Reference:

1. Pulingam, Thiruchelvi, et al. *Polymers* 14.11 (2022): 2141.
2. Li, Zibiao, Jing Yang, and Xian Jun Loh. *NPG Asia Materials* 8.4 (2016): e265-e265.
3. Ladhari, Safa, et al. *ACS Applied Bio Materials* 6.4 (2023): 1398-1430.

Mechanical Anisotropic Properties in Biofabricated Cartilage Implants

L Spauwen[1,2], A Vasilopoulou[1], A Mensinga[1], P van Veenendaal[2], M de Ruijter[1,3], J Malda[1,3]

[1]Department of Orthopaedics, University Medical Centre Utrecht, Uppsalalaan 8, the Netherlands
[2]University of Applied Sciences Utrecht, Padualaan 99, the Netherlands
[3]Department of Equine Sciences, Faculty of Veterinary Sciences, Utrecht University, Yalelaan 1, the Netherlands

Introduction

Cartilage defects pose significant challenges in terms of healing. Current treatments have limitations in size, availability and rely on donor or patient tissue[1]. Additionally, durability of total knee replacements is limited, making them unsuitable for younger patients[2]. Biofabrication aims to restore tissue functionality by placing biological active components in a pre-defined 3D-organization, typically using soft hydrogels. These hydrogels can be mechanically reinforced with microfiber box-structures created with melt electrowriting (MEW)[3]. This technology has recently been used to generate hierarchical osteochondral plugs that were able to withstand the native loading conditions[4]. To upscale towards patient-specific implants, patient-specific/anisotropic loading designs should be considered. **Therefore, this study investigates local, anisotropic mechanical properties of MEW reinforced hydrogel scaffolds**.

Methods

MEW was used to generate box-shaped scaffolds from polycaprolactone (PCL) microfibers. These boxes ranged in size from 200 x 200 µm to 500 x 500 µm in 100 µm increments (total scaffold size = 12 x 12 x 1,5 mm). Homogeneous scaffolds maintained consistent box-spacing throughout, while anisotropic designs varied the box spacing (e.g., 200 µm boxes in the center and 500 µm boxes in the surrounding areas). These scaffolds were then embedded in gelatine methacryloyl (gelMA) and crosslinked with dichloro-ruthenium (II) hexahydrate and sodium persulfate for 7 minutes with visible light (20 W, JMW20P-S, Jobmate). Mechanical properties of homogenous and anisotropic scaffolds were analyzed with a dynamic mechanical analyzer (DMA Q800, TA Instruments), focused on local compression (ø2 mm indenter) and bulk compression (compressing the entire surface of 12 x 12 mm).

Results

The homogeneous and anisotropic scaffolds were successfully printed with fiber diameters of approximately 10 µm. The embedded scaffolds demonstrated a positive relation between fiber spacing and mechanical properties ranging from 0,5 MPa to 1 MPa for bulk compression and 0,5 to 2,5 MPa for local compression (Figure 1). Significant differences were observed for local compression within the groups of local fiber spacing of 300 and 200 µm.

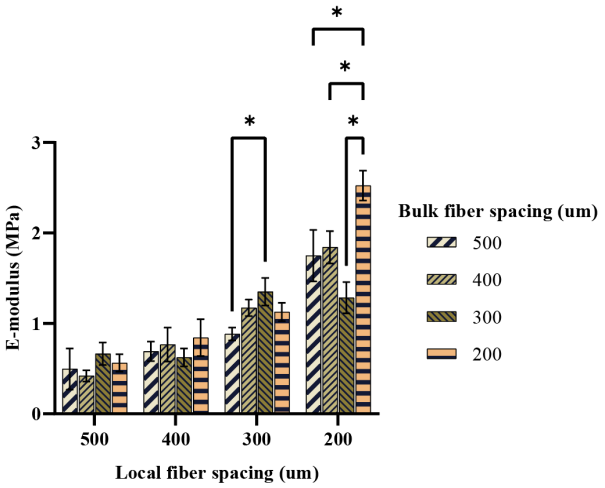

*Figure 1. Compressive modulus for **local compression** with homogenous and anisotropic scaffold designs (p<0,05 Mann Whitney-U test).*

Conclusion

This study shows the effect of anisotropic scaffolds designs on the local and bulk mechanical properties of reinforced hydrogel scaffolds. Manipulating the internal box-spacing enables to regulate the mechanical properties of the scaffold. When applying the smaller fiber spacings of 200 and 300 µm, the surrounding structure affects local compressive properties. These findings are relevant for the realization of personalized implants where patient-specific mechanical properties need to be mimicked.

References

1. Howell, M., Liao, Q. & Gee, C. W. Surgical Management of Osteochondral Defects of the Knee: An Educational Review. *Curr Rev Musculoskelet Med* **14**, 60–66 (2021).
2. Julin, J., Jämsen, E., Puolakka, T., Konttinen, Y. T. & Moilanen, T. Younger age increases the risk of early prosthesis failure following primary total knee replacement for osteoarthritis: A follow-up study of 32,019 total knee replacements in the Finnish Arthroplasty Register. *Acta Orthop* **81**, 413–419 (2010).
3. Visser, J. *et al.* Reinforcement of hydrogels using three-dimensionally printed microfibres. *Nat Commun* **6**, 1–10 (2015).
4. de Ruijter, M. *et al.* Pivotal importance of reinforcement of cartilage implants confirmed in challenging large animal model; presence of transplanted cells probably secondary. *Accepted pending minor revisions* (2023).

Can macrophage polarization be an early indicator of outcome after ACL reconstruction?

J. Spierings[1], L. Geomini[1], M. van der Steen[2], R. Janssen[1,2], K. Ito[1], J. Foolen[1]
[1]Department of Biomedical Engineering, Eindhoven University of Technology, Eindhoven, the Netherlands. [2]Department of Orthopaedic Surgery, Maxima Medical Centre Eindhoven/Veldhoven, the Netherlands

Introduction: Anterior cruciate ligament reconstruction (ACLR) with tendon autografts can display an adverse *in vivo* remodeling response. Macrophages play an important role, particularly during early graft healing [1]. Macrophages can be divided into two main types: the pro-inflammatory M1 and the pro-remodeling M2 macrophages. We propose that cytokines and DNA remnants, released by apoptotic and necrotic cells in the graft, steer macrophages more towards an M1 phenotype. We also propose that this adverse response can be prevented by graft decellularization before implantation. Our preliminary data display patient-to-patient differences in cytokine secretion from leftover graft tissue from ACLR surgery, which may be an indication of why some grafts rupture. This study aims to investigate the effect of factors released by leftover graft tissue on macrophage polarization and correlate this to patient demographics and self-reported post-operative outcomes (PROMs).

Methods: Remnant tissue of the most distal and/or proximal part of semitendinosus and/or gracilis tendons was collected after ACLR (METC N21.063). Tendons were processed immediately after retrieval (fresh (F), n=14), frozen at -20°C (fresh-frozen (FF), n=10), or decellularized [2] (partial decellularized (PD), n=8, and fully decellularized (FD), n=8). Next, paracrine influences were enabled by placing the tendon in the upper compartment and the macrophages, differentiated from the human monocytic cell line THP-1 (Sigma Aldrich lot# 16K052), in the lower compartment of a transwell system (pore size = 0.4 µm). After 24 hours, macrophage RNA was isolated, and real-time qPCR was performed to examine macrophage polarization. Gene expression was normalized to housekeeping gene GAPDH and a negative control (empty insert). Results were analyzed using a one-way ANOVA with significance set at $p < 0.05$.

Results: Expression of pro-inflammatory marker TNF-α by THP-1 cells was significantly higher for FD when compared to F ($p < 0.05$) and FF ($p < 0.01$) groups. Besides, both decellularized groups, PD and FD, showed a significantly lower gene expression in pro-remodeling marker TGF-β1 than the FF group ($p < 0.01$). Expression of both IL-1β and CD163 were not significantly affected by any treatment (Figure 1). Next to that, preliminary results showed a potential correlation between patients' age and TNF-α gene expression by macrophages (Figure 2), as younger patients tend to show higher TNF-α expression. PROM results are pending.

Discussion: Contrary to our hypothesis, gene expression of TNF-α and TGF-β1 showed that decellularized tendon tissue promotes M1 polarization of THP-1 cells. This may indicate that decellularization-induced damage-associated molecular patterns (DAMPs), e.g. collagen damage, overshadow the potential effect of dying and/or remnant cells in the tendon graft on the inflammatory response by macrophages [3]. On the other hand, a trend towards a higher TNF-α expression by macrophages exposed to tendons from younger patients (< 23 years old) was found. This is interesting as, clinically, younger patients show a higher graft-rupture rate, and it is currently not fully understood why [4]. These results reveal that pro-inflammatory polarization of macrophages may contribute to the risk of graft rupture. In the future, our data will be correlated with PROMs to improve our understanding of patient-specific recovery after ACLR and/or contribute in finding a biomarker that can help surgeons into creating personalized rehabilitation.

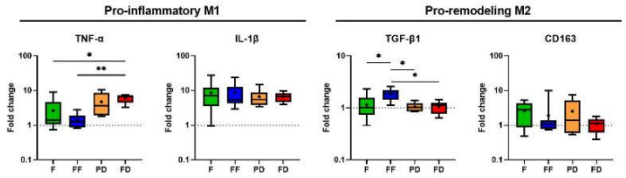

Figure SEQ Figure * ARABIC 1. Macrophage gene expression

References:

[1] Janssen & Scheffler, Knee Surg Sports Traumatol Arthrosc, 2014. [2] Uquillas, et al., JMBBM, 2022. [3] Kasravi, et al., Biomater Res, 2023. [4] Nagelli & Hewett, Sports Med, 2017.

Exploring the Role of Morphogens in Adolescent Idiopathic Scoliosis

K. Stradovnik, J. Foolen, K. Ito

Eindhoven University of Technology, Eindhoven, The Netherlands

Introduction

Adolescent Idiopathic Scoliosis (AIS) is a spinal deformity affecting 1-4% of the population, which leads to significant physical and psychological distress. While the condition's prevalence is well-documented, and the intervertebral discs (IVDs) are known to be the primary affected tissue, the precise mechanisms behind AIS development remain elusive.

One of the largely overlooked and under-researched reasons areas is the effect of morphogens (MPG) on IVD. These powerful tissue-modulating chemical signals are secreted from adjacent growth plates undergoing hyperproliferation and ossification and are responsible for growth plate cell proliferation and matrix production. However, despite the proximity of IVD cells and nothing preventing the diffusion of MPGs to the IVD tissues, we know little about their effect on the cells responsible for the AIS onset.

Objective

Our aim is to determine which MPGs and their concentrations activate signaling pathways within outer IVD tissue (i.e. Annulus fibrosus (AF)), impacting cell proliferation and matrix deposition, with a focus on collagen I, III, and elastin expression, known to vary between scoliotic and non-scoliotic patients.

In parallel, we aim to develop an improved 2.5D culture platform that facilitates the maintenance or restoration of the elongated cellular phenotype observed in vivo, in contrast to the stressed stellate shape often observed on non-patterned 2D surfaces.

Hypothesis

We hypothesize that MPGs will activate their downstream signaling pathway in AF cells, altering the collagen I, III, and elastin expression as observed in scoliotic patients.

With the fibronectin-coated polydimethylsiloxane (PDMS) platform, we will be able to establish the elongated AF cells phenotype.

Materials and Methods

We isolated AF primary cells from bovine tails (bAF) through enzymatic digestion (0.1% pronase and 0.2% collagenase II, overnight with tube rotation).

To assess morphogens concentration effects on downstream pathway activation, receptor transcription, and the expression of collagen I, II, III, and elastin, we exposed the bAF cells to various doses of morphogens for 24 h (0.1, 1, 10 ng/ml for Ihh, PTHrP, FGF-18, TGFb1, Wnt-1, IGF-1, BMP2, and 100 ng/ml for BMP2) for 24 hours. Following this, we lysed the cells and stored the lysates at -80C for further processing. RNA extraction and RT-qPCR are pending and will be performed shortly.

In parallel, we developed an improved 2.5D culture platform to promote cellular elongation. This platform utilizes a fibronectin-coated polydimethylsiloxane (PDMS) mold created from a silicon wafer featuring a 20-micrometer (20um) wide and high linear pattern of alternating raised and recessed regions.

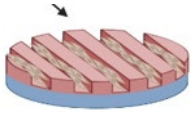

(Anticipated) Results and Discussion

In contrast to the stellate cell phenotype observed on non-patterned surfaces, our experimental constructs maintained an elongated cell phenotype within the ridges for up to 7 days. This gives us a stable platform to study the effect of morphogens on cells where their native phenotype is preserved.

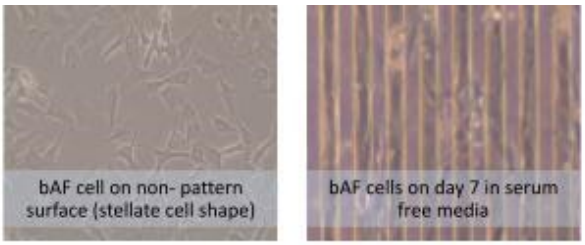

RT-qPCR and analysis of morphogen effects on AF gene expression are pending. We anticipate most MPGs to activate downstream pathways, influence receptor transcription, and modify collagen I, III, and elastin expression

Significance/Implications

By combining this enhanced 2.5D culture method, ensuring bAF cells maintain their physiologically relevant elongated phenotype with precise morphogen dosing, we aspire to create an advanced platform for investigating the impact of morphogens on AF cells, which will be in the future analyzed using RNA sequencing techniques for determination of morphogens cellular capacity for tissue remodeling.

Ultimately, our research aims to shed light on the intricate mechanisms driving scoliosis development, with a special focus on the role of growth factors. We believe this endeavor will not only advance our comprehension of AIS but also pave the way for more effective treatment strategies, and perhaps, the discovery of crucial biomarkers associated with this condition.

Wound Healing Electrospun Meshes Incorporating a Natural-based *Arrabidaea chica* Verlot extract

M.H. Taniguchi Nagahara[a,b], F. Teixeira Castro[a], A.S. Freitas[c], I.M.O. Sousa[c], M.A. Foglio[c], A.M. Moraes[b], C. Mota[a]

[a] MERLN Institute for Technology-Inspired Regenerative Medicine, Department of Complex Tissue Regeneration, Maastricht University, Universiteitssingel, 40, 6229 ER Maastricht, The Netherlands

[b] Department of Engineering of Materials and of Bioprocesses, School of Chemical Engineering, University of Campinas, Albert Einstein, 500, 13083-852 Campinas, SP, Brazil

[c] Faculty of Pharmaceutical Sciences, University of Campinas, Cândido Portinari, 200, 13083-871, Campinas, SP, Brazil

Introduction: The extract of *Arrabidaea chica* Verlot (AC), a native plant from Brazil, is popularly used in the treatment of inflammation, intestinal colic, and to promote wound healing. It is a deep-red extract characterized by the presence of anthocyanidins, phenolic compounds responsible for its antioxidant, anti-inflammatory, antifungal and antiseptic properties, as well as its capacity to promote wound healing[1,2].

Hard-to-heal lesions, e.g. chronic wounds, are frequently arrested in the inflammatory phase of wound healing, characterized by an imbalance of reactive oxygen species (ROS). In this sense, the antioxidant capacity of the plant extract could aid in managing the excess ROS that the body cannot process. As most synthetic anti-inflammatory compounds usually present side effects, alternative natural antioxidants, such as AC extract, might support ROS balance while reducing inflammation[3,4]. However, its stability is reduced in environmental conditions[1,4]. Therefore, the aim of this study is to incorporate AC extract into electrospun polycaprolactone (PCL) meshes to improve the extract stability, while ensuring controlled release envisioning wound healing applications.

Materials and Methods: A standardized AC extract was produced as previously reported[1], and its cytotoxicity to fibroblasts was assessed by metabolic activity analysis. Meshes were produced by electrospinning a 15% (wt/v) PCL solution in a mixture of chloroform and methanol (5:1), at a distance of 15 cm between the 21G needle and the rotating collector, 21 kV, and a flow rate of 5 mL/h. The extract was directly incorporated into the PCL solutions at 1, 5, and 10% (wt/wt).

The meshes were characterized regarding tensile mechanical properties, the surface hydrophilicity was analyzed through water contact angle (WCA) and the morphology by scanning electron microscopy (SEM). The controlled release of the extract was evaluated by fluorescence spectroscopy with excitation at 530 nm and emission at 585 nm for 3 days. The cytocompatibility of the meshes was evaluated using fibroblasts.

Results and Discussion: The metabolic activity analysis of the fibroblasts directly exposed to the AC extract dissolved in culture medium in different concentrations showed that cytotoxicity is observed above 1.95 µg/mL. The presence of the extract in the electrospun meshes resulted in slightly different mechanical properties. For all meshes the elastic modulus was around 8 to 9 MPa, maximum tensile stress from 2 to 3 MPa, and elongation at break of approximately 440%. The addition of AC extract decreased the maximum elongation and stress strength of the meshes but did not influence the morphological architecture, as evidenced by SEM. Regarding the interaction of the mesh surface with water, the addition of AC extract turned the surfaces of the materials more hydrophilic, in a concentration-dependent manner. The most hydrophobic surface was that of the PCL mesh with a WCA of 125°, while the least hydrophobic was the PCL mesh containing 10% of AC extract, with a WCA of 66°, considered hydrophilic.

The release of the extracts was characterized by an initial burst release followed by sustained release kinetics for up to 72 h for all the AC extract-containing meshes. The cumulative release of AC extract after 72 h ranged from 14 to 263 µg/mL depending on the initial amount of extract added. The higher the initial incorporation, the higher was the cumulative release, however, the released percentage varied from approximately 40 up to 70%, and the higher percentage released was achieved when incorporating 5% of AC extract. By incorporating the extract into the PCL mesh, we were also capable of keeping the extract more stable at 37 °C, since the free extract solution significantly degrades after 24 h, while the meshes can still release low amounts for up to 72 h.

The metabolic activity of cells seeded on top of the electrospun meshes, for a period of 7 days, increased for the mesh containing 1% of AC extract when compared to PCL alone and decreased for the ones containing 5 and 10% of extract, potentially due to the higher cytotoxic concentrations of AC extract released in the solution.

Conclusions: The results showed that the produced materials are promising candidates to be used as wound dressings for the treatment of inflamed lesions, since they are capable of controllably releasing the AC extract while also aiding in its protection from degradation at environmental conditions. Furthermore, the meshes would also be able to protect the lesion, by presenting enough elasticity to better conform to the wound site while showing higher hydrophilicity levels than PCL alone. Finally, the lowest concentration of AC extract promoted an increase in metabolic activity of fibroblasts.

Acknowledgements: The research was the supported by CNPq, CAPES and FAPESP, from Brazil, and the EU funded project PREDICTOS grant agreement 101079372.

References:

1. Sousa IMO et al. The role of spray-drying atmosphere on *fridericia chica* (bonpl.) L.G. Lohmann standardized extract production for wound healing activity. Natural Product Research 36(18):4793-4797, 2022.

2. Zorn B, et al. 3-Desoxyanthocyanidins from *Arrabidaea chica*. Phytochemistry, 56(8):831-835, 2001.

3. Arulselvan P, et al. Role of antioxidants and natural products in inflammation. Oxidative Medicine and Cellular Longevity, 2016:5276130, 2016.

4. Velnar T, Bailey T, Smrkolj V. The wound healing process: An overview of the cellular and molecular mechanisms. Journal of International Medical Research 37(5):1528-1542, 2009.

The bactericidal activity of a graphene quantum dot implant coating

L.S. van Hofwegen[1], M. Hassnain[2], P.P.S. Balraadjsing[1], S. Nizamoglu[3], S.A.J. Zaat[1]

[1]*Department of Medical Microbiology and Infection Prevention, Amsterdam UMC, The Netherlands*
[2]*Department of Biomedical Science and Engineering, KOC University, Turkey*
[3]*Department of Electrical and Electronics Engineering, KOC University, Turkey*

Introduction: One of the most common complications related to implantation of a biomaterial is biomaterial-associated infection (BAI). BAI is predominantly caused by the commensal bacteria *Staphylococcus aureus* and *Staphylococcus epidermidis*, which can become pathogenic in the presence of a biomaterial. These infections may lead to chronic inflammation and in severe cases, loss of implant function and even the need for replacement. Biomaterial surfaces coated with antimicrobials are a promising strategy for prevention of BAI, but the use of antibiotics is discouraged because of resistance development. Graphene quantum dots (GQD) may provide an alternative for antibiotics to protect against infection. GQD consist of a single layer of carbon atoms in a honeycomb-like structure with photo-activation properties. Upon photo-activation, GQD can generate reactive oxygen species (ROS) which can kill bacteria (Figure 1).

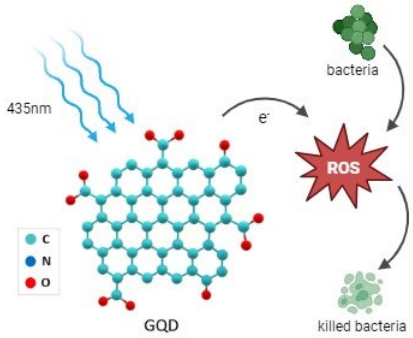

Goal: In this study, we aimed to test colloidal GQD-COOH, a carboxylated form of the GQD, as well as a novel GQD-COOH coating for their bactericidal activity against *S. aureus* and *Escherichia coli,* as representatives for Gram-positive and Gram-negative bacterial species. **Methods & Results:** To test the bactericidal activity of colloidal GQD-COOH, we used the minimal bactericidal concentration (MBC) assay. After 30 minutes of photo-activation with a 435nm blue LED light, the lowest concentrations of colloidal GQD-COOH which killed 99.9% of *S. aureus* and *E. coli* inocula were 0.8 µg/ml and 13 µg/ml, respectively. Furthermore, we tested a novel GQD-COOH coating for its bactericidal activity using the Japanese Industrial Standard (JIS) assay, where we photo-activated the GQD-COOH coating with 435nm blue light for 30 minutes. The coating consisted of alternating layers of GQD-COOH and polymer applied on glass slides. The GQD-COOH coating showed promising bactericidal activity against both *S. aureus* and *E. coli*, as photo-activation of the GQD-COOH coating resulted in complete killing of both bacterial test strains.

Conclusion: Colloidal GQD-COOH and the GQD-COOH coating show promising bactericidal activity against representative Gram-positive and Gram-negative bacteria. Therefore, a GQD-COOH coating may be a suitable candidate for application on medical devices to prevent BAI.

Influence of macromolecular crowding on collagen I fibrillogenesis in 3D printing

N.S. Vergara Vera[1], M.P. Vena[2], S. Hofmann[1], K. Ito [1,2] and M. Castilho[1,2]

[1] Orthopaedic Biomechanics, Department of Biomedical Engineering, Institute for Complex Molecular Systems, Eindhoven University of Technology, The Netherlands

[2] Department of Orthopedics, University Medical Center Utrecht, Utrecht, The Netherlands

Introduction: Collagen type I scaffolds have been stud- ied as potential alternatives to autografts for bone defecr treatment; however, their applications remain limited due to poor mechanical properties [1], often attributed to a loss of hierarchical organization. Current fabrication methods focus on bulk properties such as porosity (collagen sponges and electrospun scaffolds) and strength (composites) [1], but do not address the lack of control of the hierarchi- cal structure. Macromolecular crowding (MMC), a phenomenon based on excluded volume effects generated by large molecules, has been studied as a way to control collagen architecture [2,3]. Here, we explored the combination of MMC and extrusion printing as a means to con- trol collagen organization at different length scales in order to achieve native collagen-like structural attributes. We hypothesized that MMC enables tuning of fiber size and network density, while suspended extrusion printing enables fiber alignment and control over the macro-structure.

Materials and Methods: The MMC effects of PEG on collagen micro-structure were first studied on casted gels. Two different collagen starting materials were used: a tropocollagen solution (sColl, 5.9 mg/mL, bovine) and a suspension of collagen fibers (dColl, 5 mg/mL, bovine). PEG (20 kDa) was dissolved in PBS 1X to yield buffer solutions of different concentrations (2 to 20 mg/mL). Casted gels were prepared by combining the collagen and buffers solutions at a 1:5 (v/v) ratio, followed by incubation at 37 °C. To bring MMC into 3D printing, PEG was incorporated into the collagen ink ([Collagen] = 10 mg/mL, [PEG] = 7.5, 10 & 50 mg/mL) and meshes were printed in a support bath (4.5% gelatin type A) supplemented with PBS 1X. The bath was removed by incubating the prints at 37 °C for at least 1 hour. The degree of alignment in the prints was characterized using polarized light microscopy (PLM). Finally, the effect of MMC on fiber morphology was characterized using SEM.

Results and Discussion: The stability of the casted gels and printed constructs depended on the starting collagen material. sColl formed strong casted gels but weak printed constructs; while dColl did not form casted gels, but the printed constructs were stable. Hence, imaging was only possible on sColl casted gels and printed constructs made from dColl. SEM images revealed that MMC modified the diameter and density of collagen fibers (Figure 1), with a smaller apparent diameter (in the range of 67 13 nm – 131 27 nm) and larger packing density for higher [PEG]. Adding PEG to the ink seemed to enhance fiber alignment in the printed scaffolds, but no difference in diameter or density was observed (Figure 2). While the extrusion pro- cess itself was expected to aid fiber alignment, this effect was most noticeable in combination with MMC.

Conclusion: We demonstrated that adding PEG to a collagen solution allows tuning of fiber size and density. Preliminary results showed that incorporation of PEG in the collagen ink may influence fiber orientation in printed scaffolds. To that end, PLM is currently being explored as a semi-quantitative method to characterize alignment. Moreover, the influence of the collagen starting material on the final constructs was highlighted. Future work will focus on understanding the role of MMC in printing, and optimizing collagen/PEG inks for further control of fiber formation.

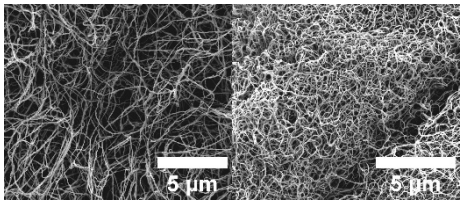

a. [PEG]= 10 mg/mL. (b) [PEG] = 20 mg/mL

Fig. 1: Collagen assembly under MMC in casted gels. Made with sColl.

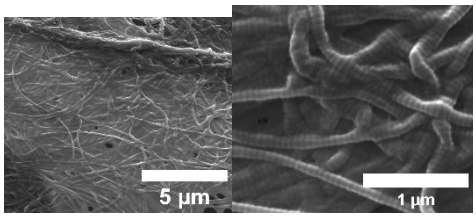

a. No PEG (b) No PEG - *D-banding*

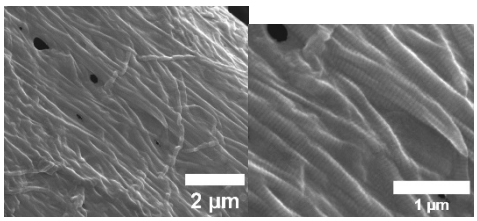

(c) [PEG] = 7.5 mg/mL (d) With PEG - *D-banding*

Fig. 2: Nanometer view of 3D-printed scaffolds under MMC conditions. Ink made from dColl. *D-banding* of collagen I was present in both cases.

REFERENCES

1. L. Fan et al.,*International Journal of Molecular Sciences*, 2023, **24**.
2. S. K. Ranamukhaarachchi et al., *Biomater. Sci.*, 2019, **7**, 618–633.
3. J.-Y. Dewavrin et al.,*Acta Biomaterialia*, 2014, **10**, 4351–4359.

Acknowledgments: This research was financially supported by the Gravitation Program "Materials Driven Regeneration", funded by the Netherlands Organization for Scientific Research (024.003.013).

Early host responses to in situ engineered heart valves

V.C. Vetter12, A.I.P.M. Smits12, C.V.C. Bouten12

1 Department of Biomedical Engineering, Eindhoven University of Technology, Eindhoven, The Netherlands 2 Institute for Complex Molecular Systems, Eindhoven University of Technology, Eindhoven, The Netherlands

Introduction

The focus of this research is to improve the understanding of cellular events occurring after implantation of tissue engineered heart valves (TEHVs) into the circulation. TEHVs are a promising alternative to overcome the limitations of current valve replacements. Although the potential and immediate functioning of several valve scaffold materials have been demonstrated, there is an insufficient understanding of the host response to these materials in a complex blood stream environment, and the resulting effects on initial tissue formation in-vivo hampers clinical translation. In our most recent study, we developed a novel approach, by coupling a micro-bioreactor system1 providing hemodynamic signals (stretch and shear), with whole blood perfusion to more closely mimic the in-vivo environment which a valve implant will experience after implantation. This system allows us to systematically improve our understanding of the cellular events that occur during the early stages of transformation of scaffolds materials into heart valves and to potentially predict in-vivo performance. In addition, both synthetic and decellularized porcine heart valves have shown to be promising heart valve scaffold materials, yet they have never been compared in one study. Here, we investigated the potential of various scaffold materials and the impact of scaffold pre-implant seeding with circulating endothelial colony forming cells (ECFCs). In addition we delved deeper into the interaction between neutrophils and biomaterials.

Methods

Electrospun polycarbonate bis-urea, poly(4-hydroxybutyrate), polycaprolactone and decellularized porcine valves were investigated under static and dynamic culture conditions with ovine whole blood. In addition, the effect of scaffold pre-seeding with donor-matched ovine ECFCs was investigated under the same conditions.

Further, human neutrophils were isolated from buffy coats to investigate the neutrophil-biomaterial response in more detail. The neutrophil responses were investigated through neutrophil characterization, activation and neutrophil extracellular trap (NET) quantification.

Results

We observed a large number platelets and neutrophils attaching to all electrospun scaffold types scaffolds in a static and flow blood environment. This result was not observed for decellularized scaffolds.

Initial data suggests ECFC pre-seeding of synthetic scaffolds under pulmonary flow reduces:
1) platelet aggregation by decreased number of CD41+ cells
2) neutrophil accumulation by a decreased number of CD11b+ cells.

Further, we observed that neutrophils pre-conditioned all electrospun scaffolds. Additionally, a significant degree of heterogeneity was observed among duplicate samples. Interestingly, this heterogeneity was not evident in the case of decellularized heart valves, where no NET formation was detected.

Conclusions & outlook

We demonstrate that we successfully assessed the interactions of immune cells attaching from the blood to our scaffold materials with the provision of hemodynamic signals. In addition, this study demonstrated the significant number of neutrophils attaching from the bloodstream and preconditioning the scaffolds. Future studies will have to investigate the impact of the neutrophils pre-conditioning on the subsequent host response.

Acknowledgement

We gratefully acknowledge the Gravitation Program “Materials Driven Regeneration”, funded by the Netherlands Organization for Scientific Research (024.003.013)

Literature

1. Smits AIPM, Driessen-Mol A, Bouten CVC, Baaijens FPT. A mesofluidics-based test platform for systematic development of scaffolds for in situ cardiovascular tissue engineering. Tissue Eng Part C Methods. 2012;18(6):475-485. doi:10.1089/ten.tec.2011.0458

Bioactive glasses vs Bacteria: Using the pH to Fight Infections in Long Bone Defects

M. Warin [a], L. Morejón [b], J. Delgado [c], M. van Griensven [a], E. Rosado Balmayor [d]

[a] Dept. cBITE, MERLN Institute for Technology-Inspired Regenerative Medicine, Maastricht University, Maastricht, The Netherlands.
[b] Center of Biomaterials, University of Havana, Havana, Cuba
[c] Faculty of Earth Sciences, University of Barcelona, Barcelona, Spain
[d] Experimental Orthopaedic and Trauma Surgery, Department of Orthopaedic, Trauma, and Reconstructive Surgery, RWTH Aachen University Hospital, Aachen, Germany

Introduction:

Every year, many people suffer from long bone fractures, and it is known that the bone defects created by those fractures can be hard to treat. Diverse factors such as trauma, bone diseases, congenital anomalies, or tumor resections can be responsible for those bone defects. While bones usually are able to regenerate themselves quite easily, this process is unsuccessful in 5 to 10% of the cases, resulting in a non-union. A non-union can be due to a critical size defect, poor mechanical stability, a lack of vascularity, a lack of soft tissue coverage, or the presence of infection among others.

The current treatments include autografts, allografts, and bone graft substitutes. A major cause of non-union is the presence of an infection at the fracture site, resulting in delayed healing or complete absence of healing. In case of an infection, the existing treatments can be combined with antibiotics, various antibacterial coatings, or Bioglass®. Sadly, those combinations often fail to eradicate the infection, causing the last option to be amputation and putting into light a tremendous need for new ways of fighting microorganisms.

Bioactive glasses release ions when degrading, thus increasing the pH, and killing bacteria**.** Some commercially available bioactive glasses are already known to have an antibacterial effect. However, the University of Havana manufactured and characterized bioactive glasses made of three types of silica sands and calcite from Cuban natural deposits, and while the formulation, rate of degradation, and bioactivity behavior of those glasses are well established (1), their bactericidal properties are still unknown.

This project aims to assess the antibacterial properties of those Cuban bioactive glasses. Bioactive glasses may be added to composite formulations in biodegradable implants to enhance bone healing while exhibiting an antibacterial effect.

Materials and methods:

The antibacterial capacity of diverse bioactive glasses such as Novamin®, Bonalive®, and newly developed phosphorous pentoxide-free bioactive glasses was investigated. The newly developed glasses, made by using Cuban extracted raw materials are composed of 52.1% SiO_2, 23.2% Na_2O, and 22.6% CaO (1).

The most encountered bacteria in long bone non-unions, and therefore the ones used in this project, are Staphylococcus aureus and Staphylococcus epidermidis.

This project also uses mesenchymal stem cells (MSCs) isolated from Bone Marrow Aspirate Concentrate (BMAC) and obtained with informed consent from patients of the Maastricht University Medical Center (MUMC+).

In order to study the antibacterial potential of the different bioactive glasses, antibacterial susceptibility assays are used. For this, the ISO standard norm ISO 20776-2:2021 was followed with no modification (2). To do so, blank antibacterial susceptibility discs were placed in Petri dishes previously inoculated with 1.5 x 10^8 CFU/ml of S. aureus and S. epidermidis, separately. Solutions made of Phosphate-buffered saline (PBS) and bioactive glasses are added to those discs. The bioactive glasses concentrations tested were the following: 100, 200, 300, 400, 500, 1000, 1500, 2000, 2500, and 5000 µg/ml. The bioactive glasses were incubated in PBS for 7 days at 37°C under mild agitation.

After overnight incubation of the Petri dishes, the zones of inhibition created by the solutions are measured. Blank discs with PBS alone and Cefazolin-loaded discs are used as negative, and positive controls, respectively.

The viability of the MSCs cultivated in the presence of the same bioactive glasses concentrations was also investigated.

Results:

The antibacterial susceptibility assays yielded negative results when using the Novamin® bioactive glass. This shows that this bioactive glass features no bactericidal effect against S. aureus and S. epidermidis.

On the other hand, the Bonalive® bioactive glass showed promising results. The antibacterial potential of the Cuban bioactive glasses shows different antibacterial properties depending on the glass composition and the concentration used. This is possibly related to the presence of different trace elements in each of the glasses. MSCs obtained from BMAC remained viable when grown in contact with the investigated bioactive glasses.

Conclusion:

In this preliminary work, we show that when used alone, the Novamin® bioactive glass does not have an antibacterial effect against S. aureus and S. epidermidis. The promising results of the Cuban bioactive glasses encourage us to think that a combination of these glasses with other biomaterials to develop bone scaffolds may allow us to create a model with a maximized antibacterial effect.

References:

1. Font Tellado S, Delgado JA, Poh SPP, Zhang W, Garcia-Valles M, Martinez S, et al. Phosphorous pentoxide-free bioactive glass exhibits dose-dependent angiogenic and osteogenic capacities which are retained in glass polymeric composite scaffolds. Biomater Sci. 2021;9(23):7876-94.
2. ISO 20776-2:2021; Clinical Laboratory Testing and In Vitro Diagnostic Test Systems. International Organization for Standardization—ISO: Geneva, Switzerland, 2021.

Steering Stem Cell Behaviour within 3D Living Composite Tissues using Stimuli-responsive Cell-adhesive Micromaterials

N.G.A. Willemen*, T. Kamperman*, C.L. Kelder, M. Koerselman, M. Becker, L. Lins, C. Johnbosco M. Karperien, and J. Leijten
Department of Developmental BioEngineering, Faculty of Science and Technology, Technical Medical Centre, University Twente, Drienerlolaan 5, 7522NB Enschede, The Netherlands. Contact: n.g.a.willemen@utwente.nl

Background

Engineered living microtissues such as cellular spheroids and organoids have enormous potential for the study and regeneration of tissues and organs.[1] These models are typically formed via self-assembly of cells via cellular adhesion.[2] Consequently, these microtissues are material-free, and thus offer little to no mechanical or biochemical control over their local microenvironment,[3] which has severely limited control over their behavior, functional performance, and on-demand adaptivity. Here, we report on the development of stimuli-responsive cell-adhesive micromaterials (SCMs) that can self-assemble with cells into 3D living composite microtissues via integrin binding, even under serum-free conditions. We demonstrate that SCMs homogeneously distribute within engineered microtissues and possess on-demand *in situ* tunable biophysical and biochemical properties, which enables cell programming via cell-material interactions by controllably designing the microtissue microenvironment. Specifically, cell behavior can be controlled based on the size, stiffness, number ratio, and biofunctionalization of SCMs in a temporal manner via orthogonal secondary crosslinking strategies.

Material & Methods

Microgel production: Microgel precursor droplets composed of dextran-tyramine-biotin (DexTAB) and horseradish peroxidase in phosphate-buffered saline were emulsified in surfactant-containing oil using a microfluidic droplet generator, and subsequently crosslinked via microfluidic supplementation of H_2O_2.[4, 5] Dex-TAB microgels were consecutively incubated with neutravidin, washed, incubated with (desthio)biotinylated molecule-of-interest (e.g., biotinylated c(RGD)fK), and washed again.

Tunable modular tissue engineering: Microgels were homogeneously co-seeded with cells into non-adherent agarose microwells. The mechanical properties of microgels could be modified post-synthesis by visible-light-induced crosslinking of tyramine moieties using ruthenium and sodium persulfate. Chemical modification of the microgels was achieved via supramolecular complexation of avidin and biotin analogs.[6]

Results

Reactive tyramine and biotin moieties in Dex-TAB microbuilding blocks could be enzymatically post-crosslinked and/or functionalized with avidin/biotin analogues, respectively. This enabled independent in situ tuning of the microbuilding blocks' mechanical and chemical properties. Stepwise functionalization of microbuilding blocks with c(RGD)fK initiated the self-assembly of cells and microbuilding blocks into living microtissues.

Incorporating microbuilding blocks within the living microtissues uniquely supported cell-biomaterial mechanotransduction, which was essential for osteogenic differentiation of 3D cultures. Material stiffness-induced lineage programming of living microtissues was dependent on the size, stiffness, number ratio of microbuilding blocks, and timing of mechanical cues.

In situ biochemical control over the microtissues was shown by temporally endowing the microbuilding blocks with (desthio)biotinylated bone morphogenetic protein (BMP)7 neutralizing nanobodies, which showed temporal control over the cellular response using a BMP-reporter cell line.

Conclusion:

In conclusion, we developed the first biochemically, biophysically, and spatiotemporally controlled smart building blocks for modular tissue engineering. This allowed for the creation of highly tunable and defined cellular microenvironments, which more accurately resembled the dynamic microenvironment of cells in native tissues.

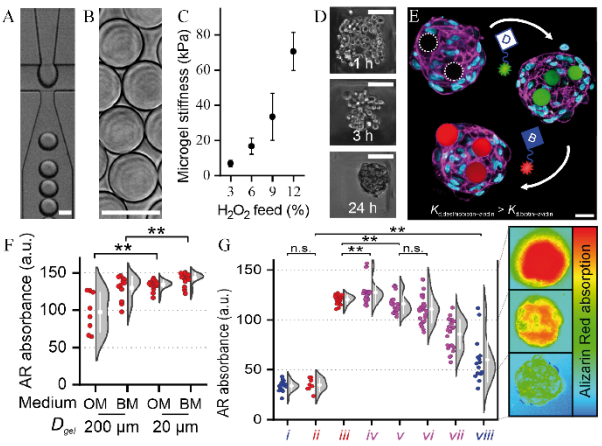

Figure 1: *A) Generation of aqueous droplets in droplet generator. B) DexTAB microgels post-crosslinking. C) Microgel stiffness was controlled by H_2O_2 supplementation. D) RGD-functionalized SCMs self-assemble with cells into microaggregates. E) In situ control over biochemical moieties using (desthio)biotin complex. F) Cell-sized SCMs induce higher osteogenic lineage commitment compared to larger SCMs. G) Osteogenic differentiation was temporally steered by in situ stiffening of soft SCMs.*

References:

[1] S. M. Oliveira *et al*, *Biotechnology Advances*, 33 (6), 2015.
[2] M. C. Decarli *et al, Biofabrication*, 13, 2021
[3] A. J. Engler *et al*, *Cell*, 126, 2006.
[4] T. Kamperman *et al.*, *Adv. Mat.*, 33, 2021.
[5] T. Kamperman *et al, Small*, 13 (22), 2017
[6] T. Kamperman *et al, Nat. Commun*, 10, 4347, 2019

Investigating the peripheral neurovascular interactions based on an in vitro model using melt electrowriting and collagen/fibrin hydrogel

H. Wu[a], P. Wieringa[a], L. Moroni[a]

[a] Complex Tissue Regeneration Department, MERLN Institute for Technology-Inspired Regenerative Medicine, Maastricht University, 6229 ET Maastricht, the Netherlands

Introduction:

Peripheral nerves and blood vessels distribute in a hierarchical and parallel pattern throughout the human body and play a critical role in maintaining homeostasis and physiological activities. Schwann cells (SCs) are known to be key players in driving parallel patterning that is observed between nerve fibers and blood vessels. Traditionally, these are viewed as the main glial cells of the peripheral nervous system that wrap around axons to form myelin sheaths, improving the speed and efficiency of nerve impulse conduction.[1] However, SCs have been found to play an important role in recruiting blood vessels to align with nerve branches.[2] In embryonic limb skin development, pre-established branches of sensory nerves and surrounding SCs express neurogenic Cxcl12 to recruit the blood vessels aligning with nerves, while neurogenic VEGF-A is also secreted to induce arterial differentiation, resulting in a mature peripheral neurovascular distribution pattern.[2]

Due to this resulting anatomical proximity and sharing a range of signals and receptors, nerves and blood vessels have a close interaction with each other.[3,4] Dysregulation of this interaction is commonly seen in chronic diseases such as type 2 diabetes and endometriosis,[5,6] which could aggravate disease severity and significantly reduce life quality. However, it is still unclear how human body regulates this interaction and its mode of effect on surrounding tissues and organs.

The aim of this study is to develop a model system that will allow us to better study this interaction, specifically how the spatial organization of one cell population can impact the other cell population. Variables of interest include the degree of cell alignment and order, the spacing between cells and the impact of collagen/fibrin hydrogel on driving mutual self-assembly of two separate cell populations. Using a combination of melt electrowriting (MEW) and hydrogels with SCs and human microvascular endothelial cells (HMVECs), we will explore these interactions between peripheral nerve and blood vessels.

Materials and Methods:

MEW was used to produce polycaprolactone (PCL) scaffolds in this study. We first used MEW to fabricate scaffolds containing a monolayer of parallel-aligned PCL fibers. According to the fiber spacing, we set four different scaffolds: 300µm, 500µm, 700µm, and 900µm. Next, SCs were seeded on the scaffold to induce the SCs encapsulated fibers. During the seeding procedure, custom-made polydimethylsiloxane (PDMS) ring molds were put above the scaffold to improve seeding efficiency. The whole system was then embedded within 3D collagen/fibrin hydrogel with different heights. To achieve this, a series of PDMS ring molds with hollow in the middle (0.4mm, 0.6mm, and 0.8mm height) were applied and put on top of the scaffold for hydrogel to crosslink. Finally, HMVECs were seeded on the hydrogel for further co-culture and to study their degree of alignment and patterning during tubulogenesis.

Results and Discussion:

According to SEM results, the actual fiber spacing of four scaffold sets was 290.71±42.02µm, 497.38±10.59µm, 707.33±14.57µm, and 924.44±11.16µm, which were consistent with the preset parameters. Parallel fiber diameters within four groups were 13.81±1.18µm, 11.70±1.45µm, 13.44±3.23µm, and 12.57±0.72µm, which were close to the diameter of peripheral nerves. Following seeding, SCs were able to wrap around fibers, forming parallel SC bundles that could maintain their shape in a 3D hydrogel environment. We anticipate that the pre-arranged SC bundles will induce vessel formation and guide the direction of vessel alignment. Furthermore, as the distance between SC bundles increases, the formation of blood vessels becomes deficient in traffic branches.

Summary:

To further understand the crosstalk between peripheral nerves and blood vessels, we here developed an *in vitro* model for assessing cell-cell interaction patterns. A series of scaffolds with controllable fiber spacing were prepared by MEW for pre-patterned cell culture, and the influence mode of SCs on the vascularization of HMVECs was explored in a hydrogel three-dimensional environment.

Keywords:

Neurovascular interaction; MEW; Hydrogel

References:

1. Zhang SH, Shurin GV, Khosravi H, et al. Immunomodulation by Schwann cells in disease. *Cancer Immunol Immunother*. 2020;69(2):245-253.

2. Li W, Kohara H, Uchida Y, et al. Peripheral nerve-derived CXCL12 and VEGF-A regulate the patterning of arterial vessel branching in developing limb skin. *Dev Cell*. 2013;24(4):359-371.

3. Mukouyama YS, Gerber HP, Ferrara N, Gu C, Anderson DJ. Peripheral nerve-derived VEGF promotes arterial differentiation via neuropilin 1-mediated positive feedback. *Development*. 2005;132(5):941-952.

4. Malheiro A, Wieringa P, Moroni L. Peripheral neurovascular link: an overview of interactions and in vitro models. *Trends Endocrinol Metab*. 2021;32(8):623-638.

5. Feldman EL, Callaghan BC, Pop-Busui R, et al. Diabetic neuropathy. *Nat Rev Dis Primers*. 2019;5(1):42.

6. Laschke MW, Menger MD. Basic mechanisms of vascularization in endometriosis and their clinical implications. *Hum Reprod Update*. 2018;24(2):207-224.

Sustainability in clinical nanogel coating technology for combating central venous catheter infection

R.Zhang, Y.Ji, P. van Rijn
University of Groningen/ University Medical Center Groningen
Department of BioMedical Engineering,
Ant. Deusinglaan 1, 9713 AV Groningen, The Netherlands
r.zhang@umcg.nl

Key words: *nanogel coating, light-switchable antimicrobial, sustainability, central venous catheter infection*

Abstract: Central venous catheter–related infections (CRIs) are high-risk infections responsible for prolonged hospitalization and significantly increased mortality all over the world. To prevent this phenomenon, increasing dosages of pharmaceuticals such as antibiotics were applied, which may induce antimicrobial resistance. Nowadays, exploring more sustainable materials and pharmaceuticals for clinical applications is becoming a long-pursued goal in the healthcare field.

Herein, we aim to develop a smart and sustainable antimicrobial nanogel coating based on bio-based material precursors and then combine it with on-demand antibiotic activation with lowered antimicrobial

resistance potential to prevent CVC infections. The nanogels are modified with cyclodextrin (CD) as the delivery vehicle and coating basis. Light-switchable azobenzene-based quinolone antimicrobial will then be incorporated into the system via the host-guest interaction with cyclodextrin.[1] Triggered by light, controllable molecular activation and on-demand drug release can be realized. This novel light-triggered antimicrobial-releasing nanogel coatings possess tremendous potential in preventing CRIs and enable sustainable biomedical materials to come to the markets.

Experimental Methods: In order to incorporate CD moieties into the cross-linking networks of the Poly(N-isopropylmethacrylamide) (p(NiPMAm)), acrylamide-modified β-cyclodextrin

(Ac-β-CD) were prepared via the reaction of per-6-amino-β-CD with acryloyl chloride under strong alkalinity condition.[2] The chemical structures and the average substitution degree of the amino groups of Ac-β-CD were investigated by the ^{1}H and ^{13}C NMR spectra and FTIR. The CD-containing p(NiPMam) nanogels were synthesized by precipitation polymerization technique. Particle size and morphology of nanogels were analysed by dynamic light scattering (DLS) measurements and transmission electron microscopy (TEM).

Results and Discussion: The modification of per-6-amino-β-CD with acryloyl chloride enables the introduction of the reactive vinyl group into the CD and further free-radical polymerizations with NiPMAm monomers to prepare CD-containing nanogel. Due to the fact that the modified CD are functionalized with numerous acrylamide groups, they can be also considered as the crosslinking reagents to substitute conventional crosslinkers such as BIS in our systems.

After incorporating 2mol% of modified CD into the p(NiPMam) nanogel system, the particle size decreased from 655 nm to 76 nm and presented a homogeneous size distribution.

Conclusions: β-CD with reactive acylamide groups on the outside surface were synthesized with per-6-amino-β-CD and acyloyl chloride under strong base condition. The CD-containing nanogels were prepared by incorporating 2mol% of Ac-β-CD into the p(NiPMam) chains. The obtained particle size was around 75 nm. In the following experimental plans, the light-switchable azobenzene-based quinolone antimicrobial will be loaded into the nanogels via the the host-guest interaction with cyclodextrin and applied as the antimicrobial coating on the central venous catheter. Then the polymeric matrix of nanogels will be substituted by the bio-based materials possessing similar chemical structures with NiPMam monomers, to achieve sustainability.[3]

References:

[1] Velema, Willem A., et al. Nature chemistry 5.11 **(2013):** 924-928.
[2] Harada, Akira, et al. Nature chemistry 3.1 **(2011):** 34-37.
[3] Hermens, Johannes GH, et al. Science Advances 6.51 **(2020):** eabe0026.

An Injectable Hydrogel Loaded with Dual-coated Nanoparticles for Wound Healing Application

Y Zhu[1], H A Santos[1,2], M-A Shahbazi[1]
[1] Department of Biomedical Engineering and W.J. Kolff Institute for Biomedical Engineering and Materials Science, University Medical Center, Groningen/University of Groningen
[2] Drug Research program, Division of Pharmaceutical Chemistry and Technology, Faculty of Pharmacy, University of Helsinki, Helsinki, Finland

Introduction

Infected wounds are a major challenge worldwide as it is responsible for delayed wound healing due to persistent infection. Currently, effective treatments for such wounds are still lacking. In recent years, photothermal therapy (PTT) has received significant attention as a promising strategy for quickly killing bacteria and promoting wound healing through precise temperature regulation(1). We are aiming to develop a dual coated core-shell nanohybrid made of polydopamine (PDA), manganese-dioxide (MnO2), and copper-oxide (CuO), which will be incorporated into an injectable hydrogel to accelerate wound healing. PDA exhibits ideal photothermal antibacterial treatment effects and has excellent photostability(2), while the MnO2 in the middle layer can convert the endogenous hydrogen peroxide (H2O2) into oxygen, which is expected to improve the hypoxic environment of the wound. The outermost layer of CuO carries antioxidant properties, which is needed for effective wound healing. Besides the nanoparticles (NPs), taurine is also incorporated into the injectable hydrogel to induce anti-inflammatory macrophage polarization for effective wound healing.

Method

PDA@MnO2@CuO NPs are prepared by simple chemical reactions for effective layer by layer coating of the PDA core. An injectable hydrogel of Farsi gum (FG) and hyaluronic acid (HA) was prepared by metal cross-linking. The size, photothermal performance, and morphology of the NPs, as well the injectability and rheological properties of the hydrogel were investigated. Subsequently, the in vitro toxicity of the hydrogel was evaluated on normal human dermal fibroblasts (NHDF).

Result

PDA@MnO2@CuO NPs had a size range of 140 to 240 nm. Transmission electron microscopy (TEM) (Fig. A) and EDX analysis proved the presence of the coating layers on PDA NPs. Then the NPs were successfully loaded into the hydrogel together with taurine (Fig. B). The mechanical properties of the pre-formed gel were measured in a dynamic oscillatory frequency sweep by a rotated rheometer. The storage (elastic) modulus (G') of all hydrogels was consistently larger than the loss (viscous) modulus (G") in the frequency range of 1–100 rad·s−1, suggesting the formation of elastic solid-like hydrogel. The final system showed good photothermal effects and could heat up 20 oC in 4 minutes at power of 1400 mW and concentration of 200 μg/ml of the NPs (Fig. C). After 4 repeated on/off cycles of NIR irradiation, it also exhibited excellent photothermal stability. Cell viability studies showed that the hydrogel system possess high safety, demonstrated by cell viability of 86.052 ± 1.162% within 24 h (Fig. D).

Fig. 1. (A) TEM images of PDA@MnO2@CuO NPs at distinct magnification; (B) Comparison of the polymer solution with the hydrogel; (C) Photothermal temperature curves under 808 nm laser; (D) Cell viability of hydrogels loaded with different concentrations of NPs in 24 h.

Conclusion

In this study, a multifunctional injectable hydrogel platform loaded with photothermal nanoparticles and taurine was successfully developed. Further, good mechanical properties, photothermal activity, and biocompatibility have been demonstrated. Nonetheless, the therapeutic ability of the final system against skin wound infection needs to be verified through in vivo analysis, and this work is ongoing.

Acknowledgement

The author is grateful for any support from Santos Lab, the University Medical Center Groningen, the University of Groningen, and the China Scholarship Council.

Reference

1. Chen Y, Gao Y, Chen Y, Liu L, Mo A, Peng Q. J Control Release. 2020;328:251-62.
2. Wang Q, Qiu W, Li M, Li N, Li X, Qin X, et al. Biomater Sci. 2022;10(17):4796-814.

Advancements in hydrogel-based inks for tissue engineering and regenerative medicine

J. Żur-Pińska[1], R. Geevarghese[1], O.C. Azuama[1], D. Parisi[2], J. Es Sayed[3], A. Amirsadeghi[3], M. Włodarczyk-Biegun[1,3]
[1]Biotechnology Centre, The Silesian University of Technology, B. Krzywoustego 8, 44-100, Gliwice, Poland
[2]Engineering and Technology Institute Groningen, University of Groningen, Nijenborgh 4, Groningen, 9747 AG, The Netherlands
[3]Zernike Institute for Advanced Materials, University of Groningen, Nijenborgh 4, Groningen, 9747 AG, The Netherlands

Introduction: The emergence of bio-fabrication techniques, particularly 3D bio-printing, has revolutionized tissue regeneration by offering precision, versatility in shape, and customization for patient-specific needs. Bioink, a printable formulation containing biomaterials, cells, and biochemical cues, is a key component of 3D bioprinting, providing an environment that mimics the physiological 3D microenvironment. Although several polymeric bioinks are available for tissue regeneration, optimizing an ideal bioink remains a challenging, time-consuming endeavor that requires interdisciplinary expertise. However, recent years have witnessed significant progress in the field of hydrogel-based bioinks for tissue engineering and regenerative medicine, aiming to address the critical need for bioinks that meet physicochemical and cytocompatibility criteria.

Aim: In our group, we are aiming to develop new 3D-printable multifunctional (bio)inks based on hydrogels composed of different polymers, including (i) hydrogels containing metal-based dynamic bonds for wound, skin and nerve regeneration, (ii) inks made of alginate (Alg), methacrylate gelatin (GelMA) and carboxymethylcellulose (CMC) for interphase tissue engineering, and (iii) inks composed of Alg and gelatine cross-linked with microbial enzymes reinforced with microparticles for drug-releasing purposes and bone tissue regeneration.

Material and methods: Hydrogels were composed of commonly used polymers, i.e. Alg, CMC, GelMA, gelatine, and quaternized chitosan. Dynamic bonds were created with $FeCl_3$ and $CuCl_2$ solutions. PLGA (poly(lactic-co-glycolic acid)) microspheres were prepared by double emulsion solvent extraction (w/o/w). Rheological studies were performed with a rheometer (TA Instruments) with 8 and/or 20 mm parallel plates, while printability was assessed by Bioscaffolder 3.3 (GeSiM). For cell culture study tenocytes and fibroblasts NIH 3T3 were used.

Results: As a result of our study, we proposed a novel ink based on quaternized chitosan-catechol, known for its unique properties and enhanced adhesion capabilities that promote cell attachment and growth. We investigated the use of catechol groups in metal-induced cross-linking mechanisms, forming reversible bonds under precise pH control. Furthermore, the dynamic network established between catechol groups and divalent or trivalent metal ions was further modified by sodium periodate to create covalent bonds. For bone tissue regeneration, our research centered on developing mechanically stable and biofunctional 3D-printed scaffolds reinforced with PLGA microspheres. These microspheres were incorporated into cell-laden Alg-gelatine-based bioink to enhance bone regeneration, which can be used in osteoporosis treatment. The 3D-printed scaffolds underwent rigorous characterization, including rheological analysis to assess physical properties, with plans to incorporate BMP-2 for further enhancing bone regeneration. For interphase tissue engineering, our primary objective was to develop a highly suitable bioink for 3D printing based on commonly used polymers, namely Alg, CMC, and GelMA. We explored different combinations of these bioink components at various ratios, aiming to establish a robust correlation between bioink rheology and its 3D printability. The ultimate goal was to identify optimal conditions ensuring excellent printability, precise shape retention, and long-term stability of 3D-printed scaffolds.

Conclusions: In our research, we are focused on detailed characterization of the systems, and the systematic approach using rheology serves as an effective tool, enabling a correlation between bioink, printability aspects, and the mechanical properties of the printed scaffolds. Such characterized systems can serve as a valuable tool for cell culture study for various tissue engineering purposes.

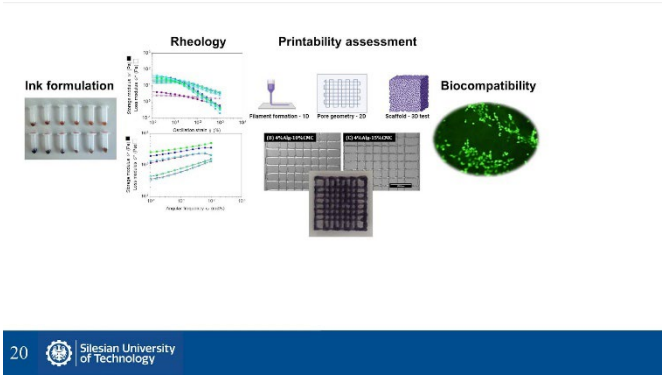

Fig. 1. Development of a new (bio)ink for tissue engineering.

Novel Bioactive Glass S53P4 cream as a bactericidal coating to prevent Biomaterial-Associated infections

Deeksha Rajkumar, Payal P.S. Balraadjsing, Martijn Riool, Sebastian A.J. Zaat

Department of Medical Microbiology & Infection Prevention, Amsterdam Institute for Infection and Immunity, Amsterdam UMC, University of Amsterdam, Meibergdreef 9, 1105 AZ Amsterdam, The Netherlands.

d.rajkumar@amsterdamumc.nl

Introduction: Biomaterial associated infection (BAI) is a frequent complication in the use of medical implants, often caused by staphylococci. BAI are generally challenging to treat due to biofilm formation and resistance to antibiotics. Bioactive Glass (BAG) S53P4 has been shown to have osteoconductive, angiogenic and antibacterial properties. BAG granules are used as a bone filler for the treatment of osteomyelitis and they are approved for local application in the treatment of bone infections without being preloaded with antibiotics. The hypothesized antimicrobial mechanism of action of BAG is that when it comes in contact with body fluids, it releases ions, increases pH and osmotic pressure. These changes result in an alkaline environment which is unfavorable for bacterial survival. Application of BAG on biomaterial surfaces may therefore provide a way to prevent BAI. A novel BAG cream has the potential to be applied on implant material surfaces. **Aim:** To investigate if BAG S53P4 cream, which consists of 50% BAG powder and 50% binder has similar or better bactericidal activity than free BAG powder or BAG granules and to see whether BAG cream has the potential to be applied on implant materials. **Method**: The bactericidal activity of BAG granules and powder against *Staphylococcus aureus* was first analysed. Then, bactericidal activity of equivalent amounts of BAG cream, powder and binder were determined. In this experiment, BAG cream or binder alone was applied on Titanium Aluminum Niobium (TAN) discs and pre-incubated in medium for 2h, 4h, 8h and 24h. The cream coating was visually inspected for stability, and eluates were collected at each time point and tested for their bactericidal activity against *S. aureus*. Additionally, pH was measured at all four time points. **Results**: The bactericidal activity and pH of BAG powder eluates was higher than of eluates of BAG granules. When comparing the bactericidal activity of equivalent amounts of BAG cream, powder and binder, BAG cream and powder had bactericidal activity but binder alone did not. It was also noted that the pH was slightly higher at 2h than at 4h, 8h and 24 h, for eluates of both BAG cream and powder. BAG cream remained adhered to the surface of the discs after submersion in medium for 24 h. **Conclusion:** BAG cream and powder show higher bactericidal activity than granules. As BAG cream applied on TAN discs adheres well and remains on the discs after submersion in medium, this suggests suitability for application on implant material surfaces.

Future research: To gain a deeper understanding of the antimicrobial mechanism of action, we intend to investigate ion release of different BAG formulations using Inductive Coupled Plasma Optical Emission Spectroscopy (ICP-OES) as well as increase in osmotic pressure and their impact on bacterial killing.

Using Bayesian Optimization to Calculate Conductivity in an Electrolytic Fluid for the Forward Problem in Electrocardiography

D. Rojas-Velazquez[1,2], A. Tonda[3], J. Garssen[1,4], A. Lopez-Rincon[1,2]

1. Division of Pharmacology, Utrecht Institute for Pharmaceutical Sciences, Utrecht University, The Netherlands.

2. Julius Center for Health Sciences and Primary Care, UMC Utrecht, The Netherlands.

3. INRAE, AgroParisTech, Université Paris-Saclay, 91120, Palaiseau, France.

4. Global Centre of Excellence Immunology Danone Nutricia Research.

Introduction. The ability of an electrolyte solution to transmit electricity is known as its conductivity, which is quantified in siemens per meter (S/m). This property is often used in various fields, including environmental and industrial sectors, to quickly and affordably determine the ionic content of a solution.

In the medical and biological fields, the measurement of electrolytic conductivity is a common practice. This is typically done by measuring the resistance of the solution between two electrodes (either flat or cylindrical) that are a fixed distance apart. To minimize water electrolysis, an alternating voltage is usually applied [1].

However, it's crucial to remember that various factors can influence conductivity values. These include temperature, electrolyte concentration, and the nature of the electrolyte. Therefore, these factors should be considered when measuring conductivity for medical applications to ensure accurate results [2]. Thus, as the calculation of the conductivity can be complex we propose to find the conductivity tensor using Bayesian Optimization (BO).

BO in material design and other problems has been an option in the last years [3][4]. BO is an optimization method that uses a small set of inputs and outputs with a Gaussian Process to predict where the global minima could be found based on a cost function characterized by the mean and the variance [5]. In contrast to other optimization methods, BO is used where the main function is costly or difficult to evaluate, and thus we can only afford a limited set of evaluations [6].

Materials. The data was downloaded from the EDGAR repository [7]. The data is from a canine heart that was perfused using the Langendorf method and supported by a second canine. The recording of the data was done using an array of electrodes placed around the heart (256 electrodes) and a torso tank (192 electrodes) for 220 time steps. The torso tank was filled with a conductive fluid that mimics the conductivity of a human torso. The electrolytic fluid was made up of sodium chloride (0.023 mol/L), sucrose (0.26 mol/L), and deionized water with a target conductivity of 500 Ωcm (0.2 S/m) similar to human torso [8].

Methods. We model the system with the Volume Conductor model of electrical activity using FEM (Finite Element Method), where the inner surface is given by the heart cage and the outer surface is the torso tank (Fig.1). Then, we try to reconstruct the conductivity tensor of the electrolytic fluid by using an Operator (T) created with FEM and BO with the measures in the heart (u_h). Then, by $Tu_h=u_{tc}$ and comparing the calculated values in the thorax (u_{tc}) to the actual measures in the (u_t) we will evaluate the quality of the conductivity tensor. The error is given by $\sum_i^{220}\frac{(u_{tc}^i-u_t^i)^2}{(u_t^i)^2}$. The tensor is described by coefficients in each axis ($cond_X$, $cond_Y$, $cond_Z$). We run the BO for 100 time steps, with 5 initial random points, using *matern* 5/2 kernel with hyperparameters solved by LBFGS-B [9] and the acquisition function by CMA-ES [10].

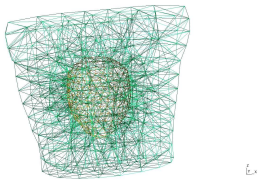

Figure 1 Geometry discretization of the Torso tank using FEM.

Results and Discussion. Using this methodology we approximated the conductivity tensor and we measured the error, being the best value for the error 0.487011 (Fig. 2-Left). Then, using the selected values we compared the actual measures to the simulated (Fig. 3-Right).

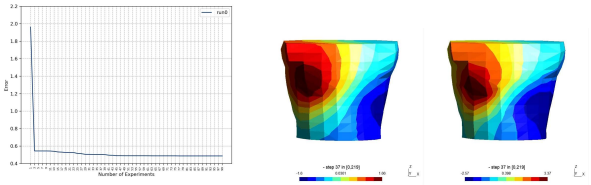

Figure 2 Error graph using BO (Left). Simulation of selected values at time step 37 (Right).

From the results we can see that even if the propagation is correct, there is a difference in the scale. In the measured values the range goes from (-1.6 to 1.66) and in the simulated goes from (-2.57 to 3.37). This error, can be given by the normalization of the geometry. Furthermore, this is a first approximation using real data. In order to validate our methodology we need to test using even more points in BO, and if possible other methodologies. In this problem each point evaluated requires around 2 minutes, this translates to a minimum 200 minutes for 100 points.

Conclusions. BO is suited for problems, where evaluation of a function is too expensive either in computer time or in resources [6]. In this first case we applied BO to find the conductivity tensor in an electrolyte solution. Nevertheless, further testing is required.

Bibliography.

[1] Moroń, Zbigniew, and Tomasz Grysiński. "How to Measure Electrolytic Conductivity Successfully." (2015).

[2]Minea, Alina Adriana. "A review on electrical conductivity of nanoparticle-enhanced fluids." (2019).

[3] Zhang, Yichi, Daniel W. Apley, and Wei Chen. "Bayesian optimization for materials design with mixed quantitative and qualitative variables." (2020).

[4] Frazier, Peter I., and Jialei Wang. "Bayesian optimization for materials design." (2015).

[5] Williams, Christopher KI, and Carl Edward Rasmussen. *Gaussian processes for machine learning*. (2006).

[6] Shahriari, Bobak, et al. "Taking the human out of the loop: A review of Bayesian optimization." (2015).

[7] Aras, Kedar, et al. "Experimental data and geometric analysis repository—EDGAR." (2015).

[8] Bergquist, Jake A., et al. "The electrocardiographic forward problem: A benchmark study." (2021).

[9] Andrei, Neculai. "Comparison LBFGS-B versus LBFGS." (2010).

[10] Hansen, Nikolaus, Sibylle D. Müller, and Petros Koumoutsakos. "Reducing the time complexity of the derandomized evolution strategy with covariance matrix adaptation (CMA-ES)." (2003).

Biofabrication of Osteogenic Spheroids from Human Dental Pulp Stem Cells of Deciduous Teeth (SHEDs)

CS Maas[1,2,*], FNO Fulfaro[1], IPB Ribeiro[1], DB Ferreira[1], HA Santos[2], KBS Paiva[1]
[1]Institute of Biomedical Sciences, University of São Paulo, São Paulo – Brazil
[2]Department of Biomedical Engineering, University Medical Center Groningen, University of Groningen, The Netherlands
*E-mail: c.soeiro.maas@umcg.nl

Introduction: Various populations of stem cells found in the oral cavity have been characterized and originated from neural crest stem cells and are considered promising for craniofacial tissue regeneration[1]. Among them, stem cells from the dental pulp of deciduous teeth (SHEDs) demonstrate a high capacity for cell differentiation, and their secretome exhibits angiogenic, neurotrophic, and immunomodulatory properties. In addition, the SHEDs are easily obtained non-invasively due to the exfoliative tooth feature. Spheroids are characterized as homogeneous, self-organized cellular aggregates grown in suspension or heterogeneously, often involving the co-culture of multiple cell types to form functional 3D tissue. Stem cell spheroids also have a high capacity to secrete autocrine and paracrine molecules. Oxygen concentration plays a fundamental role in maintaining stem cell plasticity and proliferation[2], with hypoxic conditions modulating cell secretomes[3]. Compared to other dental pulp stem cells, the proliferation potential of SHEDs under hypoxic conditions was higher in monolayer cultures[4]. However, spheroids of SHEDs and their secretome have not yet been evaluated under hypoxic conditions. In this study, our goal was the biofabrication of osteogenic spheroids from SHEDs.

Materials and Methods: SHEDs were isolated from dental pulps collected from orthodontic patients for six to seventeen years (Ethical Approval Process Number 28857920.0.0000.5467/ICB-USP). The pulp was separated from a remnant crown and then digested enzymatically (solution of 3 mg/ml collagenase type I and 4 mg/ml dispase) for 1 h at 37°C. Single-cell suspensions were by passing the cells through a 70-mm strainer[5]. Primary SHEDs were subcultured in a clonogenic medium (a-MEM + 10% FBS + antibiotics + 50 mM ascorbic acid). SHEDs were used in passage #6 to manufacture small (150-200 μm) spheroids formed in agarose micromolds with 256 circular recesses, creating in each of them a fully compacted spheroid after three days (day 0). Those spheroids were cultivated in clonogenic medium and osteogenic medium (clonogenic medium supplemented with 1 μM dexamethasone + 10 mM b-glycerophosphate) under normoxia (20% O_2) or hypoxia (2% O_2) for 28 days. Morphological (via scanning electron microscopy), ultra-structural (via transmission electron microscopy) and histological analysis were conducted.

Results and Discussion: Over time, the spheroids decreased in diameter through a continuous process of compaction, which is more pronounced when in an osteogenic microenvironment and normoxia. Regarding the cytoarchitecture, up to 7 days, the cells are more homogeneously distributed throughout the spheroid. It was also possible to observe cell aggregates inside and elongated cells on the surface of the spheroids. Results showed that the spheroid morphology is more compact in osteogenic and hypoxia environments. In addition, SHED spheroids under hypoxia presented a more homogeneous surface morphology. On the inside, it was possible to observe thicker layers composed of flat cells on layers closer to the surface. It was also possible to confirm the presence of more extracellular vesicles and a denser extracellular matrix composition of spheroids in osteogenic medium under hypoxia. Spheroids in osteogenic medium under hypoxia also presented more collagen fibres when compared to the ones under normoxia, as well as early signs of mineralisation sites.

Conclusions: So far, it has been shown spheroids from SHEDs are viable for a long time of culture and that evident differences are observed depending on the concentration of oxygen in the microenvironment. Also, morphological evidence showed that hypoxia could affect the secretome, but further investigation are currently undergoing to explore this further.

References:

[1] Paiva KBS, Maas CS, Dos Santos PM, Granjeiro JM, Letra A. Extracellular Matrix Composition and Remodeling: Current Perspectives on Secondary Palate Formation, Cleft Lip/Palate, and Palatal Reconstruction. *Front Cell Dev Biol*. 2019 Dec 13;7:340. doi: 10.3389/fcell.2019.00340. PMID: 31921852; PMCID: PMC6923686.

[2] Ma, T., Grayson, W. L., Fröhlich, M., & Vunjak-Novakovic, G. (2009). Hypoxia and stem cell-based engineering of mesenchymal tissues. *Biotechnology progress*, 25(1), 32–42. https://doi.org/10.1002/btpr.128

[3]Müller, A. S. et al. (2017). Hypoxia-based strategies for regenerative dentistry—Views from the different dental fields, *Archives of Oral Biology*. Elsevier Ltd, 81, pp. 121– 30. doi:10.1016/j.archoralbio.2017.04.029.

[4] Kanafi, M. M. et al. (2013) Influence of hypoxia, high glucose, and low serum on the growth kinetics of mesenchymal stem cells from deciduous and permanent teeth, *Cells Tissues Organs*, 198(3), pp. 198–208. doi: 10.1159/000354901

[5] Miura, M., Gronthos, S., Zhao, M., Lu, B., Fisher, L. W., Robey, P. G., & Shi, S. (2003). SHED: stem cells from human exfoliated deciduous teeth. Proceedings of the National Academy of Sciences of the United States of America, 100(10), 5807–5812. https://doi.org/10.1073/pnas.0937635100